TACTIC GROUNDWATER

GeoERA

Establishing the European Geological Surveys Research Area to deliver a Geological Service for Europe

Deliverable 5.3

Pilot description and assessment reports work package 5

Contribution partners:

IGME, ICGC, BGS, SGSS, HGI, MTI, LEGMC, LNEG, GEUS

Deliverable Data	
Deliverable number	D5.3
Dissemination level	Public
Deliverable name	Pilot description and assessment report
Work package	WP5: ASSESSMENT OF SALT-/SEA WATER INTRUSION STATUS AND VULNERABILITY
Lead WP/Deliverable beneficiary	IGME
Deliverable status	
Version	Final version
Date	25/03/2021

[This page has intentionally been left blank]

TABLE OF CONTENTS

1   INTRODUCTION

The pilot description reports are compiled in this document (as a single D5.3 document) but are separate reports from the individual pilots. Reports can include more than one pilot from the same country and present work performed in other work packages (WPs) together with the work done in work package 5. Hence, there is only one pilot report for each pilot although the pilot appears in several TACTIC work packages.

The hereby presented document include all the pilot assessments reports and results performed in WP5. Assessments in WP5 focuses on assessments of salt-/sea water intrusion status and vulnerability at the pilot scale. The pilot scale includes local and
regional scale (Fluvia and La Muga rivers delta plain, Hull & East Riding chalk aquifer, Plana de Oropesa-Torreblanca, Ravenna phreatic aquifer,Vrana lake) to small country scale (Malta Mean Sea Level Aquifer). A common method has been applied to summarise sea water intrusión status and vulnerablity in the pilots, where the available information allows to apply it. The pilots illustrate a large variety of different approaches (eg. interpolations, Sharp interface models, density dependent models) to estimate spatially distributed results.

The pilot assessment reports are ordered alphabetically and organized into separate documents within D5.4 because the individual reports are used for documentation toward local stakeholders.

Deliverable 5.3

PILOT DESCRIPTION AND ASSESSMENT

Fluvia and La Muga rivers delta plain (Catalonia)

Authors and affiliation:

Camps Clemente, Victor
Arnó Pons, Georgina
Herms Canellas, Ignasi

Geographical and Geological Institute of Catalonia

ICGC
Institut
Cartogràfic i Geològic
de Catalunya

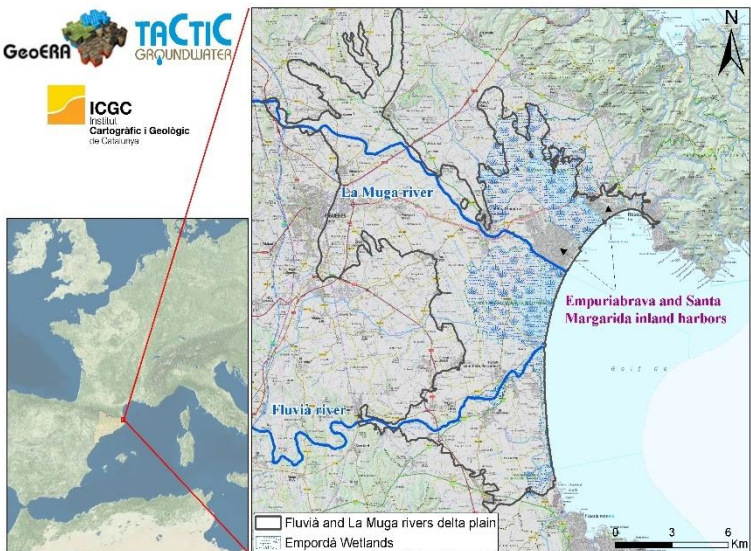| Deliverable Data	
Deliverable number	D5.3
Dissemination level	Public
Deliverable name	Pilot description and assessment
Work package	WP5: ASSESSMENT OF SALT-/SEA WATER INTRUSION STATUS AND VULNERABILITY
Lead WP/Deliverable beneficiary	IGME
Deliverable status	
Version	Version 3
Date	26/03/2021

[This page has intentionally been left blank]

LIST OF ABBREVIATIONS & ACRONYMS

ACA	Catalan Water Agency
CC	Climate Change
GC	Global Change
GSO	Geological Survey Organisations
LULC	Land Use and Land Cover
NBL	Natural Background Level
SWI	Sea Water Intrusion
TV	Threshold Value

TABLE OF CONTENTS

Pilot name	Fluvià and La Muga rivers delta plain	
Country	Spain	
EU-region	Mediterranean region	
Area (km²)	166 km²	
Aquifer geology and type classification	Sedimentary delta plain (gravel and sand layers in a silty and clay matrix). Porous media aquifer.	
Primary water usage	Irrigation / Drinking water	
Main climate change issues	The Fluvià and la Muga delta plain correspond to a very flat and low altitude area. Adjacent to the coastline there is a protected area called "the Natural Park of the Empordà Wetlands" recognized by the International Treaty of RAMSAR where mixed saline and fresh water coexists. On the north the inland harbors of Empuriabrava and Santa Margarida constructed between the 1960 and 1975 are one of the biggest marine urban areas in the world. These settings and an important demand of water for agriculture purposes combined with the expected rise in temperatures and the decrease in rainfall (consequent reduction in evapotranspiration) make this area particularly vulnerable. Additionally, the frequency of storms such "Gloria 2020" would notably increase. In this very flat area near the coastline, low air pressure during the storms causes surface salt water to move forward inland producing natural saltwater recharge from the surface to the target aquifers.	
Methods used	Assessment of the SWI status on the aquifer system by means of the proposed methods, using the **time series** available since 1995 is the main objective of this project. For the temporal evolution of the status, the proposed index methods have been used. It has been necessary to work mainly with **GIS interpolation methods** based on an iterative finite difference interpolation technique. In the future a density dependent flow 3D model of the area (not available for this project) would allow different future simulations based on climate change scenarios.	
Key stakeholders	Catalan Water Agency (ACA), agricultural irrigators communities, water supply companies.	
Contact person	Víctor Camps (ICGC); victor.camps@icgc.cat	

1 EXECUTIVE SUMMARY

The aquifer system of the Fluvià and la Muga rivers delta plain is located in the Northeast of the Iberian Peninsula. It is a porous media which consists of quaternary detrital deposits overlapping the Neogene detrital sediments of the Empordà basin. It is a typical Mediterranean fluviodeltaic aquifer system with an unconfined upper aquifer and a discontinuous confined deep aquifer. Between them a clay and silt sediments layer acts as aquitard. The extension of the aquifer is 166 km^2. The maximum thickness of the total aquifer system reaches at least 50 meters in the areas closest to the coastline. Upstream the two aquifers converge into a single aquifer of unconfined behavior.

The transmissivity of this aquifer system ranges between 200 - 3000 m^2/day (ACA, 2005) and the storage coefficient ranges from 0.15 and 10^{-4} (ACA, 2005). It should be pointed out that the aquifer system presents an important lithological spatial heterogeneity and therefore its behavior and hydraulic parameters can change substantially from one site to another one.

The study area had been mainly agricultural until the end of the 1960s and early 1970s, when (like other Mediterranean areas) the construction of tourist infrastructures were intensified. The paradigm of this situation is found in the inland harbors of Empuriabrava and Santa Margarida constructed between the 1960 and 1975 in the north of the study area. With more than 30 Km of inland navigable channels are one of the biggest marine urban area in the world. This fact caused a significant overexploitation with an increase in SWI problems in some areas. These effects were mitigated by the search for water supply alternatives in the late 1980s. Even so the largest pumping of water is related with agriculture purposes (18.9 hm^3/year), followed by water supply (2.35 hm^3/year) and other industrial uses (0.78 hm^3/year) (ACA, 2005).

Opposite to this, in an area adjacent to the coastline and surrounding the Empuriabrava harbor there is a very wild natural protected area called "the Natural Park of the Empordà Wetlands" recognized by the International Treaty of RAMSAR (site No. 592 of RAMSAR Convention Bureau, 1990) where mixed saline and fresh water coexists.

SWI has been a permanent problem in the areas closest to the coast. Therefore, a study of the available historical series can show the trend in order to complete the study in the future with a density dependent flow 3D model, which could simulate future climatic scenarios. Therefore, the main objective in this project has been to assess the status and vulnerability of the aquifer system on SWI throughout the available time series with the proposed index methods in TACTIC WP5.

For the evaluation of the status, an analysis of the available time series of the chloride concentration (data mainly provided by ICGC main stakeholder, the Catalan Water Agency) has been carried out. By defining the chloride Natural Background Level (NBL) in the Fluvià and la Muga rivers delta plain aquifer system and the corresponding chloride Threshold Value (TV), a SWI affected area has been established for each time period as proposed by the first index method (SWI status). The same affected areas and volumes estimation have been made using another kind of threshold value: the GALDIT vulnerability index. The GALDIT method has been applied to see the evolution of the moderate and high vulnerability throughout the time series. The results from both methods (the SWI status and the vulnerability assessment) have been summarized in conceptual 2D cross sections.

A slightly increase of the affected volume by SWI is observed in the last 25 years. More variability is observed in the outcomes of the SWI status method. Even so, the variation of the SWI affected areas is not homogeneous in the study area and more variability can be observed in the center and south part where the variation on the pumping exploitation rates is the most important anthropogenic process to be considered. The Empuriabrava inland harbors in the north and the Empordà Wetlands causes bigger SWI affected areas, but they existence also could favor the stability of the SWI over time.

The obtained results give a good overview of the evolution of the SWI in the area and its areal distribution concluding that the SWI status proposed method is useful in that sense. It could be applied systematically in different potential coastal areas affected by SWI and obtain comparable results among them.

It is also highlighted the need for develop 3D numerical flow and transport models (density - dependent) in the most sensible areas to simulate future scenarios related with the climate change and to obtain better and more accurate outcomes.

2 INTRODUCTION

2.1 General introduction

Climate change (CC) already have widespread and significant impacts in Europe, which is expected to increase in the future. Groundwater plays a vital role for the land phase of the freshwater cycle and has the capability of buffering or enhancing the impact from extreme climate events causing droughts or floods, depending on the subsurface properties and the status of the system (dry/wet) prior to the climate event. Understanding and taking the hydrogeology into account is therefore essential in the assessment of climate change impacts. Providing harmonized results and products across Europe is further vital for supporting stakeholders, decision makers and EU policies makers.

The Geological Survey Organizations (GSOs) in Europe compile the necessary data and knowledge of the groundwater systems across Europe. In order to enhance the utilization of these data and knowledge of the subsurface system in CC impact assessments the GSOs, in the framework of GeoERA, has established the project "Tools for Assessment of ClimaTe change Impact on Groundwater and Adaptation Strategies – TACTIC". By collaboration among the involved partners, TACTIC aims to enhance and harmonize CC impact assessments and identification and analyses of potential adaptation strategies.

TACTIC is centered around 40 pilot studies covering a variety of CC challenges as well as different hydrogeological settings and different management systems found in Europe. Knowledge and experiences from the pilots will be synthesized and provide a basis for the development of an infra structure on CC impact assessments and adaptation strategies. The final projects results will be made available through the common GeoERA Information Platform (http://www.europe-geology.eu).

2.2 The Fluvia and la Muga rivers delta plain

The present document reports the TACTIC activities in the pilot Fluvià and la Muga rivers delta plain aquifer system located in the Mediterranean coast of Spain, Girona province, in the NE of Catalonia. It is a quaternary detrital aquifer system composed by two main aquifers: an uppermost shallow unconfined aquifer and a lowermost confined aquifer. The known aquifer system thickness ranges from 10 m to more than 50 m downstream near the coastline. Upstream the two aquifers converge into a single aquifer of unconfined behavior. The detrital deposits of this aquifer system are very heterogeneous, so hydraulic parameters have a wide range of values.

The study area had been mainly agricultural until the construction of one of the biggest inland harbors in the word; the Empuriabrava and Santa Margarida marine urban area which is placed in the north of the study area. In addition to the impact on the SWI status that this civil work caused itself, the tourism pressure caused a significant increase of the exploitation of the aquifer system. Adjacent to the coastline and surrounding the Empuriabrava inland harbor there is a very wild natural protected area called "the Natural Park of the Empordà Wetlands" recognized by the International Treaty of RAMSAR (site No. 592 of RAMSAR Convention Bureau, 1990) where mixed saline and fresh water coexists. Thus, SWI has been a permanent problem in the

areas closest to the coastline and due to both natural and anthropogenic conditions. In late 1980s seawater intrusion contaminated some groundwater supply wells (ACA, 2005).

The expected climate change scenarios could push forward worsening the SWI status. Therefore, the main objective in this project has been to assess the SWI status and vulnerability assessment of the aquifer system throughout the available groundwater chloride concentrations time series by applying the proposed index methods in TACTIC WP5. These data have allowed to evaluate in a general way how the SWI status has been evolved in the last 25 years.

The assessments in the Fluvià and la Muga delta plain aquifer system have been carried out by the Hydrogeology and Geothermal Unit of the Cartographic and Geologic Institute of Catalonia (ICGC).

3.1 Site description and data

3.1.1 Location and extension of the pilot area

The pilot area is the Fluvià and La Muga rivers delta plain, which is located in the Roses Gulf within the Girona province at the NE of Catalonia (Figure 1). The study area is characterized by dry Mediterranean climate and flat terrain and it occupies an area of 166 km^2. Due to favorable climate and geographical location, the area attracts numerous tourists and is suitable for agriculture. That is, the delta plain associated with the rivers Fluvià (south) and La Muga (north) and part of the alluvial zone associated with these upstream watercourses (Figure 1). The lenght of the pilot parallel to the coastline is about 16 km. Perpendicular to the coastline, the delta plain extends over 4 km, but the extension inland following the course of the La Muga river reaches 18 km.
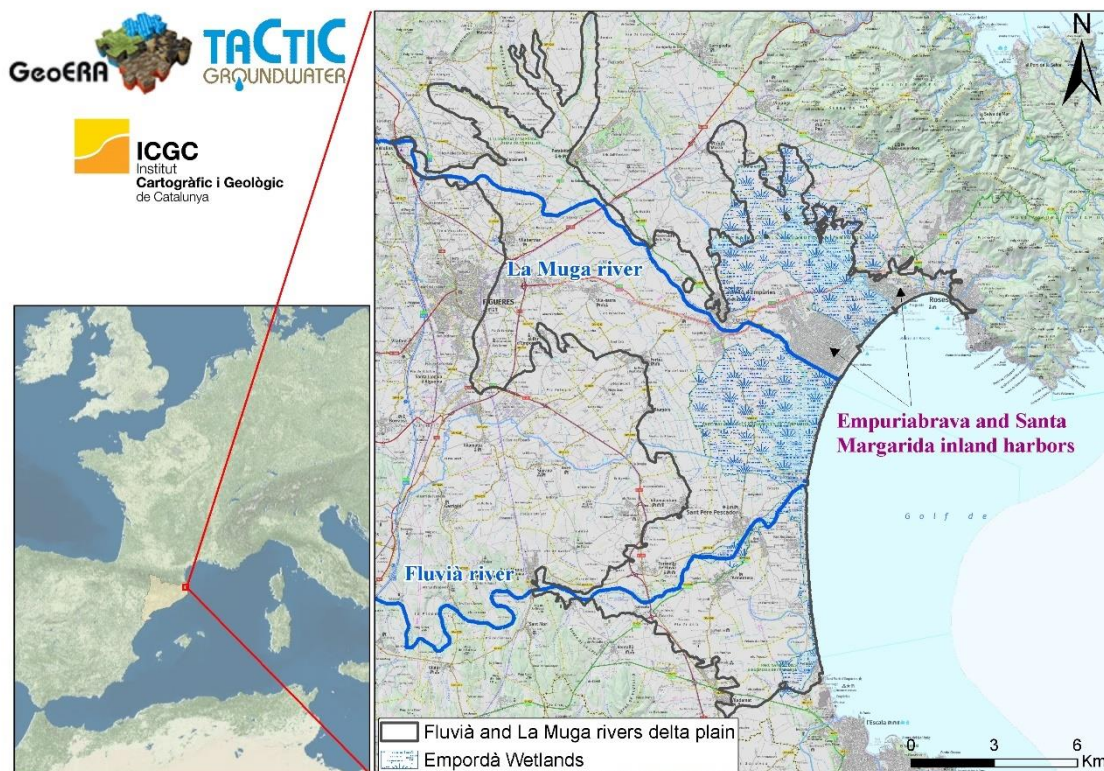

Figure 1: *Location of the Fluvià and La Muga rivers delta plain pilot area (Catalonia, ICGC).*

3.1.2 Geology/Aquifer type

The Fluvià and La Muga rivers delta plain is a quaternary detrital aquifer system. Downstream, on the flat are of the delta plain, the aquifer system is composed by two main aquifers:

a) an uppermost shallow unconfined aquifer formed by very heterogeneous detrital deposits of sands, silt, clay and gravels (ASFM in Figure 3**¡Error! No se encuentra el origen de la referencia.**). It has a thickness up to 20 meters.

b) a lowermost confined aquifer formed mainly by sands and gravels. The confined conditions are discontinuous over the study area (APFM in Figure 3). On top of this deep aquifer, silt and clay layers act as an aquitard. The confined aquifer (including the aquitard) has a known thickness of at least 30 meters. Upstream the two aquifers converge into a single aquifer of unconfined behavior.
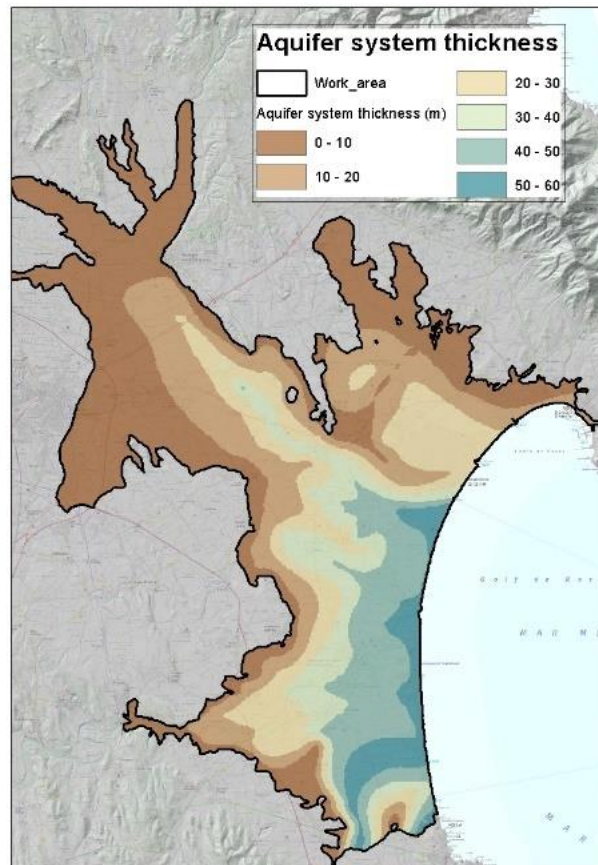

Figure 2: *Total aquifer system thickness obtained by interpolation methods. Based on the data collected from the geological and hydrogeological maps at scale 1:25.000 (ICGC, 2015) and the available hydrogeological cross sections.*

Given the heterogeneity of the aquifer system materials, the hydraulic parameters have a wide range of values. According to available pumping tests results the uppermost unconfined aquifer has a wider range of hydraulic conductivity (50-280 m/d) than the lower one (50-70 m/d). Storage coefficient range between 0.01 to 0.15 in the uppermost aquifer and reaches 10^{-4} in the deep confined aquifer. Thus, the transmissivity values range from 200 and 3000 m^2/d and the storage coefficient range from 0.15 and 10^{-4} (ACA,2005).
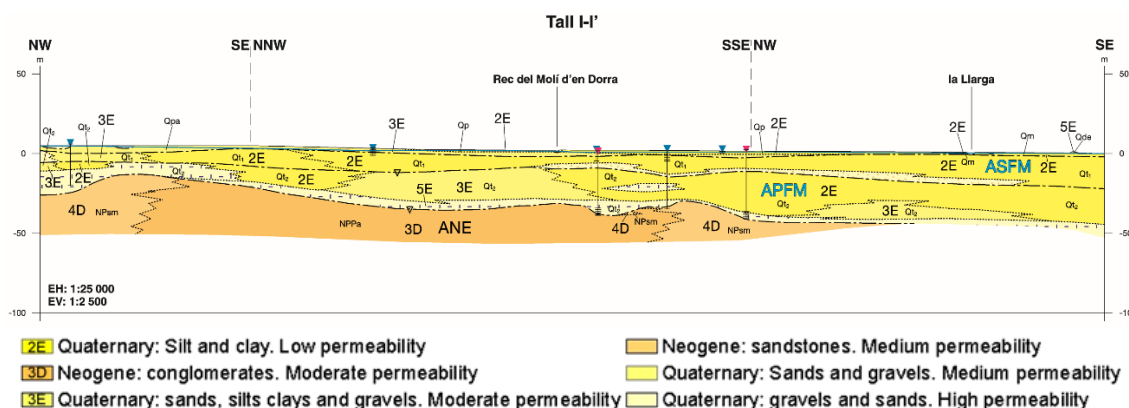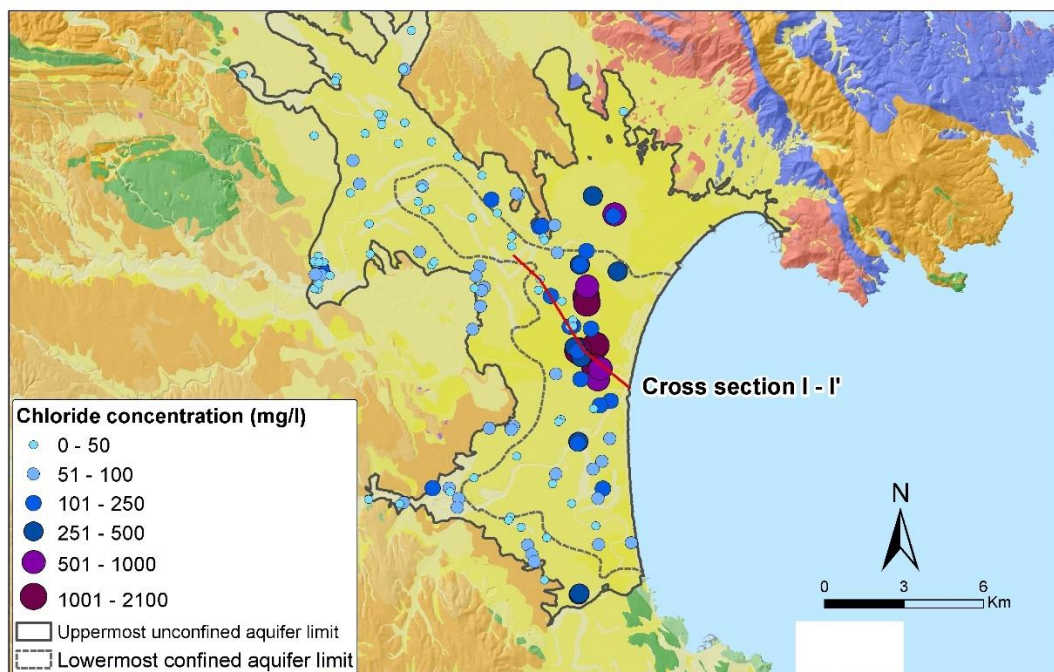
Figure 3: *Delimitation of the uppermost and lowermost aquifers and distribution of chloride concentrations (median of the historical time series analyses) . At the bottom, representative cross section of the Fluvià and la Muga rivers delta plain aquifer system (ICGC, 2015). ASFM is the upper unconfined aquifer and APFM is the deep confined aquifer. ANE corresponds to the lower Neogene aquifer system. Detrital deposits are classified into permeability classes as follows: 2E is low permeability (between 10^{-4} and 10^{-2} m/d), 3E is moderate permeability between (10^{-2} and 1 m/d), 4E and 4D is medium permeability (between 1 and 50 m/d) and 5E is high permeability (more than 50 m/d).*

3.1.3 Topography and Land Uses

The study area is very flat specially near the coastline where the topographic gradient is low. According to digital elevation model (DEM), elevation of pilot zone range between 0 to 80m a.s.l. (Figure 4).

Agriculture is the most important land use in the pilot area related mainly with rice and fruits crops. Urban areas are also important as tourism and agriculture are the main economic activities of the area. There are also forests and natural land, water bodies and beaches. Their distribution is shown on Figure 4.
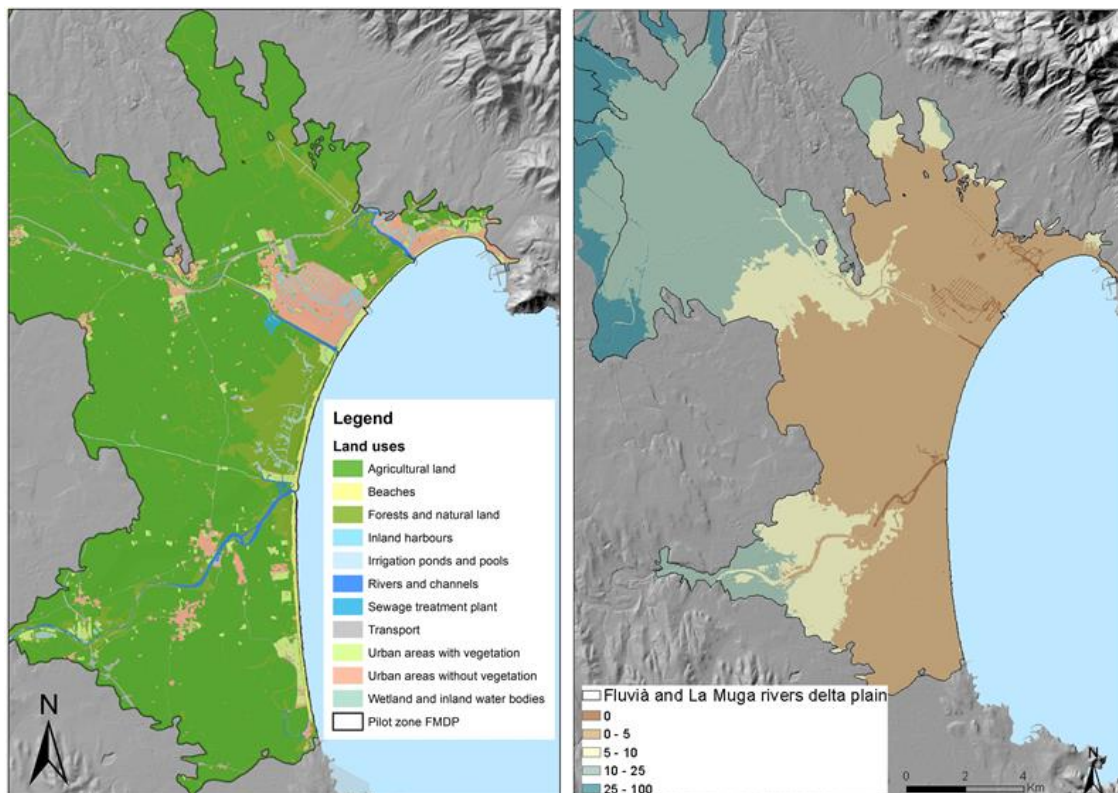

Figure 4: *Land uses map (CREAF, 2009) and digital elevation model (DEM) at 5 m resolution in the pilot zone.*

3.1.4 Surface water bodies

The most important surface water bodies in the pilot area are placed in the Natural Park of the Empordà Wetlands (4.784 Ha). There mixed saline and fresh water coexist. It is an area with high ecological interest in which there are permanently flooded bodies of water. It is recognized by the RAMSAR convention (site No. 592 of RAMSAR Convention Bureau, 1990) where is defined as *"a series of coastal saline and freshwater wetlands in the floodplains of two rivers (Fluvià and La Muga), separated from the sea by dunes. The site includes lagoons, pools, marshes and drainage channels supporting salt-resistant vegetation."*

In addition, the Fluvià and la Muga rivers, to which the studied aquifer system is associated, have a perennial stream with very variable flow rates due to the typical Mediterranean rainfall episodes with very variable yearly frequency and intensity.

The Fluvià and La Muga rivers are usually connected with the groundwater level. Depending on the area and the position of the groundwater table respect the elevation of the river surface water the rivers have an influent or effluent stream character. In the driest times of summer, the stream of the two rivers in their respective mouths are blocked by a sand bar. The area includes an extensive network of irrigation channels that spans the entire delta plain and distributes water from surface streams.

Finally, near the Empuriabrava inland harbor, there is the Castelló lake area which corresponds to an old lake drained in the 18th century that in our days is and endorheic zone used for agriculture purposes.

3.1.5 Hydraulic head evolution

Groundwater in the study area is shallow and has an overall gradient eastward ranging between 10^{-3} and $5 \cdot 10^{-3}$. Due to the discontinuity of the confined conditions of the deep aquifer, the uppermost and the lowermost aquifers have similar groundwater levels. In general, groundwater table near the coastline is around 1m asl. and inland it increases up to 10 - 12m a.s.l within the pilot area considered (Figure 5).

Piezometric groundwater level has been monitored by the Catalan Water Agency at two representative control points between 1989 and 2009 (data available at SDIM-ACA). The evolution of the piezometric levels in both aquifers is shown in Figure 6. It is observed a slight tendency to a generalized decrease on the groundwater levels (the variation throughout the observation period does not exceed 0.5 m) but a heavy seasonal oscillation that could be around 4 m at the location of the control points.

Taking into account that there are not enough data to obtain annual piezometric maps, the piezometric surface made with available data from 2011 (Figure 5) has been taken as reference piezometric surface. It is therefore assumed in this case that the final results for the SWI assessment could vary if annual piezometric surfaces were available. Even though, due to the slight tendency to a generalized decrease of groundwater levels observed in Figure 6, it has been considered that the results may be little dependent on this variable.
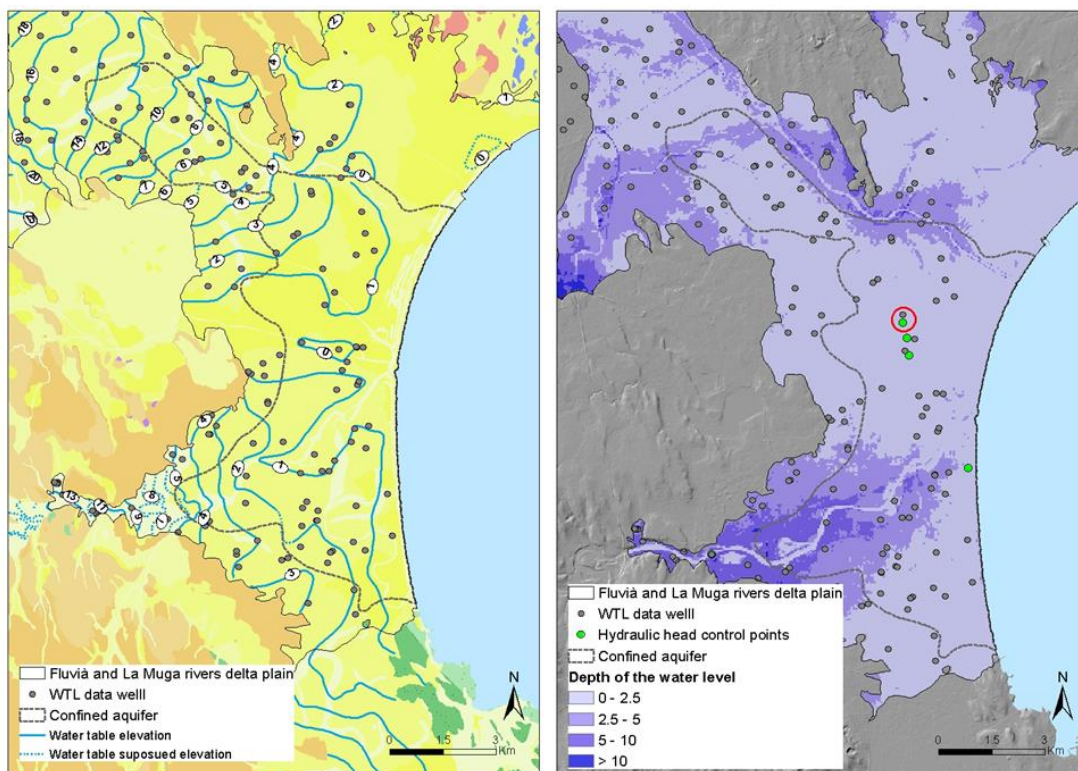
Figure 5: *Mean groundwater table distribution (left) in m asl (ICGC, 2015) and depth of the water level in the study area (right). This has been considered as the surface of the reference water table to apply the SWI status and the GALDIT vulnerability assessment method. Red circle indicates the position of the control water point of Figure 6.*
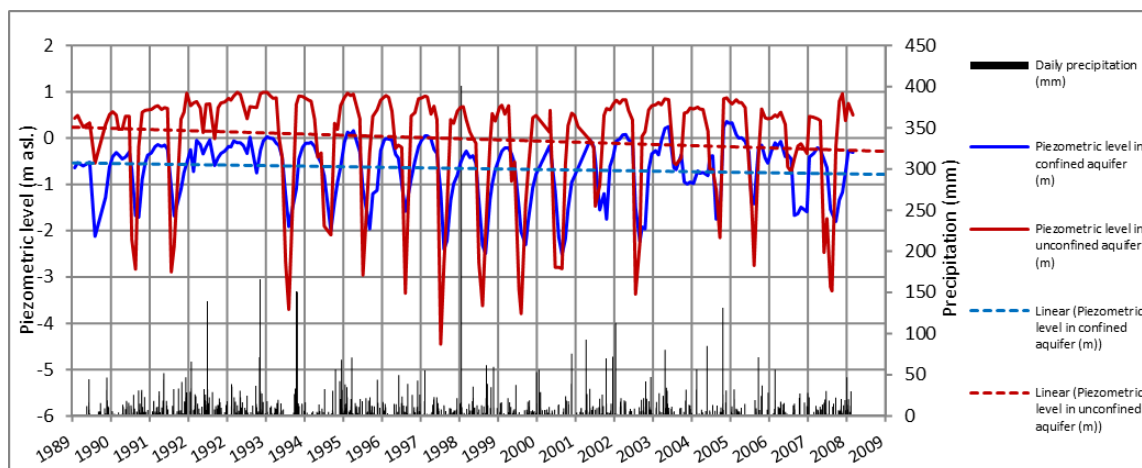

Figure 6: *Piezometric level series in the unconfined and confined aquifers between 1989 and 2009 (control piezometer is highlighted in the* Figure 5 *with red circle).*

3.1.6   Climate

Pilot area has a typical Mediterranean climate with dry summers and rainy autumn and winters. According to Köppen-Geiger climate classification, local climate belongs to Csa group, i.e., hot-

summer Mediterranean climate (Kottek M. et al 2006). The annual average temperature between 1991 and 2017 was 15⁰ C, with lowest temperatures in January and the highest ones in July. Annual precipitation was 628 mm/year during the same period.

The annual period with the highest freshwater demand coincides with lowest rainfalls rates, i.e., July has an average precipitation of 24,9 mm whereas January, October and November have higher values of 67 mm, 93 mm and 66 mm, respectively (Figure 7). The annual average potential evapotranspiration (ETP) is 889.2 mm/year, with highest rates in July (161.4 mm) and lowest ones in January (17.4 mm).
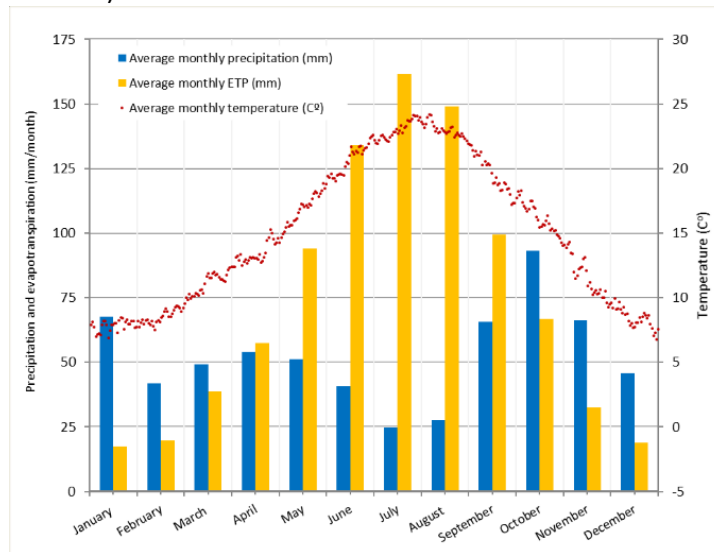

Figure 7. *Average precipitation, temperature and evapotranspiration in the study area between 1991 and 2017. ICGC (2015).*

3.1.7   *Hydrochemical data*

Hydrochemical analysis from the period 1995 to 2017 have been collected both from the Catalan Water Agency database (SDIM-ACA) and from the ICGC hydrogeological database. Regarding chloride concentrations, on which the SWI status assessment is focused, in the Fluvià and La Muga delta plain pilot area there are more than 600 available samples at around 150 water wells and control points. For each water point the number of samples available during the studied period (1995-2017) is quite variable. In some wells there are a maximum of 1 or 2 samples whereas at some control points more than 25 samples have been considered. Therefore, the spatial distribution of chloride data per year is quite variable and sometimes not enough to apply annually the SWI status and SWI vulnerability methods. The depth of sampling is not available in most cases, so it has to be assumed that is equivalent to the depth of the water point considered.

For the NBL and the corresponding TV estimation and in order to assure that long time series do not bias results and that all sampling sites contribute equally, chloride time series at each monitoring point were converted to median. Near the coastline the median values increase up to 2000 mg/l (Figure 8). Upstream, the values are quite homogeneous and range from 20 to 80 mg/l.
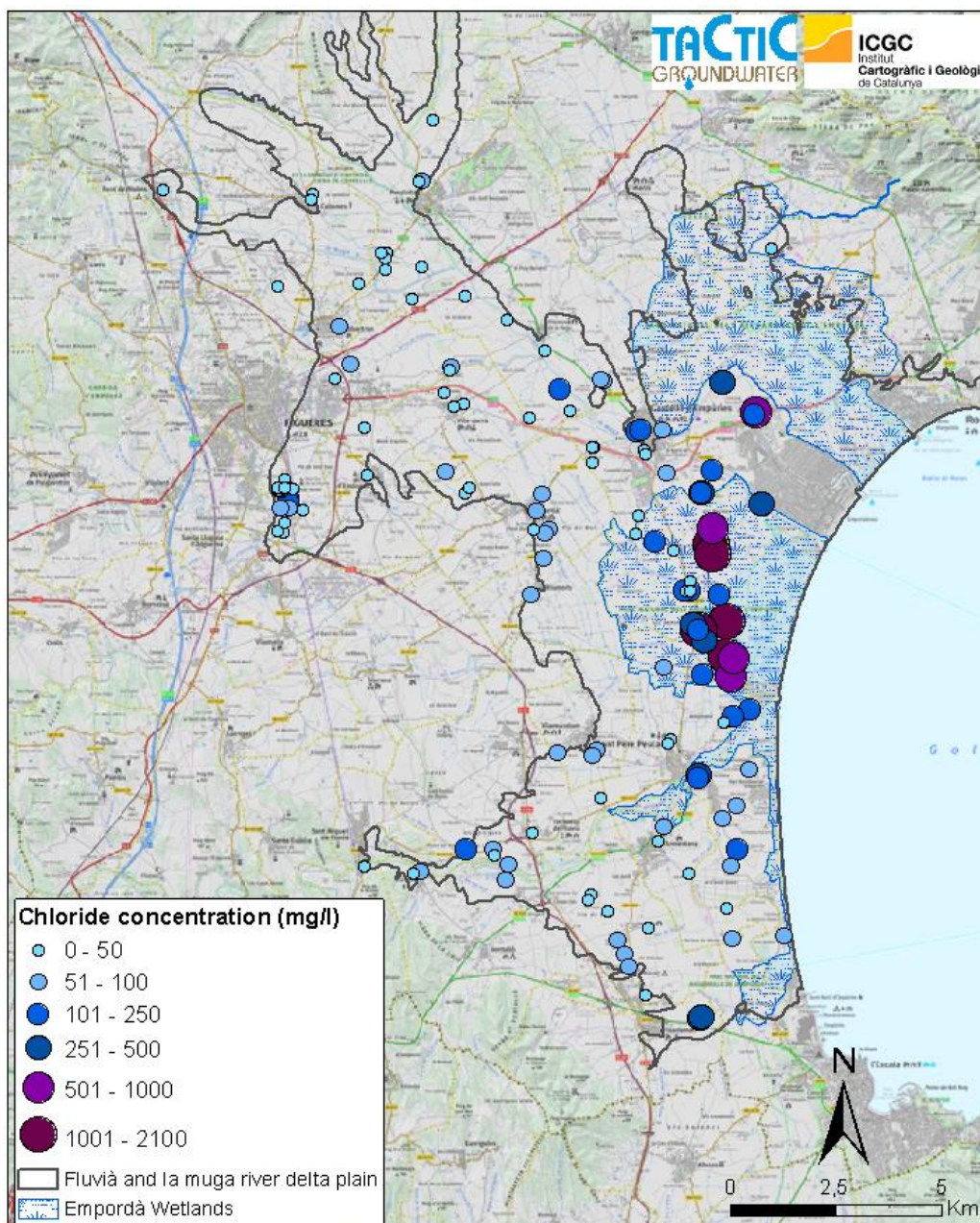
Figure 8: *Chloride concentration median values at Fluvià and la Muga rivers delta plain.*

Chloride concentration in groundwater has been monitored by the Catalan Water Agency at several representative control points between 1995 and 2017 (data available at SDIM-ACA). Taking into account individual samples, chloride concentration in control points located near the coastline registered maximums up to 1500 mg/l and in particular cases up to 3000 mg/l (Figure 9). The number of annual samples per each control point are not enough to determine annual or stational oscillations of the chloride concentration values.

Figure 9. *Chloride concentration in groundwater between 1995 and 2017.*
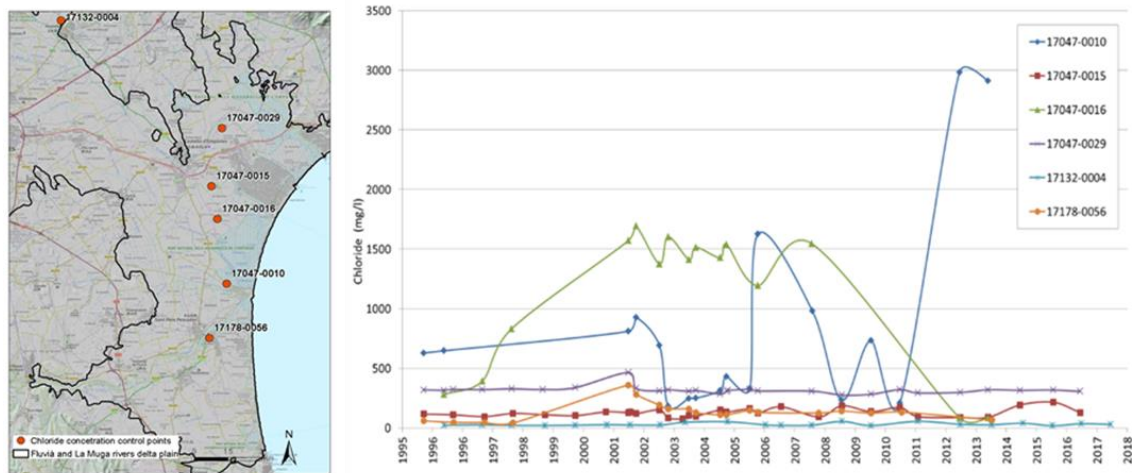
With all the available data, annual chloride concentration maps have been made using GIS interpolation methods (based on an iterative finite difference interpolation technique) to evaluate the evolution of SWI throughout the historical series (Figure 10). The number of available sampling points per year varies depending on the year between 18 and 53. Years in which the data were not enough to apply interpolation methods have been excluded of the SWI status assessment. Finally, 16 maps of chloride concentration were interpolated between 1995 and 2018.
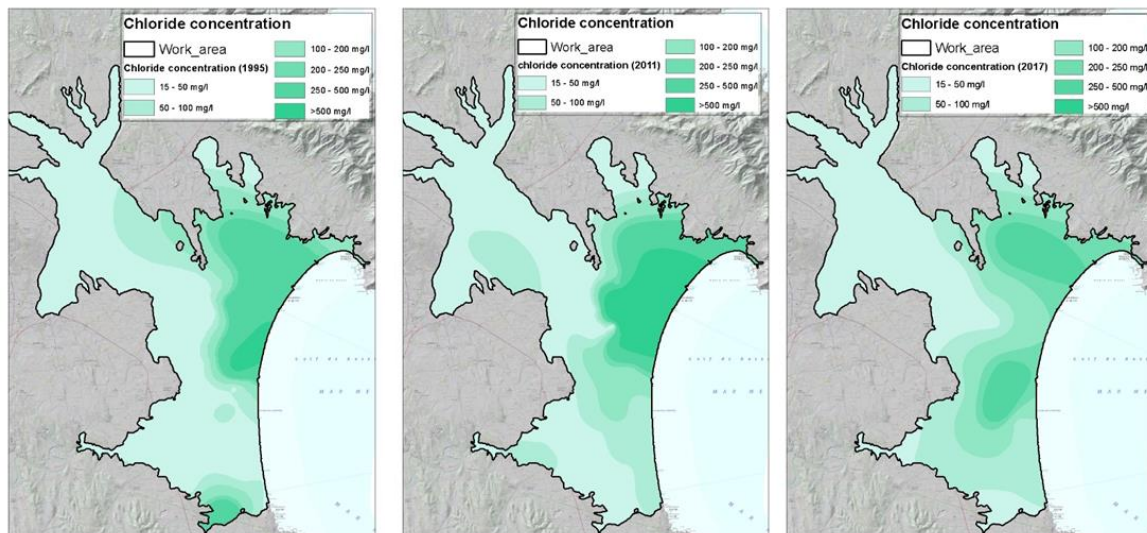
Figure 10: *Example of chloride concentration maps. Annual chloride concentration maps have been created using GIS interpolation methods. The figure shows an example of maps obtained for the years 1995, 2011 and 2017.*

In addition, concentration of other components such HCO_3^- or NO_3 have also been collected. Groundwater geochemistry available analyses indicate that groundwater is mainly Ca-HCO-SO4 type and near the coastline it becomes at certain locations to Cl-Na type. Other chemical elements, such nitrates and ammonium are significantly present as well (ACA, 2005).

3.2 Climate change challenge

According to EEA report, Mediterranean transnational region, including El Golf de Rosas, is facing inevitable consequences of climate change (EEA, 2018). It is projected that temperature will increase, and precipitation rates will decline. Consequently, it is expected that duration and intensity of heatwaves will increase, more frequent droughts will occur, water availability and river flows will decrease. Higher temperatures and lack of water would negatively affect agriculture and overall quality of life. It is expected that due to climate change crop yields would decrease, risk of desertification and fire would increase. Due to changing climate, it is possible that tourism in Mediterranean region would decrease during the summer and would potentially increase during other seasons.
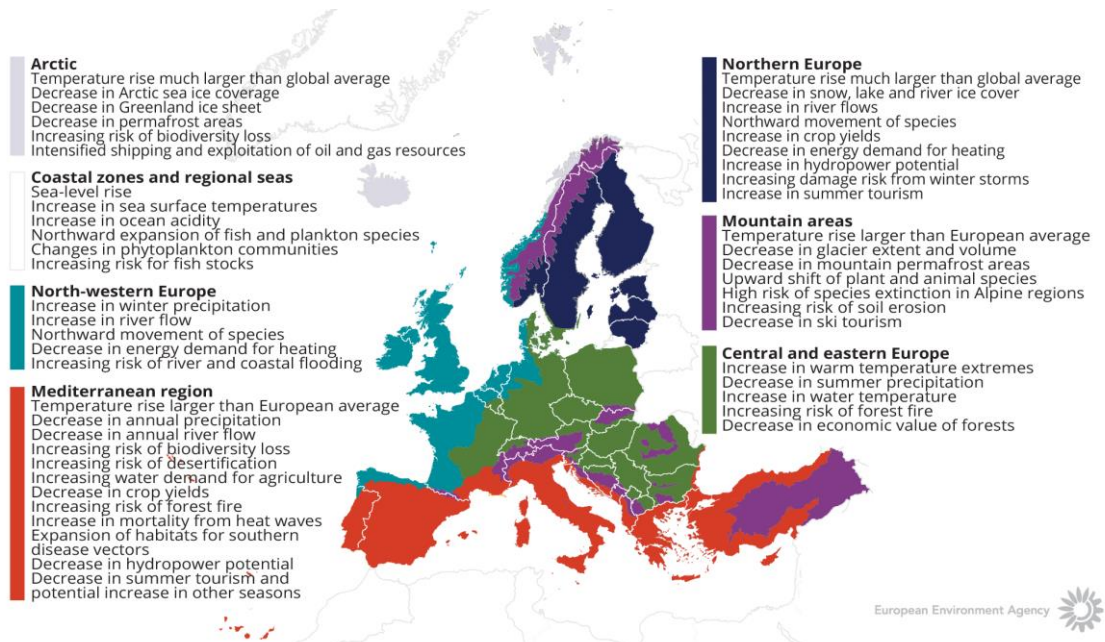

Figure 11: *How is climate expected to change in Europe. The European Environment Agency map.*

4   METHODOLOGY

The present work has been based on the historical evaluation of the SWI status and the GALDIT vulnerability assessment of the Fluvià and La Muga rivers delta plain methods (Baena-Ruiz et al., 2018). No 3D flow and transport hydrogeological model is available, thus simulation of future scenarios of the vulnerability status couldn't be performed in the framework of TACTIC WP5.

In general, both methods aim to calculate the SWI affected area and groundwater volume by considering threshold values. In the SWI status method the Threshold Value (TV) considered is a chloride concentration value based in the Natural Background Level of the aquifer (NBL), whereas for the GALDIT vulnerability assessment the limit between moderate and high vulnerability ranges is the reference TV used.

Time series analysis of the available data and **spatial Interpolation** (based on an iterative finite difference interpolation technique) of groundwater levels and chloride concentration values are the two main tools used on this TACTIC WP5 project for the Catalan pilot area.

4.1   SWI status

4.1.1   Determination of NBL and TV

For the numerical determination of the threshold value for the SWI status assessment, first it is mandatory to determine the chloride Natural Background Level (NBL). Different methods have been used and compared with the maximum chloride acceptable value provided by the Spanish drinking water legislation (RD 140/2003); the BRIDGE method (Müller et al, 2006) and the Walter probability plots method (Walter et al., 2006 and Giuliano & Blarsin, 2014).

4.1.1.1   The BRIDGE method

The "BRIDGE" EU research project (Background Criteria for the Identification of Groundwater Thresholds) was established to develop and test a methodology for derivation of groundwater threshold values to support the development of a common methodology for EU Member States. Based on the preselection of samples by considering several criteria (Müller et al, 2006), it aims first to the determination of the NBL and then determine the corresponding Threshold Value (TV).

The application of that method for the SWI status assessment in the Fluvià and La Muga rivers delta plain, has revealed some limitations regarding the preselection of valid samples to establish the NBL. Main criteria applied for the exclusion of samples (as indicated in the BRIDGE method) have been:

-   Samples with incorrect Ion balance (exceeding 10%)
-   Samples with total $[Na^+]+[Cl^-] > 1000$ mg/l
-   Samples with median nitrate concentrations above 10 mg/l
-   The REDOX conditions criterion has not been applied due to insufficient available data

In order to assure that long time series do not bias results and that all sampling sites contribute equally to the NBL derivation time series at each monitoring point are converted to median values.

The application of this criterion implies a reduction from 633 samples to 108 (more than 80%) and the reduction from 152 points with available data to 58 (almost 40%). Furthermore, the study area has characteristics that raise doubts about the suitability of these criteria:

- The pilot area is a zone with extensive and intense agricultural activity and mainly source of nitrate are the fertilizers.

- There are analysis with nitrate concentration above 10 mg/l in non-affected (SWI) area and conversely analysis with concentrations below 10 mg/l in affected (SWI) area.

With the final available and selected samples, the BRIDGE method provides a chloride NBL of 148.56 mg/l for the 90th percentile and a chloride NBL of 336 mg/l for the 97.7th percentile. These results are presumed **to be excessively high**, since the limit for the [Cl⁻] in the legislation regarding drinking water is 250 mg/l and upwards and in areas clearly not affected by SWI, the chloride concentrations in the aquifer system are below 50 mg/l.

4.1.1.2   Estimation of NBL using Probability plots (Walter et al., 2006; Giuliano & Blarsin, 2014)

Alternatively, another method has been tested. Proposed by Walter et al, (2011) it is focused on the determination of the NBL by applying an iterative statistical process using probability plots. This method seeks to eliminate extreme values (which could be considered as values affected by processes that modify natural conditions). The starting point is all the available samples.

To ensure that the time series at the same sampling point do not bias the results and that all sampling sites contribute equally to the NBL calculation, these time series are converted to median values.

The initial assumption is that there are two different families of samples: natural and affected values (for instance by SWI). This assumption must be checked by doing the normal and lognormal probability plots distribution graphics (Figure 12).
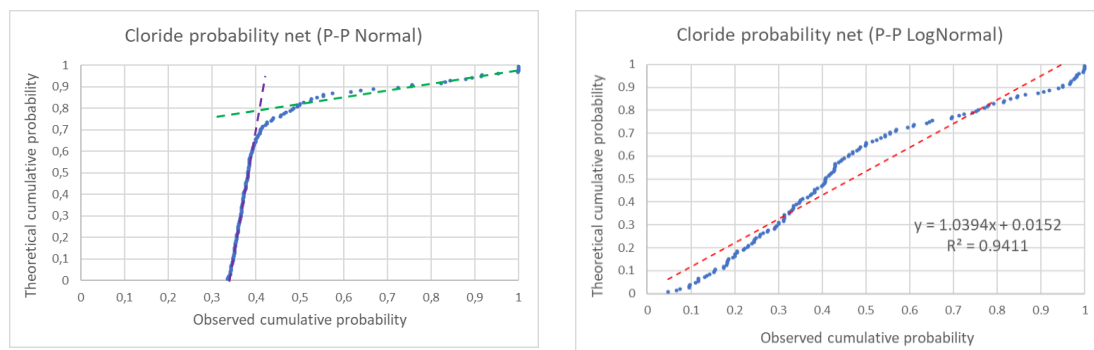

Figure 12: *Statistical distribution of chloride values from groundwater samples at Fluvià and La Muga rivers delta plain. Normal and Lognormal probability plots.*

Once this assumption has been checked, the iterative process could be applied. For the first iterative process, the 90th percentile is calculated. Data that exceed this value are excluded from the next step. For the second and consecutive steps, in which the 90th percentile is recalculated to exclude samples with a higher value. The iterative process stops when the distribution of the data is normalized. The result of the NBL is obtained from the samples that have remained (selected) by calculating the median of the studied parameter.

For the case study in The Fluvià and the Muga river delta Plain, normal distribution of the data has been achieved after 5 iterations by means of the Shapiro-Wilk test. Histograms of frequency and cumulative probability are shown on Figure 13. At this point, 99 sample points remain from the initial 150 available. The Chloride NBL ranges from 10 mg/l to 61 mg/l. A value of 37 mg/l and a value of 55 mg/l are obtained by calculating the median and he 90th percentile respectively.

The NBL value of chloride obtained by this method, is presumed to be much closer to the natural conditions of the aquifer system not affected by SWI. From that NBL value obtained, a TV of **200 mg/l** has been derived following the BRIDGE methodology.
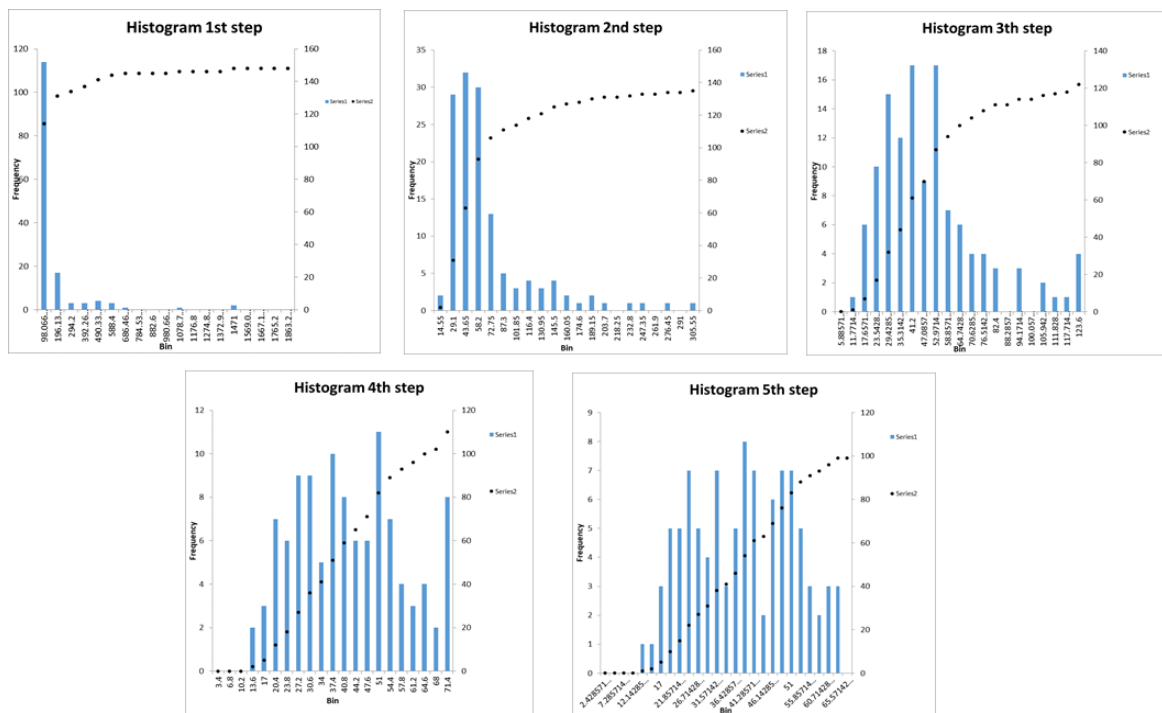
Figure 13: *Iterative process using probability plots (Walter et al, 2011). Iterative elimination of outliers (chloride concentration values above the 90th percentile is considered outliers in each iteration).*

4.1.2   Area and volume determination of the aquifer system affected by SWI

Once the threshold value has been established (200 mg/l) it has been applied to the chloride concentration interpolated maps to determine the area and volume of the affected aquifer (Figure 14). The aquifer thickness distribution map and the representative groundwater level

surface (see chapters 3.1.2 and 3.1.5) have been used in the SWI status assessment. A representative value of porosity of 0,05 for the overall aquifer system was considered.

From these values, the methodology has been applied to calculate the MaRT index, the resilience, the trend and the conceptual 2D cross sections as proposed in the **SWI status method** (Baena-Ruiz et al., 2018) and in the Deliverable 5.2.
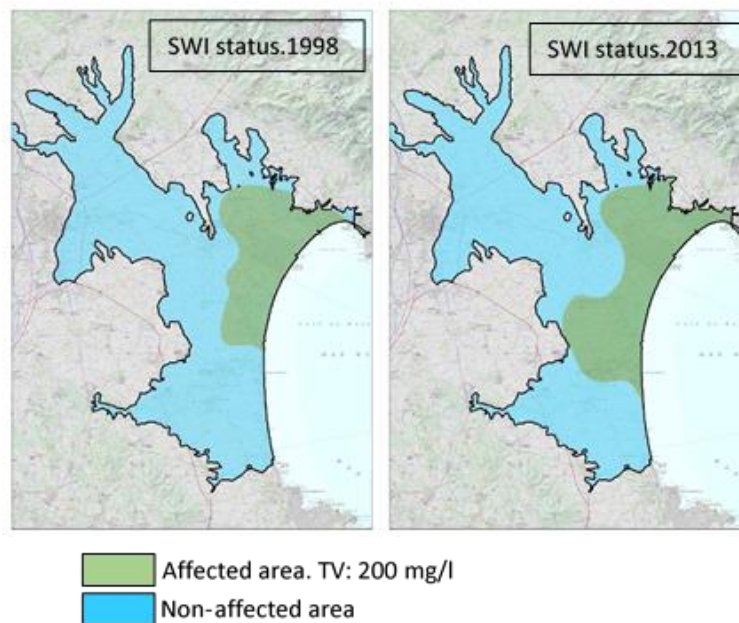
SWI Status. TV: 200 mg/l

Affected area. TV: 200 mg/l
Non-affected area

Figure 14: Examples of *SWI status maps of the years 1998 and 2013. The estimated groundwater volume by SWI is 29% and 42% respectively.*

4.2   GALDIT vulnerability assessment

Similarly, work has been done to apply the SWI vulnerability assessment method. Annual maps (from 1995 to 1998, 2002 to 2006, 2008 to 2011, 2013, 2014 and 2017) have been made following the GALDIT method (Chachadi & Lobo-Ferreira, 2001) for calculating vulnerability to SWI in the Fluvià and la Muga rivers delta plain.

For the application of the GALDIT method the type of aquifer considered ("G" parameter) was confined for the area where the lowermost aquifer is located and unconfined for the rest of the area. The hydraulic conductivity parameter of the aquifer system ("A" parameter) was defined based on the hydrogeological map of Catalonia at 1:25.000 scale (ICGC, 2015). Regarding the impact of existing status of SWI ("I" parameter) not all the samples collected with chloride concentrations had also bicarbonates values. Thus, a correlation was made between the available values of the HCO_3^-/Cl^- ratio and the Cl^- concentration values in order to map the "I" parameter.

GALDIT maps were obtained for the same years as for the SWI status method (in total 16 maps) (Figure 15). The limit between the high and the moderate vulnerability were established as the TV after considering that, based on the knowledge of the area, there are large areas characterized with moderate vulnerability that are far from the known affected areas.
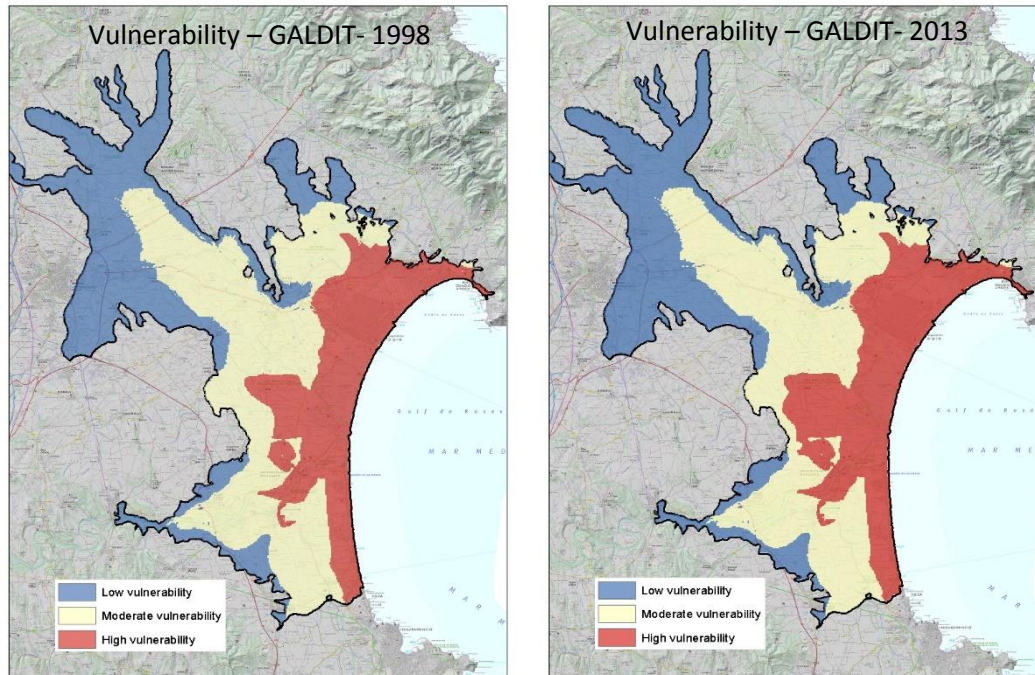

Figure 15: Example of *vulnerability maps (GALDIT method) for the years 1995 and 2013 with minimum differences of the spatial distribution of each vulnerability classes.*

From the considered threshold, affected areas and volumes have been calculated, and represented in the conceptual 2D cross sections.

5 RESULTS AND CONCLUSIONS

5.1 SWI method results: SWI status and vulnerability

From the 16 maps of SWI status and the 16 GALDIT vulnerability maps and taking into account the TV considered respectively (200 mg/l for the SWI status method and the high vulnerability class for the GALDIT vulnerability assessment method), the evolution of the total groundwater volume affected by SWI from 1995 to 2017 is shown in Figure 16 and Figure 17.

For the SWI status method, the affected groundwater volume of the aquifer system ranges between 18% and 42% with a mean value of 32% (Figure 16) whereas for the GALDIT vulnerability assessment method the obtained results show less variability in the total volume affected by SWI which ranges between 45 – 48% probably because most of the parameters considered in the GALDIT method are intrinsic of the aquifer system and therefore constant over time.
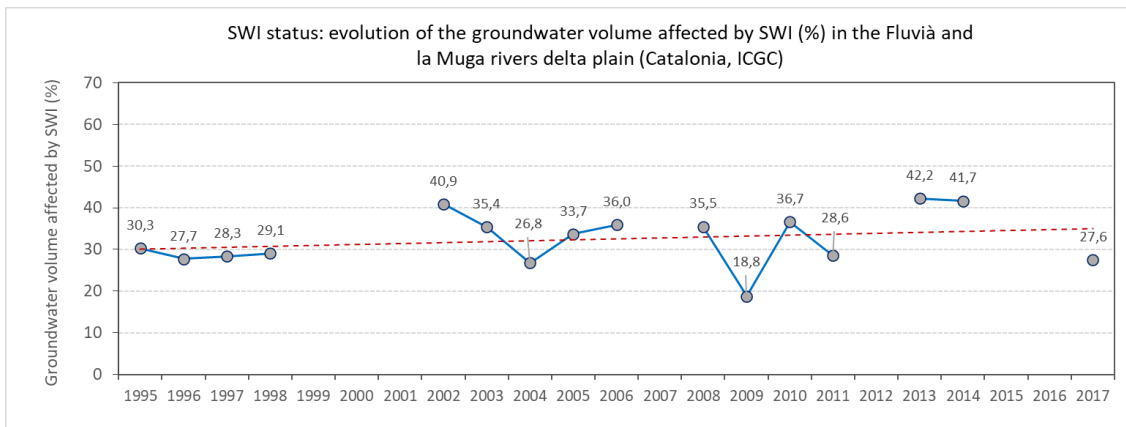

Figure 16: *Volume of the aquifer system affected by SWI (%) applying the SWI status method with a TV of 200 mg/l of chloride concentration.*
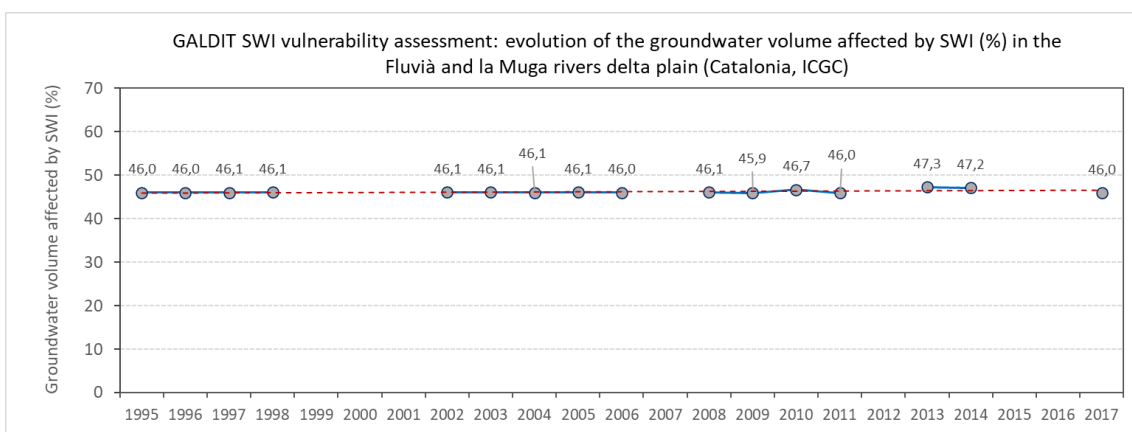

Figure 17: *Volume of the aquifer system affected by SWI applying the GALDIT vulnerability assessment method and considering the area with high vulnerability to SWI.*

These values can be considered high, since the extension of the aquifer system is large, and the maximum depth of the aquifer system is coincident with the SWI affected area. The affected volume varies depending on the year, but the trend shown by the available historical time series is slightly upward (especially considering the results obtained with the SWI status method). Even so, it is possible to establish some areas in which the SWI is permanent. As expected, in the area close to the town of Roses where the Empuriabrava and Santa Margarida inland harbor is located the SWI affectation could be considered permanent whereas the central area and south area of the delta plain (where the Natural Park of the Empordà Wetlands is located) show a more irregular affectation over time depending on the year considered. Furthermore, it can be confirmed that the inland areas of the aquifer have not been affected by SWI and can be considered as non-affected or non-vulnerable areas.

5.2   SWI method results: 2D conceptual cross-sections

In order to give a graphic idea of the groundwater volume affected by SWI, the volume and area data have been represented in conceptual 2D cross sections. The method proposed in sections 2.1.2 and 2.2.2 of deliverable 5.2 has been followed for this purpose.

The considered threshold of 200 mg/l of chloride concentration has been applied in the case of SWI status, and that of high vulnerability in the case of vulnerability to SWI. Conceptual 2D cross sections have been carried out for the year 2002, and for the mean of the entire historical series available both for the evaluation of the SWI status and vulnerability.

The results show, in the same way as previously explained, that an important part of the aquifer system in its area closest to the sea is affected by SWI. It must also be taken into account that the areas furthest from the coastline have not been affected by SWI in the entire historical series. Therefore, the proportion of volume affected would be even higher considering only the potentially affected areas.
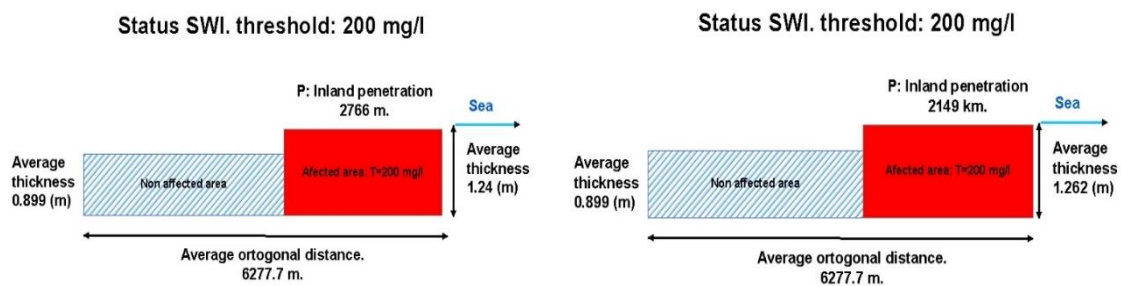

Figure 18: *2D conceptual cross-sections SWI status. Historical results in 2002 (left) and mean values for the period 1995 - 2017 (right) (Vertical exaggeration scale x1000).*
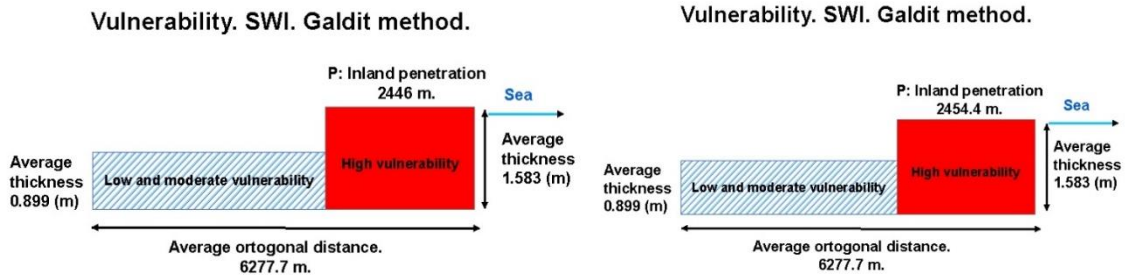
Figure 19: *2D conceptual cross-sections. Vulnerability. Historical results in 2002 (left) and mean values for the period 1995 - 2017 (right) (Vertical exaggeration scale x1000).*

5.3   SWI method results: Lumped indices Ma and L-GALDIT.

Continuing with the application of the proposed methodology, the steps described in sections 2.1.3 and 2.2.3 of deliverable 5.2 have been applied to obtain the Ma and L-GALDIT indices for the SWI status method and the GALDIT vulnerability assessment method respectively (Baena-Ruiz et al., 2018).

The Ma index provides information about the intensity of SWI (Figure 20) whereas de L-GALDIT index assess the overall vulnerability of the aquifer (Figure 21).

Figure 20: *Time series of the Ma index for the period 1995 to 2017. It is observed high variability in the Ma values, but the trend considering the entire period is slightly upward.*
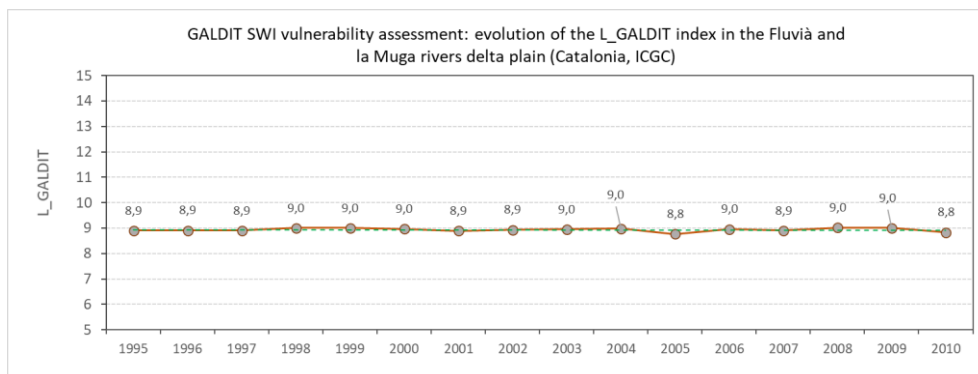
Figure 21: *Time series of the L-GALDIT index for the period 1995-2017. It is observed that the L-GALDIT doesn't present the same variability as the Ma values and there is no detectable trend considering the entire period.*

As shown by the volume of the aquifer system affected by SWI (%) applying the SWI status method (Figure 16), the Ma index evolution (which represents the i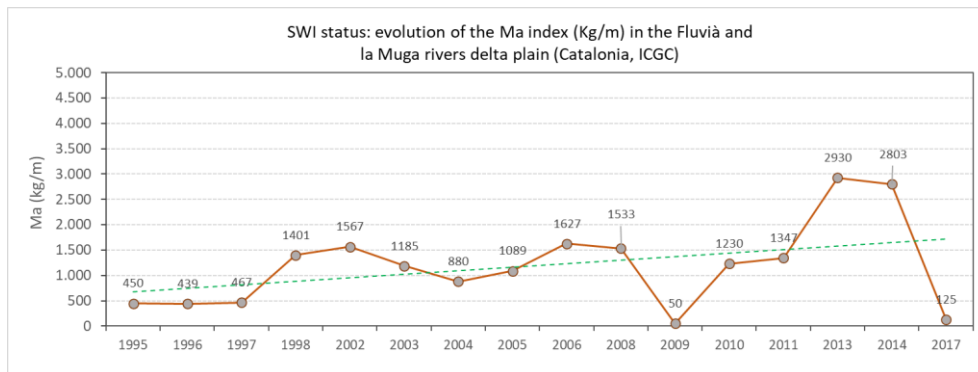ntensity of the SWI) is also coherent with the hypothesis of a SWI worsening in the area in the last 25 years. It has to be mentioned that the results could be influenced by the distribution and temporal frequency of the available samples. Even though, the obtained results give a good overview of the evolution of the SWI in the area.

On the other hand, the L-GALDIT is constant over time due to the less variability on the time series vulnerability assessment. As mentioned before, most of the GALDIT vulnerability parameters are intrinsic of the aquifer system, so permanent over time. The use of a representative groundwater table map and the low weight of the "I" parameter (which has been calculated annually) produce low variability in the vulnerability maps and consequently in the L-GALDIT index values.

These are very remarkable conclusions, and they can be considered the kickoff to go further in the study of the SWI status of the Fluvià and la Muga river delta plain by means of a density-dependent 3D model to simulate future scenarios related with the climate change and to obtain better and more accurate outcomes.

6   REFERENCES

Agència Catalana de l'Aigua (ACA), 2005. Area Fluviodeltaica del Fluvià i La Muga (401). Informe Hidrogeològic, 2005. Internal document (non published).

Baena-Ruiz, L, Pulido-Velàzquez, D, Collados-Lara, AJ. et al. Water Resources Management volume 32, pages2681–2700(2018). https://doi.org/10.1007/s11269-018-1952-2

Chachadi, A.G. and Lobo-Ferreira, J.P. (2001) Sea Water Intrusion Vulnerability Mapping of Aquifers Using GALDIT Method. Proceedings of the Workshop on Modelling in Hydrogeology, Anna University, Chennai, 143-156.

Centre de Recerca i Aplicacions Forestals (CREAF), 2009. Land Cover Map of Catalonia. 4TH edition. Available at Land Cover Map of Catalonia | CREAF.

Giuliano, M.J. & Blarasin, M.T. (2014). Hidrogeoquímica y estimación del fondo natural de nitratos del agua subterránea en un agroecosistema del pedemonte de la sierra de Comechingones. Córdoba (Argentina). Revista de la Asociación Geológica Argentina 71 (3): 378 - 392 (2014)

Hinsby, K. et al (2008). European case studies supporting the derivation of natural background levels and groundwater threshold values for the protection of dependent ecosystems and human health. September 2008. Science of The Total Environment 401(1-3):1-20. DOI: 10.1016/j.scitotenv.2008.03.018.

ICGC, 2015. Geotreball V. Mapa hidrogeològic de Catalunya 1:25.000. 78-22 and 78-23. Available at *http://www.icgc.cat/en/Public-Administration-and-Enterprises/Downloads/Geological-and-geothematic-cartography/Hydrogeological-cartography/GT-V.-Hydrogeological-map-1-25-000*

Kottek, M., J. Grieser, C. Beck, B. Rudolf, and F. Rubel (2006). *World Map of the Köppen-Geiger climate classification updated*. Meteorol. Z., **15**, 259-263. DOI: 10.1127/0941-2948/2006/0130. Retrieved from: *http://koeppen-geiger.vu-wien.ac.at/present.htm*

Müller et al. (2006). BRIDGE. Background criteria for the identification off roundwater thresholds. D18: FINAL PROPOSAL FOR A METHODOLOGY TO SET UP GROUNDWATER TRESHOLD VALUES IN EUROPE. Available at D18 BRIDGE Final Proposal for a methodology to set Groundw-205 (europa.eu)

RAMSAR Convention Bureau (1990) Directory of Wetlands of International Importance Sites Designated for the List of Wetlands of International Importance. http://www.ramsar.org/

SDIM-ACA. Catalan Water Agency database. Available at http://aca-web.gencat.cat/sdim21/

Walter, T. et al., (2006). An automated Excel-tool to determine geogenic background values using a probability net. Workshop on Groundwater Bodies in Europe and Adjacent Countries.

Berlín. October 25 - 26. Available at
https://www.bgr.bund.de/EN/Themen/Wasser/Veranstaltungen/workshop_gwbodies_2005/Poster_06_Germany_LUA_Walter_pdf.html

Walter, T. et al., (2011). Determining Natural Background Values with Probability Plots. Groundwater Quality Sustainability, Edition: IAH Selected Papers on Hydrogeology, Chapter: Chapter 26, Publisher: CRC Press, Editors: Grzegorz Malina, pp.331-342. DOI: 10.1201/b12715-32.

Deliverable 5.3

PILOT DESCRIPTION AND ASSESSMENT

Hull & East Riding chalk aquifer
(United Kingdom)

Authors and affiliation:

Vasileios Christelis, Andrew Hughes

British Geological Survey (BGS)

Establishing the European Geological Surveys Research Area to deliver a Geological Service for Europe

Deliverable Data	
Deliverable number	D5.3
Dissemination level	Public
Deliverable name	Pilots description and assessment report for saline intrusion status
Work package	WP5
Lead WP	IGME
Deliverable status	
Version	Version 2
Date	17/3/2021

[This page has intentionally been left blank]

LIST OF ABBREVIATIONS & ACRONYMS

TABLE OF CONTENTS

1 EXECUTIVE SUMMARY

Pilot name	Hull and East Riding	
Country	United Kingdom	
EU-region	North-western Europe	
Area (km^2)	2040	
Aquifer geology and type classification	Cretaceous Chalk (dual porosity aquifer)	
Primary water usage	Drinking water / Industry/ Irrigation	
Main climate change issues	Slight increase in winter and summer recharge due to rainfall increase with a risk of groundwater flooding. However, future temperature predictions indicate a higher increase in evapotranspiration compared to the rainfall increase.	
Models and methods used	Index methodologies to assess aquifer vulnerability to saline intrusion	
Key stakeholders	Government. Research institutes. Water companies.	
Contact person	British Geological Survey. (Vasileios Christelis vc@bgs.ac.uk, Andrew Hughes aghug@bgs.ac.uk)	

Seawater intrusion is not generally reported as a major issue in the UK, despite the long coastline length. Nevertheless, a screening approach based on the Catchment Data Explorer database (https://environment.data.gov.uk/catchment-planning/), developed by the Environment Agency for the implementation of the Water Framework Directive (2000/60/EC) and on Water Quality Archive (https://environment.data.gov.uk/water-quality/view/landing), was employed to identify specific groundwater bodies prone to seawater intrusion problems.

Following the above procedure, the Hull and East Riding groundwater body, which belongs to East Yorkshire Chalk formation, was identified as an appropriate pilot area. The Hull and East Riding groundwater body extends over an area of 2040 km^2. The hydrogeological conditions are mainly unconfined although may vary to semiconfined or confined in certain parts of the aquifer. Transmissivity values in the area exhibit a large spatial variation and the groundwater system receives most of its recharge from rainfall. The area has a coastline length of approximately 80 km.

Although saline intrusion affects the background chemistry in the Yorkshire Chalk, it is believed that the saline groundwater in this area is rather an old stable body of water according to previous studies (University of Birmingham, 1978, Smedley et al., 2004). In overall, the current groundwater abstraction schemes in the area do not seem to have an impact on the existing saline front as only a small percent of total recharge is being abstracted and further monitoring suggests that the saline front remained static despite the changes in the mixing zone between freshwater and saline water.

However, a model of seawater intrusion has not been previously developed in the area while the identification of those parts of the present aquifer system that might be more prone to saline intrusion could provide additional information about the general status. Given that existing information for the area under study suggests that the saline front is generally static over long periods of time, the use of sharp interface models was selected as an appropriate modelling approach. Furthermore, due to the large spatial scale of this pilot area, the sharp interface assumption provided a computationally efficient model to assess the seawater intrusion status without additional requirements for field data collection.

Different modelling scenarios were investigated based on historical and future climate recharge variations that were averaged over long time periods. The results obtained from the simulation with the sharp interface model are in good agreement with the existing known status of saline intrusion in the area. The simulation outputs also showed that the location of the freshwater/saltwater interface remains mainly unaffected in several parts of the aquifer, despite the different distribution of applied recharge. However, it was observed that for some parts of the aquifer system the location of the simulated interfaces may vary up to 700 meters, depending on the recharge scenario. In overall though, small percentage differences were obtained from the calculation of the total freshwater area for each recharge scenario. This implies that at least for the future climate scenarios investigated here, no significant changes are expected to the available freshwater area, based on the results from the sharp interface model.

Furthermore, by using the widely applied GALDIT vulnerability method an effort was made to identify the most vulnerable parts of the Hull and East Riding groundwater body to saline intrusion. Based on this preliminary investigation, a moderate to high vulnerability was observed in the upper north-eastern part of the aquifer near Bridlington and close to the Humber estuary near Kingston Upon Hull.

Future investigations in the area using more advanced seawater intrusion models, such as variable density flow and solute transport models, along with further analysis of existing data and use of updated versions of the GALDIT method, may provide additional information for possible saline intrusion problems. Nevertheless, the sharp interface model developed for this area and the use of the GALDIT vulnerability method delivered a practical computational tool to assess the status of seawater intrusion in a systematic and efficient manner. These modelling tools could provide further assistance to deal with uncertainty aspects and groundwater management practices in the area regarding the problems of saline intrusion.

2   INTRODUCTION

Climate change (CC) already have widespread and significant impacts in Europe, which is expected to increase in the future. Groundwater plays a vital role for the land phase of the freshwater cycle and has the capability of buffering or enhancing the impact from extreme climate events causing droughts or floods, depending on the subsurface properties and the status of the system (dry/wet) prior to the climate event. Understanding and taking the hydrogeology into account is therefore essential in the assessment of climate change impacts. Providing harmonised results and products across Europe is further vital for supporting stakeholders, decision makers and EU policies makers.

The Geological Survey Organisations (GSOs) in Europe compile the necessary data and knowledge of the groundwater systems across Europe. In order to enhance the utilisation of these data and knowledge of the subsurface system in CC impact assessments the GSOs, in the framework of GeoERA, has established the project "Tools for Assessment of ClimaTe change ImpacT on Groundwater and Adaptation Strategies – TACTIC". By collaboration among the involved partners, TACTIC aims to enhance and harmonise CC impact assessments and identification and analyses of potential adaptation strategies.

TACTIC is centred around 40 pilot studies covering a variety of CC challenges as well as different hydrogeological settings and different management systems found in Europe. Knowledge and experiences from the pilots will be synthesised and provide a basis for the development of an infra structure on CC impact assessments and adaptation strategies. The final projects results will be made available through the common GeoERA Information Platform (http://www.europe-geology.eu).

The present document reports the TACTIC activities regarding the Hull and East Riding groundwater body in UK. The pilot area is part of the East Yorkshire Chalk aquifer. The main land use activities in the area is agriculture, animal farming and some manufacturing and food processing industries. Average annual rainfall in the area ranges somewhere between 600 mm to over 750 mm. The hydrogeological conditions in the East Yorkshire Chalk are mainly unconfined although they may vary to semiconfined or confined in certain parts of the aquifer. Different degrees of fracturing and matrix properties exist which form a complex geological environment of mainly two porosity regimes with values greater or less than 30%. Transmissivity values in the area exhibit a large spatial variation ranging from 100 m^2d^{-1} to values greater than 10000 m^2d^{-1}. The thickness of unsaturated zone in the Yorkshire Chalk may vary from less than 10 m to over 120 m in certain regions. The groundwater system receives most of its recharge from rainfall during the first quarter of the year. The length of the coastline in the Hull and East Riding groundwater body is approximately 80 km.

The overall objective of this study is to assess the status of seawater intrusion in the Hull and East Riding groundwater system given available field data as well as via modelling and mapping tools which are considered suitable for the large spatial scale of this pilot area. As groundwater management schemes over the last 30-40 years have controlled further encroachment of seawater in the area, focus is given here on modelling the impact that different recharge scenarios may have on the extent of seawater intrusion. Thus, long-term averaged recharge periods either based on historical data or future climate scenarios are employed to simulate any

changes in the status of seawater intrusion in the area. The information generated through this investigation using mathematical models of seawater intrusion could be usefull to identify those parts of the aquifer that might be more vulnerable to seawater intrusion problems.

3 PILOT AREA

Seawater intrusion (SWI) is not reported as a major issue for UK coastal aquifers, due to the existing hydrological and geological conditions, as well as, due to groundwater abstraction policies imposed since 1970s (Environment Agency, 2006). However, by using a systematic approach, specific groundwater bodies prone to SWI problems were identified along the UK coastline. This screening approach was based on the Catchment Data Explorer database (https://environment.data.gov.uk/catchment-planning/), developed by the Environment Agency for the implementation of the Water Framework Directive (2000/60/EC), and it was used to retrieve information about the status of groundwater bodies in the UK. Furthermore, the Water Quality Archive (https://environment.data.gov.uk/water-quality/view/landing) was also utilized as a repository of water quality measurements around England for coastal and estuarine waters, rivers, lakes, ponds, canals and groundwater. Water quality measurements were available for the years 2000-2018. Both platforms provide free access to the relevant data. Based on quantitative and qualitative criteria five groundwater bodies were initially selected as potential pilot areas. The associated shapefiles of each groundwater body were then utilized to estimate the availability of monitoring points for chemical components related to salinity, as well as, of borehole data.

Following the above procedure, Hull and East Riding groundwater body, which belongs to East Yorkshire Chalk formation, was identified as an appropriate pilot area given the availability of groundwater quality and borehole data, the coastline length and the existence of a fully developed groundwater flow model by Environment Agency. The East Yorkshire Chalk constitutes a significant source of groundwater supply for the development of industrial and agricultural activities in the area, as well as, for drinking purposes (Gale and Rutter, 2006). Over the past decades, the saline groundwater in the area was mostly attributed to SWI from the Humber Estuary, as a result of uncontrolled pumping (Foster et al., 1976). Increased Cl concentrations in pumped groundwater support this assumption, however, the saline front in the area is considered stable due to groundwater management practices (Chadha, 1986). By using the methodologies proposed in this work package, our intention is to characterize the status of the selected pilot area in terms of SWI and compare with the existing known conditions.

3.1 Site description and data

3.1.1 Location of the pilot area and SWI problems

The Hull and East Riding groundwater body is part of East Yorkshire Chalk aquifer that extends from Flamborough Head southwards to the Humber Estuary. The length of the coastline is approximately 80 km and the area of the groundwater body is estimated to 1967.32 km^2. The major towns are situated on the coast of Humber and North Sea where the main SWI problems exist due to over-abstraction. Of particular interest, is the coastal aquifer part in the Hull area along the Humber estuary. In the past, over-exploitation of groundwater, mainly from industrial boreholes close to the estuary, resulted in increased salinity. Detailed studies in the early 1970s investigated the potential to control SWI along the Humber Estuary in the Yorkshire Chalk aquifer (Foster and Milton, 1976). A numerical flow model was also developed in the mid-1990s, which covered the whole of the Yorkshire Chalk, and a more recent numerical flow model was also built (ESI 2013) with updated climate and hydrogeological information.

3.1.2 Topography

The East Yorkshire Chalk topography includes impressive cliffs in the coast round Flamborough that exceed 100 m in height, while ground surface elevations in the overall area range from zero to approximately 250 m OD as shown below in Figure 1.
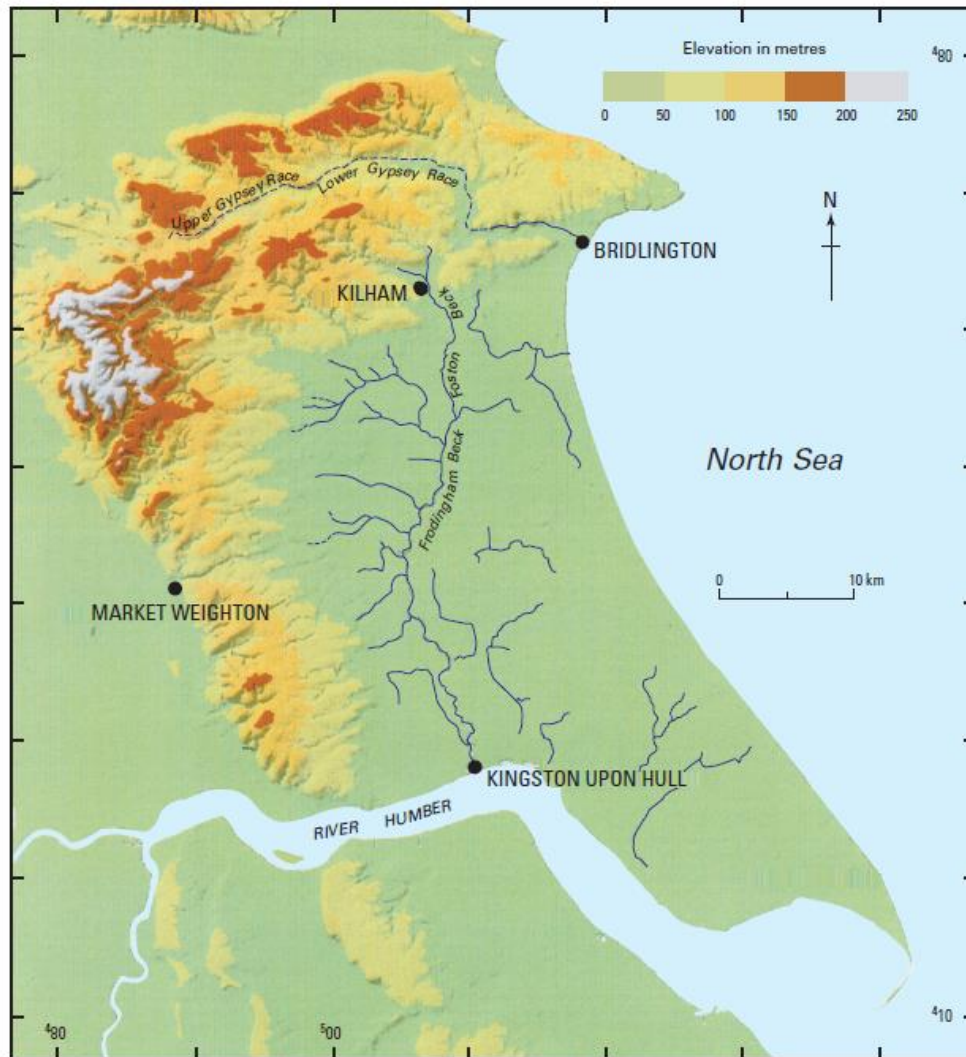
Figure 1. Topography map over the East Yorkshire Chalk (Gale and Rutter, 2006)

The Chalk is buried beneath Quaternary deposits and Holocene coastal and marsh sediments. A network of dry valleys exists across the Wolds and there is little surface drainage on the outcrop. Significant flows occur only in the Gypsey Race along the Great Wold Valley. When groundwater levels are high enough, the Gypsey Race runs along the entire length of the valley while at times of lower groundwater level the flow is increasingly intermittent. The entire Wold Valley becomes

dry in the late summer or in extended periods of drought. Springs rise in the lower reaches of the dry valleys and the tributaries of the River Hull are formed due to flow over the glacial drift.
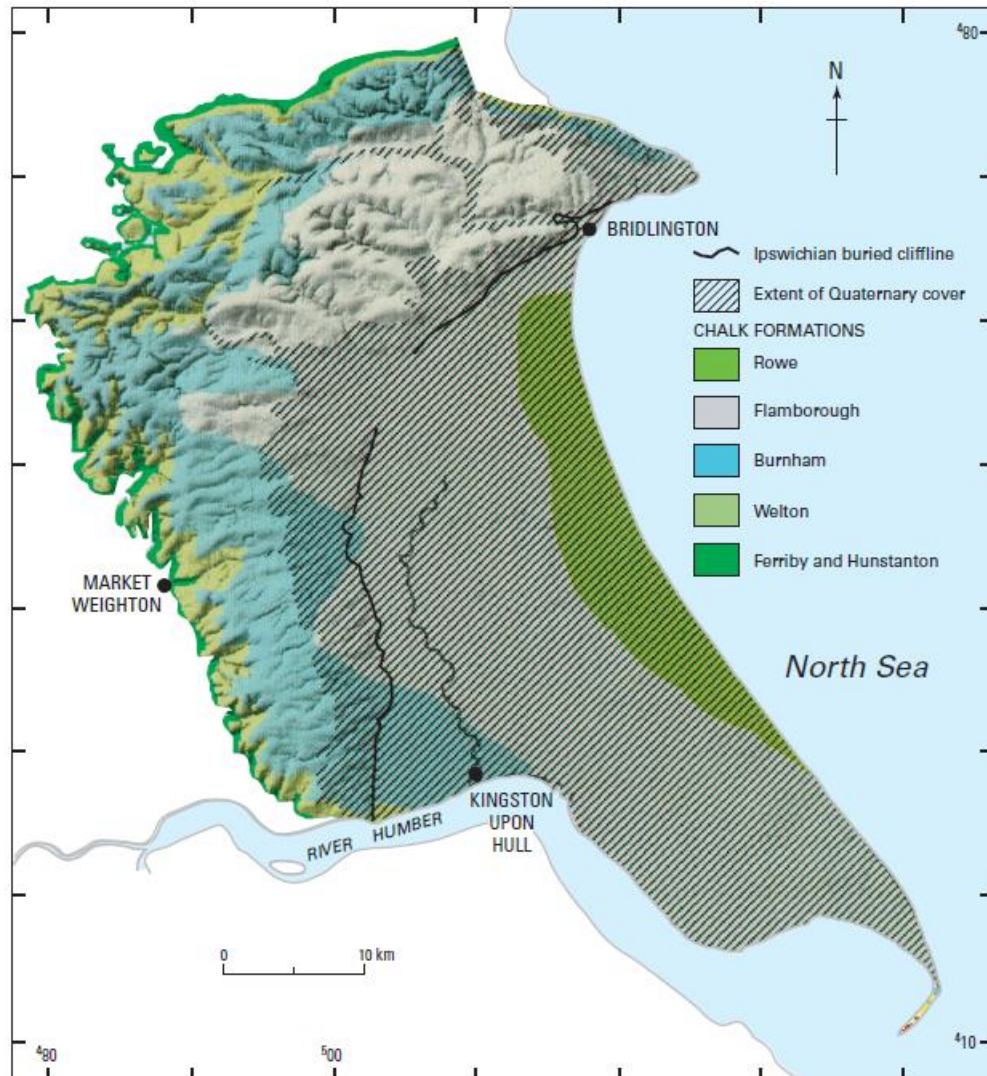
Figure 2. Geological map for the East Yorkshire Chalk (Gale and Rutter, 2006)

3.1.3   Land use

The main land use activity in the area is agriculture, focusing on arable production such as wheat and barley. Grassland comprises about 15% of arable land, oilseed rape (7%) the remainder being sugar beet, potatoes, vegetables, peas and beans. Set-aside land amounts to some 10% of the arable land cover in the Etton and North Newbald catchments. Animal farming is also important, particularly in parts of the upland Wolds where the terrain is steeper. Manufacturing is mostly related to those areas where urban centres exist, such as Hull, with food processing industry being the dominant activity. The various land use activities are depicted in Figure 3.
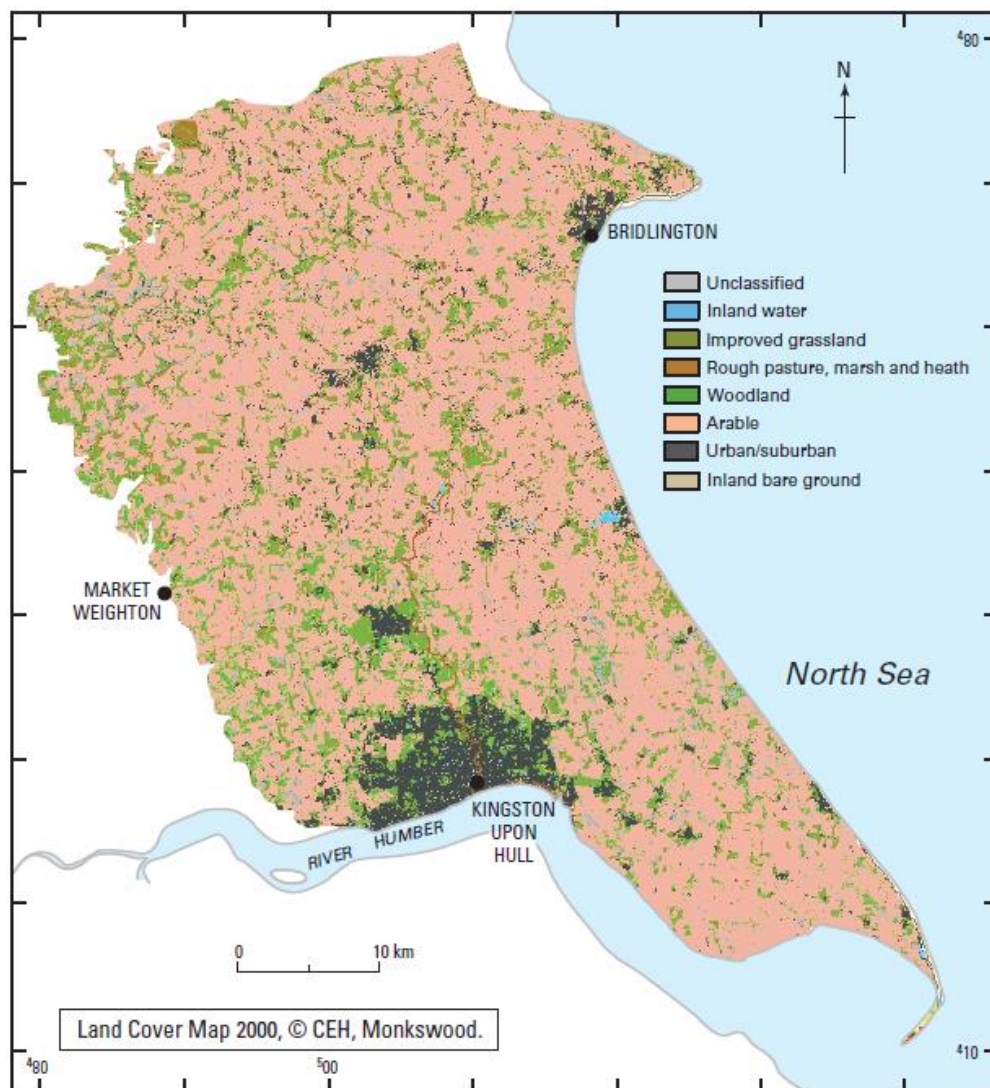
Figure 3. Map of land use over the East Yorkshire Chalk (Gale and Rutter, 2006)

3.1.4   Rainfall

Average annual rainfall in the area ranges from below 600 mm on the low-lying Holderness area to over 750 mm over the highest parts of the Wolds (Figure 4). Daily rainfall raster data (1 × 1 km) are available from the Centre for Ecology and Hydrology (CEH). Spatially distributed daily rainfall data are available starting from 1961 to 2016 (CEH). Projected (future) values of rainfall data are also available by the work of UKCP09 (Prudhomme et al., 2012; Murphy et al, 2007; Jenkins et al., 2009; Murphy et al, 2009).
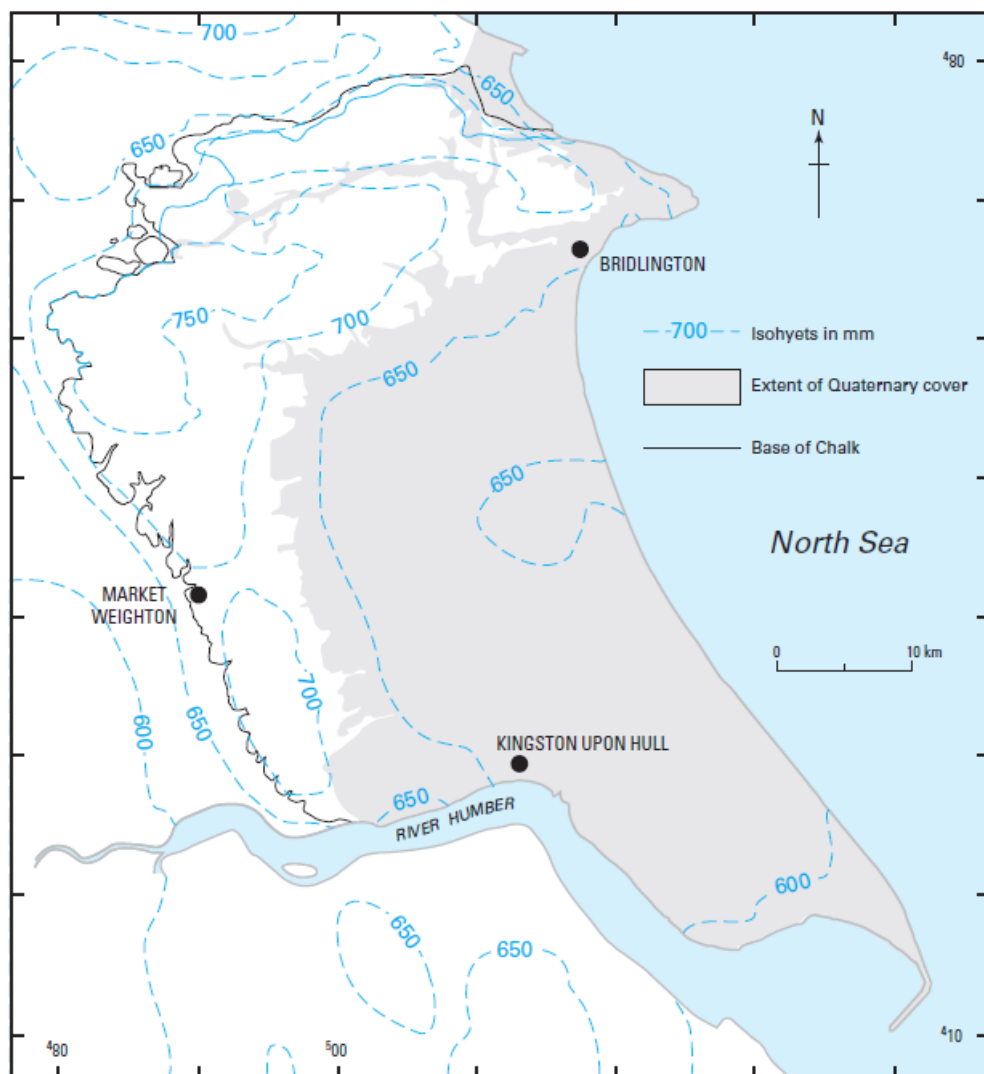
Figure 4. Spatial distribution of rainfall in the East Yorkshire Chalk (Gale and Rutter, 2006)

3.1.5 Potential evaporation

The annual potential evapotranspiration (PE) in the pilot area exhibits an average of approximately 600 mm. Monthly PE raster datasets (40 × 40 km) are available through the Met Office Rainfall and Evaporation Calculation System (MORECS), from the Met Office of the UK (Hough and Jones 1997). Figure 5 shows the distributed annual average potential evaporation data. Higher PE rates are observed to the south-southeast part of the area along the Humber estuary, while lower PE rates are observed to the middle and northeast regions.
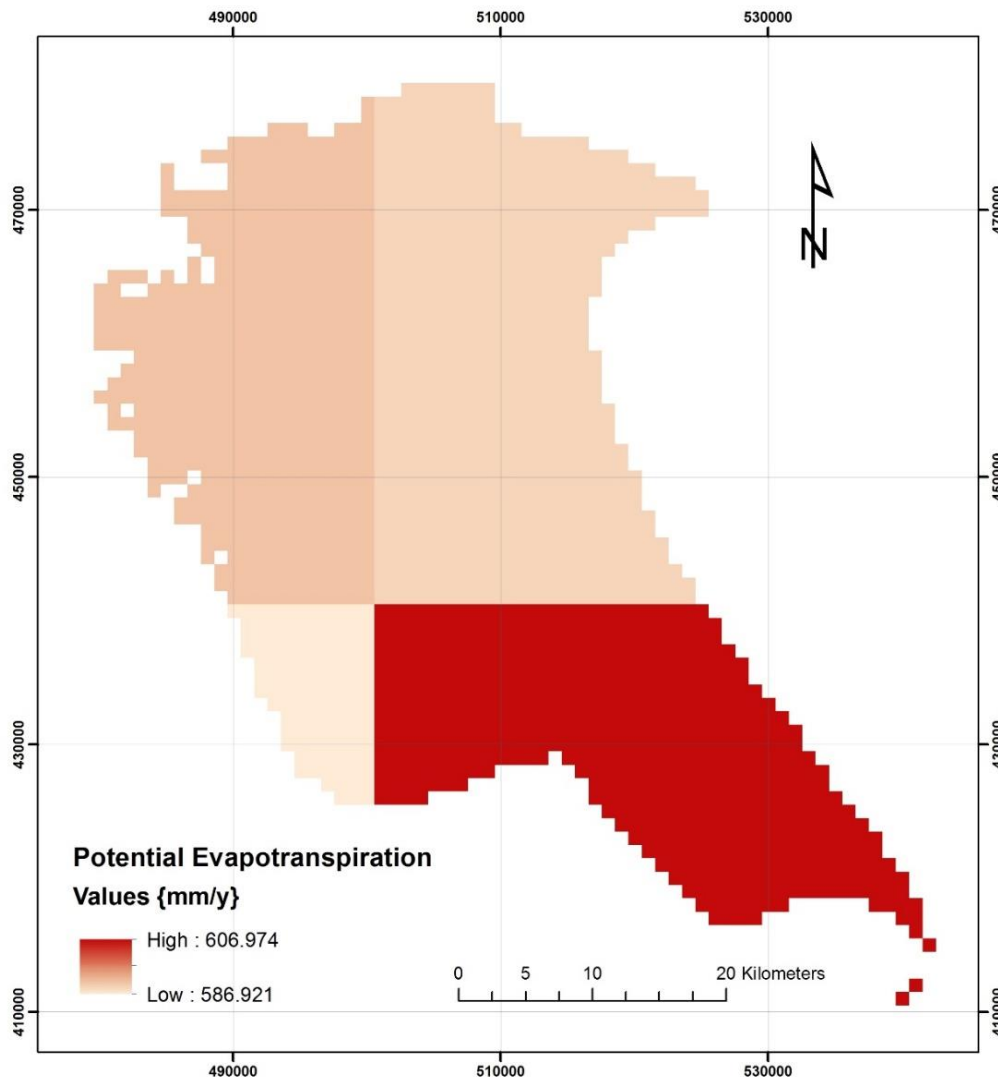
Figure 5. Spatial distribution of potential evaporation in the East Yorkshire Chalk

3.1.6 Recharge

The groundwater body in the pilot area receives most of its recharge from rainfall during the first quarter of the year. Nevertheless, the recharge process of the Chalk aquifer is generally a combination of complex flow regimes varying in timing and amount. The different rates of effective rainfall infiltration may be also affected by the presence or absence of Quaternary deposits in the surface strata. Several approaches have been applied to estimate recharge in the area. The standard Penman soil-water balance approach has been used by Environment Agency for recharge estimation. Other alternative recharge estimation approaches in the area are discussed by Rushton and Ward (1979), by Aspinwall (1995) while recently a distributed rainfall-runoff model was applied in the area to estimate recharge (ESI, 2013).

3.1.7   *Hydrogeology*

The aquifer properties of the East Yorkshire Chalk exhibit dissimilarities with southern England chalks due to different degrees of fracturing and matrix properties, which in turn, has an impact on the aquifer flow and transport capabilities. Two porosity regimes have been mainly identified in the calk of Yorkshire with values greater or less than 30%. Transmissivity values in the pilot area exhibit a large spatial variation ranging from 100 m^2d^{-1} to values greater than 10000 m^2d^{-1} as observed south west in distances less than 10 km from the Humber estuary (Figure 6). High transmissivity values of 8000 m^2d^{-1} have also been reported in the Wold Valley, northeast of the pilot area, in a study from the University of Birmingham (1985).
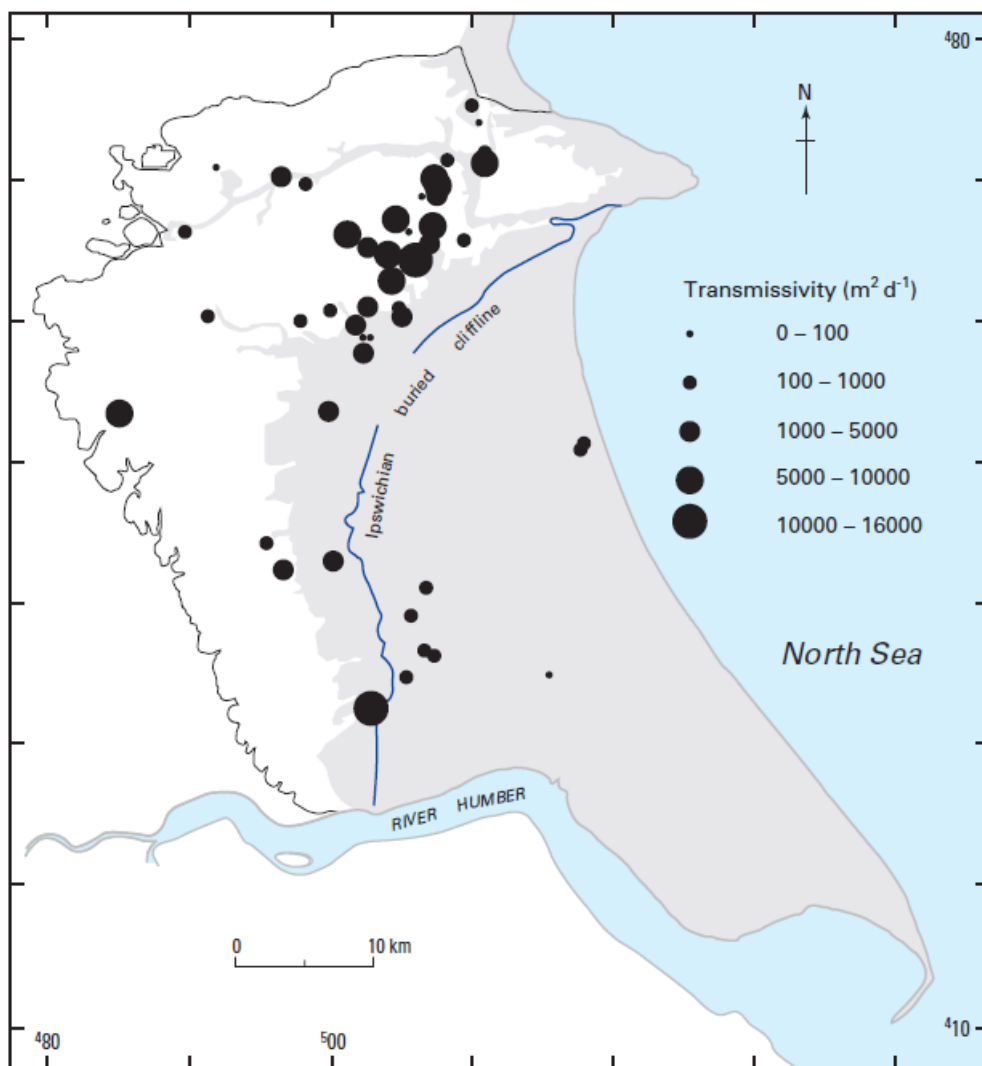
Figure 6. Spatial distribution of transmissivity values in the East Yorkshire Chalk (Gale and Rutter, 2006)

The hydrogeological conditions in the East Yorkshire Chalk vary from unconfined across the Wolds, through semiconfined conditions in the Hull catchment, to confined Chalk underlying Holderness. The latter, due to the restriction of groundwater movement and poor water quality is not being used as an aquifer. The thickness of unsaturated zone in the Yorkshire Chalk may vary from less than 10 m to over 120 m in certain regions.

The regional groundwater flow is mainly oriented along the dip of the Chalk with the major groundwater divide approximately following the line of the Chalk escarpment. The discharge of chalk groundwater takes place mainly to the North Sea, either on the beaches, or below low tide level (Foster and Milton, 1976). A network of dry valleys exists across the Wolds since the water table rarely intersects the ground surface. Just south of the Chalk outcrop, some springs occur which flow over the glacial deposits and form tributaries of the River Hull.

3.1.8 Groundwater levels

There is a network of approximately 220 boreholes in the pilot area, which monitors groundwater levels in the East Yorkshire Chalk. The longest record is Dalton Holme since 1889. Seasonal head variations are small in the confined aquifer, but may be reach 30 m in the unconfined aquifer. Smaller fluctuations of approximately 10 m have been recorded in the dry valleys (Robertson, 1984). Highest groundwater levels are recorded north west of the pilot area whereas groundwater levels in the coastal aquifer body close to Humber estuary are round zero m OD.
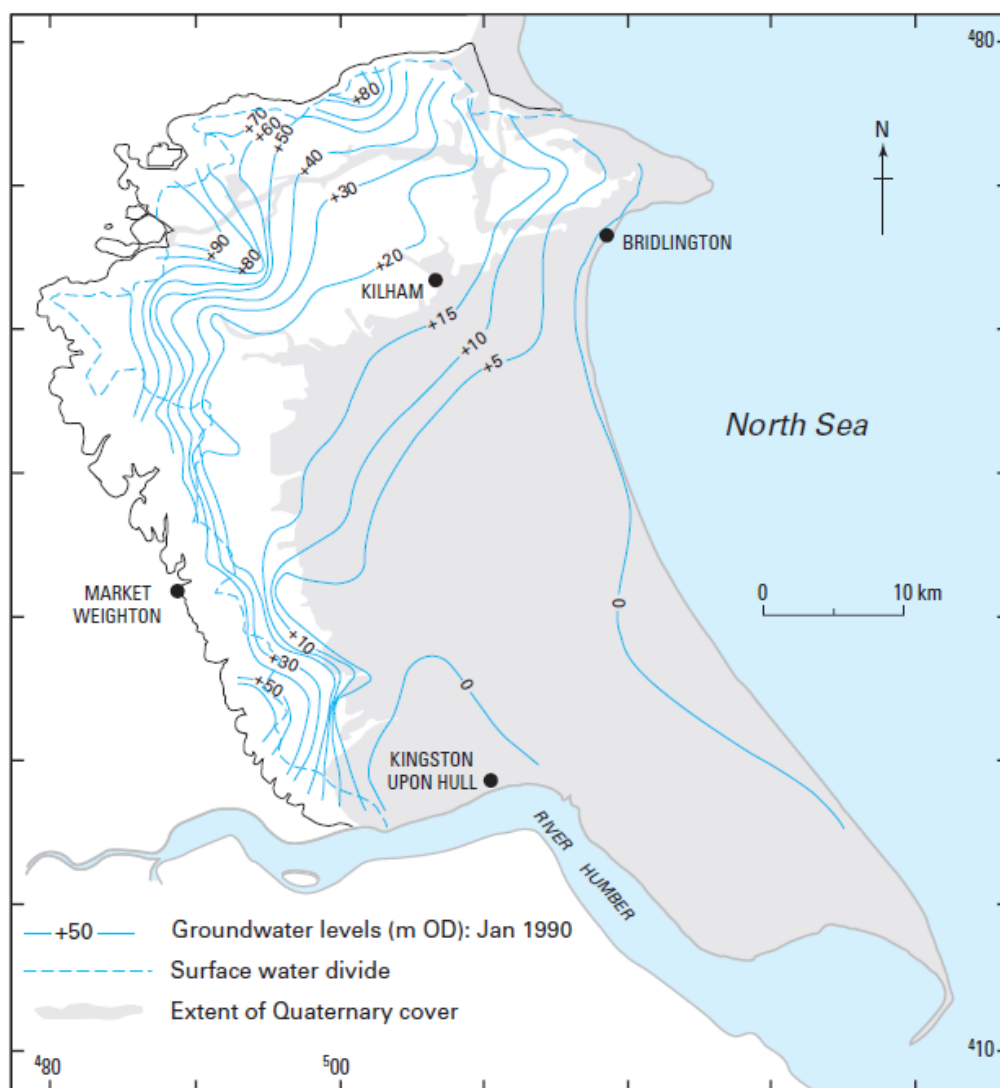
Figure 7. Spatial distribution of groundwater levels in the East Yorkshire Chalk (Gale and Rutter2006).

3.1.9   Groundwater abstraction

The amount of groundwater extracted is significant in both the confined and unconfined aquifers in the area. The majority of abstraction boreholes is located in a north–south line through Driffield and Beverley and their main major licensed abstractor within the area is Yorkshire Water Services Ltd (Aspinwall and Co., 1995a). The aquifer over-exploitation for many years resulted in SWI problems in the Kingston-upon-Hull and Holderness areas, from the Humber Estuary (Foster and Milton, 1976; Chadha, 1986). It is thought that before 1976 the total groundwater abstraction in the Kingston-upon-Hull area was in excess of the estimated annual recharge for more than 70 years.

In general, it is estimated that the current total abstraction from the Chalk is only 14% of the total recharge. It is noted that in the Hull area, which is of specific interest due to the proximity with the Humber estuary, groundwater has been extensively exploited for public water supply with indicative abstraction rates exceeding 20 Ml d^{-1}.

3.1.10   Groundwater quality and SWI

Saline intrusion is one of the main factors that affect the groundwater chemistry in the Yorkshire Chalk. Increased salinity has been observed in the confined aquifer close to the coast in the low-lying Holderness area with electrical conductivity measurements up to 17 mS cm^{-1}. However, the saline groundwater in this area is rather an old stable body of water while in the Hull area is more likely that salinity originates from a mixture of old and modern water (University of Birmingham, 1978, Smedley et al., 2004). Despite that relatively high Chloride concentrations have been recorded in the low-lying confined aquifer of the Chalk, it is not believed that this is the result of mixing with modern seawater (Figure 8).
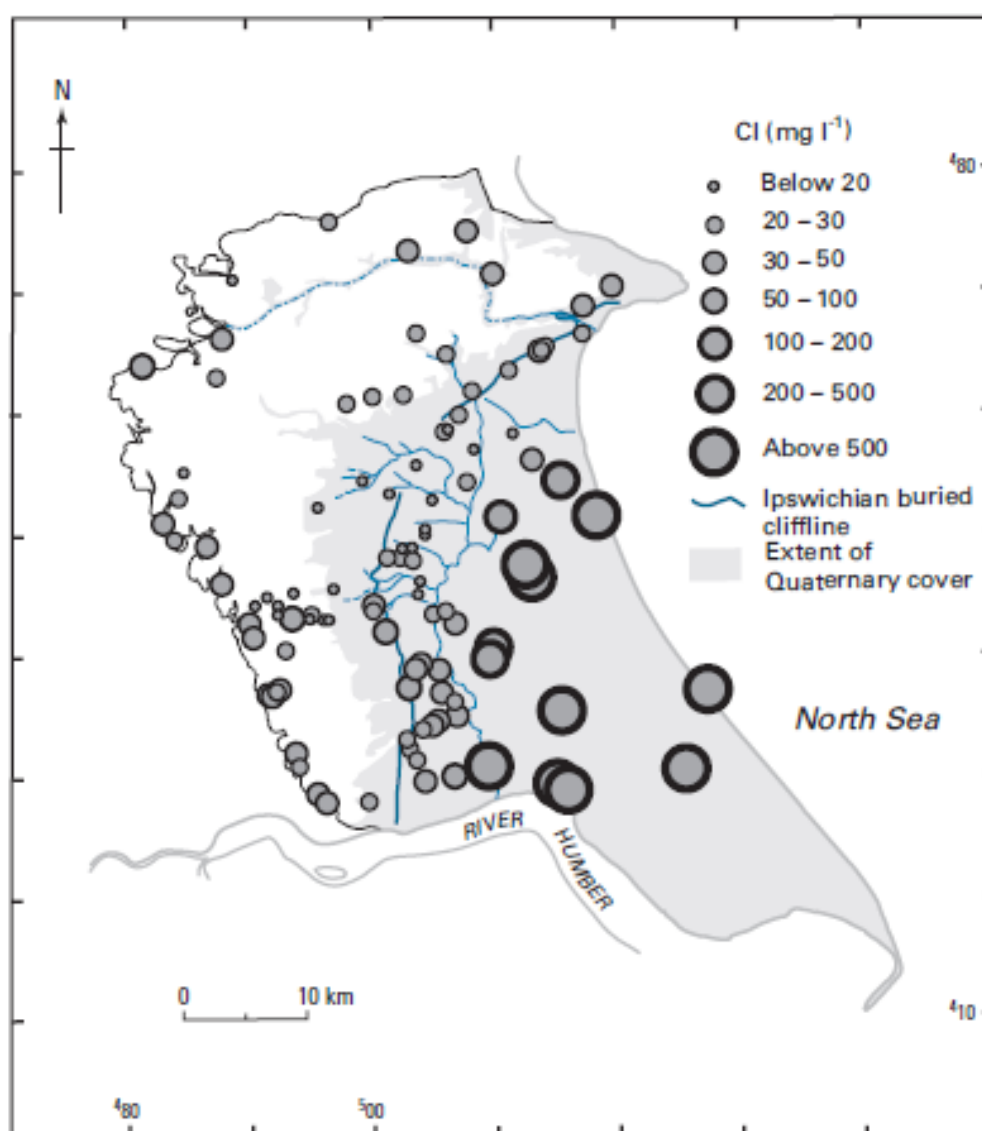
Figure 8. Spatial variation of Chloride concentrations in the groundwater of the East Yorkshire Chalk (Gale and Rutter, 2006)

Due to intensive pumping in the area, the piezometric surface was lowered down to more than 10 m below OD in some parts, allowing saline water to advance inland into the aquifer (Figure 9). Groundwater abstraction from the Chalk aquifer in Yorkshire is estimated around 38x10 m³ per year (Aspinwall, 1995a). However, further monitoring suggested that the saline front remained static despite the changes in the mixing zone between freshwater and saline water.
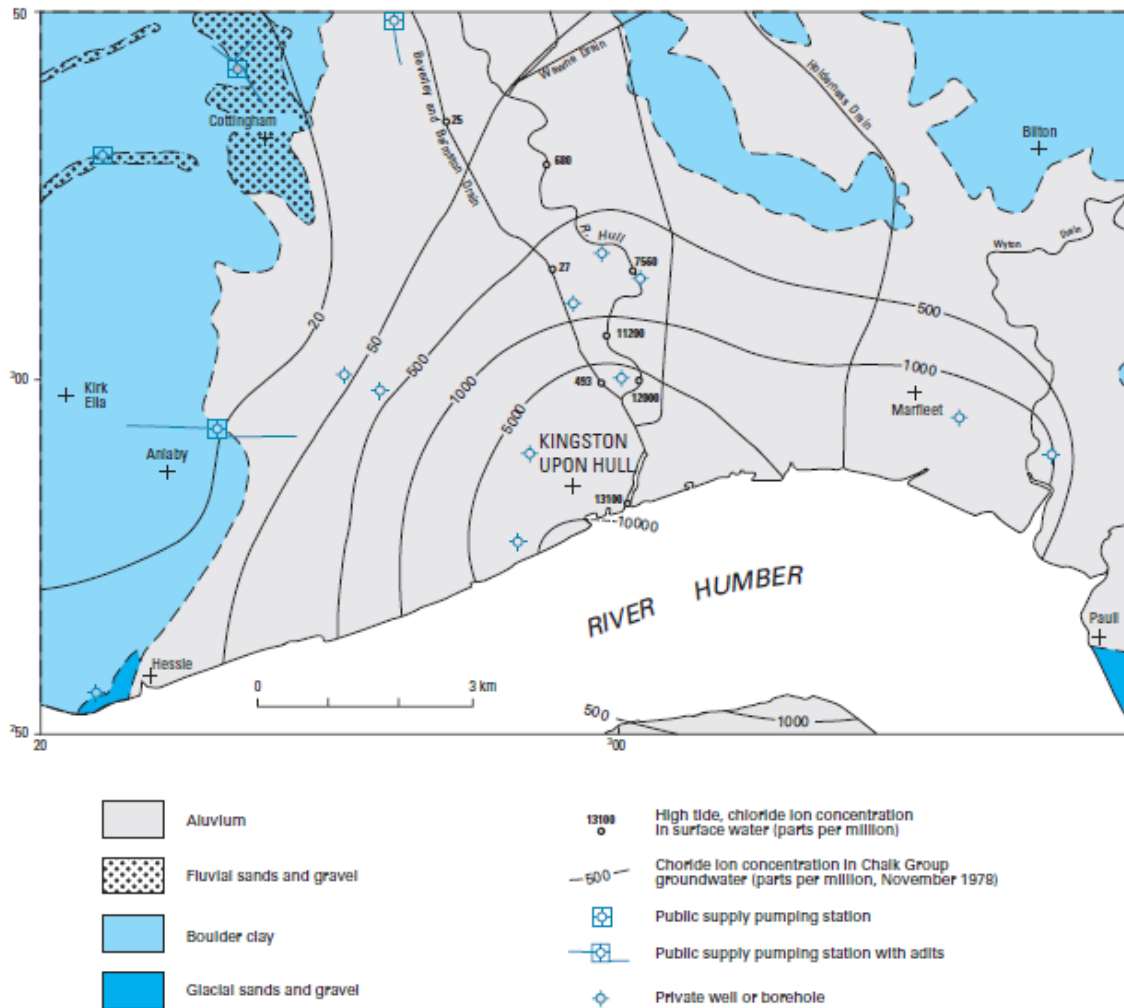
Figure 9. Extent of SWI in the Kingston-upon-Hull area (after IGS, 1980).

3.2   Climate change challenge

The assessment of impacts of climate change in the pilot area produced ambiguous results in the past since the predicted small increase in recharge may be offset by increased evapotranspiration (Gale and Rutter, 2006). Recently, the British Geological Survey (BGS) with the support of the Environment Agency (EA) BGS have undertaken a study to investigate the impact of climate change on groundwater resources using the distributed recharge model ZOODRM (Mansour and Hughes, 2018). Potential recharge values for Great Britain (England, Scotland and Wales) are produced using rainfall and potential evaporation data from the Future Flows Climate datasets (11 ensembles of the HadCM3 Regional Climate Model or RCM). This study has shown that generally the recharge season appears to become shorter, but with greater amount of recharge "squeezed" into fewer months. This conclusion is aligned with the European Environment Agency map that describes the expected climate change across the different areas in Europe (Figure 10). Impacts of climate change in the pilot area, regarding SWI, should be further investigated.
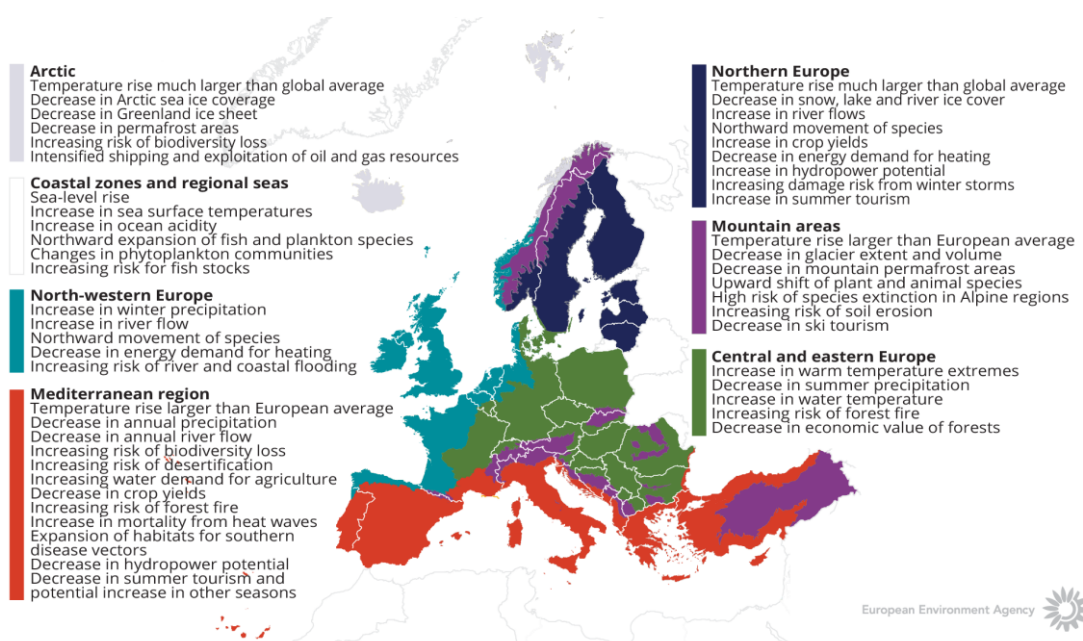
Figure 10. How is climate expected to change in Europe. The European Environment Agency map

4   METHODOLOGY

4.1   Methodology and climate data

The mathematical modelling of a Sea Water interface (SWI) is mainly based on two different conceptualizations of the freshwater and saltwater interactions. Variable density flow and solute transport models describe the formation of a transition zone between freshwater and saltwater, controlled by hydrodynamic dispersion mechanisms, and provide a more realistic representation of coastal aquifer flow processes. A coupled system of nonlinear partial differential equations is solved by using numerical codes, for example SUTRA (Voss, 1984), SEAWAT (Guo and Langevin 2002), or FEFLOW (Diersch and Kolditz 2002). Variable density flow and solute transport modelling is a high-fidelity approach in representing the dynamics and mixing of freshwater and saltwater in coastal aquifers (Werner et al. 2013). However, the application of these numerical models in regional-scale coastal aquifers might not always be straightforward due to a combination of computational challenges and spatial distribution of field data (Sanford and Pope 2010).

Another modelling approach for SWI is based on a simplification of the coastal aquifer flow where the dispersion zone is idealized as a sharp interface. It is considered as a reasonable approximation of regional coastal aquifer flow where the dispersive zone is expected to be narrow compared to the spatial scale of the area under study (Mantoglou et al. 2004). Due to the large spatial extent of the present pilot area, a sharp interface model has been employed to simulate SWI. A parsimonious SWI model was selected, based on the single-potential formulation of Strack (1976). It is suitable of providing a rough approximation of the SWI status for this pilot area within minimum computational effort. The sharp interface model of Strack (1976) is based on the Ghyben-Herzberg relation and Dupuit approximation and neglects density variability in space as well as mixing between freshwater and saltwater. The saltwater is assumed static and aquifer flow is assumed horizontal and steady-state. The depth of the interface is estimated using the Ghyben-Herzberg approximation which assumes that horizontally flowing freshwater floats above static saltwater (Essaid 1986). It is noted that sharp interface models might overestimate the extent of seawater intrusion, particularly under pumping conditions (Dausman et al. 2010; Llopis-Albert and Pulido-Velazquez 2014; Christelis and Mantoglou 2016).

Figure 11 illustrates vertical cross-sections of both confined and unconfined coastal aquifers where a sharp interface is assumed to separate freshwater from saltwater. Two distinct zones are developed. In zone 1, a confined (upper view) or an unconfined (lower view) aquifer flow is depicted whereas in zone 2 a freshwater lens floats above the static saltwater. Fresh groundwater is also pumped in zone 1.
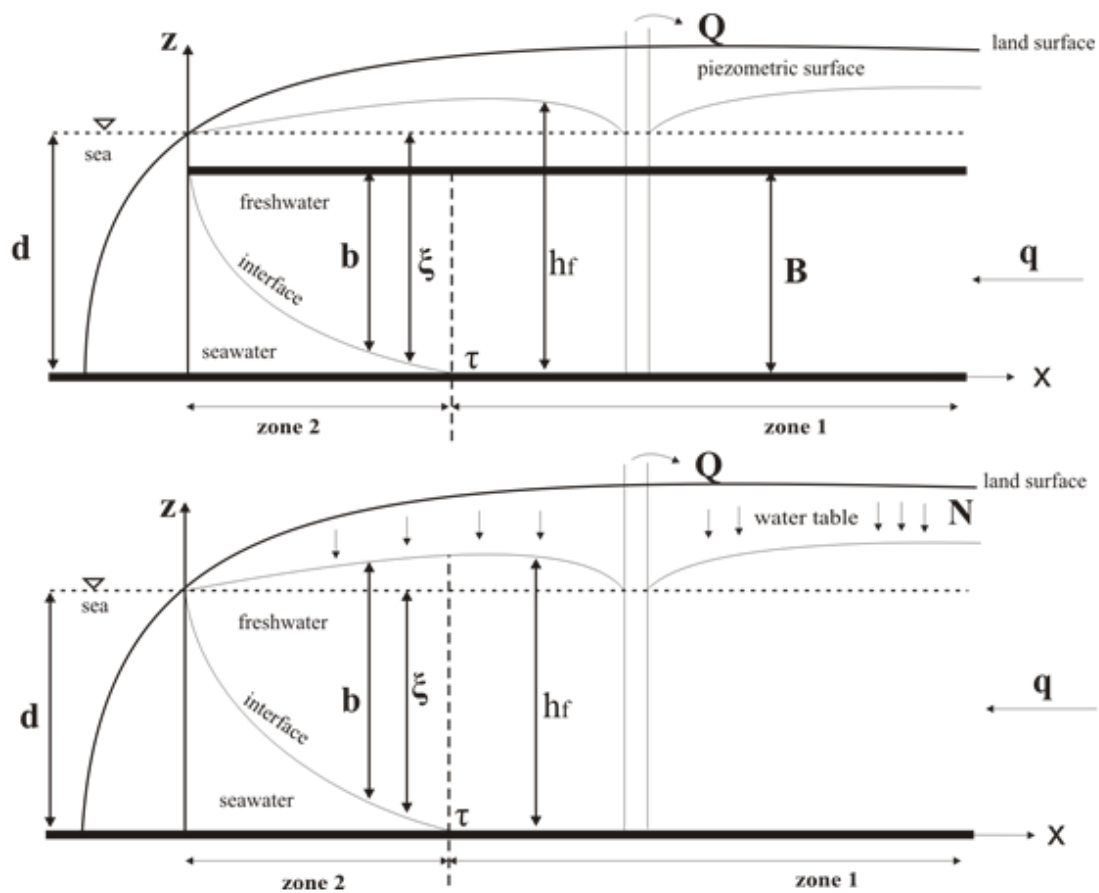
Figure 11. Schematic vertical cross-sections of a confined (upper figure) and an unconfined (lower figure) coastal aquifer, based on the sharp interface approximation (source: Christelis 2021).

Variable d $[L]$ represents the depth from sea level to the aquifer base and variable $\xi(x,y)[L]$ represents the freshwater depth from sea level to the interface. At point τ the interface intersects the base of the coastal aquifers. This point is usually called "toe" of seawater front and indicates the inland intrusion of seawater. A freshwater discharge volume rate per unit width of aquifer q $\left[\frac{L^3}{LT}\right]$ can be introduced in the model to represent inland recharge.

For the case of confined flow, variable $b(x,y)$ $[L]$ is the thickness of the confined flow region and in zone 1 equals B $[L]$, that is, the aquifer thickness defined by the two confining boundaries. In zone 2, $b(x,y) = \xi(x,y) - (d-B)$. For the case of unconfined flow, $b(x,y)[L]$ is the total freshwater depth and in zone 1, $b = h_f$ while in zone 2 $b(x,y) = h_f - d + \xi(x,y)$. Variable $h_f(x,y)$ $[L]$ is the freshwater head with reference to the impermeable aquifer base. In the case of the unconfined aquifer, a groundwater recharge rate N $[LT^{-1}]$ can be also applied to replenish the aquifer.

The Ghyben-Herzberg formula relates the hydraulic head $h_f(x,y)$ and depth $\xi(x,y)$ via the saltwater/freshwater density ratio $\varepsilon = \frac{(\rho_s - \rho_f)}{\rho_f}$ according to: $\left(\frac{1}{\varepsilon}\right)(h_f - d) = \xi(x,y)$. The following differential equations govern the aquifer flow in the confined and the unconfined case (Strack 1976; Mantoglou et al. 2004):

$$\left.\begin{array}{l} \frac{\partial}{\partial x}\left(K\frac{\partial \phi}{\partial x}\right) + \frac{\partial}{\partial y}\left(K\frac{\partial \phi}{\partial y}\right) - Q(x,y) = 0, \qquad \text{confined interface flow} \\[2mm] \frac{\partial}{\partial x}\left(K\frac{\partial \phi}{\partial x}\right) + \frac{\partial}{\partial y}\left(K\frac{\partial \phi}{\partial y}\right) + N - Q(x,y) = 0, \quad \text{unconfined interface flow} \end{array}\right\} \tag{1}$$

where ϕ $[L^2]$ is the flow potential and K $[LT^{-1}]$ is the aquifer's hydraulic conductivity. The distributed pumping rate $Q(x,y)[(L^3 T^{-1})L^{-2}]$ is $Q(x,y) = \sum_{j=1}^{M} Q_j\, \delta\left(x - x_{wj}, y - y_{wj}\right)$ where (x_{wj}, y_{wj}) are the coordinates of pumping wells $j = 1, \ldots M$ with rates Q_j and $\delta\left(x - x_{wj}, y - y_{wj}\right)$ is the Dirac delta function. In the case of confined aquifers, the flow potential is defined as (Bear et al. 1999):

$$\left.\begin{array}{l} \phi = Bh_f + \frac{\varepsilon B^2}{2} - (1 + \varepsilon)Bd \quad \text{zone 1} \\[2mm] \phi = \frac{1}{2\varepsilon}\left[h_f + \varepsilon B - (1 + \varepsilon)d\right]^2 \text{ zone 2} \end{array}\right\} \tag{2}$$

while in the case of unconfined aquifers the flow potential is expressed as (Bear et al. 1999),

$$\left.\begin{array}{l} \phi = \frac{1}{2}\left[h_f^2 - (1 + \varepsilon)d^2\right], \text{ zone 1} \\[2mm] \phi = \frac{(1+\varepsilon)}{2\varepsilon}\left(h_f - d\right)^2, \qquad \text{zone 2} \end{array}\right\} \tag{3}$$

At the location of the toe, the flow potential is calculated based on the following equations for each coastal aquifer type (Mantoglou 2003):

$$\left.\begin{array}{l} \phi_{toe} = \frac{\varepsilon}{2}B^2, \qquad\qquad \text{confined aquifer} \\[2mm] \phi_{toe} = \left[\frac{\varepsilon(\varepsilon+1)}{2}\right]d^2, \text{ unconfined aquifer} \end{array}\right\} \tag{4}$$

4.1.1 Climate data

The TACTIC standard scenarios are developed based on the ISIMIP (Inter Sectoral Impact Model Inter-comparison Project, see www.isimip.org) datasets. The resolution of the data is 0.5°x0.5°C global grid and at daily time steps. As part of ISIMIP, much effort has been made to standardise the climate data (e.g. bias correction). Data selection and preparation included the following steps:

1. Fifteen combinations of RCPs and GCMs from the ISIMIP data set where selected. RCPs are the Representative Concentration Pathways determining the development in greenhouse gas concentrations, while GCMs are the Global Circulation Models used to simulate the future climate at the global scale. Three RCPs (RCP4.5, RCP6.0, RCP8.5) were combined with five GCMs (noresm1-m, miroc-esm-chem, ipsl-cm5a-lr, hadgem2-es, gfdl-esm2m).

2. A reference period was selected between 1981 – 2010 and an annual mean temperature was calculated for the reference period.

3. For each combination of RCP-GCM, 30-years moving average of the annual mean temperature where calculated and two time slices identified in which the global annual mean temperature had increased by +1 and +3 degree compared to the reference period, respectively. Hence, the selection of the future periods was made to honour a specific temperature increase instead of using a fixed time-slice. This means that the temperature changes are the same for all scenarios, while the period in which this occur varies between the scenarios.

4. To represent conditions of low/high precipitation, the RCP-GCM combinations with the second lowest and second highest precipitation were selected among the 15 combinations for the +1 and +3 degree scenario. This selection was made on a pilot-by-pilot basis to accommodate that the different scenarios have different impact on the various parts of Europe. The scenarios showing the lowest/highest precipitation were avoided, as these endmembers often reflects outliers.

5. Delta change values were calculated on a monthly basis for the four selected scenarios, based on the climate data from the reference period and the selected future period. The delta change values express the changes between the current and future climates, either as a relative factor (precipitation and evapotranspiration) or by an additive factor (temperature).

6. Delta change factors were applied to local climate data by which the local particularities are reflected also for future conditions.

For the analysis in the present pilot the following RCP-GCm combinations were employed:

Table 1. Combinations of RCPs-GCMs used to assess future climate

		RCP	GCM
1-degree	"Dry"	rcp6p0	noresm1-m
	"Wet"	rcp4p5	miroc-esm-chem
3-degree	"Dry"	rcp4p5	hadgem2-es
	"Wet"	rcp8p5	miroc-esm-chem

4.2 Tool(s) / Model set-up

The flow equations presented in Equation 1 can be solved numerically using a groundwater flow code to account for coastal aquifers of irregular shape. Here, the groundwater model version of MODFLOW-2005 (Harbaugh, 2005) was utilized to solve the flow equations based on a block-centered finite-difference numerical scheme. Unconfined and steady-state, two-dimensional coastal aquifer flow conditions were simulated using a spatial discretization of $\Delta x = \Delta y = 500 m$. A simplified river flow network was included in the model, given the availability of existing data for river stages in the pilot area. Spatially distributed hydraulic conductivity and recharge values were used as inputs to the model to simulate the extent of seawater intrusion in the area. A single simulation run requires approximately 0.17 seconds which is indicative of the very low computational cost associated with this sharp interface model.

In particular, the impact of several recharge scenarios on the extent of SWI was investigated. As discussed previously, this particular sharp interface model assumes steady-state flow conditions and thus all recharge maps were averaged over specified time periods. First, a baseline simulation was performed using the long-term average of a historical recharge calculation of 50 years produced using the UK national scale model (Mansour et al., 2018). Then, the 50 years of historical recharge were disaggregated into five decadal recharge periods to investigate for possible differences in the simulated SWI extent. Finally, the future recharge values estimated using the UK national scale recharge model and the change factors of the four selected climate scenarios presented in Table 1, were applied in the SWI model to assess their effect on the simulated location of the freshwater/saltwater interface in the pilot area.

4.3 Model calibration

The historical recharge values applied to simulate the groundwater potentials for the baseline case are obtained from the work published by Mansour et al. (2018). In this work a national scale recharge model was calibrated by comparing the simulated long-term average overland flows to the observed ones at selected gauging stations located at major rivers. Figure 12 shows a Q plot for the simulated vs observed long term average runoff values at the selected gauging stations. The estimated recharge values are also compared with recharge values estimated using other tools and by other researchers and governmental bodies such as the Environment Agency.

The values of the hydraulic parameters, mainly the hydraulic conductivity, are obtained from an ongoing research project called Hydro-JULES. This a research program supported by NERC National Capability funding (Grant number: NE/S017380/1) to the Centre for Ecology & Hydrology (CEH), British Geological Survey (BGS) and National Centre for Atmospheric Science (NCAS). Under this work a numerical groundwater model is developed for the Chalk aquifer which covers the Humber estuary. A stochastic approach was used to produce a spatially distributed map of the hydraulic conductivity values. In this approach, hydraulic conductivity data available across the Chalk aquifer were interpreted stochastically to produce a large number of statistically acceptable hydraulic conductivity maps. These are then processed using the numerical model. Simulated and observed groundwater levels at selected observation boreholes are compared and a selected number of best performing models are selected. Finally, and to address the uncertainty associated with the used data and the stochastic approach, maps showing the 25th, mean and 75th percentile hydraulic conductivity values and obtained from the

hydraulic conductivity maps are produced. In this work, the spatially distributed mean hydraulic conductivity values are used to investigate the saline intrusion in the aquifer.
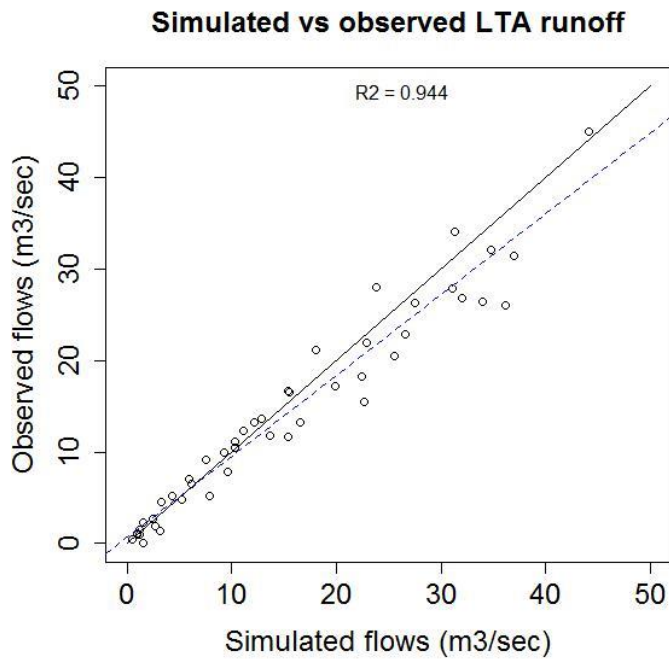
Figure 12 Q plot for the simulated vs observed long term average runoff values at the 56 gauging stations shown in **¡Error! No se encuentra el origen de la referencia.** after Mansour et al. (2018)

5 RESULTS AND CONCLUSIONS

5.1 Saline intrusion using the historical long-term average recharge values

Initially, SWI was simulated for the case of a long-term average recharge input distributed spatially in the area. Figure 13 presents the specific contour which corresponds to the flow potential of the interface location as calculated by equation 4. The sharp interface approach separates the aquifer into a freshwater zone (the area indicated by Zone F in Figure 13) and into a saltwater zone (the area indicated by Zone S in Figure 13).
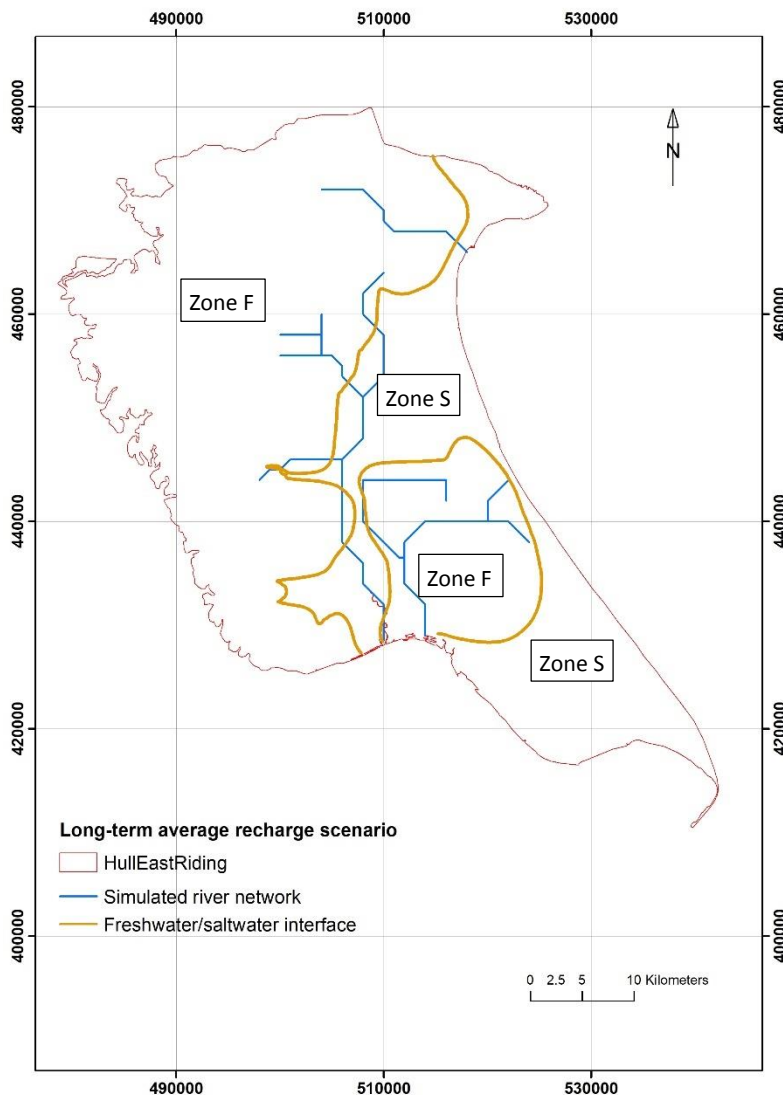
Figure 13. Baseline scenario presenting the simulated intrusion of seawater for a long-term average recharge of 50 years period

In overall, the simulated interface reasonably approximates the distribution of chloride data shown in Figure 8. The saltwater intruded area simulated by the sharp interface model, mostly

encompasses the quaternary cover of the aquifer where, according to Figure 8, increased chloride values have been recorded. From a qualitative point of view, the model appears to reproduce well the status of SWI based on the historical chloride data which are indicative of saline groundwater in the area along the coastline and inland (Figure 14).
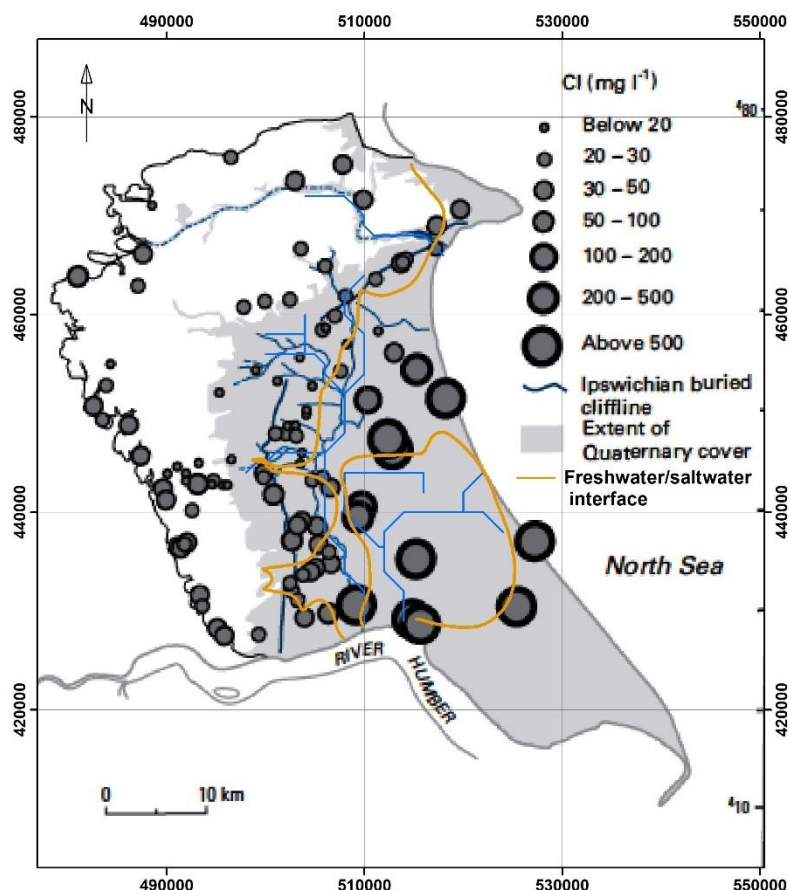

Figure 14. The freshwater/saltwater interface plotted on top of the available chloride map of figure 8.

5.2   Variation of saline intrusion on a decadal basis

Next, the simulated interfaces are presented based on the time-averaged decadal recharge periods (Figure 15). Results show that by simulating different historical recharge periods the extent of seawater intrusion exhibits a similar pattern for all of these periods. However, the differences among the interface locations may range from as low as 10 meters up to 700 meters, depending on which part of the Hull and East Riding groundwater body is considered. For example, large differences are observed in the upper north-eastern part near Bridlington and close to the Humber estuary near Kingston Upon Hull.
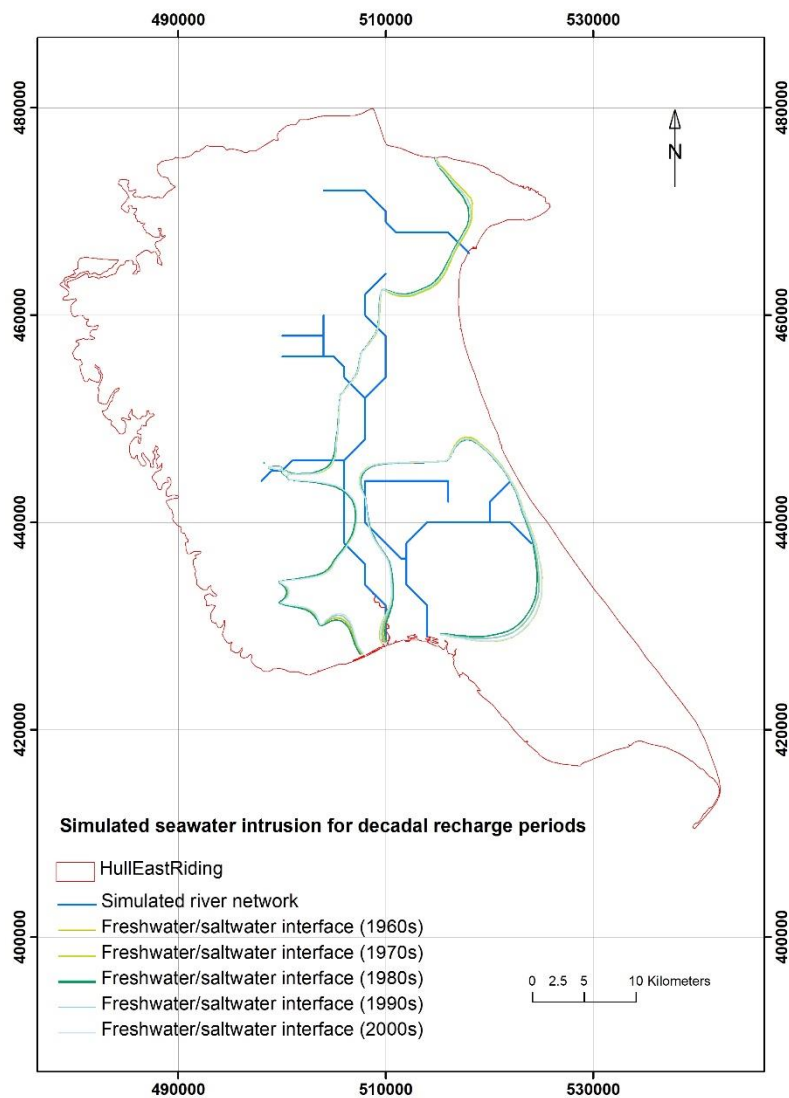
Figure 15. Location of freshwater/saltwater interfaces for 5 different decadal recharge periods.

Another metric to quantify the differences among the decadal recharge periods is to calculate the freshwater area as this is separated from the saltwater intruded area using the simulations with the sharp interface model. The results demonstrate that the recharge period from 1980-1990 (i.e. 1980s), had a smaller calculated freshwater area than the other periods with a 1.8% difference from the corresponding freshwater area obtained from the baseline simulation. This is attributed to the reduced recharge during that period which is 11.74% less than the long-term average recharge.
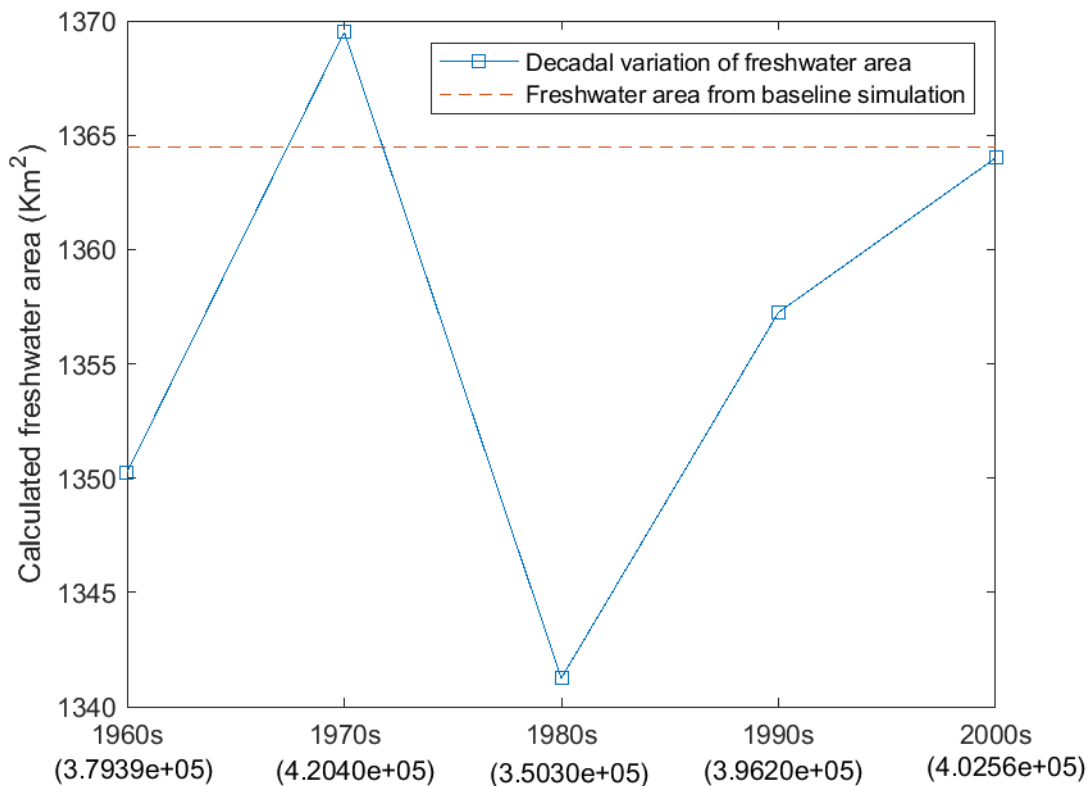
Figure 16. Calculated freshwater area for the 10-year averaged periods between 1960s-2000s. In parenthesis is the total groundwater recharge (m^3) applied in the SWI model.

5.3 Saline intrusion under future climate scenarios

A set of four SWI simulations were also performed to assess the impact of future climate recharge projections on the interface position. The recharge inputs for each SWI simulation are based on the climate scenarios presented in Table 1. As it is shown in Figure 17, there are parts of the aquifer where the simulated interfaces are close to each other while the range of these distance differences may vary from 30 meters to 760 meters. Apart from the total recharge input applied in the SWI model, the interface location in the area also depends on local hydraulic conductivity and local river network features. Thus, a decrease or an increase in total recharge is not always the major factor to trigger a smaller or larger extent of seawater intrusion as demonstrated by the simulated interfaces. However, it is observed that in the case of the 3-degree "Wet" climate scenario, the recharge input has a significant impact on the simulated extent of seawater intrusion. The interface line corresponding to this scenario (3 degree "Wet" in Figure 17) remains always closer to the coast boundary compared to the other interfaces.
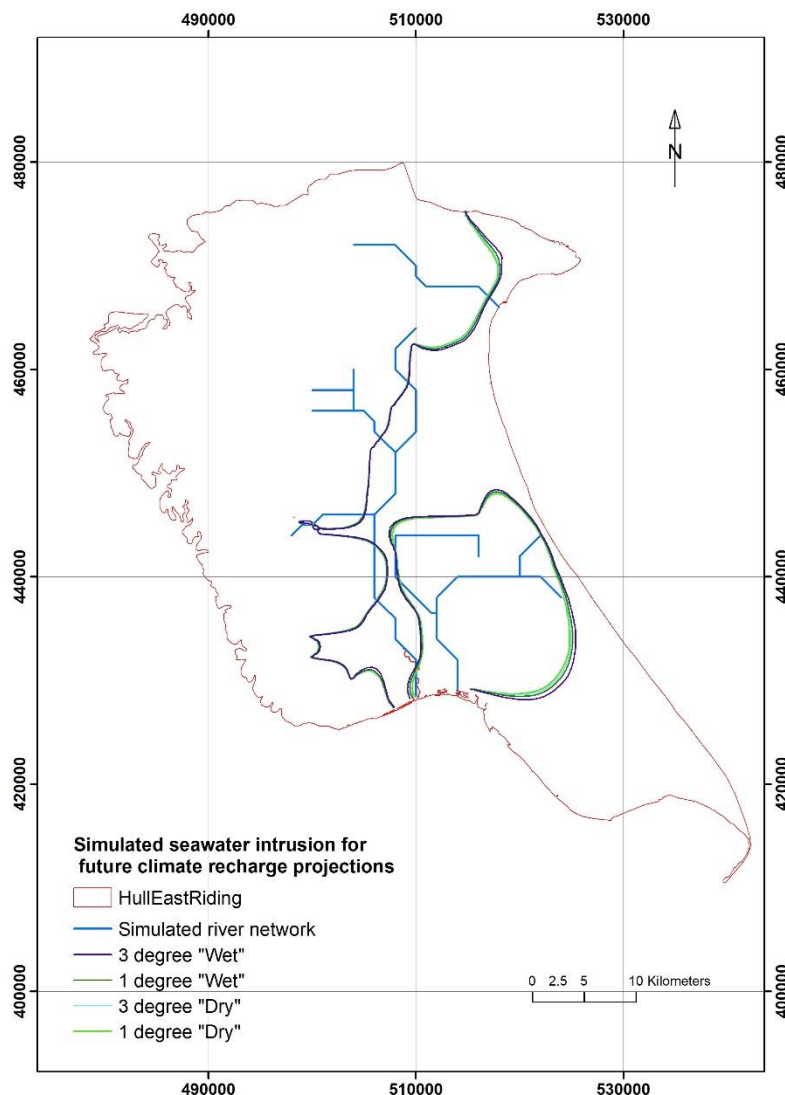
Figure 17. Location of freshwater/saltwater interfaces for the four climate scenarios.

The freshwater areas were also calculated for the climate scenario simulations. The impact of the 3-degree "Wet" climate scenario on mitigating seawater intrusion is evident by providing the largest freshwater area. Interestingly, the 3-degree "Dry" climate scenario provided a slightly larger freshwater area than the 1-degree "Dry" climate scenario which contradicts to the hypothesis that the former is a drier scenario than the latter. This could be attributed to that the 3-degree "Dry" scenario may include short-period high intensity rainfall storms that generate large amounts of recharge and compensate for the dry periods. This could be more extreme in the 3-degree "Dry" than in the 1-degree "Dry" climate scenario yielding a long-term average recharge that is slightly higher.
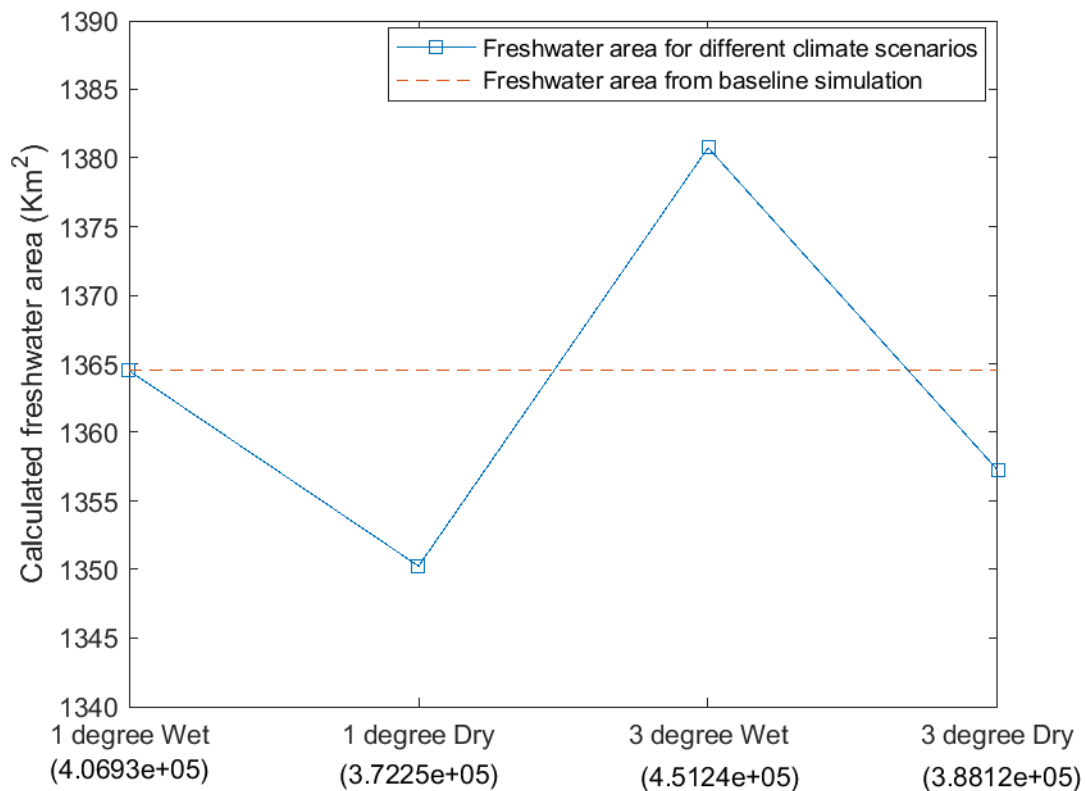
Figure 18. Calculated freshwater area for the different future climate recharge projections. In parenthesis is the total groundwater recharge (m^3) applied in the SWI model.

5.4 Assessment of saline intrusion vulnerability using the GALDIT method

One popular approach to assess the vulnerability of a coastal aquifer to seawater intrusion is the GALDIT method (Lobo-Ferreira et al. 2005), an index-based ranking approach which provides a practical tool to map those parts of an aquifer that are more prone to the encroachment of seawater (Recinos et al. 2015). Enhancement of the currently available data, mostly regarding salinity levels in the area, might lead to a different interpretation of the seawater intrusion vulnerability in the area. Nevertheless, the method identified certain areas which appear to have moderate or high vulnerability score and further modelling analysis and data collection could provide insights regarding the seawater intrusion status for future groundwater management.
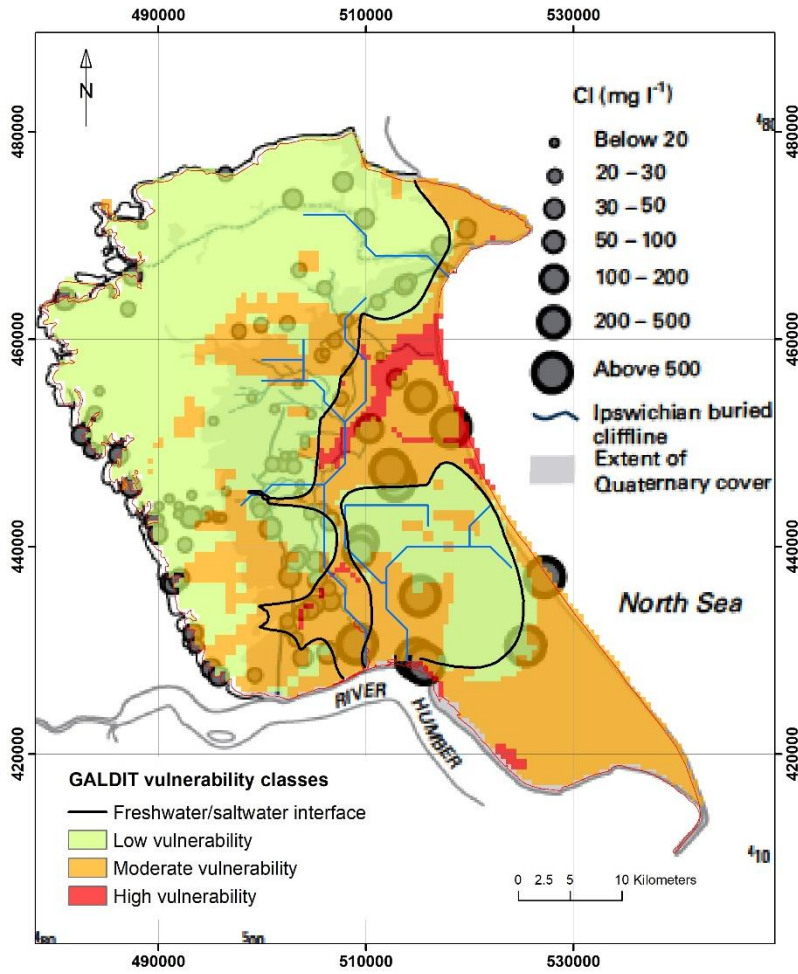
Figure 19. Characterization of the vulnerability of the pilot area to seawater intrusion based on GALDIT method.

REFERENCES

Aspinwall and CO. 1995a. Yorkshire Chalk groundwater model. Report prepared for National Rivers Authority and Yorkshire Water plc, Leeds.

Aspinwall and CO. 1995b. Development of groundwater models for the Kilham area of the East Yorkshire chalk aquifer. Report NR1709B prepared for the National Rivers Authority, Leeds.

Chaddha, D. S. 1986. Saline intrusion in the Chalk aquifer of North Humberside, UK. In Bockelman, R. H. et al. (editors). Proceedings of the 9th Salt Water Intrusion Meeting (SWIM), Delft, The Netherlands.

Christelis V. and Mantoglou A. 2016. Coastal aquifer management based on the joint use of density-dependent and sharp interface models. Water Resources Management, 30(2), 861–876.

Christelis V. 2021. Surrogate-based optimization methods for coastal aquifer management. PhD thesis, National Technical University of Athens, Athens, Greece. https://dspace.lib.ntua.gr/xmlui/handle/123456789/53074

Dausman A., Langevin C., Bakker M., and Schaars F. 2010. A comparison between SWI and SEAWAT—the importance of dispersion, inversion and vertical anisotropy. 21st Salt Water Intrusion Meeting, Gov. of Azores, Azores

Environment Agency. 2006. Date. The state of groundwater in England and Wales.

ESI 2013. East Yorkshire Chalk Aquifer Investigation: Numerical model report. Report reference: 60271 R2D1. Prepared for the Environment Agency.

Essaid, H.I., 1986. A comparison of the coupled fresh water-salt water flow and the Ghyben-Herzberg sharp interface approaches to modeling of transient behavior in coastal aquifer systems. Journal of Hydrology, 86(1-2), pp.169-193.

Foster, S. S. D., Parry, E. L., and Chilton, P. J. 1976. Groundwater resource development and saline intrusion in the Chalk aquifer of North Humberside. Report of the Institute of Geological Sciences, 76/4.

Foster, S. S. D., and Milton, V. A. 1976. Hydrogeological basis for large-scale development of groundwater storage capacity in the East Yorkshire Chalk. Report of the Institute of Geological Sciences, 76/7.

Gale, I. N., and Rutter, H K. 2006. The Chalk aquifer of Yorkshire. British Geological Survey Research Report, RR/06/04. 68pp.

Harbaugh, A.W., 2005, MODFLOW-2005, the U.S. Geological Survey modular ground-water model -- the Ground-Water Flow Process: U.S. Geological Survey Techniques and Methods 6-A16.

Hough, M. N. & Jones, R. J. A. 1997. The United Kingdom Meteorological Office rainfall and evaporation calculation system: MORECS version 2.0 – an overview. Hydrology and Earth System Sciences, 1, 227–239.

Jenkins, G.J., Murphy, J.M., Sexton, D.S., Lowe, J.A., Jones, P. and Kilsby, C.G. 2009, UK Climate Projections: Briefing report, Met Office Hadley Centre, Exeter, UK.

Lobo-Ferreira, J.P., Chachadi, A.G., Diamantino, C., and Henriques, M.J. 2005. Assessing aquifer vulnerability to sea-water intrusion using GALDIT method: Part 1 – Application to the Portuguese Aquifer of Monte Gordo. IAHS and LNEC, Proceedings of the 4th The Fourth Inter Celtic Colloquium on Hydrology and Management of Water Resources, held at Universidade do Minho, Guimarães, Portugal, July 11- 13, 2005.

Llopis-Albert, C. and Pulido-Velazquez, D., 2014. Discussion about the validity of sharp-interface models to deal with seawater intrusion in coastal aquifers. Hydrological Processes, 28(10), pp.3642-3654.

Mansour, M. M. and Hughes, A. G. 2018. Summary of results for national scale recharge modelling under conditions of predicted climate change. British Geological Survey Internal report. Commissioned Report OR/17/026.Mansour, M. M., Wang, L., Whiteman, Mark, Hughes, A. G. 2018. Estimation of spatially distributed groundwater potential recharge for the United Kingdom. Quarterly Journal of Engineering Geology and Hydrogeology, 51 (2). 247-263. https://doi.org/10.1144/qjegh2017-051

Mantoglou, A., Papantoniou, M. and Giannoulopoulos, P., 2004. Management of coastal aquifers based on nonlinear optimization and evolutionary algorithms. Journal of Hydrology, 297(1), 209-228.

Murphy, J.M., Booth, B.B.B., Collins, M., Harris, G.R., Sexton, D.M.H., and Webb, M.J. 2007. A methodology for probabilistic predictions of regional climate change from perturbed physics ensembles. Phil. Trans. R. Soc. A 365, 1993–2028.

Murphy, J.M., Sexton, D.M.H., Jenkins, G.J., Boorman, P.M., Booth, B.B.B., Brown, C.C., Clark, R.T., Collins, M., Harris, G.R., Kendon, E.J., Betts, R.A., Brown, S.J., Howard, T. P., Humphrey, K. A., McCarthy, M. P., McDonald, R. E., Stephens, A., Wallace, C., Warren, R., Wilby, R., and Wood, R. A. 2009, 'UK Climate Projections' Science Report: Climate change projections. Met Office Hadley Centre, Exeter.

Prudhomme, C., Dadson, S., Morris, D., Williamson, J., Goodsell, G., Crooks, S., Boelee, L., Davies, H., Buys, G., Lafon, T. and Watts, G., 2012. Future Flows Climate: an ensemble of 1-km climate change projections for hydrological application in Great Britain. Earth System Science Data, 4(1), pp.143-148.

Recinos, N., Kallioras, A., Pliakas, F. and Schuth, C. 2015. Application of GALDIT index to assess the intrinsic vulnerability to seawater intrusion of coastal granular aquifers. Environmental Earth Sciences, 73, 1017–1032.

Robertson, A. S. 1984. BGS contribution to the Yorkshire Water Authority Kilham area river augmentation scheme. British Geological Survey Technical Report, WD/ST/84/9R.

Rushton, K. R., and Ward, C. T. 1979. The estimation of groundwater recharge. Journal of Hydrology, Vol. 41 345–361.

Smedley, P.L., Neumann I. and Farrell, R. 2004. Baseline Report Series 10: The Chalk aquifer of Yorkshire and North Humberside. British Geological Survey Commissioned Report No. CR/04/128N.

Strack, O.D.L., 1976. A single-potential solution for regional interface problems in coastal aquifers. Water Resources Research, 12(6), 1165-1174.

University of Birmingham. 1978. South Humberside Salinity Research Project: Final Report to the Anglian Water Authority. Departments of Geological Science and Civil Engineering, University of Birmingham.

University of Birmingham. 1985. Yorkshire Chalk Groundwater Model Study: Final Report to Yorkshire Water Authority. Departments of Geological Science and Civil Engineering, University of Birmingham.

Deliverable 5.3

PILOT DESCRIPTION AND ASSESSMENT

Malta Mean Sea Level Aquifer, Malta

Authors and affiliation:

Manuel Sapiano
Henry Debattista

Deliverable Data	
Deliverable number	D*5.3*
Dissemination level	Public
Deliverable name	*Pilot description and assessment*
Work package	WP*5, WP6*
Lead WP/Deliverable beneficiary	*IGME*
Deliverable status	
Version	*V1.1*
Date	Date 26/02/2021

[This page has intentionally been left blank]
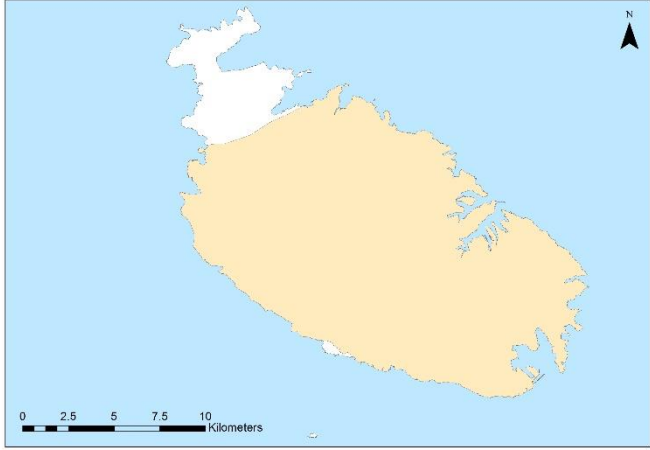
LIST OF ABBREVIATIONS & ACRONYMS

CC	Climate Change
GHB	General Head Boundary
GL	Globigerina Limestone
GSO	Geological Survey Organisation
HFB	Horizontal Flow Barrier
EEA	European Environment Agency
ERA	Environment and Resources Authority
EWA	Energy and Water Agency
LCL	Lower Coralline Limestone
MSLA	Mean Sea Level Aquifer
RBMP	River Basin Management Plan
WFD	Water Framework Directive
WSC	Water Services Corporation

TABLE OF CONTENTS

1 EXECUTIVE SUMMARY

Pilot name	Malta MSLA	
Country	Malta	
EU-region	Mediterranean Region	
Area (km²)	216.6Km²	
Aquifer geology and type classification	Limestone (sedimentary-fractured aquifer)	
Primary water usage	Drinking Water, Agricultural Irrigation	
Main climate change issues	Increasing temperatures, Decreasing Recharge (both due to decreasing rainfall and changing rainfall patterns) and Sea-Level rise	
Models and methods used	Groundwater numerical models, water balance equations.	
Key stakeholders	Water Services Corporation, Environment and Resources Authority	
Contact person	Manuel Sapiano, Energy and Water Agency, manuel.sapiano@gov.mt	

The Malta Mean Sea Level Aquifer system is by far the most important groudnwater body in the Maltese islands sustaining around 80% of the available renewable freshwater resources. The aquifer system sustains a groundwater body which takes the form of a lens of freshwater floating on the denser sea-water, and therefore an arrangement where freshwater is in lateral and vertical contact with sea-water. These aquifer systems are therefore highly vulnerable to sea-water intrusion in response to abstraction activities, and groundwater abstraction needs to be carefully managed to ensure the quality of the abstracted water. The level of sea-water intrusion depends on several factors including the rate of abstraction, the hydro-dynamic properties of the aquifer matrix and the distance of the bottom of the abstraction point to the freshwater-seawater interface. The position of the interface depends, in accordance with the Ghyben-Herzberg principle, on the piezometric levels. Therefore any lowering of the piezometric surface due to Climate Change impacts is construed as potentially contributing to an exacerbation of the sea-water intrusion levels arising under pumping conditions,

The study represented in this report models the impact on the piezometric levels of the Mean Sea Level aquifer system arising from the occurrence of three potential climate change scenarios entailing a reduction in rainfall, an increase in abstraction and a rise in sea-level respectively.

The study also undertakes a comparative analysis of the impact arising from these three Climate Change scenarios with that arising from due to anthropogenic activities such as different levels of overabstraction and recharge reduction.

The results of the numerical models show that the piezometric surface under the modelled Climate Change conditions is generally lower than that resulting when the aquifer is modelled under reference conditions. In general, however, the impact of climate change on the groundwater body seems to be of a lower concern when compared with modelled results for scenarios testing the application of poor groundwater management practices. However, the onset of Climate Change is expected to exacerbate the effects of poor aquifer management practices, due to an increase in the vulnerabilty of the new aquifer reference conditions. Hence the need to optimise existing groundwater management strategies to ensure a high level of protection for these vulnerable natural freshwater resources.

2   INTRODUCTION

Climate change (CC) already have widespread and significant impacts in Europe, which is expected to increase in the future. Groundwater plays a vital role for the land phase of the freshwater cycle and has the capability of buffering or enhancing the impact from extreme climate events causing droughts or floods, depending on the subsurface properties and the status of the system (dry/wet) prior to the climate event. Understanding and taking the hydrogeology into account is therefore essential in the assessment of climate change impacts. Providing harmonised results and products across Europe is further vital for supporting stakeholders, decision makers and EU policies makers.

The Geological Survey Organisations (GSOs) in Europe compile the necessary data and knowledge of the groundwater systems across Europe. In order to enhance the utilisation of these data and knowledge of the subsurface system in CC impact assessments the GSOs, in the framework of GeoERA, has established the project "Tools for Assessment of ClimaTe change ImpacT on Groundwater and Adaptation Strategies – TACTIC". By collaboration among the involved partners, TACTIC aims to enhance and harmonise CC impact assessments and identification and analyses of potential adaptation strategies.

TACTIC is centred around 40 pilot studies covering a variety of CC challenges as well as different hydrogeological settings and different management systems found in Europe. Knowledge and experiences from the pilots will be synthesised and provide a basis for the development of an infra structure on CC impact assessments and adaptation strategies. The final projects results will be made available through the common GeoERA Information Platform (http://www.europe-geology.eu).

This report provides an outline of the studies carried out under the TACTIC project in the pilot area of Malta's Mean Sea Level Aquifer system (MSLA). The MSLA extends over an area of 216km^2, south of the bounding Pwales Fault system. From a hydrogeological perspective the groundwater body is sustained in the Lower Coralline Limestone and is bounded by the Pwales fault in the North and the freshwater-saltwater interface at the coast.

The study concerns the development of the MSLA under three scenarios which assume potential climate change impacts related to reduced recharge (due to changing rainfall patterns), increased abstraction (due to increased irrigation needs as a result of higher temperatures and increased losses due to evapotranspiration) and sea-level rise. These assessments are important to guide the development of future management frameworks for this groundwater body, which is the most important natural freshwater resources in the Maltese islands. Malta's 2nd River Basin Management Plan (2nd RBMP) identifies this aquifer system in poor quantitative status with the main abstraction pressures arising due to groundwater abstraction for municipal supply and agricultural irrigation purposes. The 2nd RBMP sets out the development of an abstraction management framework as one of the key measures to enable this groundwater body to progressively achieve good quantitative status – that is a balance between recharge and abstraction. Studies on the development of the groundwater body under climate change conditions are important to enable water management frameworks to be sufficiently flexible to effectively address future challenges.

The protection of the status of the Malta Mean Sea Level aquifer system is a central feature in Malta's water management strategies due to the strategic importance of this natural freshwater body for water supply purposes. The "floating-lens" typology of this groundwater body makes it highly vulnerable to the intrusion of sea-water in response to abstraction activities, in particular where sustainable abstraction rates are exceeded. This leads to the salinisation of the groundwater resource further constraining its use. Therefore, the results obtained under TACTIC will also support the development of the groundwater protection measures under Malta's 3rd RBMP, intended to secure the sustainability of this groundwater resources in the future. The results of this project will in particular contribute to the climate-proofing assessments of the 3rd RBMP's measures, thereby supporting the achievement of the EU's Water Framework Directive's (WFD) Environmental Objectives.

3   PILOT AREA

The Maltese archipelago consist of three inhabited islands: Malta, Gozo and Comino, located approximately 96km south of Sicily and 290km north of Tunisia. The total surface area of the archipelago is approximately 316km^2, with Malta and Gozo, the two largest islands occupying 246km^2 and 67km^2 respectively.   The Malta mean sea-level aquifer system is located in the island of Malta south of the bounding Pwales fault, which juxtaposes the aquifer formation – the Lower Coralline Limestone with the impermeable Blue Clay formation creating a natural boundary condition. The MSLA develops over an area of 216km^2 and is primarily sustained in the Lower Coralline Limestone. The freshwater body takes the form of a lens dynamically floating on the more saline water, having a convex piezometric surface and conversely a concave interface, both tapering towards the coast.

The MSLA is by far the most important groundwater body in the Maltese islands, sustaining around 80% of the total groundwater yield. It is however, also under sustained quantitative pressures – with the analysis undertaken as part of Malta's 2nd RBMP qualifying the groundwater body to be under poor quantitative status conditions. The 2nd RBMP identifies groundwater abstraction for municipal and agricultural irrigation purposes as the two most significant quantitative pressures on this aquifer system. The MSLA's floating lens structure entails a direct relationship between quantitative and qualitative aspects, due to the intrusion of saline waters in response to over-abstraction events.

The effective protection of this aquifer system is of strategic importance for the Maltese islands due to the important contribution it provides to Malta's water production resource base. Groundwater abstraction from the MSLA contributes around 34% of the municipal water supply, whilst also sustaining around 40% of the water demand of the agricultural sector. The collapse of this aquifer system would therefore have social, economic and environmental repercussions on the country. Malta's 2nd RBMP introduces a water management framework intended to offer a high level of protection to groundwater resources by promoting the conjunctive use of water demand management and water supply augmentation measures. This management framework seeks to introduce alternative water resources to supplement groundwater supplies thus easing the pressures on these fragile natural resources.

The 2nd RBMP identifies Climate Change as another important factor which needs to be engrained in Malta's medium to long-term water management frameworks. The impacts of Climate Change are expected to lead to changes in rainfall patterns (lower rainfall depth and increased propensity of high intensity rain events) and increasing temperatures, both of which can potentially have a profound effect on groundwater resources. In the case of the MSLA, the impacts of these changes could be further compounded by impacts related to sea-level rise. The studies undertaken under the TACTIC project attempt to model the effect of these Climate Change impacts on the status of the Malta Mean Sea Level aquifer system, in order to enable these impacts to be considered during the development of current water management frameworks such as the 3rd RBMP.

3.1   Site description and data

3.1.1 - Location

The Mean Seal Level aquifer system is developed over an area of 216km² in the island of Malta. It is bounded by the Pwales fault (a natural impermeable boundary) to the North, and by the freshwater-saltwater interface at the coast. The groundwater body is sustained in the Lower Coralline Limestone formation and the Globigerina Limestone formation where this occurs at sea-level.
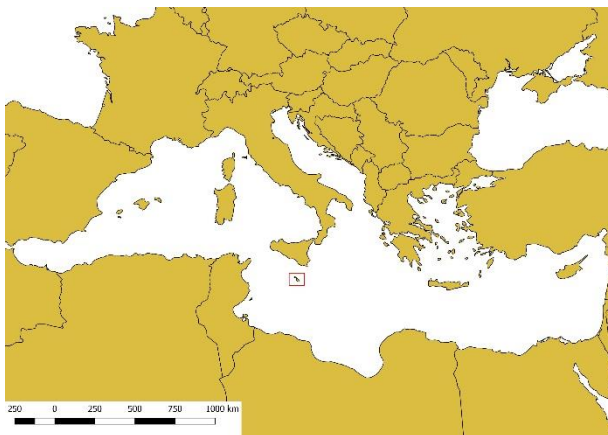

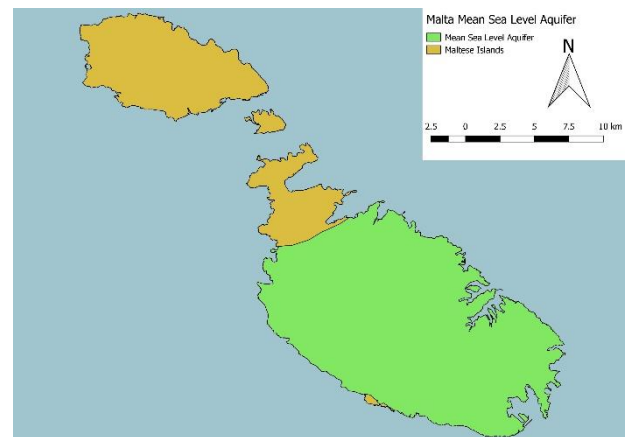Figure 1 - Location of the Maltese Islands (marked in red)

Figure 2 - Extent of the Malta Mean Sea Level Aquifer System

3.1.2 – Climate

The climate of the Maltese Islands is typically semi-arid Mediterranean with characteristic mild, wet winters and hot, dry summers. The average annual precipitation is of 550mm. Rainfall exhibits a high intra-annual variability with some years being excessively wet, whilst other relatively dry. The seasonal distribution of rainfall defines a wet period between the months of October and March (with around 85% of the total annual rainfall occurring during this period), and a dry period between April to September. Another important characteristic of the semi-arid climate is the high natural losses of water due to evapotranspiration. In fact the potential evapotranspiration rate (Penman Monteith) for the Maltese islands is estimated at 1391mm, whilst the effective evapotranspiration is estimated to exceed 60% of the mean annual rainfall. Evapotranspiration and losses due to surface runoff further limit the natural recharge to the aquifer systems.

The main climatic characteristics that are of particular relevance to water management include:
- high variability in interannual and intra-annual rainfall;
- high-intensity, short-duration rainfall events;
- seasonal scarcity of precipitation when the water requirements of the agriculture and tourism sectors are highest (normally from June to August);

- frequent occurrence of low rainfall years when groundwater recharge is likely to be low; and
- frequent occurrence of high rainfall years when runoff is likely to be high.

3.1.3 - Topography

The Maltese islands present a generally flat topography gently sloping from the highlands in the west to the coastal areas in the east. The highest elevations in the island, located on the Rabat-Dingli plateau reach around 250m above mean sea-level. Deep incised or broad dry-valley systems guide the flow of rainwater runoff in an eastern direction long this sloping terrain, the valley typology depending on the nature of the outcropping geological formations. These valley systems serve as the main natural drainage lines for the conveyance of rainwater runoff to the coastal zone.
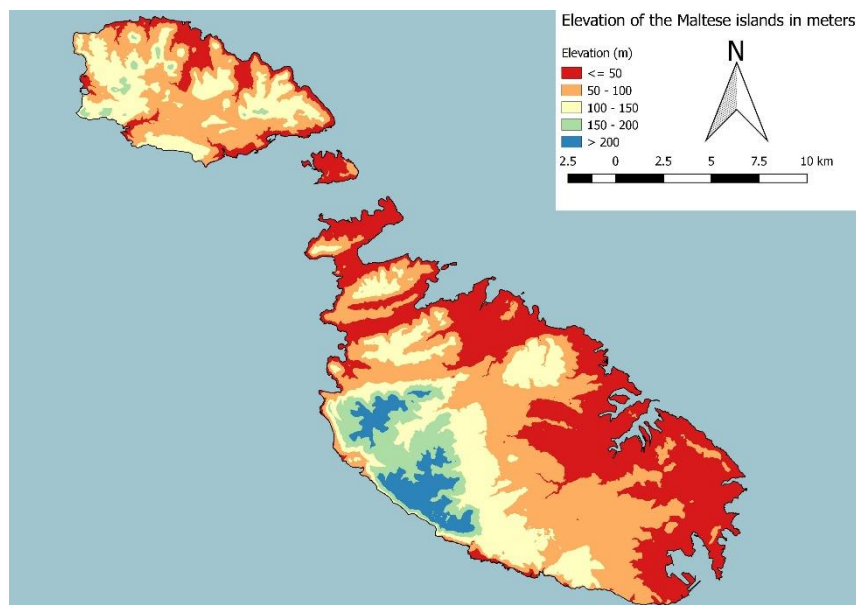
Figure 3 - Elevation Map of the Maltese Islands

3.1.4 – Land Use

The main land-use categories in the Maltese islands are Urban and Agricultural areas which account for around 25% and 50% of the total area of the Islands respectively. The Maltese islands thus present an uncharacteristically high rate of urban development, arising primarily due to the high population density of the island, which at around 1500 inhabitants/km^2 is by far the highest in Europe.

The high population density also leads to an intensive use of available land resources, which results in a mixed-land use scenario, which is not common in larger continental countries.

Various activities are thus commonly found operating side by side, and large areas of pristine land are generally lacking.
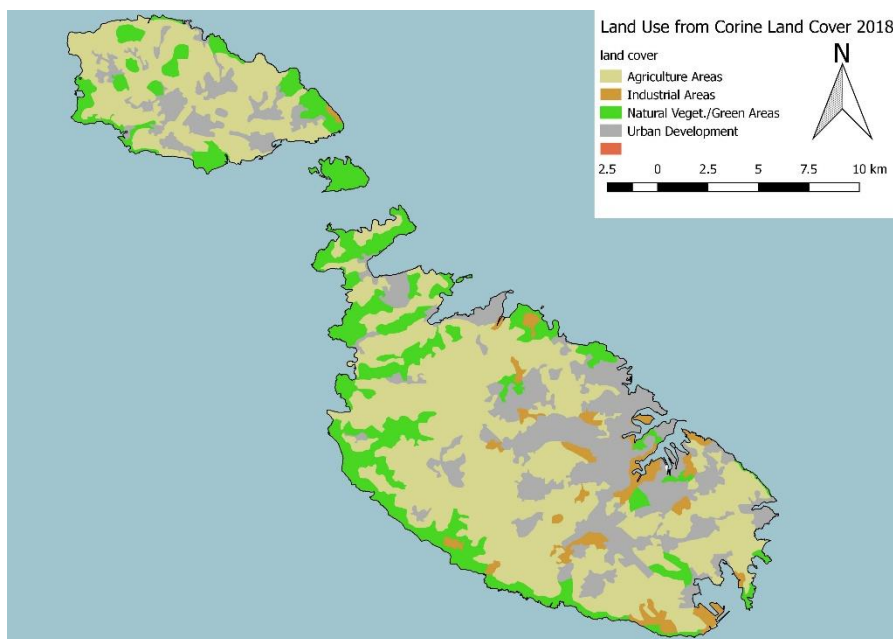
Figure 4 - Land-Use Map of the Maltese Islands (CORINE 2018)

3.1.5 – Soil Types

Maltese soils are derived from local geology, are highly calcareous and affected by cultural elements. D. M. Lang (1960) classified Maltese soils formations as Carbonate, Xerorendzinas, Terra and soil complexes, further subdivided into subtypes (series) named after the localities where the first examples were noted. The depth of the soil and soil material is very variable. On the ridges, plateau and plains (erosion surfaces), the soils are very shallow ranging in depth from less than 20cm to about 60cm. Deeper soils occur only in isolated pockets. In valleys, the soils are deeper (150cm), but patches of shallow soils are very common, especially near the valley edges.

3.1.6 – Geology and aquifer type

3.1.6.1 - Geology

The geology of the Maltese islands compromises a succession of tertiary limestones and marls with scarce Quaternary deposits. Essentially, the islands are geologically made up of a core of clays and marls, the Blue Clay and the Globigerina Limestone formations stacked between two coralline limestone formations known as the Upper and the Lower Coralline Limestone. The oldest formation, the Lower Coralline Limestone is chronologically dated to the Upper Messinian age and possibly extending into the early Pliocene.

The lithological different natures of these formations, together with their geological position enable the development of two broad aquifer typologies: the upper aquifers (perched), in the Upper Coralline Limestone and the lower (mean sea-level) aquifers in the lower limestone units (the Lower Coralline Limestone and where fractured the Globigerina Limestone).

The Upper and Lower Coralline Limestones are therefore considered to function as the main aquifer formations in the islands. The Globigerina Limestone functions only locally as an aquifer formation, only where it is fractured and/or is located at sea level, and is commonly expected to allow groundwater flow exclusively through fractures and fissures. The Blue Clay is normally impermeable and underlines the perched aquifer systems.

3.1.6.2 – Aquifer typology

The Lower Coralline Limestone formation represents the most important aquifer formation of the Maltese islands, sustaining the major sea level groundwater bodies, which by far are the primary sources of freshwater for the islands. As the formation is predominantly composed of algal limestone with sparse corals, it has moderate, irregular and channel-like permeability.

The largest and by far the most important of these sea level bodies of groundwater is the mean sea level aquifer system occurring in the island of Malta. This aquifer stretches across and area of 216km^2, primarily south of the bounding Pwales fault. The body of groundwater sustained by the Malta MSLA yields an estimated 66% of the total groundwater abstracted in the country and under optimum conditions, the aquifer system is estimated to be capable of storing up to 1.5 billion m^3 of groundwater.
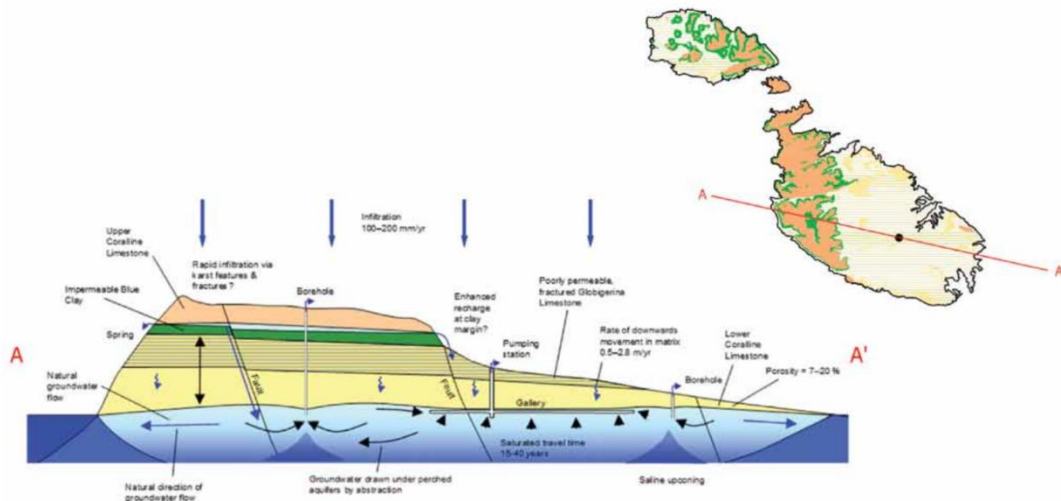

Figure 5 - Conceptual Understanding of the Malta Mean Sea Level Aquifer System

The groundwater body occurring in this sea level aquifer system is in lateral and vertical contact with seawater. Due to the density contrast of freshwater and saltwater a Ghyben-Herzberg system is developed. The outcome is a lens shaped body of freshwater that is dynamically

floating on more saline water, having a convex piezometric surface and conversely a concave interface, both tapering towards the coast where there is virtually no distinct definition between the two surfaces. Maximum hydraulic heads of 4-5m amsl were measured for the groundwater sustained in the Malta MSLA in the 1940s, when the system was largely unexploited. The lens sinks to a depth below sea level roughly 40 times its piezometric head at any point, fading into more saline water across a transition zone, the thickness of which highly depends on the hydrodynamic characteristics of the aquifer formation, and the dynamic effects of pumping. The limits of this transition zone are commonly defined by the surface of the 1% and 95% seawater context, based on the total dissolved solids, or chloride content.

3.1.7 – Surface water bodies

The small size and geomorphology of the islands precludes the development of economically exploitable surface water resources such as rivers and lakes. Inland surface water systems are generally very small and limited to specific areas in dry valley systems in the vicinity of perched aquifer springs.
.

3.1.8 – Abstraction/Irrigation

Groundwater abstraction, from all the groundwater bodies in the Maltese Water Catchment District, is estimated to reach around 38 million m^3, or 61% of the total national water demand. The sector with the highest dependence on groundwater resources was the agricultural sector, which accounted for almost half of the total groundwater abstraction in the Maltese islands.

Groundwater abstraction tends to have a regional dimension, with the perched aquifer systems being important groundwater sources to sustain the traditional irrigated land-areas of the Maltese islands, whilst abstraction by the Water Services Corporation gains more relevance in the mean sea-level aquifer systems.

The assessments leading to Malta's 2nd RBMP classified the mean sea level aquifer system as being under poor quantitative status, namely that the mean annual abstraction is estimated to exceed the mean annual recharge. The 2nd RBMP identifies groundwater abstraction of municipal supply purposes as the most important groundwater abstraction typology from this aquifer system, followed by abstraction for agricultural irrigation. The water balance framework of the MSLA is presented in figure 6 below. The water balance assessment outlines the quantitative pressures on the aquifer system, with water outflows from the system being estimated at higher levels to water inflows in the system.
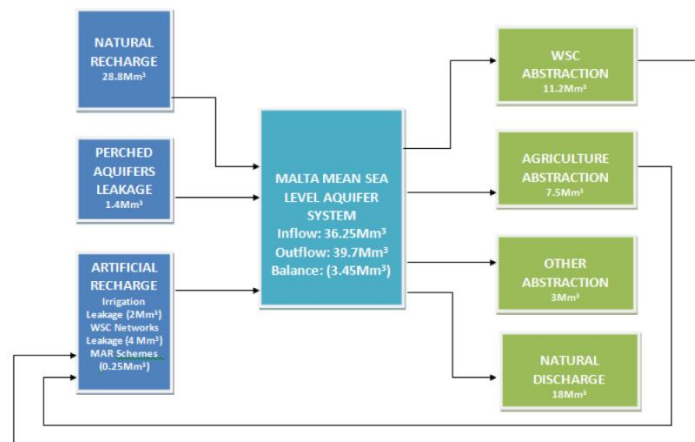
Figure 6 - Water Balance Assessment for the Malta Mean Sea Level Aquifer system (2nd RBMP)

3.2 Climate change challenge

In the Mediterranean region, climate change is expected to negatively affect water resources and current climate change studies outline the following expectations:

- An increase in air temperature in the range of 2.2 C° to 5.1 C° for the countries of the Mediterranean region by 2100 with respect to the period 1980 – 1999 (IPCC 2007, scenario A1B);
- A significant decrease in rainfall, ranging between -4 and -27 % for the countries of the Mediterranean region (IPCC 2007, scenario A1B);
- Extreme events, such as heat waves, droughts or floods, are likely to be more frequent and violent.
- An increase of the sea level which, according to specific studies, could be around 35 cm up to the end of the century.

In the case of the Maltese islands, Climate Change is thus expected to result in the gradual increase in temperature and the decrease in the mean annual rainfall. The increasing temperatures would also entail an increase in natural water losses due to evapotranspiration which would lead to increased irrigation requirements. Rainfall patterns are also expected to change, with a prevalence of more high intensity rain events and increased periods with less precipitation, both factors contributing to lower recharge rates to groundwater. These important changes would also be complemented by a rise in sea-level, which however is considered as being of less importance with regards to the development of the sea-level aquifer systems.
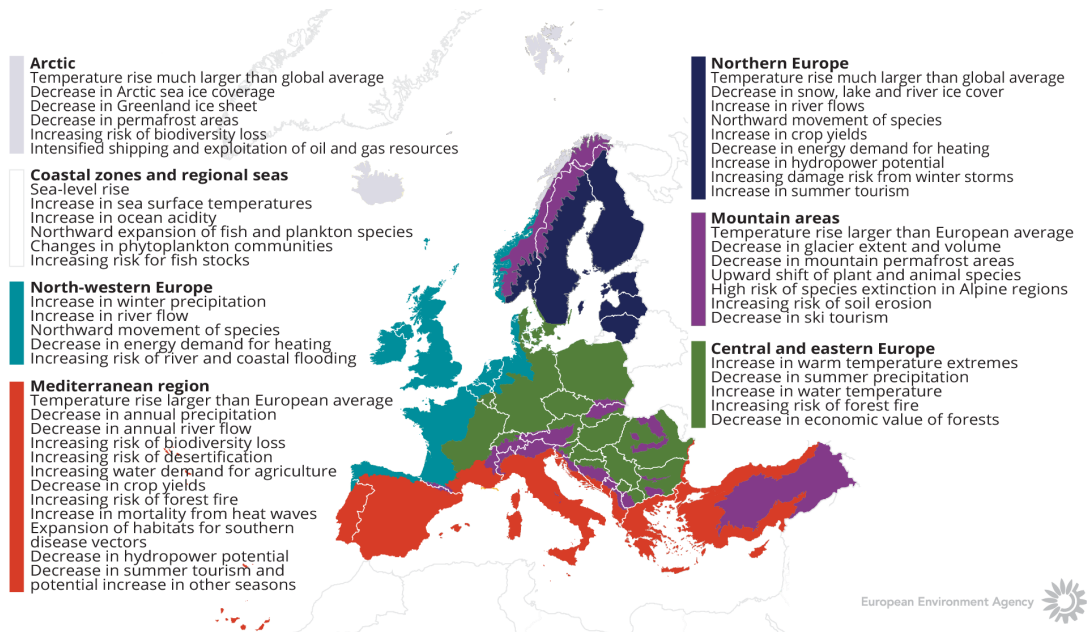
Arctic
Temperature rise much larger than global average
Decrease in Arctic sea ice coverage
Decrease in Greenland ice sheet
Decrease in permafrost areas
Increasing risk of biodiversity loss
Intensified shipping and exploitation of oil and gas resources

Coastal zones and regional seas
Sea-level rise
Increase in sea surface temperatures
Increase in ocean acidity
Northward expansion of fish and plankton species
Changes in phytoplankton communities
Increasing risk for fish stocks

North-western Europe
Increase in winter precipitation
Increase in river flow
Northward movement of species
Decrease in energy demand for heating
Increasing risk of river and coastal flooding

Mediterranean region
Temperature rise larger than European average
Decrease in annual precipitation
Decrease in annual river flow
Increasing risk of biodiversity loss
Increasing risk of desertification
Increasing water demand for agriculture
Decrease in crop yields
Increasing risk of forest fire
Increase in mortality from heat waves
Expansion of habitats for southern disease vectors
Decrease in hydropower potential
Decrease in summer tourism and potential increase in other seasons

Northern Europe
Temperature rise much larger than global average
Decrease in snow, lake and river ice cover
Increase in river flows
Northward movement of species
Increase in crop yields
Decrease in energy demand for heating
Increase in hydropower potential
Increasing damage risk from winter storms
Increase in summer tourism

Mountain areas
Temperature rise larger than European average
Decrease in glacier extent and volume
Decrease in mountain permafrost areas
Upward shift of plant and animal species
High risk of species extinction in Alpine regions
Increasing risk of soil erosion
Decrease in ski tourism

Central and eastern Europe
Increase in warm temperature extremes
Decrease in summer precipitation
Increase in water temperature
Increasing risk of forest fire
Decrease in economic value of forests

European Environment Agency

Figure 7 – EEA Projections for Climate Change Impacts in different regions in Europe

4   METHODOLOGY

4.1   Methodology and climate data

4.1.1   Tools/ model description

The numerical model of the Mean Sea Level aquifer system was developed using the MODFLOW-2005 numerical code (Harbaugh, 2005), mainly through the GIS-integrated user interface FREEWAT. A transient-state numerical model of the Mean Sea Level aquifer was developed, based on the conceptual model of the aquifer system. The development of the groundwater body was considered over a long-term period (1600 – 2018) to reflect its different exploitation scenarios throughout the years. The main result of the model presented the hydraulic heads (and interface) under reference conditions.

The availability of this baseline model enables the investigation of the development of the aquifer system under different scenarios. Scenario modelling is the activity that shows the usage of numerical models in a dynamic approach, namely the application of models as effective tools to assess future (or alternative) settings due to the variation of anthropic or natural conditions, such as management of water resources, abstraction policy, land use variation, climate change conditions, etc.

For the purpose of the TACTIC project, the baseline model was run on three scenarios which take into account the foreseen climate change effects on the water balance with reference to:
(i) Scenario 1: This scenario assumes an estimated decrease in infiltration caused by the existing trends in rainfall decrease and temperature rise. Applying the estimated variation of the water balance term as a consequence of the Climate Change RCP8.5 scenarios for the central Mediterranean (Malta area) an overall reduction of about 10% of the reference recharge has been calculated for the year 2050;
(ii) Scenario 2: This scenario projects an increasing abstraction for agriculture to compensate the demand due to higher losses by evapotranspiration. Whilst maintaining the recharge decrease of the 1st scenario, this second scenario increases agricultural abstraction with respect to the reference model by 10%; and
(iii) Scenario 3: This scenario focuses on sea-level rise where the sea-level at the coast is gradually increased till it reaches an elevation of +0.40m over reference conditions.

The reference model of the mean sea-level groundwater body and the testing of different groundwater management scenarios were undertaken in the frame of the implementation of the LIFE 16 IPE MT 008 Project -LIFE-IP-RBMP-Malta - Optimising the implementation of the 2nd RBMP in the Maltese River Basin District.

4.1.2   Climate data

The TACTIC standard scenarios are developed based on the ISIMIP (Inter Sectoral Impact Model Intercomparison Project, see www.isimip.org) datasets. The resolution of the data is 0.5°x0.5°C global grid and at daily time steps. As part of ISIMIP, much effort has been made to standardise the climate data (a.o. bias correction). Data selection and preparation included the following steps:

1. Fifteen combinations of RCPs and GCMs from the ISIMIP data set where selected. RCPs are the Representative Concentration Pathways determining the development in greenhouse gas concentrations, while GCMs are the Global Circulation Models used to simulate the future climate at the global scale. Three RCPs (RCP4.5, RCP6.0, RCP8.5) were combined with five GCMs (noresm1-m, miroc-esm-chem, ipsl-cm5a-lr, hadgem2-es, gfdl-esm2m).
2. A reference period was selected as 1981 – 2010 and an annual mean temperature was calculated for the reference period.
3. For each combination of RCP-GCM, 30-years moving average of the annual mean temperature where calculated and two time slices identified in which the global annual mean temperature had increased by +1 and +3 degree compared to the reference period, respectively. Hence, the selection of the future periods was made to honour a specific temperature increase instead of using a fixed time-slice. This means that the temperature changes are the same for all scenarios, while the period in which this occur varies between the scenarios.
4. To represent conditions of low/high precipitation, the RCP-GCM combinations with the second lowest and second highest precipitation were selected among the 15 combinations for the +1 and +3 degree scenario. This selection was made on a pilot-by-pilot basis to accommodate that the different scenarios have different impact in the various parts of Europe. The scenarios showing the lowest/highest precipitation were avoided, as these endmembers often reflects outliers.
5. Delta change values were calculated on a monthly basis for the four selected scenarios, based on the climate data from the reference period and the selected future period. The delta change values express the changes between the current and future climates, either as a relative factor (precipitation and evapotranspiration) or by an additive factor (temperature).
6. Delta change factors were applied to local climate data by which the local particularities are reflected also for future conditions.

Precipitation and Evapotranspiration projections were based on HadGEM2-ES data for the RCP8.5 scenario (3 degree global change – maximum), whilst precipitation projections were based on GFDL-ESM2M data for the RCP8.5 scenario (3 degree global change – minimum).

The tables below outline the estimated variation of the water balance term in the model as a consequence of the Climate Change data projections available for the Maltese islands, through the application of the foreseen variation of precipitation, temperature and evapotranspiration. The water balance terms were applied in the numerical model to develop the Climate Change scenarios.

Temperature (Deg C)	Oct	Nov	Dec	Jan	Feb	Mar	Apr	May	Jun	Jul	Aug	Sept
Average temperature (1980-2010)	21.5	17.6	14.2	12.7	12.5	13.9	16.0	19.7	23.8	26.6	27.1	24.6
T change under 3 deg C global change (max)	2.0	1.8	1.9	1.7	1.7	1.7	1.8	2.0	2.1	2.3	2.1	2.1
Projected Temperature	23.5	19.4	16.1	14.4	14.2	15.6	17.8	21.6	25.9	28.8	29.2	26.7

Precipitation (mm/month)	Oct	Nov	Dec	Jan	Feb	Mar	Apr	May	Jun	Jul	Aug	Sept
Average PR (1980-2010_	68.6	102.9	108.6	92.9	56.9	37.9	20.8	8.5	4.0	0.2	5.6	56.0
Change in PR under 3 deg global change (min)	0.924	0.814	0.683	0.686	0.503	0.745	0.930	0.677	0.500	1.000	0.762	0.701
Projected Precipitation for scenario (2050)	63.43	83.75	74.22	63.72	28.63	28.26	19.35	5.77	2.01	0.21	4.26	39.29

Potential Evapotranspiration (mm/month)	Oct	Nov	Dec	Jan	Feb	Mar	Apr	May	Jun	Jul	Aug	Sept
Average PET (1980-2010)_	97.6	66.9	46.0	36.0	29.5	37.2	44.5	64.2	87.6	116.6	131.3	114.4
Change in PET under 3 deg global change (max)	1.052	1.050	1.060	1.056	1.056	1.053	1.053	1.052	1.051	1.051	1.046	1.048
Projected PET for scenario (2050)	102.7	70.3	48.8	38.0	31.1	39.2	46.8	67.5	92.1	122.6	137.4	119.9

Table 1: Temperature, Precipitation and Evapotranspiration Projections for the water balance assessment of the Malta Mean Sea Level Aquifer System

4.2 Tool(s) / Model set-up

The main settings of the model are summarized in Table 2 below. In transient state, stress periods related to the abstraction of groundwater and other water losses and the temporal and spatial redistribution of natural recharge were included.

Domain	Width ~19 km (along the SW-NE direction), length ~27 km (along the NW-SE direction) with a rotation of 53°.
Horizontal discretization	Cell size 100x50m; total 105536 cells, 388 rows by 272 columns.
Active domain	1022386 cells.
Vertical discretization	1 model layer, representing the lithology Globigerina Limestone (GL) and Lower Coralline Limestone (LCL). The model top is set as the top of GL. The elevation of model bottom is firstly calculated as (TOP-180m), to mimic a constant saturated thickness. Where this returns a bottom elevation higher than -180 m, the value is lowered to -180 m, so that eventually almost the whole aquifer has a constant bottom equal to -180 m.
Boundary conditions	The sea level is represented by the third type condition (GHB – General Head Boundary package in MODFLOW). A value of 0.15 m is set to represent the sea level (slight larger than in the steady state model after an analysis of tidal variation over the years of interest). The conductivity of GHB is a value parametrized and object of calibration, with a starting value of 50 m2 /day. The

	main faults in the islands are accounted for by applying the HFB (Horizontal Flow Barrier) package of MODFLOW code. For all cells the same value of HFB input parameters is used, namely K = 8.64 m/day for fault hydraulic conductivity and 1 m as fault thickness. Estimation of the conductivity is done along the calibration process. Galleries, public boreholes and private wells are represented as WEL package, same as the water losses from pipes which inject water rather than extracting it from the system.
Hydrogeological parameters	Horizontal hydraulic conductivity values are object of calibration (with associated prior information from the data analysis). Vertical hydraulic conductivity is supposed to be 1/10 of the horizontal one. Storage coefficient and porosity are assumed to be constant all over the domain with the following values: porosity = 0.2; specific storage = 5E-6 − 1E6 m-1; specific yield = 0.05 - 0.1 (Freeze and Cherry, 1979)

Table 2: Main Characteristics of the numerical model for the Malta MSLA

4.3   Tool(s)/ Model calibration/ test

The calibration process was set to adjust the parameters not only to reproduce the observed heads, but also to respect the parameters' prior information, trying to find the agreement between hard and soft data along with the model behavior.

In order not to overfit the heads (i.e., calibrating "too well"), heads observations were provided a weight proportional to their reliability, and the measurement Objective Function was assigned a lower threshold, given the uncertainty of the original data. Elements that were taken into account in setting a threshold for the measurement Objective Function were:
- the geostatistical interpolation of heads which provided a RMSE of 0.43 m;
- the average SD of heads time series is about 0.2 m;
- the borehole elevation error, which can be higher than 1 m in places;
- the tidal oscillations which make the heads oscillate accordingly, with differences that range from a few millimetres to 0.2-0.3 m.

Considering the above list, the Objective Function was set to provide a RMSE related to heads residuals not lower than 0.43 m.

Besides heads, additional "parameter observations" were added to the calibration process in order to make the inverse problem solvable. The weight assigned to the prior information was iteratively adjusted to reach a compromise between respecting the head data given the above constraints, while limiting the overfitting with advantage of the parameter preferred value coherence.
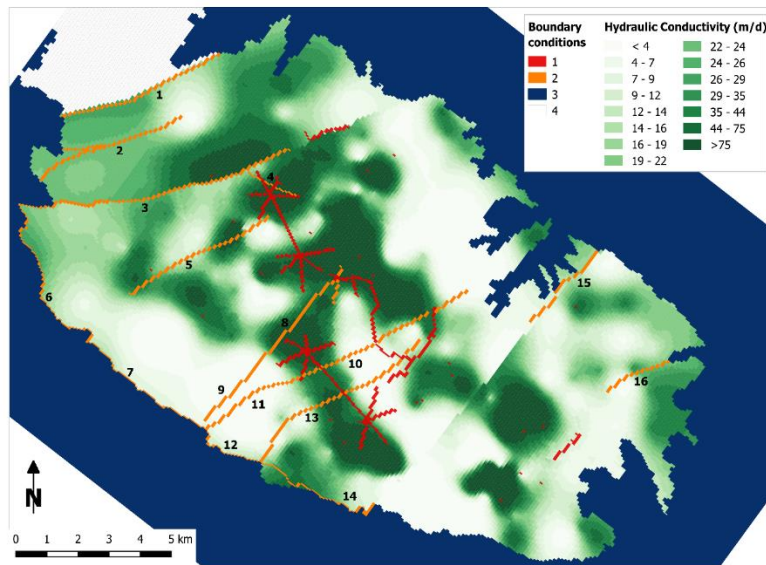
Figure 8 - One of the calibration process results outlining a possible spatial distribution of the hydraulic conductivity (m/d) that calibrates the MSLA head data.

5   RESULTS AND CONCLUSIONS

The application of the Malta-MSLA numerical groundwater body model to the climate change scenarios assessed under the TACTIC project portray the development of groundwater body piezometric (and interface) levels under the additional stresses induced by climate change, and enable a comparative assessment to the aquifer development under reference conditions. The main model outputs for the reference conditions and each of the three climate change induced scenarios are represented in the plots hereunder:

(i) Reference Conditions
Simulated heads (m asl) resulting from the application of the numerical model under reference conditions are presented hereunder. The reference year is 2012.
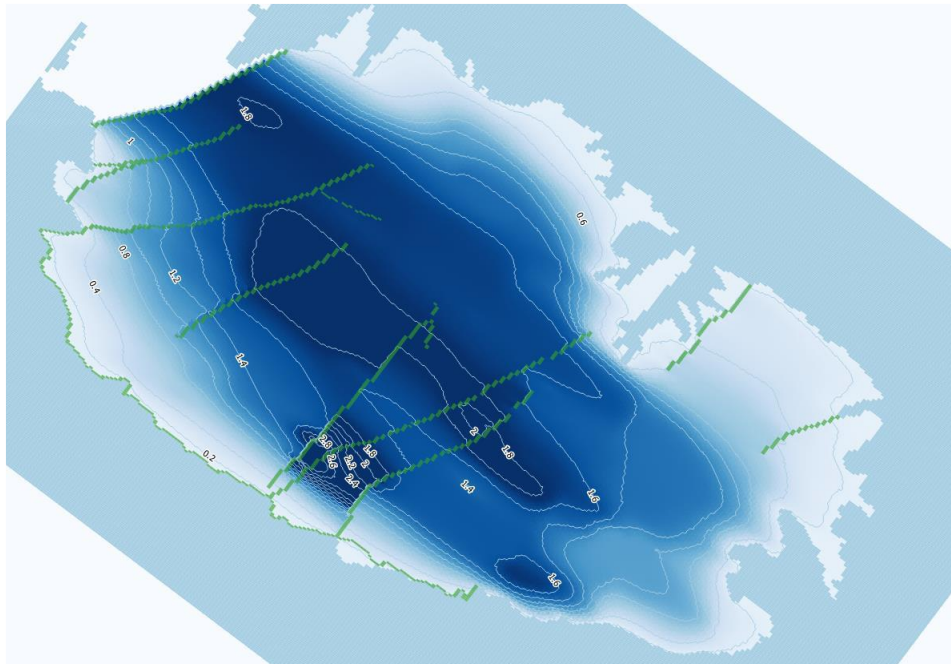
Figure 9 - Malta MSLA - Piezometric Surface under Reference Conditions (2012)

(ii) Climate Change Scenario 1 – reduction in reference recharge
Simulated heads (m asl) resulting from the application of the numerical model under the first Climate Change scenario are presented hereunder.
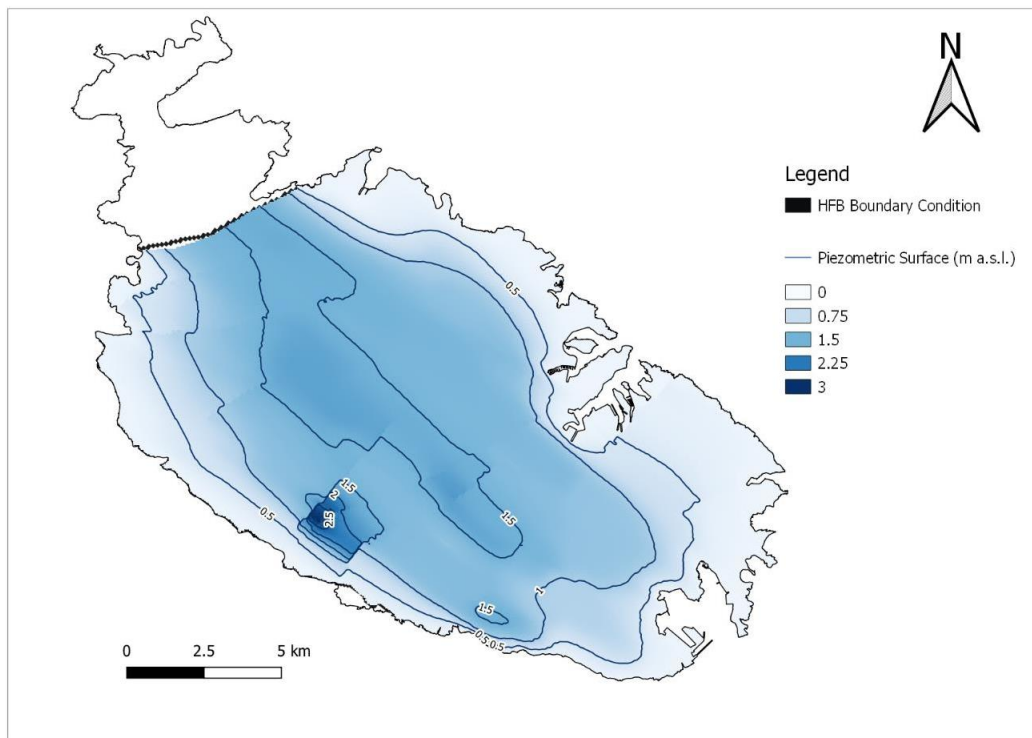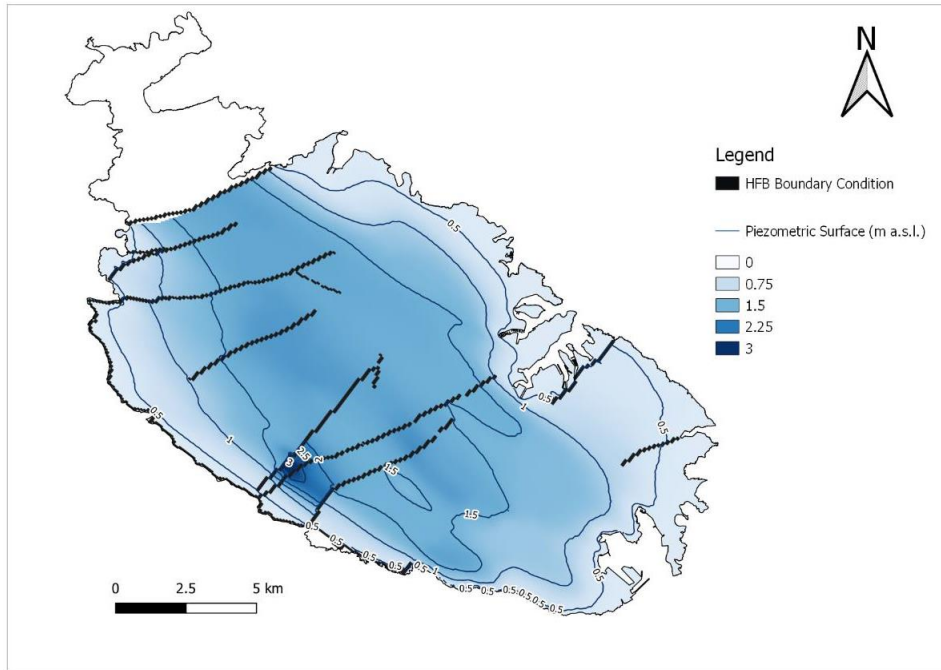
Figure 10 - Malta MSLA - Piezometric Surface under Climate Change Scenario 1 projections

(iii) Climate Change Scenario 2 – increase in agricultural groundwater abstraction
Simulated heads (m asl) resulting from the application of the numerical model under the second
Climate Change scenario are presented hereunder.
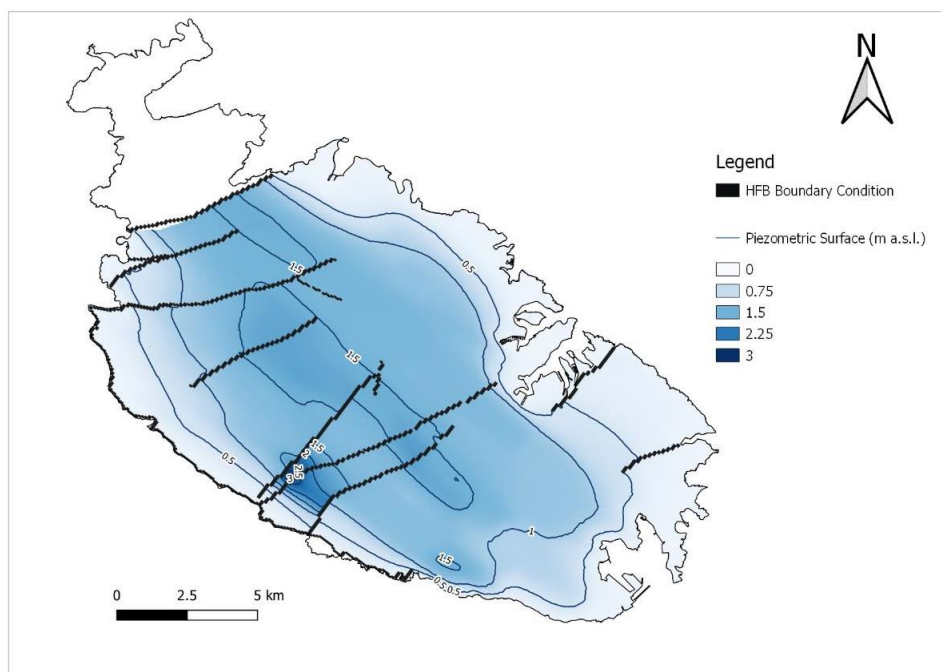
Figure 11 - Malta MSLA - Piezometric Surface under Climate Change Scenario 2 Projections

(iv) Climate Change Scenario 3 – sea-level rise

Simulated heads (m asl) resulting from the application of the numerical model under the third Climate Change scenario are presented hereunder.

Figure 12 - Malta MSLA - Piezometric Surface under Climate Change Scenario 3 projections

5.1 Results of assessments

The projected piezometric levels emerging from the application of the three Climate Change scenarios to the numerical model of the Malta mean sea-level aquifer system are summarized hereunder:

(i) Climate Change Scenario 1: the resultant piezometric levels are lower than those under the reference situation, which is an expected outcome since the piezometric head is directly dependent on the long-term mean annual recharge levels. However, the reduction in the piezometric level is generally contained to the central regions of the island, where a decline in head of up to 0.5m occurs. However, it is important to note that compared to other water management scenarios, in general, the projected impact of climate change under these conditions seems to be extremely less threatening when compared to poor groundwater management practices such as high levels of over-abstraction.

(ii) Climate Change Scenario 2: in this scenario the resultant piezometric levels are similarly lower than those under the reference condition, but the projected deterioration is close to that registered under the first scenario. In fact this scenario projects the central region of the aquifer system to maintain hydraulic heads of the order of 1.5m amsl. This could be a resulting effect of the groundwater body settling into a lower steady state (under lower hydraulic heads) which

would enable the groundwater body to sustain the marginally increased abstractions. Similarly to the first scenario, therefore, the impact of climate change seems to be extremely less threatening when compared to the impact of poor groundwater management practices. It should be noted however, that these results do not preclude further deterioration in the status of the groundwater bodies should more marked Climate Change impacts occur.

(iii) Climate Change Scenario 3: The piezometric head projected under the sea-level rise scenario are practically of the same order of the levels projected under the reference situation. The only visible effect over the aquifer volume is a boundary reduction along the coast generated by the reduction of emerged land. Therefore, also under this third scenario, the impact of climate change seems to be less marked when compared to the impacts on the aquifer systems arising due to aquifer mismanagement scenarios.

The modelled results of the three Climate Change scenarios undertaken under the TACTIC project, outline the development of a highly resilient groundwater body under conditions of reduced recharge, increased abstraction and sea-level rise. The projections seem to indicate that the groundwater body would, under the Climate Change related conditions assumed in the respective scenarios, reach lower steady state conditions. Hence, the impact of Climate Change according to the assumed climate models would not be expected to result in a severe impact on the mean-sea level groundwater body.

However, the reduced piezometric levels registered under each scenario would make the groundwater body more vulnerable to aquifer mismanagement practices such as over-abstraction. The conditions prevailing under the three Climate Change scenarios would facilitate the occurrence of localized sea-water intrusion and the salinization of wells under abstraction conditions. Hence, the need for the development of sound aquifer management frameworks to enable the sustainable management of this groundwater body of strategic national importance.

6 REFERENCES

- Adaptation to Climate Change | Malta Resources Authority. 2019. *Adaptation to Climate Change | Malta Resources Authority*. [ONLINE] Available at: http://mra.org.mt/climate-change/adaptation-to-climate-change/. [Accessed 10 January 2019]

- Barbagli, A., et. al, 2021. Geological and hydrogeological reconstruction of Maltese archipelago's main aquifers, submitted.

- De Filipps, G., et. al, 2017. The FREEWAT platform for the assessment of water availability and quality. *Acque Sotterranee – Italian Journal of Groundwater, 6(3/149);65-66, in Italian.*

- Environment and Resources Authority, E., 2011. *The First Water Catchment Management Plan*. 1st ed. Malta: Environment and Resources Authority.

- European Investment Bank, Study on Climate Change and Energy in the Mediterranean, EIB 2008.

- Freeze R.A. and Cherry J.A. (1979). Groundwater: Englewood Cliffs, NJ, Prentice-Hall.

- Galdes, C., 2011. *The Climate of Malta: statistics, trends and analysis*. 1st ed. Malta: National

- Lang, D.M, 1960. Soils of Malta and Gozo. Colonial Research Series N.29, London: HMSO

- Lotti, F., et. al, 2021. Numerically enhanced conceptual modelling (NECom) applied to the Malta Mean Sea Level Aquifer. *Hydrogeology Journal, in press.*

- Malta Environment and Planning Authority, M., 2006. *State of the Environment Report 2005*. 1st ed. Malta: Malta Environment and Planning Authority.

- Mangion, J., et. al, 2008. *The Mean Sea Level Aquifer, Malta and Gozo*. 1st ed. United Kingdom: Blackwell Publishing Ltd.

- Macdonald, D M J et al 2020. Review of existing studies and documentation on hydrological and hydrogeological characteristics of the Maltese islands: CT3069/2019 – Activity 1.2 Report. *British Geological Survey Commissioned Report,* CR/20/052. 113 pp.

- Pedley, M., 2002. *Limestone Isles in a Crystal Sea - The Geology of the Maltese Islands*. 1st ed. Malta: Publishers Enterprises Group

-   Schembri, P., 1997. *The Maltese Islands: Climate, vegetation and landscape*. 1st ed. Netherlands: GeoJournal

    Sustainable Energy and Water Conservation Unit,, 2015. *The 2nd Water Catchment Management Plan for the Malta Water Catchment District 2015 - 2021*. Malta

-   Vella, S., 2001. *Soil information in the Maltese islands*. 1st ed. Bari: CIHEAM.

Deliverable 5.3 and 6.3

PILOT DESCRIPTION AND ASSESSMENT

Plana de Oropesa-Torreblanca

Authors and affiliation:

David Pulido-Velazquez, Leticia Baena-Ruiz, AJ. Collados-Lara, Juan de Dios Goméz-Gómez.

Geological Survey of Spain (IGME)

Version	Final version
Date	05/11/2020

[This page has intentionally been left blank]

[This page has intentionally been left blank]

LIST OF ABBREVIATIONS & ACRONYMS

CC	Climate Change
GC	Global Change
LULC	Land Use and Land Cover
SWI	Sea Water Intrusion
GSO	Geological Survey Organisations

TABLE OF CONTENTS

1 EXECUTIVE SUMMARY

Pilot name	Plana de Oropesa-Torreblanca	
Country	Spain	
EU-region	Mediterranean region	
Area (km²)	89 km²	
Aquifer geology and type classification	Coastal sedimentary plain (gravel and sand levels in a silty clay matrix). Porous aquifer.	
Primary water usage	Irrigation / Drinking water	
Main climate change issues	The increasing population since 1970, especially in summer, and the transformation from dry to irrigated croplands led to an increase in pumping volume that extended over two decades (1975-1995, especially in the period 1985-1995), provoking a drop in groundwater level and seawater intrusion (SWI) problems. From 1995 to 2010 there was a progressive reduction in pumping due to the abandonment of certain crops and irrigated areas. Impact studies are proposed to assess status and vulnerability taking into account future climatic and global change (GC) scenarios. In general, in the Mediterranean area an increase in temperature and a decrease in precipitation are expected. The available potential future scenarios show higher evapotranspiration, a lower groundwater recharge and an increase of the sea level. In coastal areas the problem is exacerbated due to overexploitation, intensifying SWI. In order to reduce the impacts of climate change (CC) on SWI, different adaptation strategies could be applied. Measures to reduce aquifer demands (Adaptation strategies are mainly focused on changes Land Use and Land Cover in the area) and measures on the offer (eg. Water reuse) could be applied to obtain complementary resources to supply demands.	
Models and methods used	Generation of potential future climate change scenarios and definition of adaptation scenarios (Land Use and Land Change scenrios and complementary resources to supply demands). Propagation with a chain of auxiliary models (recharge, agricultural) to generate inputs for a density dependent flow model (The finite-difference numerical code SEAWAT). An index method to summarize results using different spatial resolution (maps, cross sections and lumped indices). Distributed model (3D finite-difference numerical code SEAWAT); index method.	

Key stakeholders	Jucar River Basin Authority, agricultural associations, water supply companies.
Contact person	L. Baena and D. Pulido, IGME (Spain), l.baena@igme.es; d.pulido@igme.es

The Plana de Oropesa-Torreblanca aquifer is a detrital Mediterranean aquifer, which extends over 75 km^2. This Plio-Quaternary aquifer is unconfined and heterogeneous and consists of a silty clay matrix with gravel and sand levels. The aquifer is wedge shaped and it can reach 90 m thickness near the coast. The transmissivity varies between 300 and 1000 m^2/day and the storage coefficient ranges from 2 to 12%. In the study area, there have been important land use changes from the 1970s. Before 1995 there was a significant transformation in the crop water demand due to new irrigated lands appeared. From this date to 2010, the main change was an increase of artificial surfaces (mainly residential Lan Use and Land Cover [LULC] along the coast) and an improvement in the efficiency of irrigation techniques. Pumping was deduced from historical data. The mean annual pumping in the historical period is 22 Mm^3/year approximately. The land use changes are reflected in the evolution of total pumping in the Plana de Oropesa-Torreblanca aquifer. First, the transformation into irrigated croplands from 1975 to 1995 produced an increase in pumping from 15 Mm^3/year to a maximum of 35 Mm^3/year. It produced a drop in Groundwater level and higher SWI problems. Later on, the transformation of irrigation techniques and land uses led to a reduction in pumping to a minimum rate around 13 Mm^3/year. Nevertheless, SWI has been a significant issue in this aquifer during the historical period that might be exacerbated in the future. Therefore, the main challenge of this work is to assess and summarise impacts of potential future CC and GC scenarios on SWI in the aquifer, and to identify and study potential adaptation strategies.

An impact and adaptation assessment has been performed for future potential scenarios. Representative future CC scenarios are generated and a future LULC scenario was defined in accordance with the plan approved by the local government (PGOU Torreblanca, 2009). Four GC scenarios were defined by combining the LULC scenario and the CC scenarios. These GC scenarios and a LULC scenario without CC have been propagated to assess hydrological impact by simulating them within a coupled modelling framework based on a density-dependent model whose inputs are defined by a sequential coupling of different models (rainfall-recharge models, crop irrigation requirements and irrigation return models). Finally, based on the outputs of this chain of models, a method is applied to summarise the impacts of GC scenarios in the global status and vulnerability to SWI at the aquifer scale including some management strategies. It allows to compare the significance of the SWI problems in different historical and future periods for an aquifer and between different aquifers. The effect of CC in the GC scenarios is also analyzed.

Results show that GC scenarios would imply a greater deterioration in the aquifer than LULC scenario. The adaptation strategies will produce a reduction of pumping in some areas of the aquifer, which would reduce the impacts of the potential future LULC and GC scenarios. The lumped indices reveal that GC would involve more variability in SWI problems (global status and vulnerability) and CC would increase the degradation of the aquifer. On average, it is expected

that a greater area affected by intrusion and extreme climatic conditions might produce an increase in the vulnerability of the aquifer. GC would produce a greater impact on SWI global status than in the aquifer's vulnerability. Nevertheless, the resilience capacity of the aquifer would allow recovering from the impacts of the extreme climatic conditions.

.

2 INTRODUCTION

It is a detrital Mediterranean aquifer, which extends over 75 km^2. It has a length of 21 km and a width of between 2.5 and 6 km. This Plio-Quaternary aquifer is unconfined and heterogeneous and consists of a silty clay matrix with gravel and sand levels. The aquifer is wedge shaped and it can reach 90 m thickness near the coast. The transmissivity varies between 300 and 1000 m^2/day (Renau-Pruñonosa et al. 2016) and the storage coefficient ranges from 2 to 12%. Different Researchers and technicians from the Spanish Geological Survey (IGME) have participated in the assessment summarised in this report.

The overall objective of this study is to assess and summarise impacts of potential future CC and GC scenarios on SWI in the aquifer, and to identify and study potential adaptation strategies. SWI has been a significant issue in this aquifer during the historical period. In general, the available potential future scenarios show higher evapotranspiration, a lower groundwater recharge and an increase of the sea level. In coastal areas the problem is exacerbated due to overexploitation, intensifying SWI. In order to reduce the impacts of CC on SWI, different adaptation strategies could be applied. Measures to reduce aquifer demands (adaptation strategies are mainly focused on LULC changes in the area) and measures on the offer (eg. Water reuse) could be applied to obtain complementary resources to supply demands. In this report we analyse some potential adaptation strategies and their influence on future SWI. Therefore, the information generated could be usefull to identify and assess potential future sustainable management strategies to reduce SWI problems.

3 PILOT AREA

The Plana de Oropesa-Torreblanca is not a large coastal groundwater body (75 km^2), but it is very relevant for the local water supply and to maintain the optimal environmental conditions in a RAMSAR wetland area, "the Prat de Cabanes", which is located just above the aquifer and is hydraulically connected to it (Sanz-Garrido and Capilla 2015). There is no permanent rivers on this area and some of them only show runoff immediately after a long rainfall period. The increasing population since 1970 and the continuing agricultural exploitation have produced SWI problems of different entity in this aquifer (Baena-Ruiz et al. 2018).

This problem might be exacerbated in the future due to CC impacts. In this project we intend to assess and analyse impacts of future potential CC and GC scenarios on SWI and evaluate some adaptation strategies. We will consider measures to reduce groundwater demand (LULC changes) and measures based on the offer to obtain complementary resources to supply demands (water reuse and desalination).

3.1 Site description and data

- Location and extension of the pilot area (figure)
The Plana de Oropesa-Torreblanca aquifer is located in the Mediterranean region of EU, in the province of Castellón in Spain (See Fig. 1). It is a coastal aquifer that extends for 21 km parallel to the coast in a NE-SW direction, with a width of between 2.5 and 6 km, covering approximately 75 km^2 (Renau-Pruñonosa et al. 2016).

- - - Municipal sector
☐ Plana de Oropesa-Torreblanca aquifer
▓ Prat de Cabanes Natural park
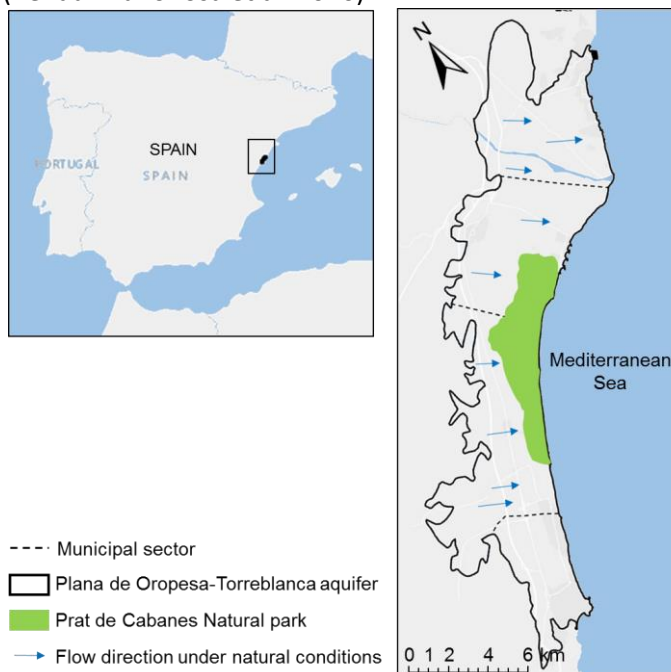→ Flow direction under natural conditions

Fig. 1. Location of the pilot area

- Geology/Aquifer type

The Plana Oropesa-Torreblanca is an unconfined, heterogeneous, detrital and multilayer aquifer composed of gravel and sand levels in a silty clay matrix (Ballesteros et al. 2016). The Plioquaternary detrital materials comprising limestone pebbles, gravel and conglomerates derived from the adjacent mountain ranges, with abundant lenses of coarse sand, silt and clays. There are frequent lateral and vertical changes in facies and the overall distribution is irregular. The aquifer is overlain by more recent alluvial fans, colluviums, dunes and peatlands. The transmissivity ranges from 300 to 1000 m^2/day (García-Menéndez et al. 2016) and the storage coefficient varies between 2 and 12%. Fig. 2 shows the geological map and two representative cross sections.
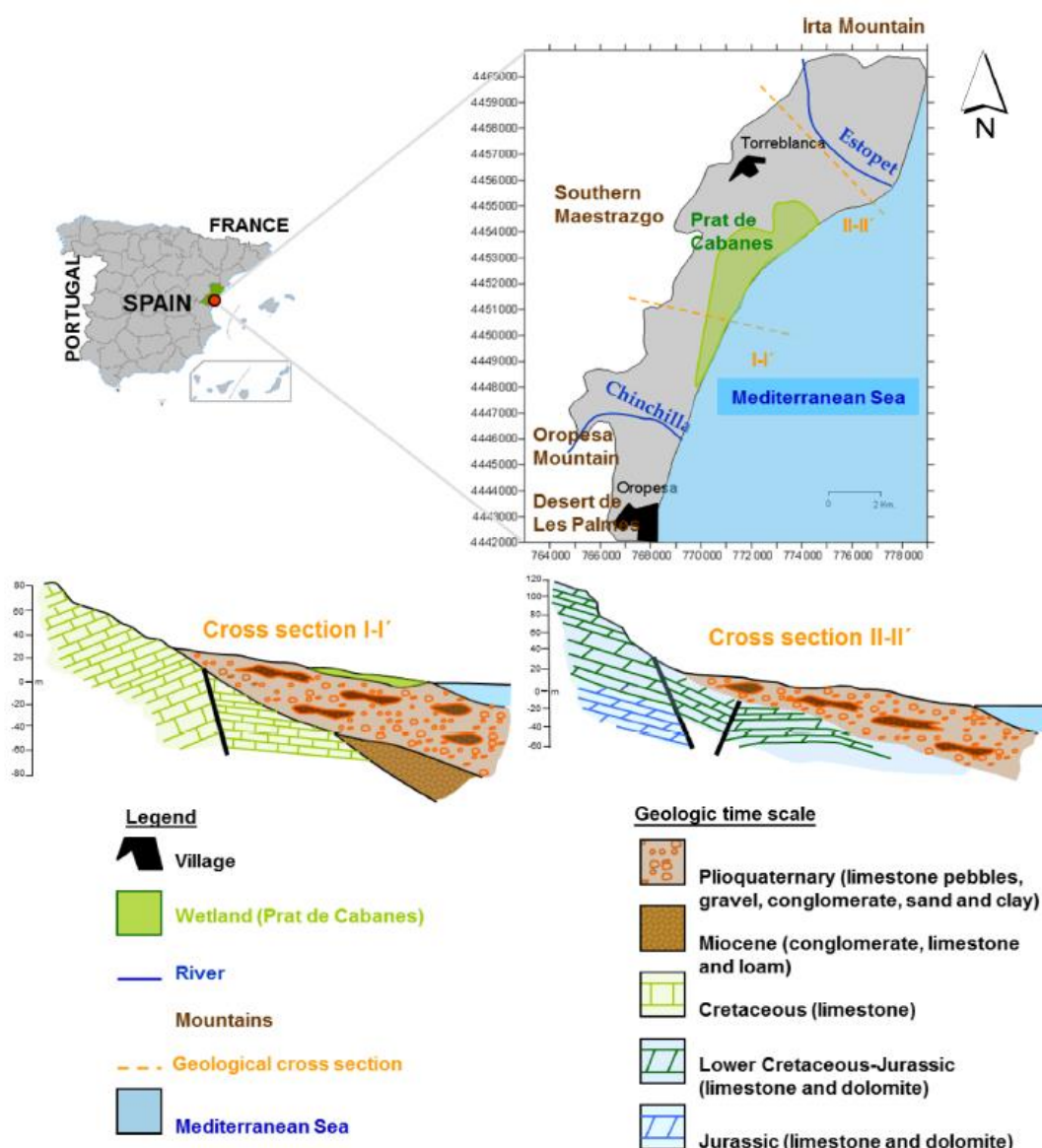
Fig. 2 Geological map and cross sections (Pulido-Velazquez et al. 2018)

- Geometry, Topography and soil types

The Plana de Oropesa Torreblanca is located in the eastern coast of Spain, in the Mediterranean Sea (Fig. 1). It is formed by an underlying aquifer which has the same name. Fig. 3 shows a representation of topography and bottom surface of the Plana de Oropesa-Torreblanca aquifer. This aquifer is wedge-shaped being the maximum thickest located near to the coastline, where it can reach 90 m thick. The area is predominantly flat and it is surrounded inland by mountain ranges. The soils in the Plana de Oropesa-Torreblanca mainly belong to the Entisol group (71.6%) and the Inceptisol group (28.4%) (IGME-DGA 2015)
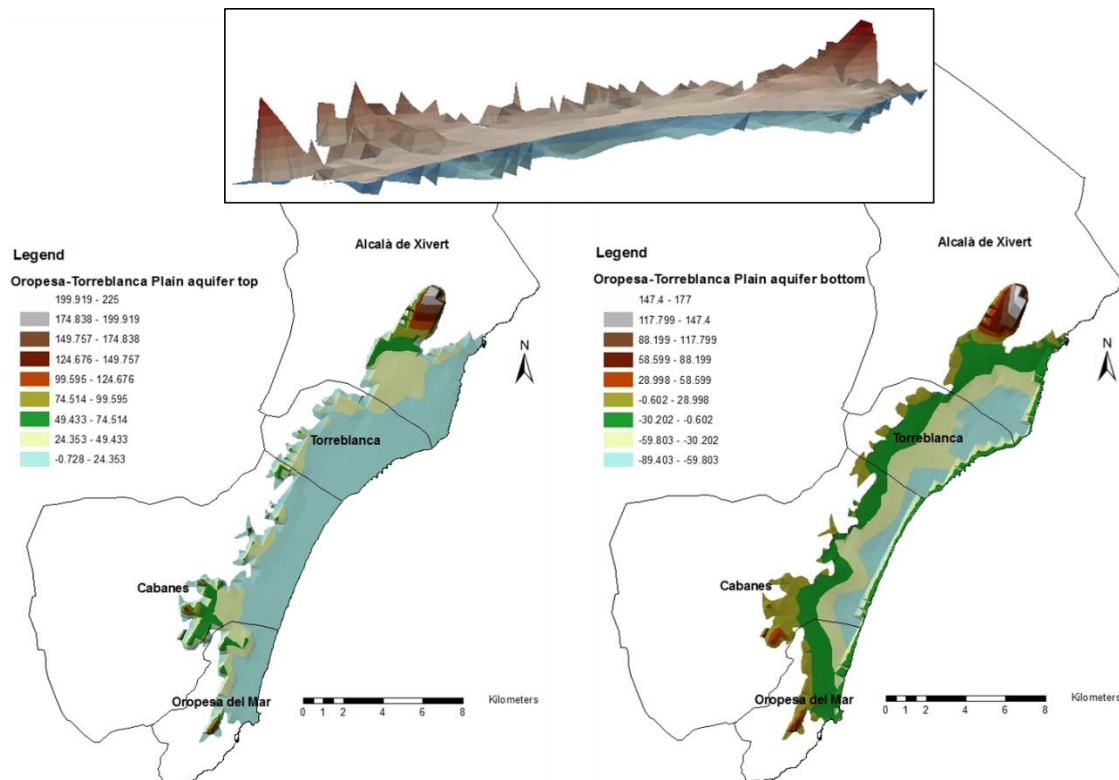
Fig. 3 Aquifer Geometry (top and bottom of the aquifer)

- *Surface water bodies*

There is a wetland area of high environmental value known as "Prat de Cabanes". It is one of the largest in the Region of Valencia (812 ha), and is listed under the RAMSAR convention (Convention on Wetlands of International Importance)—site No. 458 (RAMSAR Convention Bureau 1990). There is a well-developed typical wetland vegetation with submerged and emergent plants, halophytic and dune communities. There are also a number of endemic plants, fish, and invertebrates, and the area supports several species of nesting birds. Thus, it is also a Special Protection Area (SPA), as recognized under the European Union Directive on the Conservation of Wild Birds (Directive 2009/147/EC). The area extends from Torrenostra to Torre la Sal, with a transversal dimension of 1.5 km. It is permanently flooded, with a relatively slow process of siltation. It was developed through the long-term sedimentation of a coastal lagoon, underlain by extensive areas of peat, and is separated from the sea by a dune complex (Sanz-Garrido and Capilla 2015).

The seasonal variation of the rainfall and the groundwater table usually results in a very important reduction of the surface water in the wetland during late spring and early summer. In fact, according to the conclusions from different studies developed for the Spanish National Hydrologic Plan (Alfonso 2002), the hydrologic equilibrium of the area is seriously threatened and it is posing a severe risk for the wetland in terms of water balance and water quality (Sanz-Garrido and Capilla 2015).

- *Hydraulic head evolution*

In the Plana de Oropesa-Torreblanca the hydraulic head usually varies between 0.25 and 0.5 m near the coast and it is depressed at certain times in zones close to the coast. At points furthest from the coast the hydraulic head is about 1.5-2.5 m a.s.l. Hydraulic head decreases from June to October and increase from Novemeber to May.

The increasing population since 1970 and the continuing agricultural exploitation have produced SWI problems of different entity in these aquifers. A continuous decreasing trend is observed from 1974 in a yearly scale.

Fig. 4 shows the hydraulic head in dry, medium and wet years. The main differences are the variation in the hydraulic gradient and the appearance of inverted flow in the south and east areas. In the southern sector, there are permanent SWI problems. To the east of Torreblanca there are also situations of piezometric depression in the dry years, although they seem to be restored in the middle and wet years.
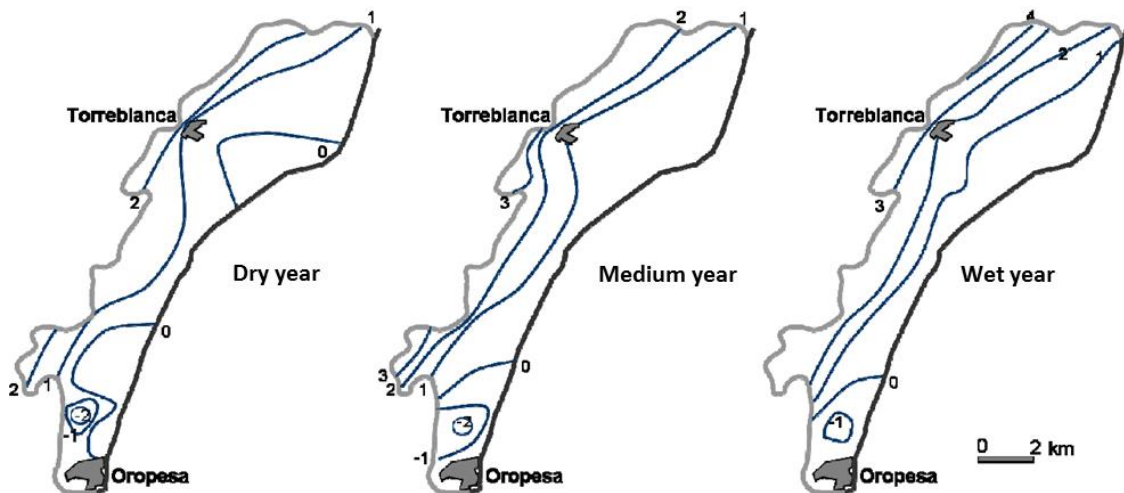

Fig. 4. Hydraulic head in dry, medium and wet years (modified from Renau-Pruñonosa 2013)

The hydraulic head tamporal evolution for some representative observation wells has been also represented in Fig. 5.
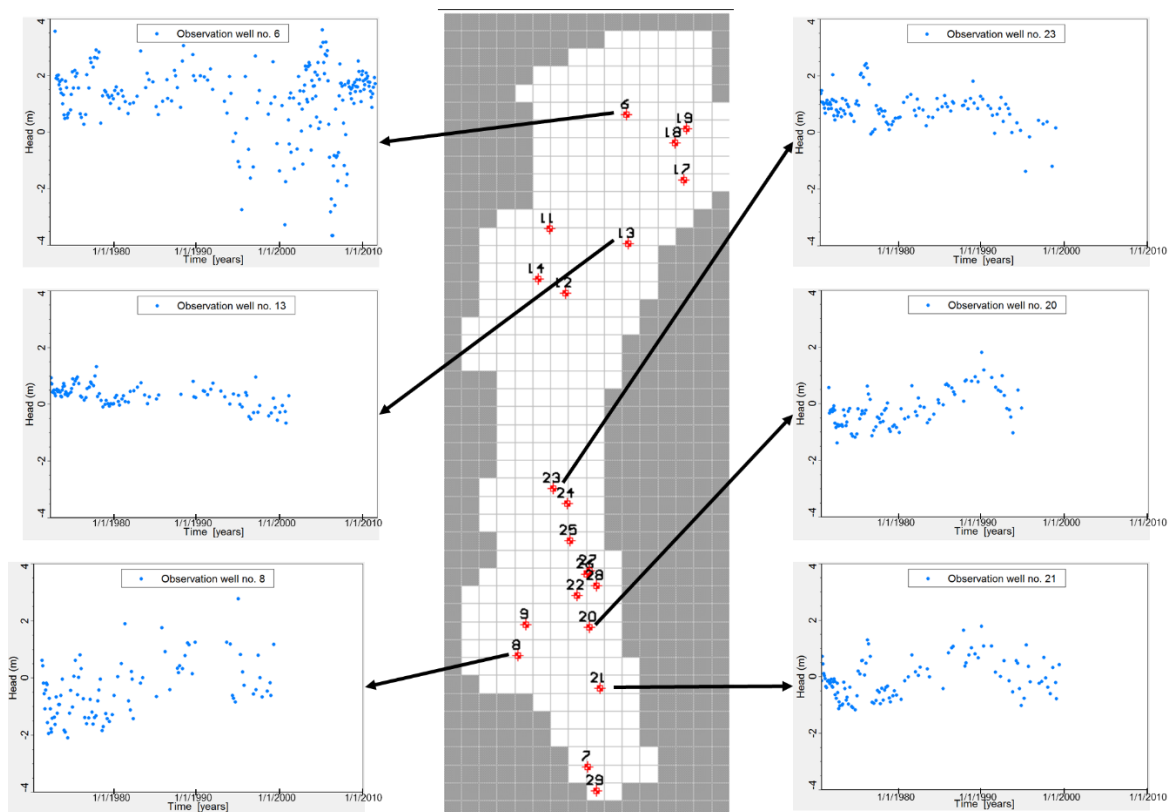
Fig. 5. Historical evolution of hydraulic head at some observation points

- *Climate*

The Plana de Oropesa Torreblanca has a Mediterranean climate with hot, dry summers and wet winters. Historical monthly average precipitation (1973-2010) varied between 20-30 mm in summer and it reached almost 80 mm in the rainiest month. The monthly average Temperature changes from 12ºC to 28ºC throughout the year. Yearly scale does not show a clear trend in precipitation and temperature. Fig. 6 shows rainfall and temperature for the period from 1973 to 2009. Evapotranspiration in the wetland is estimated to be around 10.80 Mm^3/year.
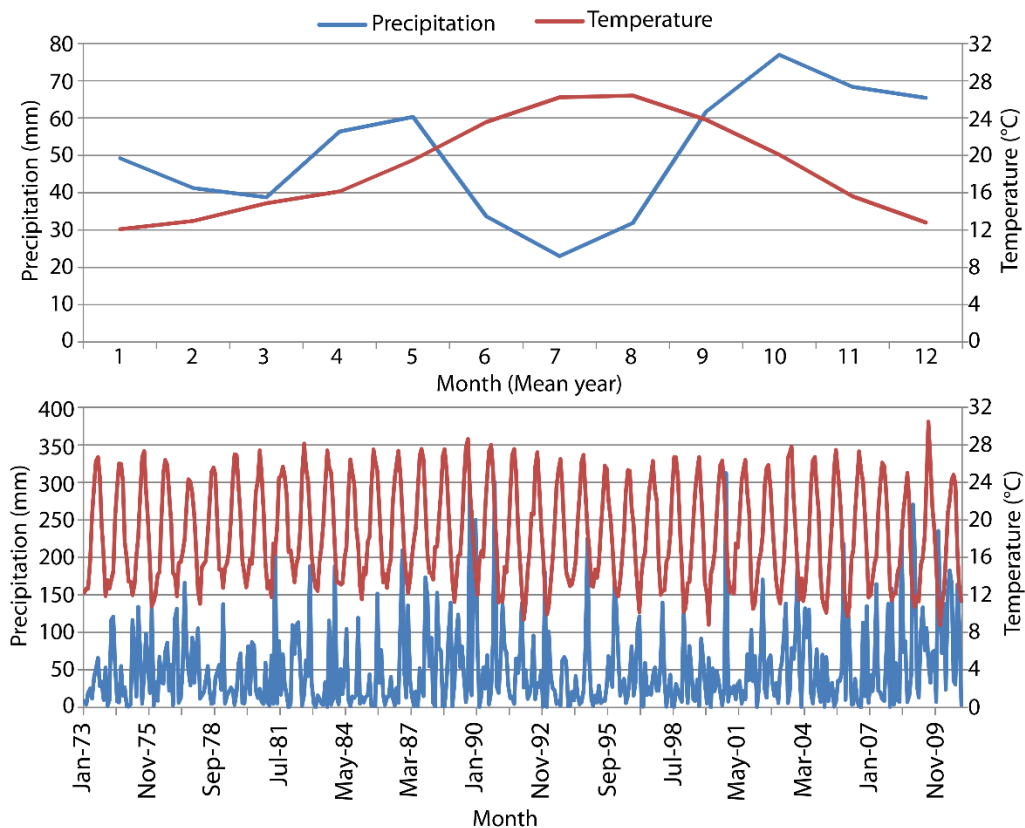
Fig. 6. Historical rainfall and temperature in Plana de Oropesa-Torreblanca aquifer (modified from Pulido-Velazquez et al. 2018)

- Land use

In the 1960s and early 1970s the Oropesa-Torreblanca Plain was sparsely populated and land was dedicated mostly to non-irrigated cropping. From 1975 to 1995 there was a significant transformation from dry to irrigated lands, especially in the period 1985–1995 (Pulido-Velazquez et al. 2018). From 1995 to 2010 the main change was an increase of artificial surfaces (mainly residential LULC along the coast) (Feranec et al. 2010) and an improvement in the efficiency of irrigation techniques (CHJ 2015). Fig. 7 shows the CORINE land use map in 2006 (Feranec et al. 2010).
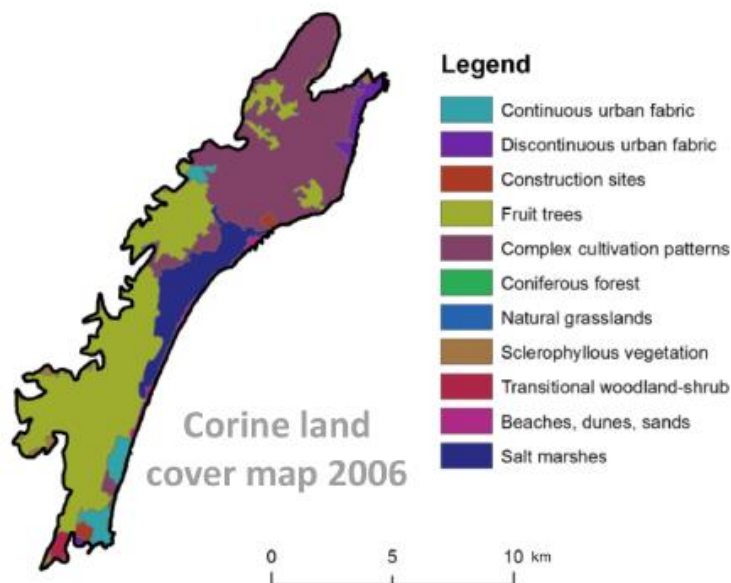
Fig. 7 CORINE Land use maps in 2006 (modified from Pulido-Velazquez et al. 2018)

- *Abstractions/irrigation*

The land use changes are reflected in the evolution of total pumping in the Plana de Oropesa-Torreblanca aquifer. The transformation into irrigated croplands from 1975 to 1995 produce an increase in pumping and drawdowns of groundwater levels. In this period the SWI problem has grown. Later on, the transformation of irrigation techniques and land uses led to a reduction in pumping (Pulido-Velazquez et al. 2018).

Agriculture is the main economic pillar, with a greater water demand than other activities such as tourism or industry. The pumping for agricultural use is 32.5 Mm^3/year and for human consumption are 3.35 Mm^3/year making a total of 35.85 Mm^3/year (IGME-UJI 2009).

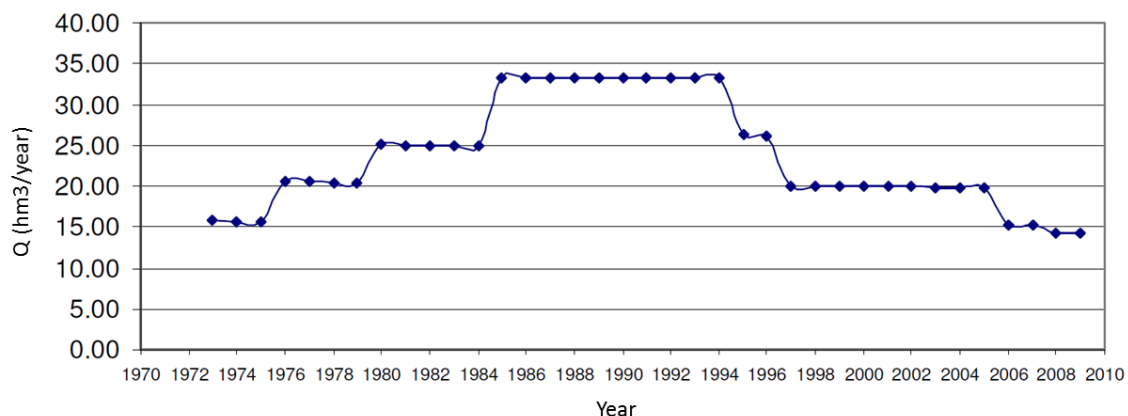Fig. 8 shows the annual historical temporal evolution of the pumping.

Fig. 8 Historical temporal evolution of pumping (Mm^3/y). (modified from Renau-Pruñonosa 2013)

- *Flow balance components*

The main Groundwater flow direction is NW-SE under natural conditions (Morell and Giménez 1997; Renau-Pruñonosa et al. 2016). The aquifer is laterally connected with adjacent aquifers that produce inflows to the system. There is recharge that comes from infiltration of precipitation and irrigation returns. The groundwater outflows are produced by Pumping, discharge to the Prat de Cabanes wetland, and groundwater discharges to sea (Pulido-Velazquez et al. 2018). The mean flow balance in the period 1948-1983 is sumarized in Table 1.

Inflow/outflow	Flow balance
Inflows (Mm^3/yr)	
Rainfall recharge	7
Lateral transfer	4.3
Seepage from irrigation	12.7
Total inflows	**24**
Outflows (Mm^3/yr)	
Outflows to the sea	3.9
Drains	1.5
Groundwater pumping	18.6
Total outflows	**24**

Table 1. Approximate water balance in the Plana de Oropesa-Torreblanca aquifer in the period 1948-1983 (IGME 1989).

3.2 Climate change challenge

In accordance with the EEA map the main expeted issues due to CC in this case study are those described in Fig. 9 for the Mediterranean regions. Existing national assessments show significant potential reductions (around a 18% for the RCP8.5 emission scenario in the horizon 2071-2100) of the future aquifer recharge in the area (see Pulido-Velazquez et al., 2018)

The main challenge is to find adaptation measures to maintain a sustainable use of the groundwater body with a balance between supply water demands (different uses) under future climate change conditions and maintaining a good status in the aquifer (constraining SWI problems) and the related ecosystem.
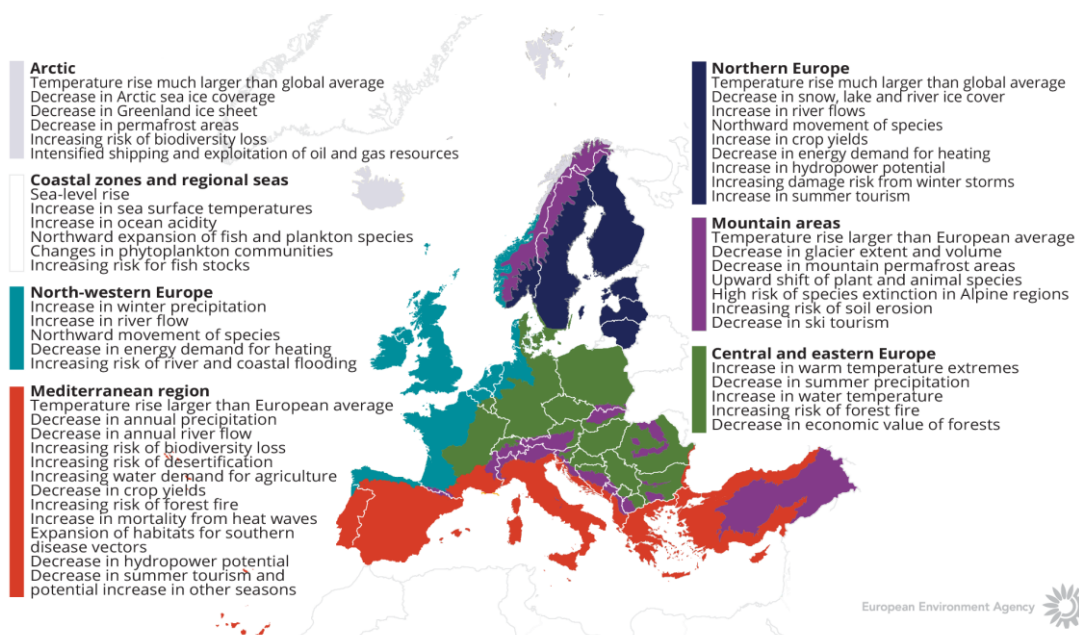
Figure 9. How is climate expected to change in Europe. The European Environment Agency map

4   METHODOLOGY

4.1   Methodology and future scenarios

4.1.1   Tools/ model description

An impact and adaptation assessment has been performed for historical and some future potential GC scenarios. In order to assess the hydrological impacts of those climatic and management scenarios we simulate them within a modelling framework based on a density-dependent SEAWAT model whose inputs are defined by a sequential coupling of different models (rainfall-recharge models, crop irrigation requirements and irrigation return models). It allows to estimate hydraulic head and chloride concentration fields within the aquifer from the historical period and other potential scenarios.

Representative future CC scenarios were generated by ensembles of different local projections and a future LULC scenario was defined in accordance with the plan approved by the local government (PGOU Torreblance, 2009). Four GC scenarios were defined by combining the LULC scenario and the CC scenarios. These GC scenarios have been propagated by simulating with the cited calibrated chain of models.

Finally, based on the outputs provided by this chain of models in the historical and future potential scenarios assessment, we will apply a method based on indices and variables to summarise SWI status and vulnerability at aquifer scale. It is described in detail in the Deliverable 5.2. The **inputs** required **and the steps to be followed** to apply the method are compiled in that cited report. Information on the aquifer volume affected by SWI at different spatial scales will be generated, moving from areal maps to representative conceptual cross section and lumped indices. The sensitivity of the affected volumes to the threshold employed to define them should be also tested. This threshold is defined from the natural background level in the aquifer. The proposed indices-based method has been implemented in a general GIS tool (Baena-Ruiz and Pulido-Velazquez., ur) to facilitate its application and comparison between SWI problems in different groundwater bodies and temporal periods. The resilience and trend of the system to SWI can be deduced from the time series of the proposed indices. Impacts of potential GC scenarios (CC and LULC change scenarios) can be also analysed. A published paper in Environmental Earth Science journal (Baena-Ruiz et al., 2020) shows an application of this method to analyse potential climatic scenarios. The method has been also applied to perform historical assessment (Baena-Ruiz et al., 2018). The deliverable 5.2 was made by compiling the methodological descriptions included in the cited papers. The partner will test the applicability of the method to different typologies of aquifers depending on the available information and previous modeling activities.

4.1.2   Future scenarios. Climate and land use data

Several future local CC scenarios have been generated for a short term horizon (2011-2035) under the most pessimistic emission scenario RCP8.5 included in the IPCC Fifth assessment

report (AR5). Their impacts on SWI will be estimated by propagating them within the cited modelling framework. The outputs generated will be employed as inputs of the proposed method to analyze and summarize SWI at aquifer scale.

4.1.2.1 TACTIC standard Climate Change scenarios

The TACTIC standard scenarios are developed based on the ISIMIP (Inter Sectoral Impact Model Intercomparison Project, see www.isimip.org) datasets. The resolution of the data is 0.5°x0.5°C global grid and at daily time steps. As part of ISIMIP, much effort has been made to standardise the climate data (a.o. bias correction). Data selection and preparation included the following steps:

1. Fifteen combinations of RCPs and GCMs from the ISIMIP data set where selected. RCPs are the Representative Concentration Pathways determining the development in greenhouse gas concentrations, while GCMs are the Global Circulation Models used to simulate the future climate at the global scale. Three RCPs (RCP4.5, RCP6.0, RCP8.5) were combined with five GCMs (noresm1-m, miroc-esm-chem, ipsl-cm5a-lr, hadgem2-es, gfdl-esm2m).
2. A reference period was selected as 1981 – 2010 and an annual mean temperature was calculated for the reference period.
3. For each combination of RCP-GCM, 30-years moving average of the annual mean temperature where calculated and two time slices identified in which the global annual mean temperature had increased by +1 and +3 degree compared to the reference period, respectively. Hence, the selection of the future periods was made to honour a specific temperature increase instead of using a fixed time-slice. This means that the temperature changes are the same for all scenarios, while the period in which this occur varies between the scenarios.
4. To represent conditions of low/high precipitation, the RCP-GCM combinations with the second lowest and second highest precipitation were selected among the 15 combinations for the +1 and +3 degree scenario. This selection was made on a pilot-by-pilot basis to accommodate that the different scenarios have different impact in the various parts of Europe. The scenarios showing the lowest/highest precipitation were avoided, as these end members often reflects outliers.
5. Delta change values were calculated on a monthly basis for the four selected scenarios, based on the climate data from the reference period and the selected future period. The delta change values express the changes between the current and future climates, either as a relative factor (precipitation and evapotranspiration) or by an additive factor (temperature).
6. Delta change factors were applied to local climate data by which the local particularities are reflected also for future conditions.

For the analysis in the present pilot the following RCP-GCm combinations were employed:

Table 2. Combinations of RCPs-GCMs used to assess future climate

		RCP	GCM
1-degree	"Dry"	rcp4p5	hadgem2-es

	“Wet”	rcp6p0	noresm1-m
3-degree	“Dry”	rcp4p5	hadgem2-es
	“Wet”	rcp6p0	hadgem2-es

4.1.2.2 Local climate change scenarios generated in addition to the TACTIC standard

In Plana de Oropesa-Torreblanca, the generation of future local GC scenarios (including CC and LULC scenarios), and the description of the modeling framework employed to propagate their impacts is presented in detail in the paper Baena-Ruiz et al., (2020). Four potential future climate scenarios (CC scenarios) were generated for a short term horizon (2011-2035) under the most pessimistic emission scenario RCP8.5. They were defined by ensembles of 36 different local climatic projections generated by applying different statistical corrections (correction of first and second order moments) taking into account historical data and climatic projections simulated with 9 different climatic models, obtained by combining results from 4 RCMs nested to some GCMs (results from 5 GCM were employed, but the RCMs simulations were only available for some of those GCMs) generated in the framework of the CORDEX Project (2013). They have been generated under two conceptual approaches or downscaling techniques: bias correction techniques and delta change techniques (Räisänen and Räty, 2012).

We considered four options to define representative future scenarios by applying different ensembles of corrected projections. All of them will produce practically the same monthly changes in temperature and precipitation (Figure 12), but differences in other monthly statistic of the series as the standard deviation or the variability of the series. They are described in detail in Baena-Ruiz et al., (2020). Two ensemble scenarios were generated by an equi-feasible linear combination of all the future series generated by delta change (E1) or bias correction (E2). The bias correction techniques are based on the analysis of the statistical difference between the climatic variables in the historical data and the control simulations produced by the climate models for the same period. They aim to define a transformation function to correct the control series to obtain a better approximation of the historical statistic. They assume that in the future the bias between model and data will be the same as observed in the historical period (e.g. Watanabe et al., 2012; Haerter et al., 2011). The delta change approaches assume that the model can obtain a good approximation of the relative changes in climate variables' statistics, but do not provide a good prediction of the absolute values. Accordingly, they try to characterize the “delta change” produced in the main statistics of the climatic variables by analysing the relative difference between the future and control scenario
simulations. The future series will be obtained by perturbation of the historical series in accordance with the estimated “delta change” (e.g. Pulido-Velazquez et al., 2011a, 2014; Räisänen and Räty, 2012). Two other options were defined by non-equifeasible ensembles defined by combining only the models (E3, for the delta change approach) or combinations of models and correction techniques (E4, for the bias correction techniques) that were “not inferior” (better calibrated) in terms of approaching the historical statistics (mean, standard deviation and asymmetry coefficients). These non-equifeasible ensembles we do not consider the inferior models because they provide worst approximations to the historical series that make us mistrust their predictions.

All these ensemble climate scenarios showed (Figure 10) an increase in mean temperature (≈ 1 °C on average) with respect to the historical period (1973–2010). The future mean rainfall showed a decrease (up to 24% monthly) for every month except September and October, in which a relative increase was predicted (up to 30%). These months are the rainiest in the study area and frequent storms occur. The local future scenarios show an increment in these extreme rainfall events (Pulido-Velazquez et al. 2018).
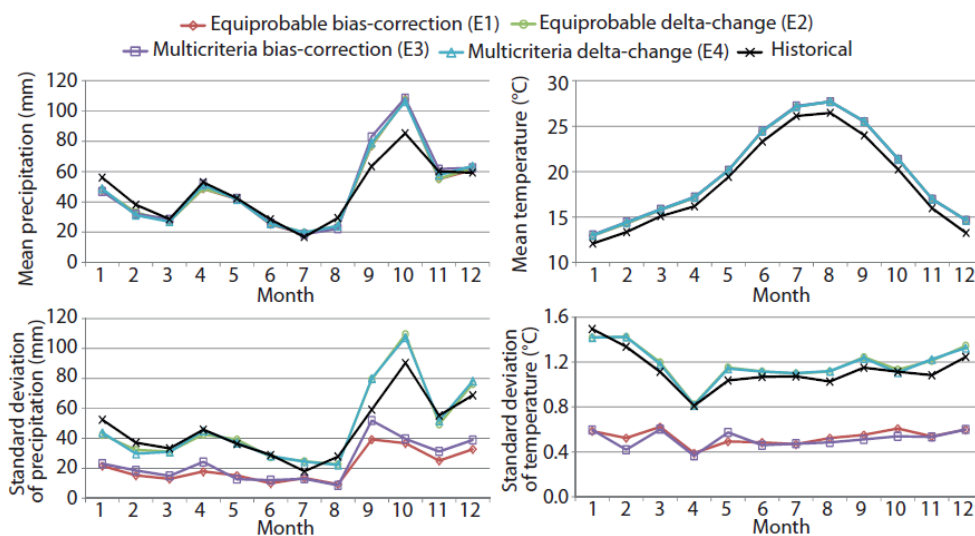
Figure 10. Monthly mean and standard deviation of future temperature and precipitation for the four ensemble scenarios (taken from Pulido-Velazquez et al., 2018)

The changes in LULC were obtained from both fieldwork undertaken in the area and from the European CORINE Land Cover database (Feranec et al., 2010). These data were used to estimate the pumping and the irrigation returns.

The transformation from dry to irrigated croplands led to an increase in pumped abstractions that extended over 2 decades (1975–1995, especially in the period 1985–1995), provoking a drop in groundwater level and seawater intrusion problems. From 1995 to 2010 there was a progressive reduction in pumping due to the abandonment of certain crops and irrigated areas. The LULC information was used to estimate agricultural water requirements following a procedure to compute crop water requirements based on the FAO Irrigation and Drainage Paper (Allen et al., 1998). The estimated irrigation demands have also been employed to assess pumping taking into account information about the origin of the water that supplies each demand. The irrigation demands are multiplied by the irrigation return coefficients obtained for the crops in this area in previous studies (Tuñon, 2000) to assess recharge from irrigation.

The predicted future changes in LULC over the Plana Oropesa-Torreblanca are of greater magnitude than the historical ones and could drastically modify the rural and urban landscape (See Figure 11). The already-approved tourist developments (the public urbanization work – PAI – for the Marina d'Or Golf in Oropesa and Cabanes, and the General Town Plan – PGOU – for Torreblanca) anticipate an increase in population of more than 130 000 inhabitants, as well as

the disappearance of most of the agricultural activity in the area. These significant changes in LULC will produce significant impacts on water demands, and, therefore in pumping and recharge and so to the hydrodynamics of the aquifer. In contrast, there are no significant changes to LULC anticipated in the area belonging to the municipality of Alcalà de Xivert, also situated on the Plana. These changes are described with more detail in Pulido-Velazquez et al., (2018).
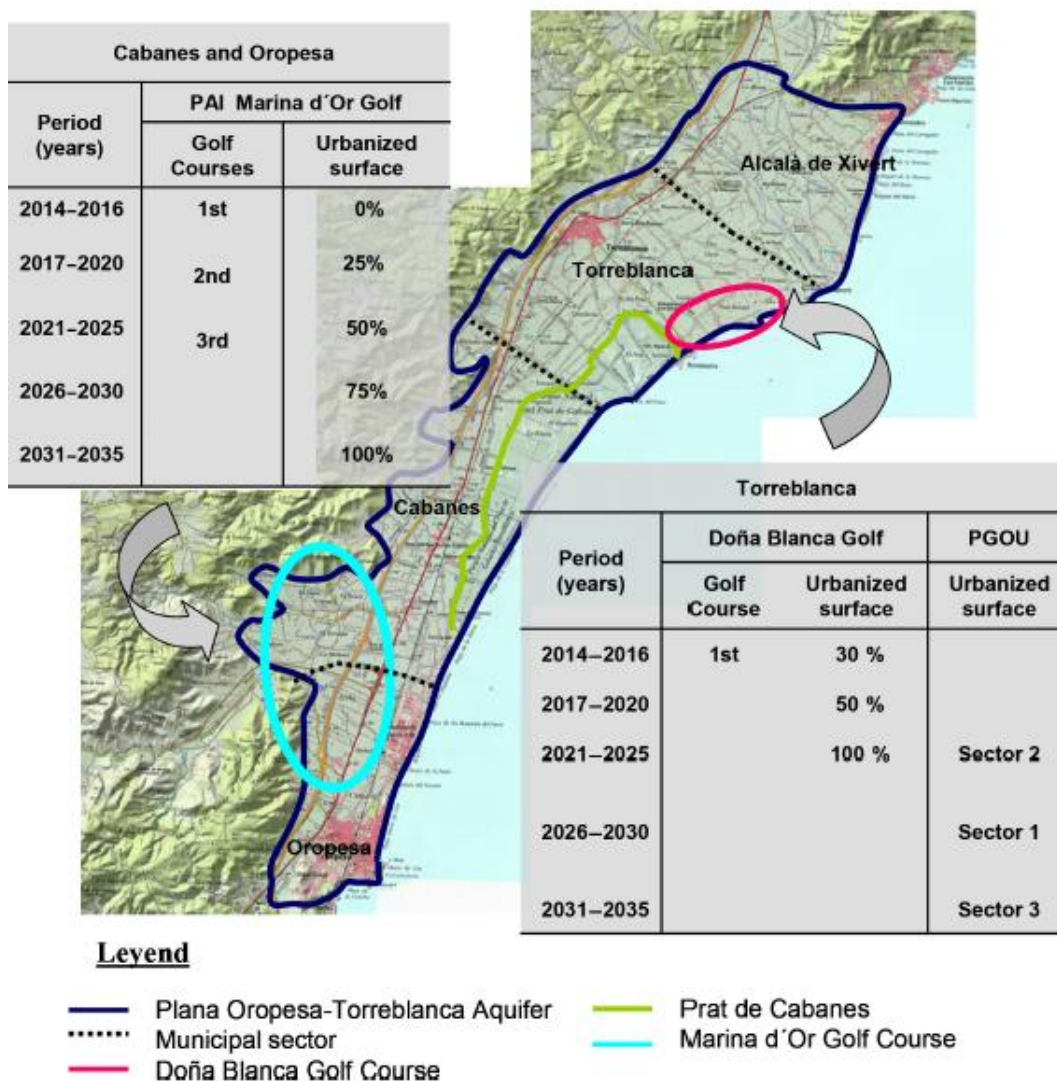

Cabanes and Oropesa		
Period (years)	PAI Marina d´Or Golf	
	Golf Courses	Urbanized surface
2014–2016	1st	0%
2017–2020	2nd	25%
2021–2025	3rd	50%
2026–2030		75%
2031–2035		100%

Torreblanca			
Period (years)	Doña Blanca Golf		PGOU
	Golf Course	Urbanized surface	Urbanized surface
2014—2016	1st	30 %	
2017—2020		50 %	
2021—2025		100 %	Sector 2
2026—2030			Sector 1
2031—2035			Sector 3

Leyend

───── Plana Oropesa-Torreblanca Aquifer
········· Municipal sector
───── Doña Blanca Golf Course
───── Prat de Cabanes
───── Marina d´Or Golf Course

Figure 11. Future land use scenarios in 2035. (taken from Pulido-Velazquez et al., 2018)

Finally we considered 4 potential future scenarios:
- Baseline (BL) scenario: no LULC change and no CC
- LULC scenario: it considers the described future LULC scenario and assumes that there is not CC.
- GC scenarios (GC1, GC2, GC3, GC4) assuming constant sea level: we consider four GC scenarios that simultaneously consider the potential impacts of the described future LULC

scenario under the four generated CC scenarios (E1, E2, E3 y E4). The comparison of these scenarios with the BL provides information about the GC impacts.

4.2 Tool(s) / Model(s) set-up: chain of models (SEAWAT simulations) and proposed SWI assessment method (status and vulnerability)

A chain of models was defined to assess the impacts of the future scenarios on the hydraulic head and the chloride concentration within the aquifer. It is described in detail in Pulido-Velazquez et al., 2018. It includes a sequential coupling of three "auxiliary models" (rainfall-recharge models, crop irrigation requirements and irrigation return models) with this density dependent model SEAWAT model, in which the outputs of the auxiliary models are used as inputs of the groundwater model. The density dependent SEAWAT flow model was defined in accordance with the conceptual approach deduced from the available information in our case study. The aquifer is unconfined, heterogeneous, detrital and multilayer composed of gravel and sand levels in a silty clay matrix (Ballesteros et al., 2016). The transmissivity in the Plio-Quaternary Plana de Oropesa-Torreblanca aquifer ranges from 300 to 1000 m^2/day (García-Menéndez et al., 2016) and the storage coefficient varies between 2 and 12%. Groundwater flow approximately follows a NW-SE direction before discharging to the sea. The range of piezometric levels varies in the Plana de Oropesa-Torreblanca reaching maximum about 3 m a.s.l. at points furthest from the coast. The piezometric level is depressed in zones close to the coast. Aquifer geometry is derived from previous 3D models (Renau Pruñonosa 2013). The Plana de Oropesa-Torreblanca aquifer is wedge-shaped being the maximum thickest located near to the coastline, where it can reach 90 m thick.

The SEAWAT model was calibrated in accordance with the available historical information about hydraulic head (described in Section 3.1. See Figure 5) and chloride concentration within the aquifer. There are no chloride concentration data for this study area from 1988 to 1989 neither from 2001 to 2005. The number of monitoring points of chloride concentration varies over time between 12 and 34, while the monitoring points of hydraulic head ranges between 9 and 1.

The chloride concentration exceeds 1000 mg/l in zones close to the coast. Points inland exhibit lower concentrations that are more stable through time. Concentrations increased over the 1980s as a consequence of the expansion in irrigated croplands, associated with a period of scarce rainfall. Subsequently, there was a drop in mean chloride concentrations due to the reduction in pumping, together with improved hydrological planning (Figure 12).
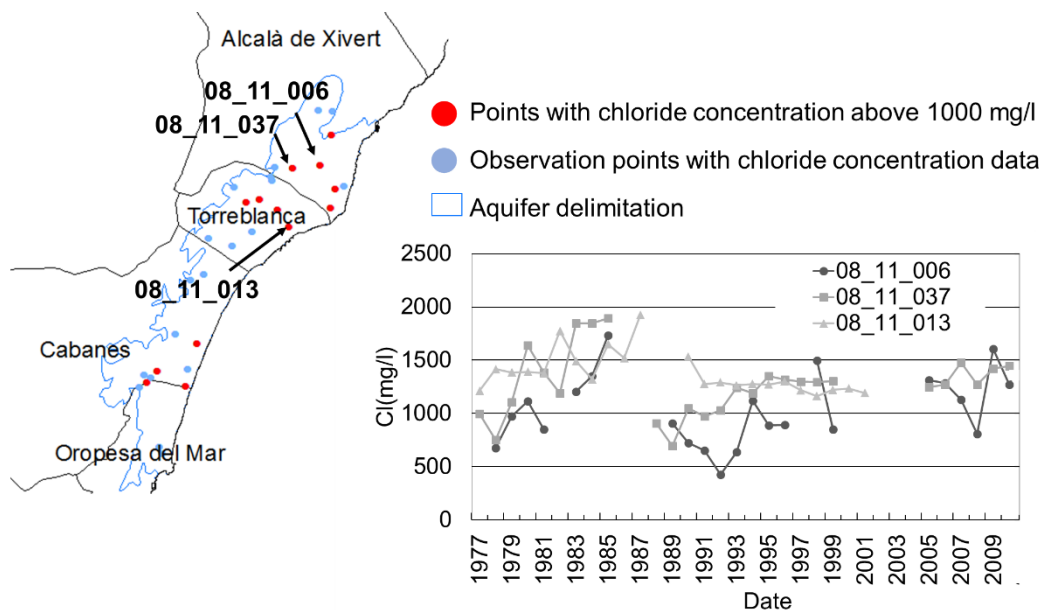
Figure 12 Location of the observation points in Plana de Oropesa-Torreblanca and evolution of the chloride concentrations in monitoring points (modified from Baena-Ruiz et al., 2018)

Groundwater flow approximately follows a NW-SE direction before discharging to the sea. The range of piezometric levels varies in the Plana de Oropesa-Torreblanca reaching maximum about 3 m a.s.l. at points furthest from the coast. The piezometric level is depressed in zones close to the coast. Aquifer geometry is derived from previous 3D models (Renau Pruñonosa 2013).

The chain of models were employed to assess the information required by the proposed **method/tool (Deliverable 5.2) in order to assess and summarize the status and vulnerability** to SWI through visual pictures and time series. The **inputs** of this method have been taken from the outputs and data integrated within the chain of models. They include variables (to characterize the historical evolution of hydraulic head and chloride concentration) and parameters (to define aquifer geometry and hydrodynamic behavior) to determine the overall status of the aquifer. For the vulnerability assessment and analyses, other intrinsic information (aquifer type, conductivity, distance from the shoreline, bicarbonate concentration) is also needed as inputs to apply the proposed method. It is based on the SWI vulnerability maps generated by applying the GALDIT method (Chachadi and Lobo-Ferreira 2005), which is described in detail in Deliverable 5.2. A chloride concentration threshold is used to determine the volume of aquifer affected by SWI. Different method can be applied to define this threshold value (see deliverable 5.2). In this application we have performed a sensitivity analysis of the proposed method results to the adopted threshold values, by assuming two different potential values. The **final results** SWI status and vulnerability results will be summarized by using: 1. Maps of SWI affected aquifer volumes; 2. 2D conceptual cross-sections (with mean penetration and thickness in specific dates or mean values in periods); 3. Lumped Index (Mass of affected area and lumped vulnerability index) to summarise the global dynamic of SWI within the aquifer.

4.3   SEAWAT Model calibration / test

The SEAWAT model was calibrated by a trial and error procedure to minimize the differences between the model results and the observations. It is described in detail in Pulido-Velazquez et al., 2018.

4.3.1   Observation data

The model reproduce with a reasonable accuracy the trends and dynamic of the historical hydraulic head and chloride concentration (see Figure 13a and 13b respectively) for the period 1973–2010.
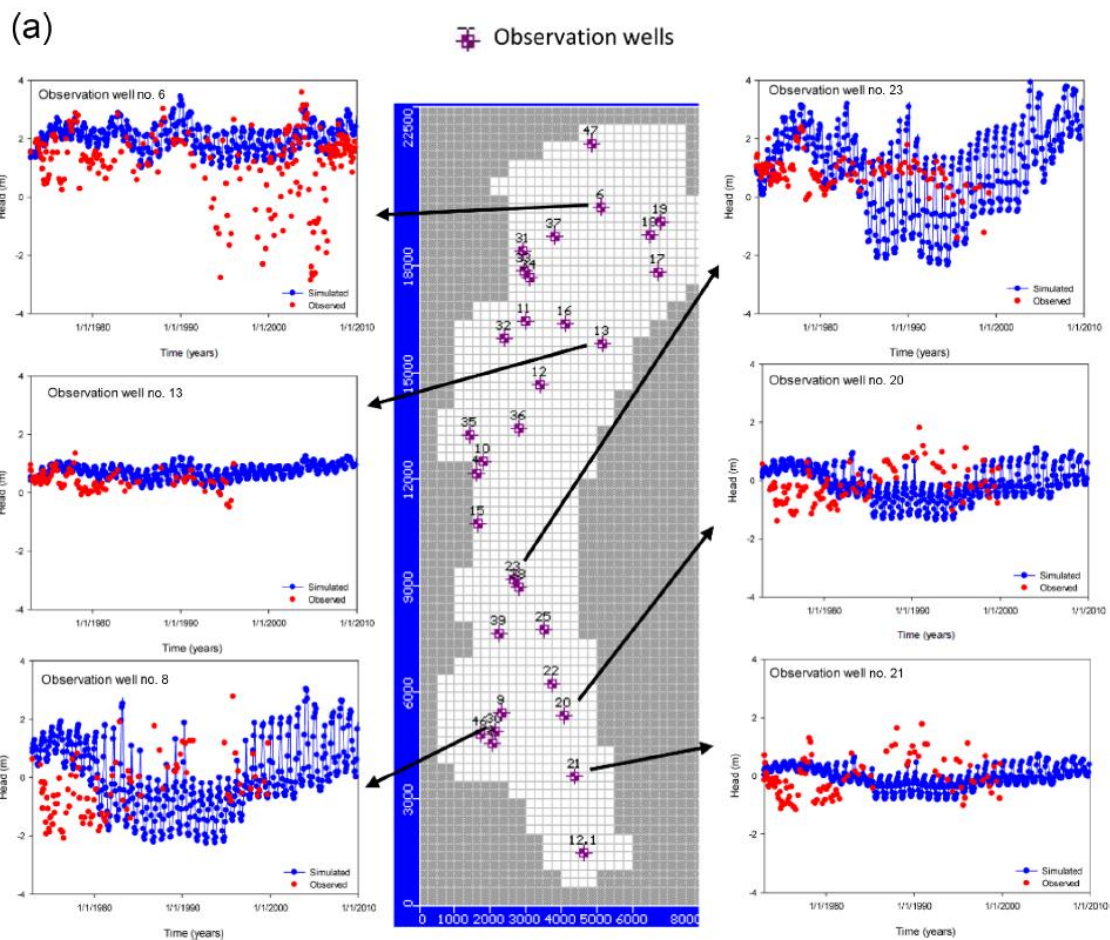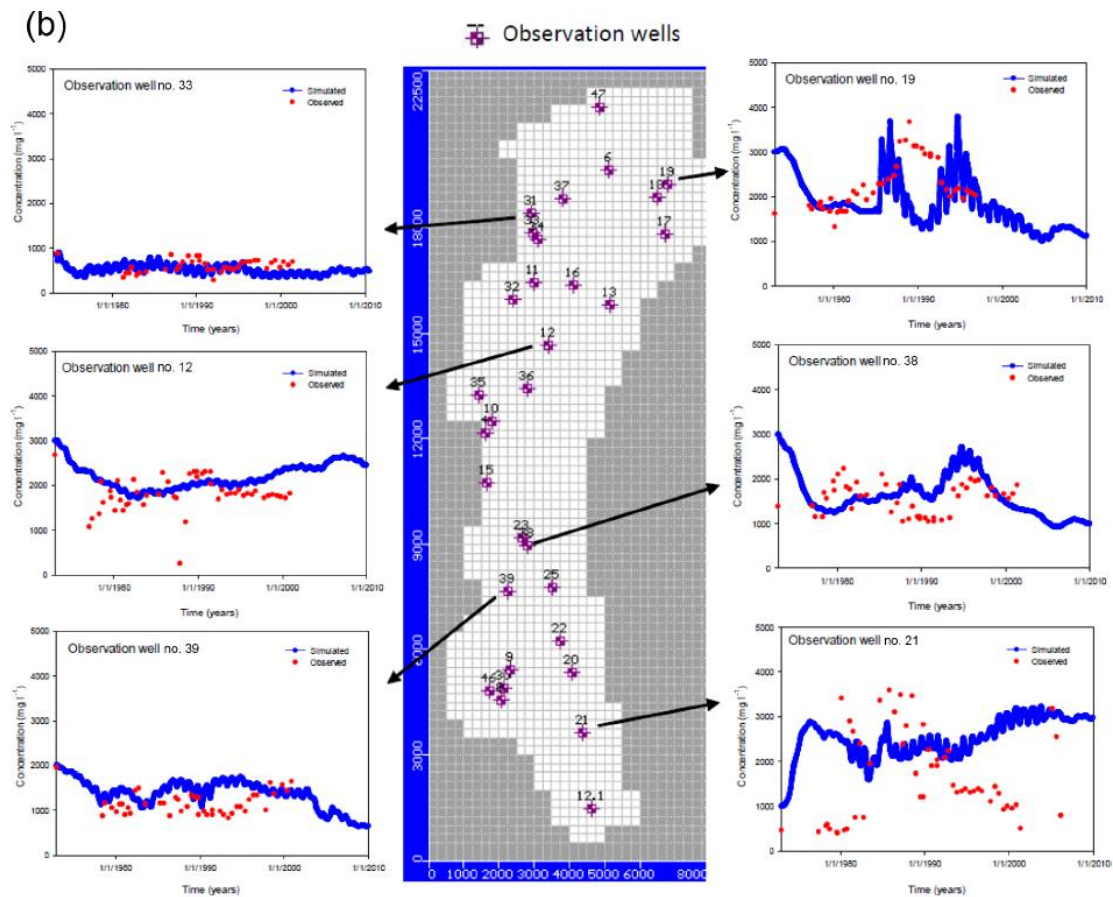
Figure 13. (a) Hydraulic head obtained with the models vs. data at some observation points. (b) Salinity obtained with the models vs. Data at some observation points. (Figure taken from Pulido-Velazquez et al., 2018)

The chain of cited models were employed to estimate the information required by the proposed method/tool (Deliverable 5.2)

5 RESULTS AND CONCLUSIONS

In this section we show the results for the historical and future potential scenarios assessment. We have split them in: results from the chain of models that integrates SEAWAT simulations (described in subsections 5.1, 5.2 and 5.3), which were employed to generate the inputs of the proposed method to assess SWI status and vulnerability; and results obtained when applying the proposed index method to assess and summarise SWI status and vulnerability (subsections 5.4, 5.5 and 5.6).

5.1 SEAWAT simulation of historical conditions. Inputs required to apply the proposed method to assess historical SWI.

We include an example of the historical maps of chloride concentration and groundwater volumes/resources (Figure 14) generated to apply the method to assess and summarize SWI status. They were generated from the described chain of models that includes SEAWAT simulations. In the presented maps for October 1985, we have represented the mean chloride concentration in the aquifer depth. The historical status shows that the majority of the aquifer is affected by high chloride concentration. In most of the aquifer area (more than 80 %), the salinity is above 1100 mg/l, and, therefore, it is in general affected by intrusion.
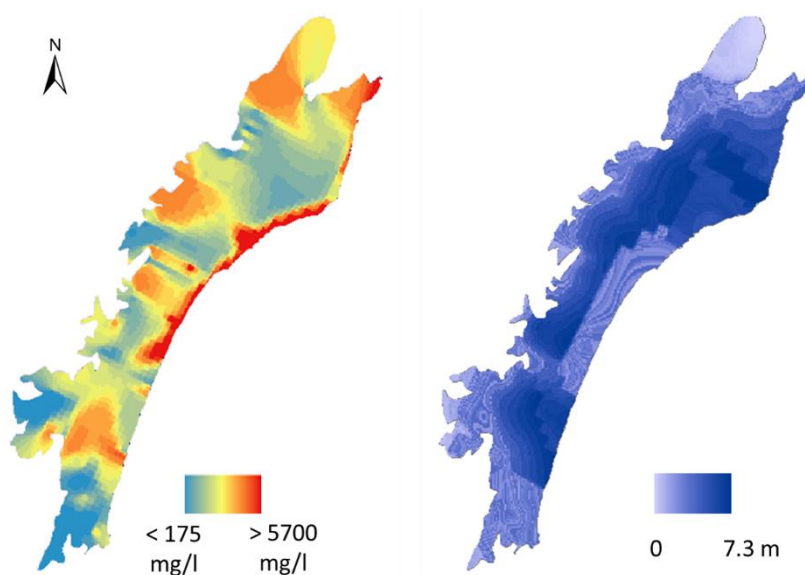
Figure 14. Historical maps of chloride concentration (left) and groundwater resources (right) (October 1985)

We also show an example of the historical vulnerability maps required to assess SWI vulnerability (Figure 15). In general, the Plana de Oropesa-Torreblanca aquifer is highly vulnerable due to the characteristics of its formation (it is an aquifer lying parallel to the coast

with a wedge shaped geometry, very shallow inland, thicker close to the coastline, and with high conductivity) and to the elevated chloride concentration along the coastline.
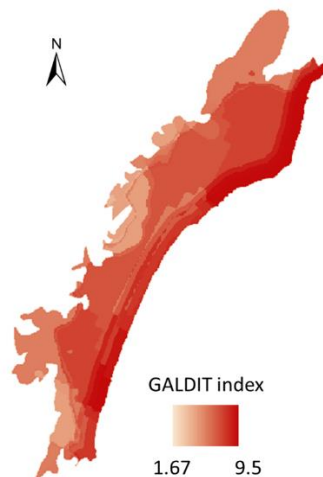

Figure 15 Historical maps of vulnerability (October 1985)

5.2 SEAWAT simulations of future scenarios. Inputs required to apply the proposed method to assess future SWI.

This section shows an example of the future maps of chloride concentration and groundwater resources (Figure 16) required to apply the method to assess and summarize impacts on SWI status. They were generated by propagating the described GC scenarios. The expected future climatic conditions would have a negative impact on the salinization of the aquifer resources, and also on the aquifer vulnerability to SWI.
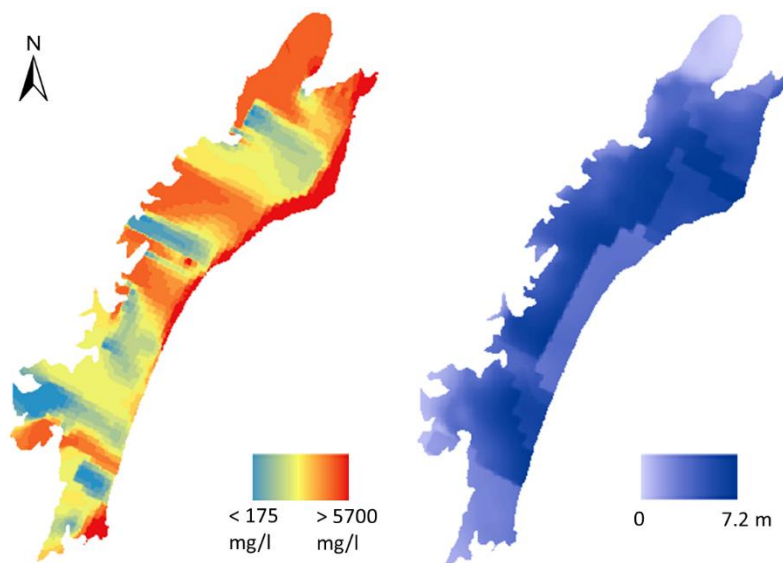
Figure 16. Maps of potential future chloride concentration and groundwater resources for the simulated scenario GC4 (September 2027)

We have also included an example of the future vulnerability maps for the simulated scenario GC4 (Figure 17). It shows that the vulnerability is less sensitive to CC due to other factors that are used in the index (conductivity and distance from the coast), which have greater weight and are invariant in time.
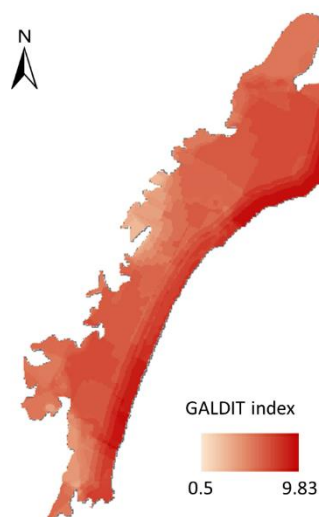
Figure 17 Maps of potential future vulnerability for the simulated scenario GC4 (September 2027)

5.3   Uncertainty on future impacts simulated with SEAWAT

There are significant uncertainties in future GC conditions and their impacts. In this report we do not intend to perform a detailed analysis of hydrological uncertainty. For an appropriate uncertainty analyses of hydrological impacts it would be more appropriate to obtain results from each individual climate model projections instead to the ensemble scenarios employed in this study. Note that it would require us to deal with different sources of uncertainty (Matott et al., 2009). The complexity is even greater for the presented methodology, since it entails the coupling of several numerical codes and a large amount of data and a long simulation time period.

5.4 SWI Method results: Maps of SWI status and vulnerability

Following the steps described in section 2.1.1 and 2.2.1 of Deliverable 5.2 we obtain the maps of affected volumes in terms of SWI status and vulnerability respectively. We assumed two different chloride concentration threshold values to identify groundwater volumes affected by SWI. The adopted thresholds are 250 mg/l, which is the consumption limit and the default value adopted in other previous studies (Ballesteros et al. 2016); and 1100 mg/l. It allows us to show the sensitivity of the results to this parameter.

The affected volume using a threshold of 250 mg/l is much greater than when using a 1100 mg/l threshold (Figure 18). This phenomenon highlights the need to determine properly this threshold in each aquifer, since the assessment of whether there are SWI problems is quite sensitive to this value. Nevertheless, in both cases the majority of the aquifer volume is affected by SWI.
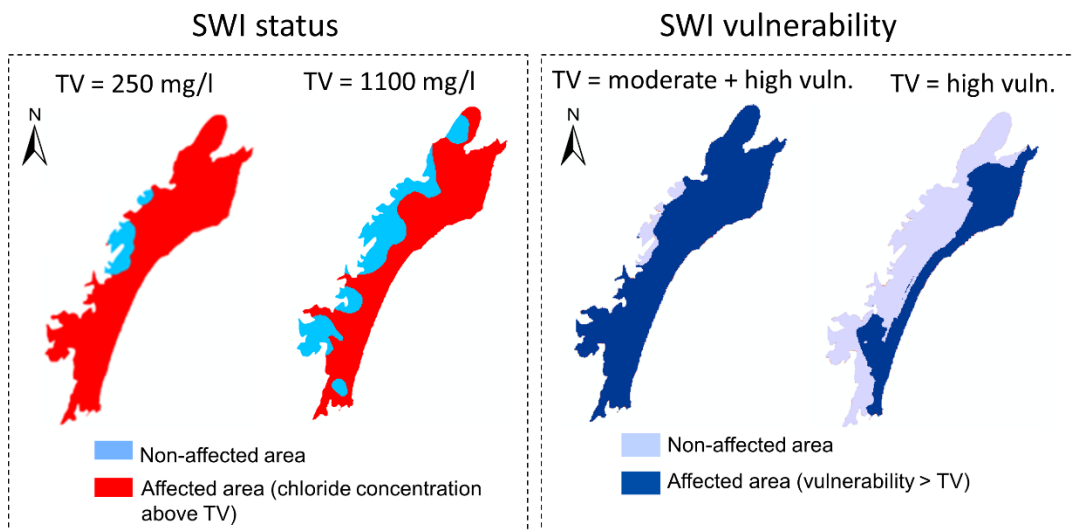

Figure 18. Maps of historical SWI status and vulnerability "affected volumes" (October 1985)

In the future assessment, we have considered only one threshold value (1100 mg/l for SWI status and the high vulnerability values of the GALDIT index to assess vulnerability to SWI). In terms of SWI status, the worst hypothetical scenario is the GC4, in which practically the whole aquifer

would have a chloride concentration above 1100 mg/l (Figure 19). In GC4 scenario the aquifer would suffer an increment of 10% in the affected volume compared to the baseline scenario in 2010 (the starting point of the future period in this study). Nevertheless, the aquifer already had a large affected volume in 2010 (more than 80%) (Pulido-Velazquez et al. 2018). The affected areas in terms of high vulnerability is significantly smaller (less than 40%). The GC4 scenario shows a zone of high vulnerability at the north of the aquifer that corresponds with an area with high conductivity.
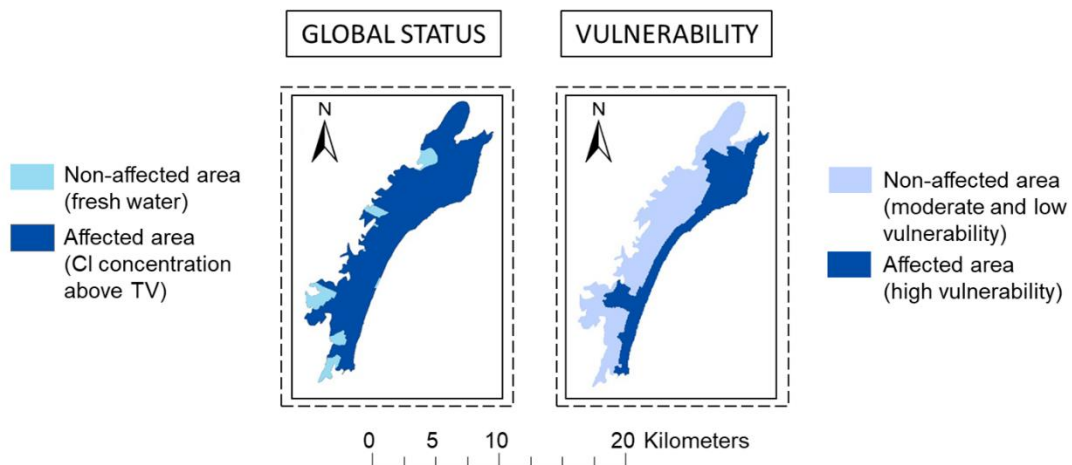
Figure 19. Maps of potential future SWI status and vulnerability "affected volumes" for the GC4 simulated scenario (September 2027)

5.5   SWI Method results: 2D conceptual cross-sections (mean penetration and thickness)

Following the steps described in section 2.1.2 and 2.2.2 of Deliverable 5.2 we obtain the conceptual cross section to summarise results in terms of SWI status and vulnerability respectively. They are also obtained for two different values of the thresholds values in the historical period to SWI status (250 mg/l and 1100 mg/l) and vulnerability (moderate + high vulnerability and high vulnerability) to show the sensitivity of the results to this parameter (Figure 20). Again, this conceptual-visual approach show the high volume of groundwater affected by seawater intrusion within the aquifer, and the sensitivity of the results to the adopted threshold.
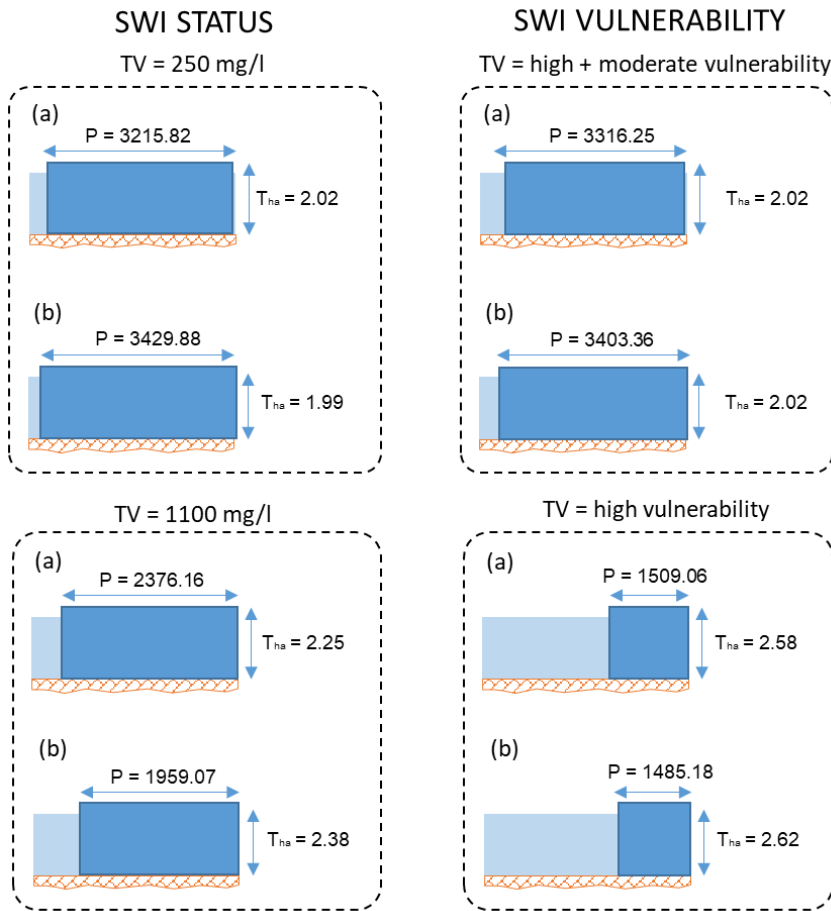
Figure 20. 2D conceptual cross-sections. Historical results in October 1985 (a) and mean values for the period 1973-2010 (b) (units in m)

In the future assessment we considered only one threshold value (1100 mg/l for SWI status and the high vulnerability values of the GALDIT index to assess vulnerability to SWI) (Figure 21).
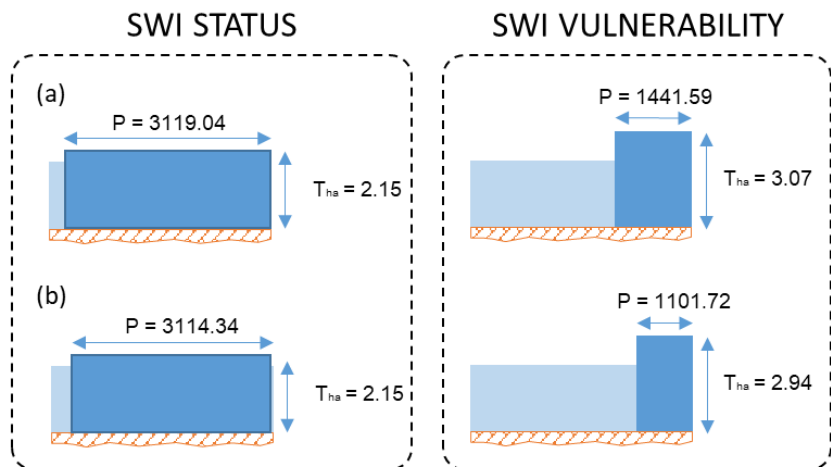
Figure 21.   2D conceptual cross-sections. Potential Future Results for the simulated scenario GC4 in September 2027 (a) and mean values for the period 2011-2035 (b) (units in m)

All potential future GC scenarios would undergo an increase in the average affected volume in accordance with the conceptual cross section, although the aquifer was largely affected in the historical period (Pulido-Velazquez et al. 2018).

5.6   SWI Method results: Lumped indices Ma and L-GALDIT.

Following the steps described in section 2.1.3 and 2.2.3 of Deliverable 5.2 we obtain the lumped indices Ma and L-GALDIT, to summarise the global dynamic of affected volumes in terms of SWI status and vulnerability respectively (Figure 22).
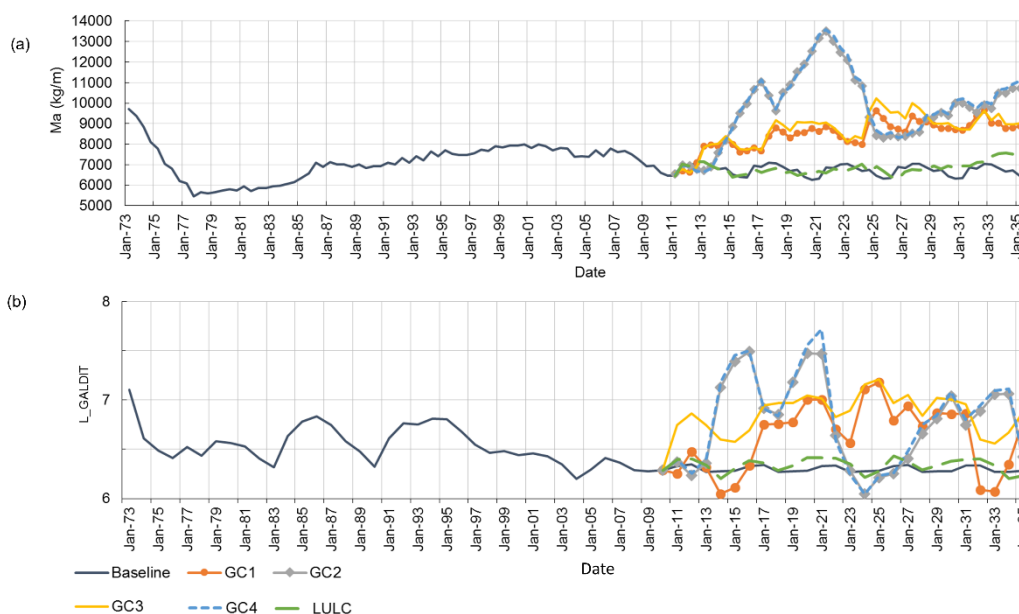
Figure 22.   Time series of the indices Ma and L-GALDIT in the historical (1973-2010) and potential future results for the simulated scenarios in the horizon 2011-2035 (modified from Baena-Ruiz et al., 2020).

The result show that the future LULC changes scenario would not produce a clear deterioration of the global status and vulnerability of the aquifer. The continuous growing trend (in the LULC and GC scenarios) in the Ma index observed from 2025 is related to the impacts of the planned urbanization of a large area in Torreblanca, which produces an increase of chloride concentrations. GC scenarios forecast a large affected mass in the future, which is mainly due to the potential climatic conditions. The maximum values of the lumped indices (Ma and L_GALDIT) during the GC scenarios are induced by periods with high temperature and low precipitation. The LULC scenario does not produce significant changes in the vulnerability. The vulnerability is more sensitive to the GC scenarios. All of them show a significant increase in its variability and

a mean increase in the vulnerability, but there are some periods in which the vulnerability even decreases.

From this future series we can assess the recovery/degradation rate (see Deliverable 5.2) of the lumped index Ma (Figure 23).
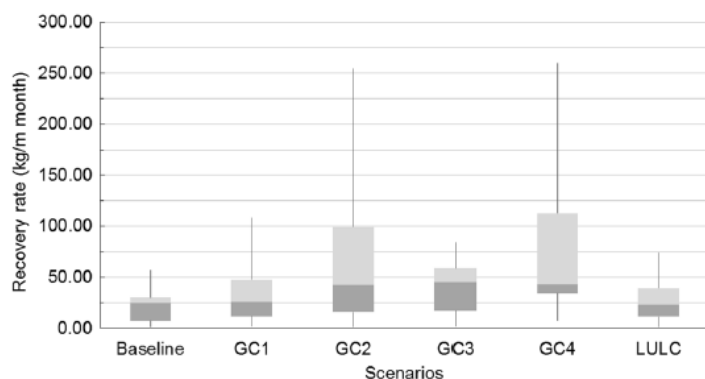

Figure 23. Statistics of recovery rate for all scenarios analyzed in the simulated scenarios in the horizon 2011-2035.

It shows that the aquifer is able to respond to the severe climatic conditions estimated in GC scenarios. Based on the calibrated model, GC2 and GC4 scenarios present more extreme values, but also show higher recovery rates.

6 REFERENCES

Alfonso, C. (2002) Entrevista a Francisco Cabezas Calvo-Rubio, Subdirector General de Planificación Hidrológica: Evaluación Ambiental Estratégica del PHN. Revista Ambienta, Volume 9. www.revistaambienta.es

Allen, R. G., Pereira, L. S., Raes, D., and Smith, M.: Crop evapotranspiration – Guidelines for computing crop water requirements, FAO Irrigation and drainage paper 56, FAO, Rome, http://www.fao.org/docrep/X0490E/x0490e00.htm (last access: May 2018), 1998.

Baena-Ruiz, Leticia & Pulido-velazquez, David & Collados-Lara, Antonio-Juan & Renau-Pruñonosa, Arianna & Morell, Ignacio & Senent-Aparicio, Javier & Llopis-Albert, Carlos. (2020). Summarizing the impacts of future potential global change scenarios on seawater intrusion at the aquifer scale. Environmental Earth Sciences. 79. 10.1007/s12665-020-8847-2.

Baena-Ruiz, Leticia & Pulido-velazquez, David, u.r. GIS-SWIAS: tool to summarize seawater intrusion status and vulnerability at aquifer scale. Special issue: Scientific Programming Tools for Water Management. Journal: Scientific Programming

Special issue: Scientific Programming Tools for Water Management
Journal: Scientific Programming

Baena-Ruiz, L, Pulido-Velazquez, D, Collados-Lara, AJ. et al. Water Resour Manage (2018) https://doi.org/10.1007/s11269-018-1952-2

Ballesteros BJ, Morell I, García-Menéndez O, Renau-Pruñonosa A (2016) A standardized index for assessing seawater intrusion in coastal aquifers: the SITE index. Water Resour Manag 30(13):4513–4527. https://doi.org/10.1007/s11269-016-1433-4

CHJ (2015) (Júcar Water Agency) Júcar River Basin Plan. Demarcación hidrográfica del Júcar. Confederación Hidrográfica del Júcar. Ministry of Agriculture, Food and Environment, Spain

Directive 2009/147/EC of the European Parliament and of the Council of 30 November 2009 on the Conservation of Wild Birds. http://eur-lex.europa.eu/legal-content/EN/TXT/?uri=CELEX:32009L0147

Feranec, J., Hazeu, G., Soukup, T., and Jaffrain, G.: Determining changes and flows in European landscapes 1990–2000 using CORINE land cover data, Appl. Geogr., 30, 19–35, 2010.

García-Menéndez O, Morell I, Ballesteros BJ, Renau-Pruñonosa A, Esteller MV (2016) Spatial characterization of the seawater upconing process in a coastal Mediterranean aquifer (Plana de Castellón, Spain): evolution and controls. Environ Earth Sci 75:728. https://doi.org/10.1007/s12665-016-5531-7

Haerter, J. O., Hagemann, S., Moseley, C., and Piani, C.: Climate model bias correction and the role of timescales, Hydrol. Earth Syst. Sci., 15, 1065–1079, https://doi.org/10.5194/hess-15-1065-2011, 2011.

IGME (1989). Las aguas subterraneas en la comunidad valenciana. Uso, calidad y perspectivas de utilizacion. Report, Geological Survey of Spain, Ministerio de Industria y Energía, Madrid, Spain, 298 pp.

Instituto Geológico y Minero de España; Dirección General del Agua (IGME - DGA, 2015). Apoyo a la caracterización adicional de las masas de agua subterránea en riesgo de no cumplir los objetivos medioambientales en 2015. Demarcación hidrográfica del Júcar. Instituto Geológico y Minero de España y Dirección General del Agua. Madrid

Instituto Geológico y Minero de España; Universitat Jaume I de Castelló (IGME - UJI, 2009). Estudio piloto para el cálculo de descargas ambientales al mar en las masas de agua subterránea costeras de la provincia de Castellón (Cuenca del Júcar). Instituto Geológico y Minero de España y Dirección General del Agua. Madrid

Morell, I. and Giménez, E (1997) Hydrogeochemical analysis of salinization processes in the coastal aquifer of Oropesa (Castellón, Spain), Environmental Geology, 29(1/2), 118-131

Pulido-Velazquez, D, Renau-Pruñonosa, A, Llopis-Albert, C, Morell, I, Collados-Lara, A.-J, Senent-Aparicio, J, and Baena-Ruiz, L (2018) Integrated assessment of future potential global change scenarios and their hydrological impacts in coastal aquifers–a new tool to analyse management alternatives in the Plana Oropesa-Torreblanca aquifer. Hydrology and Earth System Sciences, 22(5), 3053

Pulido-Velazquez, D., García-Aróstegui, J. L., Molina, J. L., and Pulido-Velázquez, M.: Assessment of future groundwater recharge in semi-arid regions under climate change scenarios (Serral-Salinas aquifer, SE Spain). Could increased rainfall variability increase the recharge rate?, Hydrol. Process., 29, 828– 844, https://doi.org/10.1002/hyp.10191, 2014.

Pulido-Velazquez, D., Garrote, L., Andreu, J., Martin-Carrasco, FJ, Iglesias, A. 2011a. A methodology to diagnose the effect of climate change and to identify adaptive strategies to reduce its impacts in conjunctive-use systems at basin scale. Journal of Hydrology 405: 110–122 doi:10.1016/j.jhydrol.2011.05.014.

RAMSAR Convention Bureau (1990) Directory of Wetlands of International Importance Sites Designated for the List of Wetlands of International Importance. http://www.ramsar.org/

Räisänen, J. and Räty, O.: Projections of daily mean temperatura variability in the future: cross-validation tests with ENSEMBLES regional climate simulations, Clim. Dynam., 41, 1553– 1568, https://doi.org/10.1007/s00382-012-1515-9, 2013.

Renau-Pruñonosa, A (2013) Nueva herramienta para la gestión de las aguas subterráneas en acuíferos costeros. Volumen ecológico de remediación (VER). Metodología y aplicación a la Plana de Oropesa-Torreblanca (MASub 080.110), Universitat Jaume I

Renau-Pruñonosa, A, Morell, I, and Pulido-Velazquez, D (2016) A methodology to analyse and assess pumping management strategies in coastal aquifers to avoid degradation due to seawater intrusion problems, Water Resources Management, 30(13), 4823-4837, doi:10.1007/s11269-016-1455-y

Sanz-Garrido, I. and Capilla, J.E. (2015) Assessment of Saltwater Intrusion and Discharges to a Wetland with a 3D Transient Variable Density Flow Model: The Coastal Plane Oropesa-Torreblanca Aquifer, Spain. Journal of Water Resource and Protection, 7, 749-768. http://dx.doi.org/10.4236/jwarp.2015.79062

Tuñon, J.: Determinación experimental del balance hídrico del suelo y evaluación de la contaminación asociada a las prácticas agrícolas, PhD Thesis, Universitat Jaume I de Castellón, Castellón, Spain, 2000.

Watanabe, S., Kanae, S., Seto, S., Yeh, P. J.-F., Hirabayashi, Y., and Oki, T.: Intercomparison of bias-correction methods for monthly temperature and precipitation simulated by multiple climate models, J. Geophys. Res., 117, D23114, https://doi.org/10.1029/2012JD018192, 2012.

TACTIC GROUNDWATER

GeoERA

Establishing the European Geological Surveys Research Area to deliver a Geological Service for Europe

Deliverable 5.3

PILOT DESCRIPTION AND ASSESSMENT

Ravenna phreatic aquifer

Authors and affiliation:

Paolo Severi, Luciana Bonzi, Lorenzo Calabrese, Marcello Nolè

[Geological, Seismical and Soli Survey of Emilia – Romagna Region - Italy]

Deliverable Data	
Deliverable number	Dx.2
Dissemination level	Public
Deliverable name	Pilot description and assessment
Work package	WP5
Lead WP/Deliverable beneficiary	IGME
Deliverable status	
Version	Version nr 1
Date	Date 25/01/2021

[This page has intentionally been left blank]
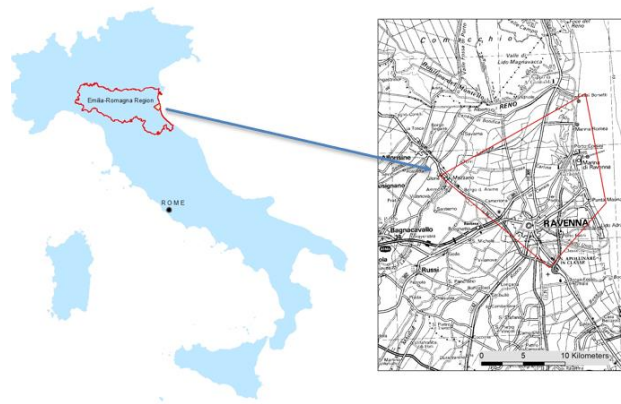
LIST OF ABBREVIATIONS & ACRONYMS

CC	Climate Change
GC	Global Change
LULC	Land Use and Land Cover
SWI	Sea Water Intrusion
GSO	Geological Survey Organisations
EC	Electric Conductivity

TABLE OF CONTENTS

1   EXECUTIVE SUMMARY

Pilot name	Ravenna phreatic aquifer	
Country	Italy	
EU-region	Mediterranean Region	
Area (km^2)	About 200	
Aquifer geology and type classification	Strand plain and delta front sands and silts; porous semi-confined to phreatic coastal aquifer	
Primary water usage	domestic use, coastal ecosystem maintenance	
Main climate change issues	Drought, Sea level rising	
Models and methods used	3d geological and geotechnical modelling of aquifers (Leapfrog) integrated with piezometric and salinity monitoring data	
Key stakeholders	Local municipality, tourism operators, enviromental heritage authorities	
Contact person	SGSS . Paolo Severi (paolo.severi@regione.emilia-romagna.it)	

The study area of this pilot is located in northern Italy, in the Emilia-Romagna Region in the province of Ravenna and it is about 200 km^2 large. From a geological point of view, it is a porous phreatic aquifer composed by amalgamated medium to fine sand of beach/dune complexes and delta-front. The project for monitoring the salt-water intrusion into this sandy phreatic aquifer began in 2009 and is still active today. The intrusion of the saline wedge is a phenomenon that must be monitored because it can damage crops, as well as the delicate ecosystems that make the coastal territory a reserve of biodiversity.

The monitoring network consists of 10 piezometers which pick up the entire thickness of the aquifer and which are currently measured twice a year. At each control point the water level is measured and, starting from this, for each meter of depth, the specific electrical conductivity (EC) and temperature are measured. The comparison between the trend of these parameters in the different measurement campaigns allows to verify the possible progress of the the salt - water intrusion into the shallow aquifer.

Within this pilot project a 3D model with the lithological distribution was created and then, in order to include the EC distribution into the 3D model of the aquifer, we selected from our dataset the four most complete measurement campaigns (October 2009, March 2010, September 2013 and October 2019) and we determined for each campaign an average piezometric level. This model, created using sw Leapfrog, represents the changes of the EC in the groundwater of the coastal phreatic aquifer in this area. Until now, no clear trend in salt-water intrusion in this aquifer has been observed in the last decade. These models could be used in future groundwater numerical model to evaluate water availability in future climatic change contest.

2   INTRODUCTION

Climate change (CC) already have widespread and significant impacts in Europe, which is expected to increase in the future. Groundwater plays a vital role for the land phase of the freshwater cycle and has the capability of buffering or enhancing the impact from extreme climate events causing droughts or floods, depending on the subsurface properties and the status of the system (dry/wet) prior to the climate event. Understanding and taking the hydrogeology into account is therefore essential in the assessment of climate change impacts. Providing harmonised results and products across Europe is further vital for supporting stakeholders, decision makers and EU policies makers.

The Geological Survey Organisations (GSOs) in Europe compile the necessary data and knowledge of the groundwater systems across Europe. In order to enhance the utilisation of these data and knowledge of the subsurface system in CC impact assessments the GSOs, in the framework of GeoERA, has established the project "Tools for Assessment of ClimaTe change ImpacT on Groundwater and Adaptation Strategies – TACTIC". By collaboration among the involved partners, TACTIC aims to enhance and harmonise CC impact assessments and identification and analyses of potential adaptation strategies.

TACTIC is centred around 40 pilot studies covering a variety of CC challenges as well as different hydrogeological settings and different management systems found in Europe. Knowledge and experiences from the pilots will be synthesised and provide a basis for the development of an infra structure on CC impact assessments and adaptation strategies. The final projects results will be made available through the common GeoERA Information Platform (http://www.europe-geology.eu).

The present document reports the TACTIC activities in the pilot called Ravenna phreatic aquifer, located in the Adriatic coast of Emilia-Romagna Region, Italy.

It is a sandy costal aquifer, which extends for about 200 km². The shape and the dimension are indicated in figure 1; along the Adriatic coast the length is about of 16 km, and the pilot area enters towards the alluvial plain of the Po river for 15 km.

The pilot consists in a porous phreatic aquifer composed by amalgamated medium to fine sand of beach/dune complexes and delta-front, deposited during the progradational phase of the Holocenic trasgressive-regressive sedimentary cycle. Aquifer thickness varies from 7 until 21 meters. Thanks to hundreds of geognostic tests (CPT, CPTU, corings, water-wells), it has been possible to produce a detailed geological and hydrostratigraphic reconstruction of the aquifer limits and characteristic (top and bottom surfaces; thickness). Five different geological units were recognised and mapped in a 3D model (using the sw Leapfrog), corresponding to the main depositional environments present in the area (marine shallow water/deltaic to alluvial systems). Sand of the delta-front and strand plain constitues the Coastal Phreatic Aquifer.

The overall objective of this study is to use all the geological and hydrogeological data available to obtain a 3D geological model and a 3D EC distribution model of the aquifer during time.

These models could be used in future groundwater numerical model to evaluate water availability in future climatic change contest.

3   PILOT AREA

Overall introduction to the site and its challenges

In the coastal area of the Emilia-Romagna region many different and precious environments, where ground, fresh water and sea water live together in a delicate balance, are influenced by the characteristics of natural depositional systems and morphological setting of this sector. The rapid urbanization of the coast has mobilized this balance and created numerous water-supply problems that involve coastal aquifers. The increased water demands by expanding population, the increased water requirements for commercial and agricultural purpose and the development of extensive drainage networks for disposal of excess water have added the magnitude and complexity of these problems.

Salt water intrusion and contamination into the phreatic shallow aquifer, could lead to very critical consequences as deterioration of water quality, salinisation of soils, desertification of the coastal plain, with damages for the agricultural and tourist sectors.

We consider that the knowledge framework founding on the reconstruction of geometry and lithological features of the aquifer body is the basic tool to understand flow pattern and processes and to support the actions for mitigation of the nowadays criticisms and planning the future management of water resources.

3.1   Site description and data

- *Location of pilot area (Figure 1):* Pilot area is located in the eastern margin of Po Plain, facing the Adriatic Sea. It belongs to the Emilia-Romagna Region and it is included into the Ravenna Municipality. The aquifer is located on the coastal territory characterized by a huge articulated deltaic plain.
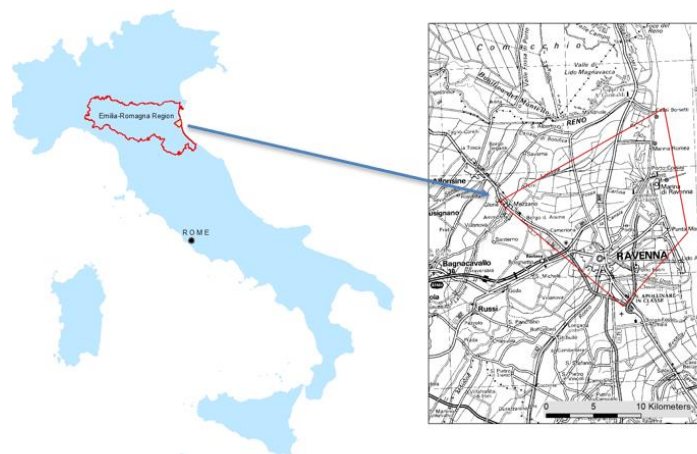

Figure 1 – Location of pilot area

- *Climate*
  - *climate type* is sub-continental/temperate type, with moderately cold winters (the average seasonal temperatures are about 5° C) and hot summers, with temperatures that stand at average values around 23 ° C. The average temperature in Ravenna is about 13.3 °
  - *precipitation and evapotranspiration:* The average annual rainfall is about 650 mm. Rain falls throughout the year in Ravenna. Most of the rain falls around November, with an average total accumulation of 63 millimeters. The least amount of rain falls around July, with an average total accumulation of 29 millimeters.

- *Topography (Figure 2):* the territory is flat and low, with average altitudes about 1.5 m and a maximum around 4 m, made up of anthropic structures (road ramps), river banks and dunes. Some areas are below sea level and correspond mainly to wetlands.
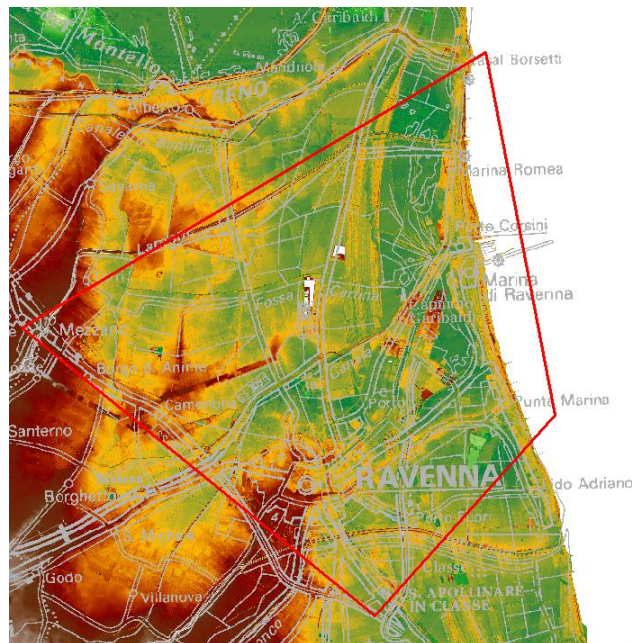
Figure 2 – Topography of the pilot area

- *Land use (Figure 3):* The southern sector of the pilot area is developed around the city of Ravenna and its harbour and it is characterized by urban area (grey colours, red); the central and northern sectors are mainly agricultural areas (mainly light yellow and orange) as in the eastern margin wet areas are widespread (light blue) with extensive pine forests (green colours) towards the sea. The coast is low and sandy, characterized by local touristic towns and a continuous dune/beach system.
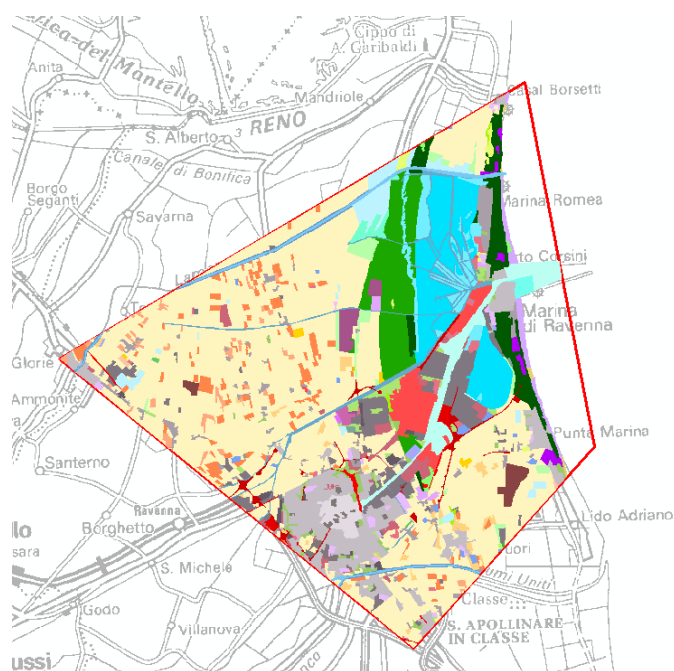
Figure 3 – Land use

- *Soil types (Figure 4):* Soils in this area are mainly calcaric-moderately alkaline; 1D type are soils of the coastal plain and they have a coarse texture; 2A type are soils in morphologically depressed areas of the alluvial plain and they have a fine texture; 3A type are soils in morphologically higher areas of the alluvial plain and they have a medium texture. Polygons indicated with CA correspond to a superficial body of water.
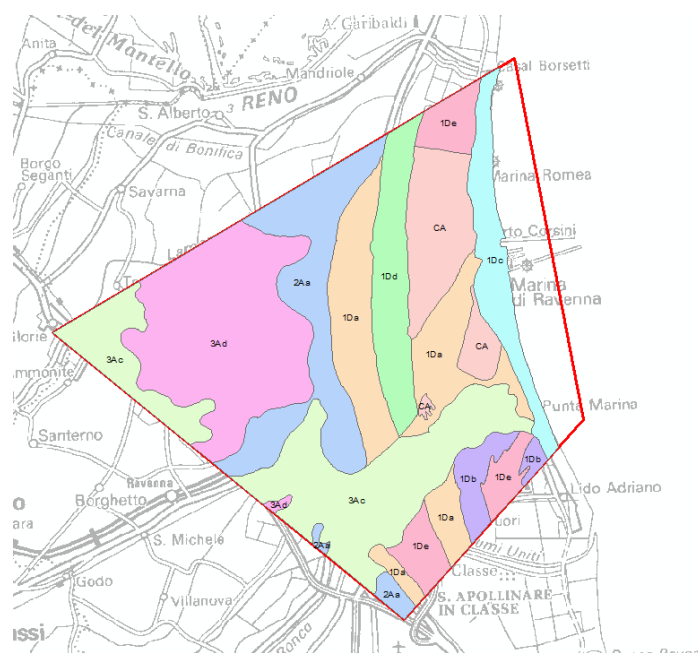

Figure 4 – Soil Types

- *Geology/Aquifer type (Figure 5)*: in this pilot area, alluvial deposits characterize the western sector (yellow to rose) while coastal dune (blue) and lagoonal and swamp deposits outcrop in the eastern sector. Aquifer is porous, phreatic in the eastern sector where it reaches maximum thickness (about 15 m) as pinches out westward, where it becomes semi-confined; it's mainly composed by medium to fine sand of beach/dune complexes and delta-front, deposited during the progradational phase, since 6 ky BP, of the Holocenic ransgressive-regressive sedimentary cycle.
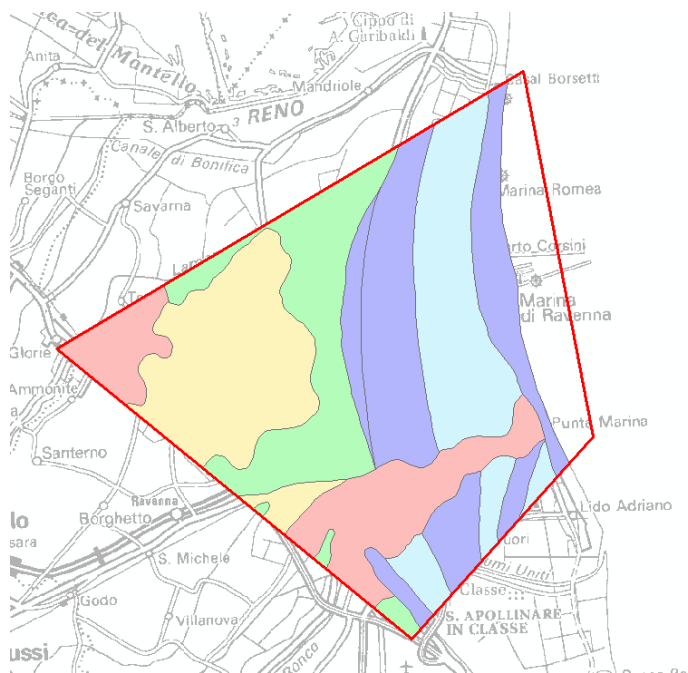
Figure 5 – Surface geology at 1:250.000 scale

- *Surface water bodies (Figure 6)*: The territory is characterized by a dense network of artificial channels (green lines), used for irrigation purposes and for the drainage of surface waters. In the southern margin there is the major river of the area, the Fiumi Uniti River (blue). In the north-eastern area there are large wetlands (blue and light blue polygons), mainly brackish.
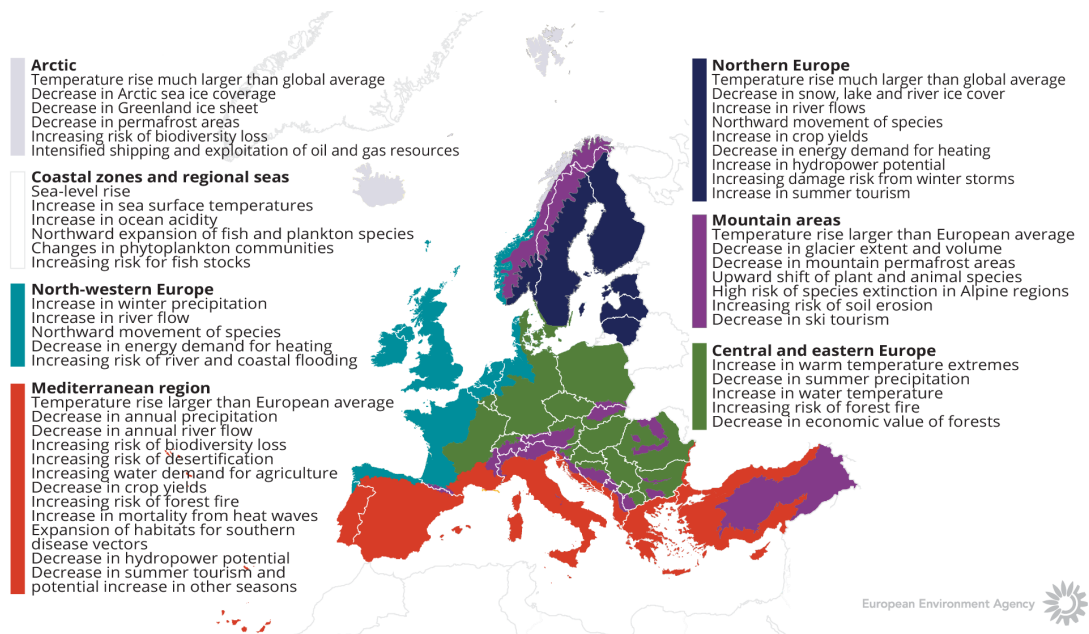
Figure 6 – Surface water bodies

Abstractions/irrigation: in this area only few withdrawals of water from the subsoil are allowed through deep wells because of a great subsidence occurred in the past few years; the large part of the wells existing in this area are very shallow (less than 10 m) and have only a domestic use. Water for irrigation comes only from the channel network presented in Figure 6.

3.2 **Climate change challenge**

In accordance with the EEA map the main expeted issues due to climate change in this case study are those described in the Figure 7 for the Mediterranean regions, with strong rising in summer temperatures, rainfall reduction with a result of drought increasing and salinization of solis and groundwaters.

The main challenge is to find adaptation measures to maintain a good status in the related ecosystem or to promote their controlled and sustainable tranformation; it's important to support a dynamic management of groundwater bodies through a in-depth knowledge of balance between subtraction of fresh water and recharge of the aquifer troughtout the future climate change conditions.

In this context, we consider that the geological reconstruction of the aquifer could be one of the basic tools to support the necessary actions to mitigate the changes in the availability of surface and groundwater induced by climate change.

Arctic
Temperature rise much larger than global average
Decrease in Arctic sea ice coverage
Decrease in Greenland ice sheet
Decrease in permafrost areas
Increasing risk of biodiversity loss
Intensified shipping and exploitation of oil and gas resources

Coastal zones and regional seas
Sea-level rise
Increase in sea surface temperatures
Increase in ocean acidity
Northward expansion of fish and plankton species
Changes in phytoplankton communities
Increasing risk for fish stocks

North-western Europe
Increase in winter precipitation
Increase in river flow
Northward movement of species
Decrease in energy demand for heating
Increasing risk of river and coastal flooding

Mediterranean region
Temperature rise larger than European average
Decrease in annual precipitation
Decrease in annual river flow
Increasing risk of biodiversity loss
Increasing risk of desertification
Increasing water demand for agriculture
Decrease in crop yields
Increasing risk of forest fire
Increase in mortality from heat waves
Expansion of habitats for southern
disease vectors
Decrease in hydropower potential
Decrease in summer tourism and
potential increase in other seasons

Northern Europe
Temperature rise much larger than global average
Decrease in snow, lake and river ice cover
Increase in river flows
Northward movement of species
Increase in crop yields
Decrease in energy demand for heating
Increase in hydropower potential
Increasing damage risk from winter storms
Increase in summer tourism

Mountain areas
Temperature rise larger than European average
Decrease in glacier extent and volume
Decrease in mountain permafrost areas
Upward shift of plant and animal species
High risk of species extinction in Alpine regions
Increasing risk of soil erosion
Decrease in ski tourism

Central and eastern Europe
Increase in warm temperature extremes
Decrease in summer precipitation
Increase in water temperature
Increasing risk of forest fire
Decrease in economic value of forests

European Environment Agency

Figure 7 - Climate expected change in Europe. The European Environment Agency map

4 METHODOLOGY

4.1 Methodology and climate data

4.1.1 Tools/ model description

The approach to the impact and adaptation assessment started from the characterization of hydrogeological dynamics on the base of historical data.

Therefore, the activity focused on the reconstruction of the physical, lithological and hydrogeological features of the coastal phreatic aquifer and on the integration of the three-dimensional model created with the geological and hydrogeological monitoring data available.

Five different geological units were recognised and mapped in 3D (with sw Leapfrog) in the pilot area, corresponding to the main depositional environments present (marine shallow water/deltaic to alluvial systems, figure 8a); the orange unit includes delta-front and strand plain sands and constitutes the Coastal Phreatic Aquifer.

The groundwater monitoring started in 2009 and is still in progress; it is carried out with a probe that measures water level, temperature and electrical conductivity every meter in piezometers with a depth between 7 and 21 meters. An example of how we collect the data is shown in figure 8b, where the trend of EC, temperature and piezometric level are illustrated with reference to one of the monitoring points.

The Holocene succession has been studied for the creation of the 3D model, with a particular attention to the upper sandy portion, where the coastal phreatic aquifer develops, consisting of prograding dunes, beach ridges and delta front deposits.

The data were integrated, and it was possible to identify the groundwater bodies for each survey and the three-dimensional variation of the parameters mentioned above. With reference to September 2013 survey, the EC 3D and 2D distribution are represented in figure 9 a, b and c. In the reported example EC varies from < 2.5 ms/cm to > 30 ms/cm; only a little portion of the aquifer is saturated in fresh water (blue area in left upper portion), while a large amount of the costal phreatic aquifer is saturated by salt water (green areas). We consider that this could be the natural distribution of the EC, due to the equilibrium from the recharge in fresh water from the rain, rivers and irrigation, and the salt intrusion from the Adriatic Sea and from the canals where marine water enters during storm and tide.

The aim is to provide a solid base-knowledge, when the data and models will be available to develop future scenarios. At the moment, in fact, no new tools have been produced nor those proposed within the project have been used due to the lack of fundamental necessary information, first of all the quantification of the contribution of the various factors in the flow balance. It is hoped that these data will be available in the future.
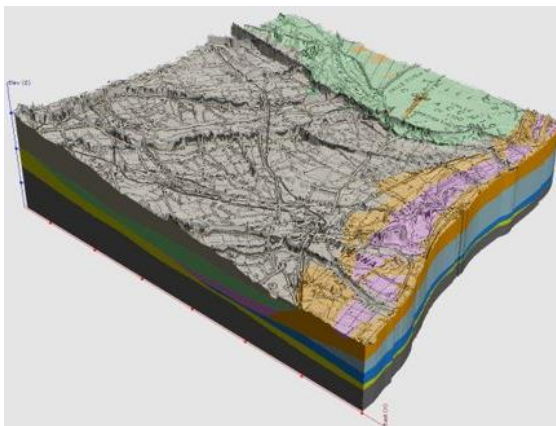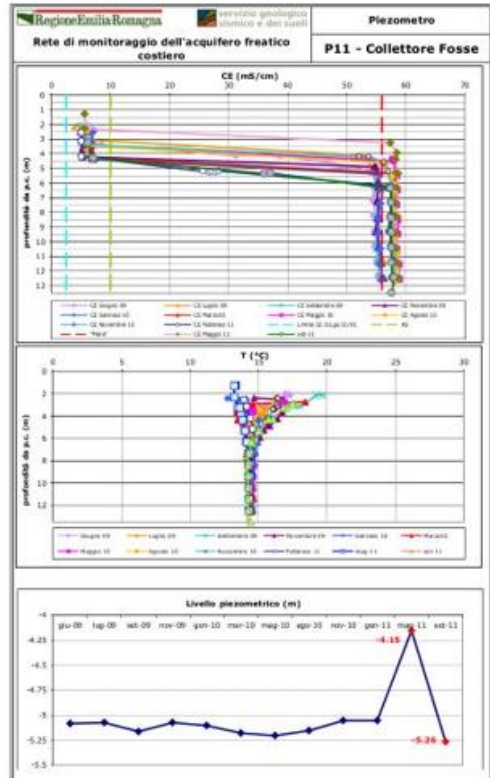
Figure 8: 3D geological model of the Ravenna pilot site, orange colour represents the phreatic aquifer (a). Example of electrical conductivity (EC mS/cm), temperature, and piezometric level available from monitoring surveys (b)

a

b
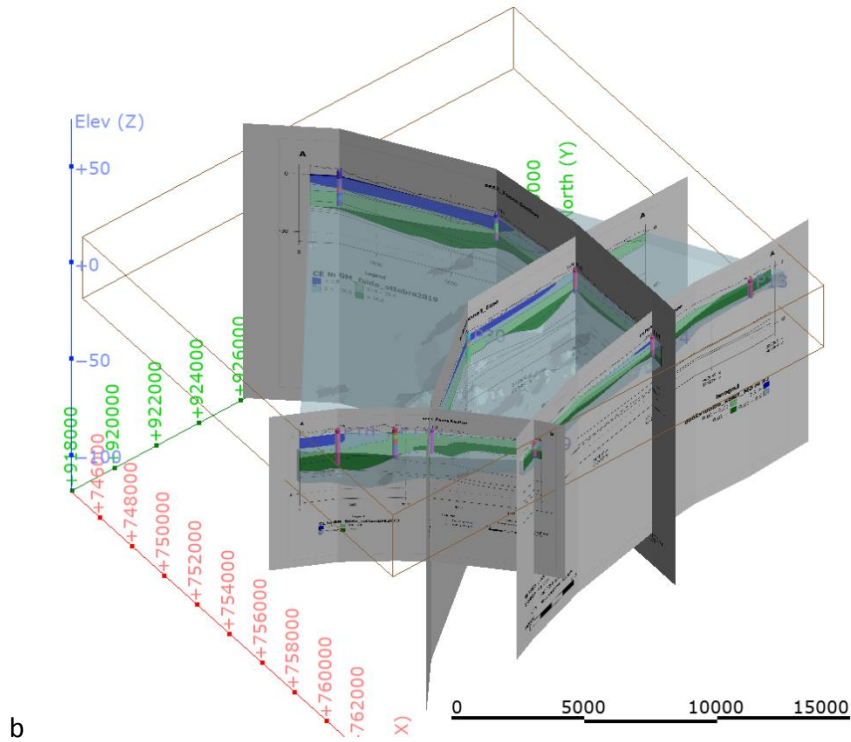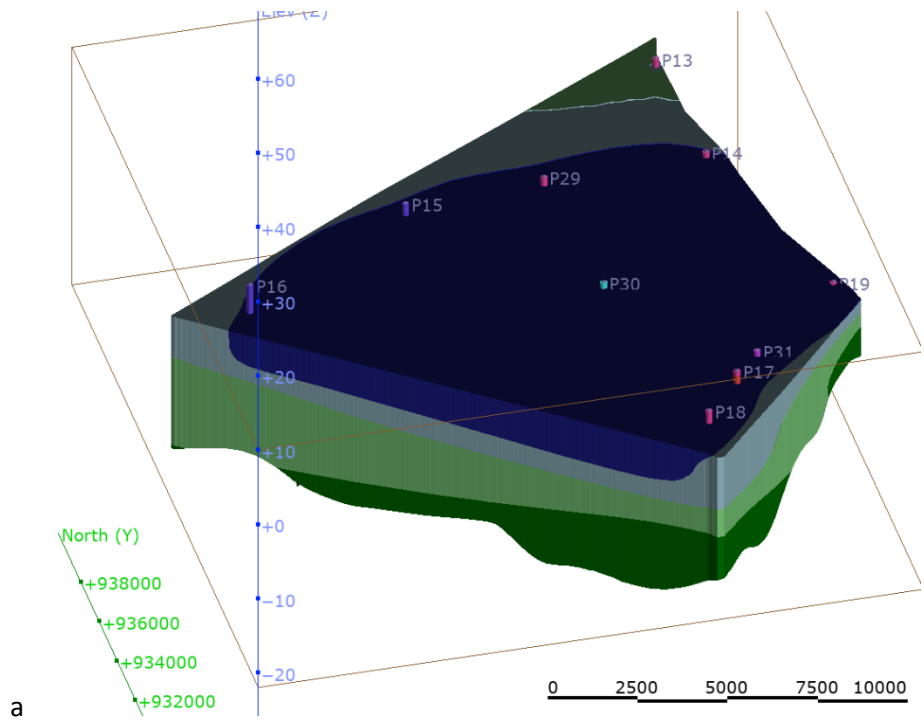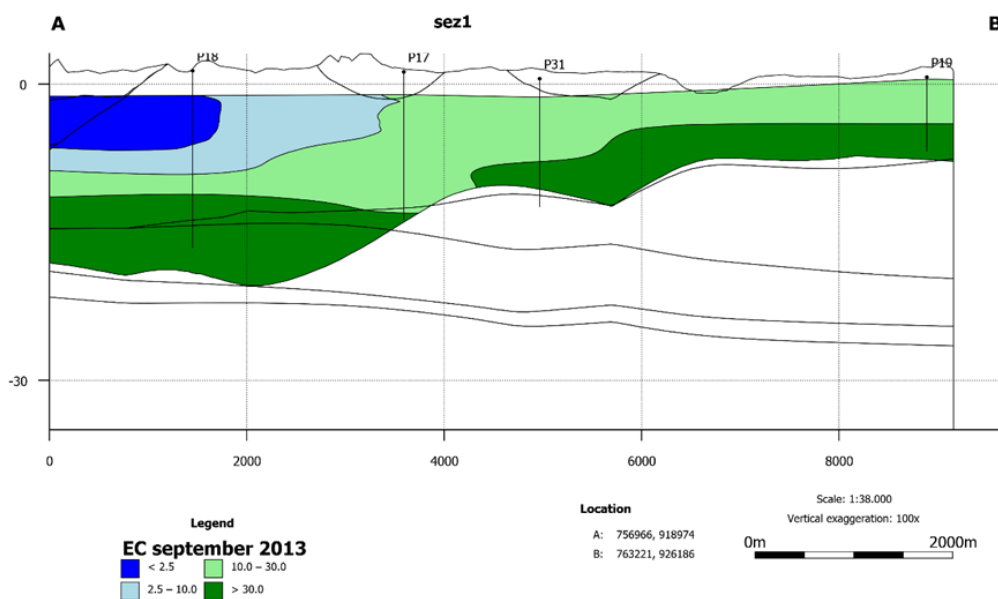
c

Figure 9: integration of EC data with geological model: a) 3D variation of EC within the aquifer; b) representative cross-section network; c) cross-section with geological units (black line) and EC distribution within the aquifer (coloured from dark blue to dark green).

The aquifer volume in the Ravenna pilot affected by brackish (EC from 10 to 30 mS/cm) and saltwater (EC > 30 mS/cm) intrusion varies between 79% and 61%, considering the four monitoring surveys in the period 2009-2019 (Table 1).

	October 2009	March 2010	September 2013		October 2019
Volume of total groundwater within aquifer (mc)	2.543.800.000	2.755.700.000	2.607.700.000		2.664.500.000
Volume of groundwater with EC>10 mS/cm within aquifer (mc)	2.008.530.000	1.681.840.000	1.916.780.000		1.656.360.000
% of EC>10 water	79	61	74		62
Volume of water with EC>30 mS/cm	930.530.000	608.740.000	865.480.000		657.940.000

within aquifer (mc)					
% of EC>30 water	37	22	33		25

Table 1: Volume of total and brackish to salt water within the aquifer.

The results show that the condition of the aquifer in the last ten years is quite stable with a strong natural contamination of brackish and salt water by sea. Changes in EC lateral and vertical distribution are associated to variation in total rainfall in the different years and also to groundwater flow, that influenced the intrusion of salt water (EC> 30 mS / cm) in depth.

On the basis of these results, no particular trends potentially associated with ongoing climate change for the period analyzed are observed. A long-term future projection, also in the light of the recent scenarios of the meteo-climatic forcings, could highlight important changes in the SWI. The fact remains that, due to the trend towards an increase in temperatures and drought periods (see below), an escalation of the phenomenon must be expected.

4.1.2 Future scenarios. Climate and land use data

In this case study, for the reasons mentioned above, no modeling was developed for a quantitative assessment of the changes in groundwater due to climate change. However, it is possible to already have an idea of how the climate will vary in the future in Emilia-Romagna and foresee a clear deterioration of the water resources in question.

Arpae-Emilia-Romagna Region has conducted several studies on the impact of the climate on the environment at a regional and local scale; in particular, the effects of rising temperatures on the water resource have been investigated (EU Interreg IVC Water CoRe Project). The results show that in the climatic projections predict an increase in the average annual temperature for the Italian peninsula, between 1.5 and 2 ° C, in the period 2021-2050. In the same period, for the Emilia-Romagna region there is a signal of 2 ° C increase for both the minimum and maximum temperatures. The change in the last part of the century, 2071-2100, will be much more marked, in which an even more marked increase in the average annual temperature will occur, around 3.5-4 ° C and for the summer season an increase in the maximum number of consecutive days without precipitation is expected. There will therefore be an increase in both mean and extreme values. This means that very hot (with positive anomalies of 3-4 degrees) and relatively prolonged periods, which today are extreme events, will be more frequent in the 2021-2050 period and will be the norm at the end of the century. In the Emilia-Romagna Region in recent years there is evidence of the impacts of climate change on natural areas and cities, but ecosystems, such as forests and wetlands, biodiversity, the availability of drinking water resources and the agriculture are also affected by climate change.

When the SWI modelling will be applied, the use of the local scenario weather-climatic data (Arpae) or ISIMIP (Inter Sectoral Impact Model Intercomparison Project, see www.isimip.org) datasets will be evaluated, considering also the expected rising of the Adriatic Sea.

What we have done until now is to realise a 3D geological model and a 3D distribution of EC over time, which could be used in future groundwater numerical model to evaluate water availability in future climatic change contest.

5   RESULTS AND CONCLUSIONS

The SWI assessment was based on the reconstruction of the aquifer architecture and on the lithological and hydrogeological characterization. This was possible thanks to the amount of data archived in the Geognostic Database of the Emilia-Romagna Region. The aquifer has also been monitored for 12 years through a network of piezometers by which groundwater level, EC and temperature, has been measured several times a year.

The type of data favors the definition of the basic structure of the aquifer, SWI state and its evolution. Until now, on the basis of monitoring data, no particular trends potentially associated with ongoing climate change for the period analyzed are observed.

The future scenarios, on a modeling basis, was not dealt with, which would be the proper integration to the work done so far. The application of a model was conditioned by the lack of quantification of the system's water balance. The current approach in the study was: knowing the past in order to predict the future. When the SWI modelling will be applied, the use of the local scenario weather-climatic data (Arpae) or ISIMIP (Inter Sectoral Impact Model Intercomparison Project, see www.isimip.org) datasets will be evaluated, considering also the expected rising of the Adriatic Sea. What we have done until now is to realise a 3D geological model and a 3D distribution of EC over time, which could be used in future groundwater numerical model to evaluate water availability in future climatic change contest. These 3D models have been published on GEOERA web site, according to GIP-P colleagues.

6   REFERENCES

Amorosi A., M. C. Centineo, M. L. Colalongo, G. Pasini, G. Sarti, e S. C. Vaiani (2003) - Facies Architecture and Latest Pleistocene–Holocene Depositional History of the Po Delta (Comacchio Area), Italy. The Journal of Geology, 111, 39–56

Barlow P.M., 2003. Ground water in freshwater-saltwater environments of the Atlantic Coast. USGS Circular 1262.

Carbognin L., Rizzetto F., Tosi L., Teatini P., Gasparetto-Stori G., 2005. L'intrusione salina nel comprensorio lagunare veneziano. Il bacino meridionale. Giornale di Geologia Applicata 2 (2005) 119-124.

Carbognin L., Rizzetto F., Tosi L., Teatini P., Gasparetto-Stori G., 2005. L'intrusione salina nel comprensorio lagunare veneziano. Il bacino meridionale. Giornale di Geologia Applicata 2 (2005) 119-124.

Esca S., Venturini L., 2006. Hydrogeological impact of wellpoint dewatering upon unconfined coastal aquifer of the municipality of Cervia (Ravenna – Italy). Proceedings 1st SWIM-SWICA Joint Saltwater intrusion Conference, Cagliari-Chia Laguna, Italy – September 24-29, 2006, 71-77.

Gargini A., Spensieri P., Rossi M. (2001). Monitoraggio dei parametri idrogeologici ed idrochimici della rete freatimetrica costiera della provincia di Ferrara nel periodo 1989-1999. Università degli Studi di Ferrara, Provincia di Ferrara. Italia tipolitografia (Fe).

Martini A., Semenda srl, Daniele G., Angelelli A., 2007. La cartografia Geologica e dei Suoli online. Rapporto Interno, Servizio Geologico Simico e dei Suolo, Luglio 2007.

Piccinini L., Vincenzi V., Gargini A., 2008. Modellazione di flusso a densità variabile di un acquifero freatico salinizzato. Giornale di Geologia Applicata 2008, 9 (2) 249-261.
Post V.E.A., 2005. Fresh and saline groundwater interaction in coastal aquifers: Is our technology ready for the problems ahead? Hydrogeol J, 16: 120-123.

Rizzini A. (1974) – Holocene sedimentary cycle and heavy mineral distribution, Romagna-Marche coastal plain, Italy. Sedimentary Geology, 11, 17-37.

Stefani M. e S. Vincenzi (2005) - The interplay of eustasy, climate and human activity in the late Quaternary depositional evolution and sedimentary architecture of the Po Delta system. Marine Geology, 222-223, 19-48

Ulazzi E., M. Antonellini, G. Gabbianelli (2007) - Characterization of the Coastal Phreatic Aquifer of the Cervia Area (NE Italy). Mem. Descr. Carta Geol. d'It., 76, 277-288

Venturini L. (2008) - Impatto idrogeologico degli scavi sotto-falda in ambito costiero (Dewatering dei terreni di fondazione). Presentazione orale in: Idrogeologia in Emilia-Romagna risorsa, applicazioni e tutela, 3 ottobre 2008 Palazzo del Podestà Castell'Arquato Piacenza.

Deliverable 5.3 and 6.3

PILOT DESCRIPTION AND ASSESSMENT

Vrana lake, Croatia

Authors and affiliation:

Andrej Stroj

Croatian geological survey (HGI-CGS)

Deliverable Data	
Deliverable number	D*5.3* & D6.*3*
Dissemination level	Public
Deliverable name	Pilot description and assessment
Work package	WP5: **ASSESSMENT OF SALT-/SEA WATER INTRUSION STATUS AND VULNERABILITY**; WP6: **GROUNDWATER ADAPTATION STRATEGIES**
Lead WP/Deliverable beneficiary	IGME
Deliverable status	
Version	*Version 3*
Date	*1/4/2021*

[This page has intentionally been left blank]
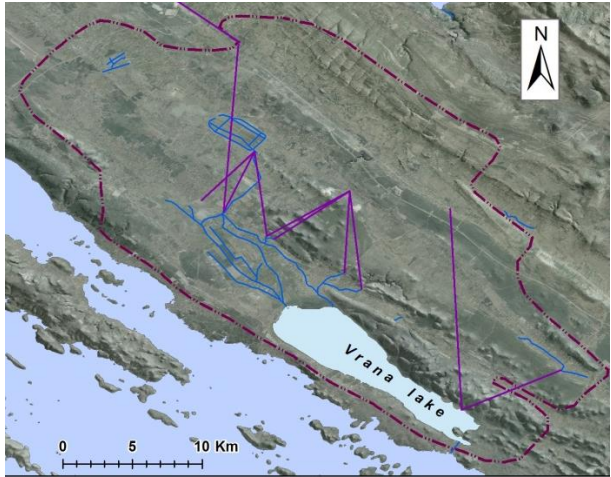
LIST OF ABBREVIATIONS & ACRONYMS

CC	Climate Change
GC	Global Change
LULC	Land Use and Land Cover
SWI	Sea Water Intrusion
GSO	Geological Survey Organisations
PET	Potential evapotranspiration

TABLE OF CONTENTS

1 EXECUTIVE SUMMARY

Pilot name	Vrana lake	
Country	Croatia	
EU-region	Mediterranean region	
Area (km^2)	516 km^2	
Aquifer geology and type classification	Karstic limestones, Fissured aquifer	
Primary water usage	Drinking, irrigation	
Main climate change issues	Vrana lake is situated in the close vicinity of Adriatic Sea coast in highly karstified terrain (Dinaric Karst region). The lake is declared as a nature protection area. Permeable terrain between the lake and the sea enable underground inflow of sea water into the lake during dry periods when lake level is low. Therefore, the lake eco system is highly vulnerable to increasing duration of draughts as well as sea level rising. Pumping of groundwater for public water supply and irrigation in the catchment presents additional pressure on the lake system.	
Models and methods used	Time series analysis, conceptual and lumped model (GARDENIA-BRGM, METRAN-TNO)	
Key stakeholders	Vrana lake nature park (public institution), water supply company, private farmers	
Contact person	Andrej Stroj, Croatian Geological Survey, astroj@hgi-cgs.hr	

Vrana lake is situated in Croatian coastal region Dalmatia, separated from the Adriatis Sea by a narrow carbonate ridge less than 1 km wide in its narrowest parts. The lake and its immediate surrounding is declared as a nature protection area. Carbonate ridge, which separates the lake from the sea, is intensely karstified, i.e. permeable for groundwater flow. This enables sea water intrusion (SWI) to the lake through permeable subsurface during the low lake water levels. Lake water level above the sea level is the main factor that prevent SWI. Although occasionally slightly brackish lake water is natural characteristic of the lake, inflow of a sea water during prolonged draught periods, which are generally concurrent with summer seasons in the area, produce excessive salinization of the lake and a major threat to the ecosystem. The most important cause for lowering the lake water levels during relatively hot summer seasons is direct evaporation from the lake. High water and air temperatures, together with large lake surface area (approx. 30 km^2) and shallow depth (up to a few meters) produce very high rates of evaporation. Lake level and salinization dynamics shows significant inertia, so major lake salinization events typically occur when the lake was not sufficiently replenished during preceding wet season, resulting in low water level and increased salinity at the beginning of summer/draught periods.

The lake is fed solely by groundwater from the extensive karstic catchment with approx. area of 500 km^2. Pumping of groundwater for public water supply and irrigation in the catchment presents additional pressure on the lake system, as sufficient fresh water inflow is essential to control SWI to the lake. Additional unfavourable factor presents presence of artificial channel for evacuation of the lake water during high water levels. The channel was firstly built in 18th century, reconstructed additionally several times afterwards, with the aim to drain the extensive wetlands in the area upstream from the lake. Before the channel construction the lake was drained naturally through the permeable subsurface, but channel considerably fastens that process resulting with lower water levels at the beginning of dry summer periods, when lake water losses continue by strong evaporation. Intensive agriculture is still present in the area upstream from the lake, and closing of the channel during the wet seasons would cause flooding of the agricultural lands. This prevents restoration/closing of the channel in order to re-establish natural conditions.

As already explained, SWI feed lake during low lake water levels, resulting in lake level stabilization at levels slightly below sea water level despite high evaporation and low fresh water inflow during prolonged draughts. Therefore, CC, which results in increasing temperature and prolonged draughts in the area, presents major thread to the lake ecosystem. Increasing trend of the sea water level, which is also a consequence of CC and GC, would additionally amplify lake salinization processes in the future. In depth understanding and significance estimation of all processes, influencing the lake SWI is necessary to predict future CC scenarios, as well as to consider potential adaptation and mitigation strategies.

All available data time series, related to the historical lake level and salinity dynamics, were collected: over 70 years of the lake level data; almost 60 years of rainfall, air temperature and relative humidity data which served also for calculation of potential evapotranspiration (PET) data based on Turc method (Etp Turc software developed by BRGM); data on direct evaporation from the lake surface; and 18 years of monthly lake salinity measurements. Preliminary time series analysis was carried out including descriptive statistics, autocorrelation and cross correlation functions to examine system inertia and interdependence of different parameters. After the preliminary time series analysis, lumped modelling tools were used to model lake level dynamics based on precipitations, PET and direct lake evaporation. GARDENIA (developed by BRGM), METRAN (developed by TNO) and AQUIMOD (developed by BGS) lumped modelling tools were tested for modelling purposes. Although all used tools were principally developed for modelling groundwater levels in aquifers, they were tested for modelling lake level, which is in strong connection with the surrounding karst groundwater. Water fluxes to the lake are happening mainly dispersedly through the karst subsurface, and consequently impossible to be directly measured and monitored. This prevents modelling the lake level based on direct inflow, outflow and lake geometry. Lumped groundwater modelling tools were used as an option to overcame this problem. GARDENIA and AQUIMOD models enable level modelling based on precipitations and additionally pumping dynamics, which was used as equivalent process to direct evaporation from the lake. METRAN model is pure transfer function model which can use several input time series in order to model output series. Simple transfer function was also used to model lake salinity response to the low lake levels.

Best results for lake level modelling were obtained by GARDENIA software due to effective way to take evaporation effect into account as a pumping. GARDENIA software calibrates pumping influence with pumping coefficient, determined automatically through calibration. AQUIMOD software also has option to include pumping to the model, but its influence is not calibrated through coefficient, resulting in largely overestimated effect when it was expressed in

recommended units. Therefore, pumping/direct evaporation was not included in the AQUIMOD model, resulting with low final model efficiency. Moreover, we experience additional problems with automatic calibration process: final parameters for the model were calibrated manually. METRAN software succeeded to produce relatively efficient model based by two input series: precipitations and air temperatures. Direct lake evaporation is strongly correlated to air temperature, and together with the precipitation is main controlling factor for the lake level dynamics. This enables good efficiency of the METRAN model. Main problem with the METRAN is that it is not user friendly in the present form, so all the modelling work had to be done by TNO expert who developed the tool.

The second considered model for the lake salinity study was dependence of the lake salinity on the lake levels. First, critical lake level was determined, below which salinity start to increase. Afterwards, only levels below critical level were taken as a input series, and lake salinity values as an output. Simple transfer function that summed influence of 10 months historical period of lake levels below threshold value produced good agreement with the observed vales. Finally, usage of lake level model and lake salinity model together enabled possibility for prediction of future lake salinity, based on predicted precipitations and air temperature from various CC scenarios.

2 INTRODUCTION

Climate change (CC) already have widespread and significant impacts in Europe, which is expected to increase in the future. Groundwater plays a vital role for the land phase of the freshwater cycle and has the capability of buffering or enhancing the impact from extreme climate events causing droughts or floods, depending on the subsurface properties and the status of the system (dry/wet) prior to the climate event. Understanding and taking the hydrogeology into account is therefore essential in the assessment of climate change impacts. Providing harmonised results and products across Europe is further vital for supporting stakeholders, decision makers and EU policies makers.

The Geological Survey Organisations (GSOs) in Europe compile the necessary data and knowledge of the groundwater systems across Europe. In order to enhance the utilisation of these data and knowledge of the subsurface system in CC impact assessments the GSOs, in the framework of GeoERA, has established the project "Tools for Assessment of ClimaTe change ImpacT on Groundwater and Adaptation Strategies – TACTIC". By collaboration among the involved partners, TACTIC aims to enhance and harmonise CC impact assessments and identification and analyses of potential adaptation strategies.

TACTIC is centred around 40 pilot studies covering a variety of CC challenges as well as different hydrogeological settings and different management systems found in Europe. Knowledge and experiences from the pilots will be synthesised and provide a basis for the development of an infra structure on CC impact assessments and adaptation strategies. The final projects results will be made available through the common GeoERA Information Platform (http://www.europe-geology.eu).

The present document reports the TACTIC activities in the pilot Vrana lake located in the Adriatic Sea coast of Croatia, in Dalmatia province. The lake is declared as a nature protection area (Nature Park) because of its rare natural habitats and biodiversity. It has been included in the list of Important Bird Areas in Europe and became Ramsar site. Lake is fed mainly by a groundwater from a large karstic catchment. The lake is separated from the sea by relatively narrow (in places less than 1 km wide) carbonate tidge. Carbonate ridge is intensely karstified, what enables SWI to the lake during low lake water levels through the permeable subsurface. Although occasionally brackish lake water is natural characteristic of the lake, more and more pronounced draught periods, increasing temperatures and sea level rising due to a CC and GC are the main thread for the vulnerable lake ecosystem. Detailed knowledge of all processes, influencing the lake SWI, is necessary to assess and summarise impacts of potential future CC and GC scenarios, and to identify potential measures for mitigation of adverse consequences and to estimate their impact. Therefore, the Vrana pilot was included in TACTIC WP5: *Assessment of salt-/sea water intrusion status and vulnerability* and WP6: G*roundwater adaptation strategies* in order to examine potential future CC scenarios for the lake SWI, as well as to consider potential adaptation and mitigation strategies. Within the TACTIC project different modelling tools were used and tested for modelling the lake level based on historic climatic measurements, as well as future CC predictions, which were developed and provided by partner GSOs (GARDENIA by BRGM, AQUIMOD by BGS and METRAN by TNO).

3 PILOT AREA

3.1 Site description and data

3.1.1 Location and extension of the pilot area

The pilot area is located in the western part of Croatia (Dalmatia) beside the Adriatic Sea coast (Fig 1). It is located within the broader Dinaric Karst region which spreads across the several countries (Slovenia, Croatia, Bosnia and Herzegovina, Montenegro, northern Albania) parallel to the eastern Adriatic sea coast. Vrana lake catchment area belongs to Mediterranean region and covers approx.. 515 km^2 (Fig. 1).
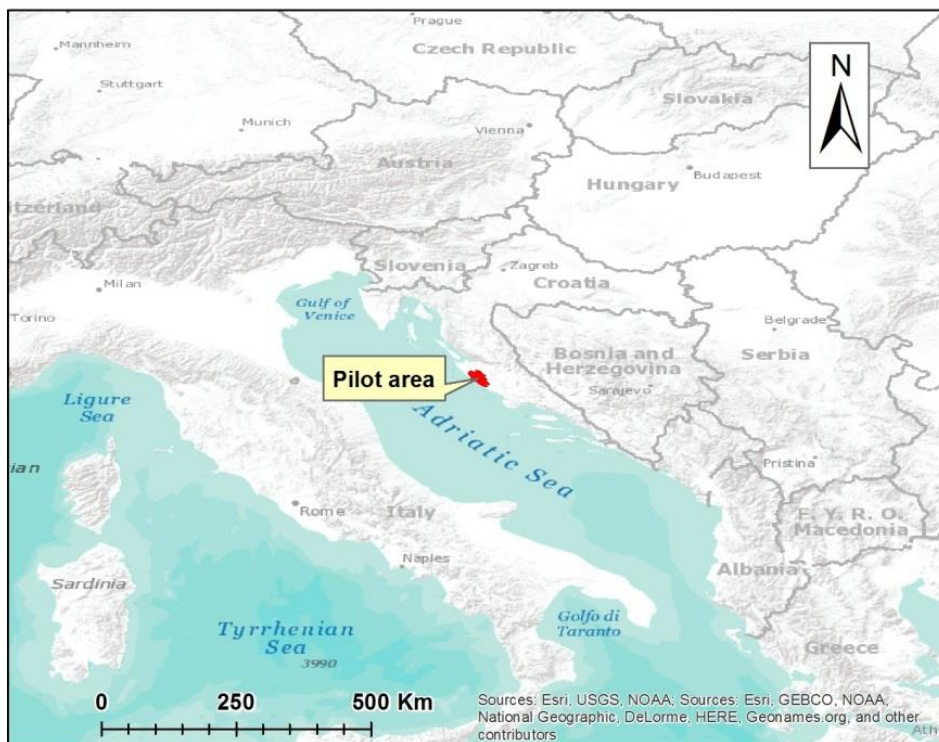
Figure 1. Location of the pilot area

Vrana lake is situated in the close vicinity of Adriatic Sea coast in highly karstified terrain (Dinaric Karst region). It is located in a shallow kryptodepression with the bottom at –3.5 m a.s.l. Lake water levels vary annually approx. in the range 0–2.5 m a.s.l. Permeable terrain between the lake and the sea enable underground SWI into the lake during dry periods, in conditions when the lake level drop close or even slightly below sea level. Therefore, the lake eco system is highly vulnerable to increasing duration of draughts as well as sea level rising.

Upstream of the lake, within the same karstic catchment, there is agricultural lowland area called Vrana polje (45 km^2). Agricultural activities include groundwater abstractions for irrigation purposes (mostly uncontrolled). Public Water Supply Company also use groundwater from the catchment with pumping stations located on the major freshwater springs upstream from the lake, mostly at the NE edge of the Vrana polje.

In the SE part of the lake, across the narrowest part of the carbonate ridge that separates the lake from the sea, there is an 850 m long artificial channel for evacuation of the lake water during high water levels. The channel was firstly excavated in 18th century, additionally reconstructed and deepened afterwards, with the aim to drain the extensive wetlands in the area upstream from the lake (Vrana polje, agricultural area that was marshy area prior the channel). Before the channel construction the lake was drained only through the permeable (karstified) subsurface, and channel considerably fastens that process. Although the channel bottom is slightly above average sea water level, fast drainage through the channel in high lake level conditions results with lower water levels at the beginning of dry summer periods. During low lake levels, when drainage through the channel ceases, lake water losses continue by strong evaporation. As intensive agriculture is present in the area upstream from the lake, closing of the channel during the wet seasons would cause flooding of the agricultural lands. This prevents restoration/closing of the channel as a measure to re-establish natural conditions.

3.1.2 Climate

Climate in the area of Vransko Lake is typically Mediterranean, with mild, considerably short and rainy winter periods, and dry, hot summers. By Köppen, this type of climate is called "Olive tree climate". Holm oak forests, maquis (Mediterranean scrubland) and dry grasslands on rocky karst terrain characterize its vegetation.

Mean annual temperature varies within the watershed in the range 12-15°C, and average annual precipitation amounts 950 mm/y (Zaninović et al. 2008). Warmest months of the year are July and August (21-24°C monthly averages), and January and February are the coolest (5-8 °C). October and November have the highest precipitation (approx. 120 mm monthly average), and June and July are the driest months (approx. 50 mm monthly average). Infiltration coefficient is estimated to be approx. 0.2-0.3. Based on the estimated infiltration coefficient, mean annual recharge is approx. 250 mm, which equals 129×10^6 m^3/y.

3.1.3 Topography and soil cover

Water catchment of Vrana Lake consists of levelled surfaces of karst poljes, separated by moderately elevated hills and ridges. All the morphological features are elongated in NW-SE direction, known as a Dinaric strike direction. Elevation of the area ranges from 0-300 m a.s.l. (Fig. 2), generally rising in NE direction. Soil cover of variable thickness covers levelled surfaces, while on elevated hilly areas soil cover is almost absent with bare limestone rock outcrops on the surface.
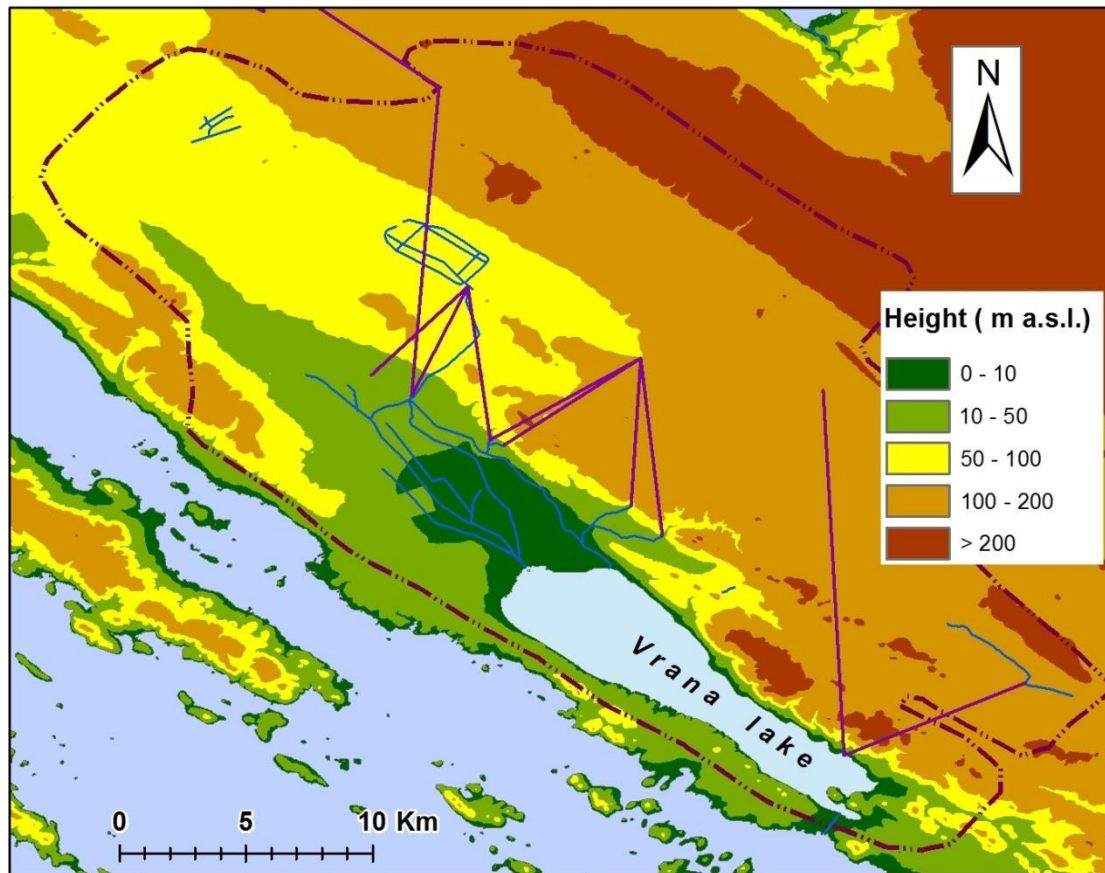
Figure 2. Topography of the pilot area.

3.1.3 Land use

Vrana lake and its immediate surrounding is declared as a nature protection area (Nature park) because of its rare natural habitats and biodiversity. It has been included in the list of Important Bird Areas in Europe and became Ramsar site. Lake is fed mainly by a groundwater from a large karstic catchment (>500 km^2). Nature protected area, which is in natural condition, presents only a small part of the catchment (approx. 57 km^2, of which 30 km^2 is extent of the Lake).

Vrana polje area was historically occasionally flooded swampy area upstream from the lake. Artificial drainage of the Vrana polje begun in 18th century with construction of the channel connecting the lake with the sea. The Channel serve for evacuation of the lake water during high water levels up to present day. Additional network of drainage channels across the polje area converted wetland to arable land. Today Vrana polje is agricultural area which is both drained and partly irrigated during dry seasons.

There are additional agricultural areas in the catchment area, typically situated within the elongated shallow valleys and levelled surfaces (karst poljes), separated with rocky hills and ridges. Rocky carbonate hills are covered with shrubs and Mediterranean woods. Larger settlements are located at the see coast (downstream from the lake), while inner parts of the catchment are relatively sparsely inhabited, without larger individual settlements.

3.1.3 Geology/Aquifer type

Study area is dominantly built of limestones (karst rocks) of Cretacious and Paleogene age, and in lesser extent of flysch rock complex of Paleogene age (Fig. 3). Flysch rocks are generally covered by soil cover, while soil cover is almost absent on limestones (Fig. 3). Area is tectonically folded and thrusted, with dominant NW-SE strike of the structures (faults and fold axes). The Flysch rocks, representing the stratigraphically youngest rocks, are situated in the core areas of the synclines. Thrust faults often intersect and deform continuation of synclines and anticlines in the area.

Limestones are well karstified, proven by a number of tracing tests performed in the area (Fig. 3). Surficial water flows are mostly absent on the limestone areas, and precipitations quickly infiltrate into the epikarst (surficial most intensively karstified zone, usually few to ten meters thick). Infiltrated water is partly transported from epikarst further to the deeper karst conduit networks, but it is also partly lost through evapotranspiration processes as epikarst zone is typically within the reach of plant roots.

Ground water flow in karst terrains is concentrated within karst conduits, while surrounding rock mass usually have very low porosity and consequently low permeability. Low permeability of the rock mass is reflected by general unproductiveness of wells that failed to intercept significant conduits. Storage of water is mainly related to shallow epikarst zone, as well as fractured rock mass within the deeper vadose and phreatic zone. Exact significance of epikarst zone and deeper zones for water storage is still relatively unclear. However, storage and regulation capacity of the karst system is limited, resulting in typical extreme oscillation of spring discharges during dry and wet seasons. This causes occasional floods of low lying karst terrains during wet seasons, as well as water scarcity in dry seasons.

Flysch rock complex consist of intercalation of marl, sandstone and limestone beds. In contrary to limestone terrains, flysch terrains are generally non-karstified and impermeable, forming hydrogeological barriers in the subsurface. Therefore, in flysch areas water flow mostly on the terrain surface. Position of flysch rocks above limestones within synclines often form "hanging" groundwater flow barriers which enable deep karstic flows beneath them (Fig. 4).
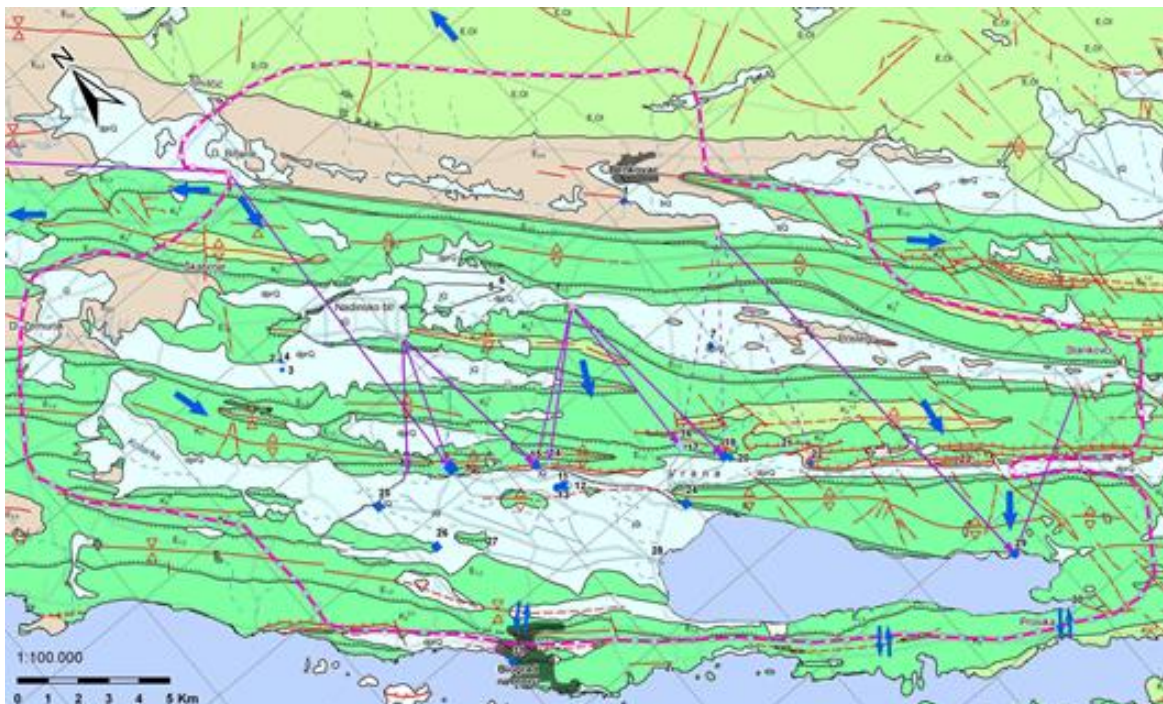
Figure 3. Hydrogeologic map of the Vrana lake catchment (karst rocks in green colors, low permeable flysch rocks in brown, unconsolidated sediment cover in light blue, ground water tracing connections are marked with purple lines, groundwater flow directions with blue arrows, adapted from Stroj 2012).

While majority of the karstic springs in the Vrana polje area discharges fresh water, there are also a few springs discharging brackish water. SWI on the springs is not controlled directly by their distance from the sea coast, but rather by depth of water circulation (Fig. 4). More precisely, springs that are fed by the water from deep lying karst conduits, which are situated below fresh water-brackish water interface, discharges brackish water. Seawater share in the spring water is variable depending on hydrological conditions, i.e. inflow of fresh water to the conduit system.

Vrana karst polje
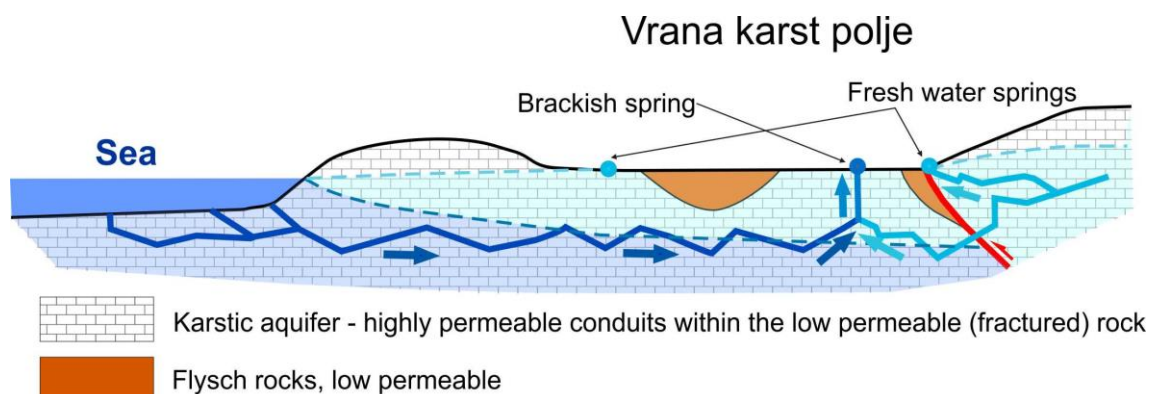
Figure 4. Conceptual model of sea water intrusion affecting some of the inland springs on the Vransko polje area (upstream/NE from the lake, Fig. 2).

Vrana Lake is separated from the sea by karstified limestone ridge, on the narrowest part slightly less than 1 km wide. This allows fast drainage of fresh water from the lake to the sea during wet periods, both through the artificial surface channel for high water evacuation and karstified subsurface. On the other hand, lowering of the lake level near or even slightly below the sea level due to the high evaporation during summer draught periods enable direct SWI through the karstified subsurface into the lake (Fig. 5). This direct SWI to the lake is the main cause for the major lake salinization events, as salinity of the brackish springs are below the lake salinity in such periods. In addition, highest salinity is typically measured in the lake area closest to the Sea coast (SE part of the lake). Therefore, the main factor for prevention of excessive salinization of the lake is sufficiently high lake level above the sea level, what directly prevents SWI.
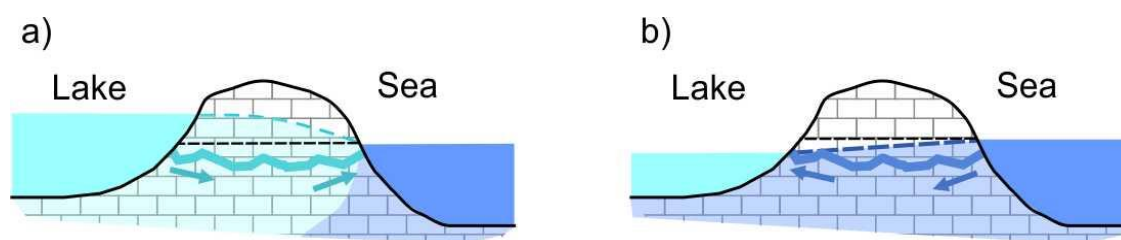
Figure 5. Conceptual model of sea water/fresh water dynamics between the lake and the sea: a) high lake water level during wet season; b) low lake water level during draught periods.

3.1.3   Surface water bodies

Vrana lake with its surface of approx. 30 km^2 and average depth of 1-2 m is major surface water body in the area. It is separated from the Adriatic Sea by a narrow land stretch. The lake is fed by karstic springs, majority located across Vransko polje area and its edges, and some located immediately at the lake coast (Fig. 3). Springs located upstream in the Vrana polje area form relatively short and intermittently dry watercourses which inflow to the lake. Watercourses are

mostly modified and incorporated in a network of artificial drainage channels, which spreads across the Vrana polje area.

3.1.3 Abstractioms/irrigations

Major fresh water karst springs in the Vrana polje area are captured and pumped for the public water supply. During dry season water level in the spring pools (and shallow wells, digged or drilled at spring locations) are pumped bellow the terrain surface, drying the watercourses downstream. Estimated mean annual pumping rates are approx. 100 l/s, with maximum pumping capacity of 180 l/s.

Groundwater is additionally pumped for irrigation purposes on a number of shallow digged wells in the polje area, typically excavated at intermittent spring locations. Irrigation pumping quantities are mostly uncontrolled. Estimated yearly mean abstraction for irrigation is approx. 200-300 l/s.

Both abstractions for agriculture and drinking water supply are most intensive during relatively dry and hot summer seasons. Pumping of groundwater in the catchment presents additional pressure on the lake system, as it lowers fresh water supply to the lake during draughts.

3.2 Climate change challenge

In accordance with the EEA map, the main expected issues due to CC in the broader area are those described in Fig. 9 for the Mediterranean regions. Main expected changes are increasing temperatures, especially during summer season (Croatian Meteorological and Hydrological service, www.meteo.hr). In addition, draught periods during summer seasons are expected to be more frequent and severe. Increasing temperatures will intensify direct evaporation from the lake, resulting in decreased lake levels in summer periods. This, together with rising trend of the sea level, will enhance SWI to the lake, what presents major threat for the lake ecosystem. Fresh water inflow to the lake during summer season is also expect to lower due to a combination of expected decrease of groundwater recharge within the karstic catchment and increase in demands for water abstractions for irrigation during summer seasons.
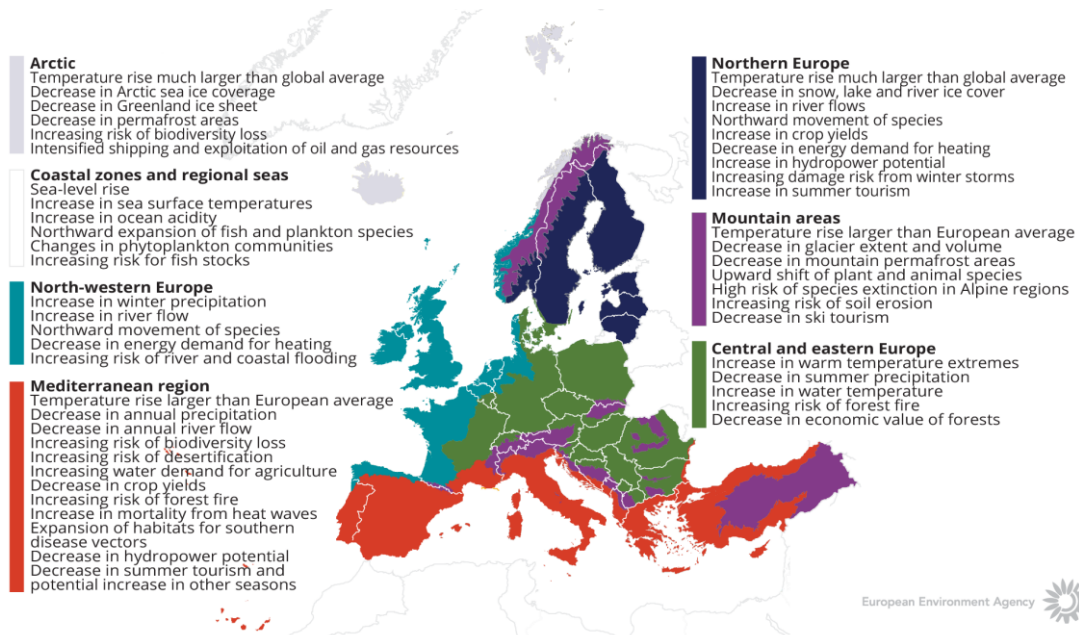
Figure 6. How is climate expected to change in Europe. The European Environment Agency map

4 METHODOLOGY

4.1 Methodology and climate data

4.1.1 Tools/ model description

Assessment of Vrana lake pilot area was done using several lumped modelling softwares/tools: GARDENIA (including EtpTurc module), METRAN and AQUIMOD modelling tools, all included in the TACTIC Toolbox (WP2). Prior to modelling, preliminary analysis of available data time series was done by usage of common statistical softwares (Excel, XLSTAT). Lumped modelling was used to model lake level response to precipitation and temperatures in the catchment, as well as lake water salinity in response to critically low lake levels. Modelling lake levels based on precipitations and temperatures within the catchment as a first step, and lake salinity based on lake levels as a second step enabled analysis how CC future scenarios will affect SWI to the lake. Very heterogeneous nature of karstic subsurface, together with generally scarce data on subsurface parameters, especially regarding karst conduits geometry, prevents usage of spatially distributed groundwater flow models.

GARDENIA is a lumped hydrological model for the simulation of relationships between series of stream or spring flow data at the outlet of a watershed, and/or groundwater level data at an observation well situated in the underlying aquifer and the rainfall received over the corresponding watershed. Withdrawals by pumping groundwater can be considered if necessary. The calibration phase of the model is done automatically by the software under control of the user.
GARDENIA enables to set a hydrological balance for the basin: actual evapotranspiration, runoff, infiltration, recharge. The hydrological balance can be used for the evaluation of natural groundwater recharge of aquifers. GARDENIA gives the extension of river flow, groundwater level or recharge data over a long period for which precipitation and potential evaporation data are known.
EtpTurc module, installed with the GARDENIA, allows the calculation of the potential evapotranspiration at daily, ten-weekly or monthly time steps by using the monthly Turk formula (1961). Calculated PET is further used in GARDENIA together with precipitation as an input file.

AQUIMOD is a simple, lumped-catchment groundwater model. It simulates groundwater level time-series at a point by linking simple algorithms of soil drainage, unsaturated zone flow and groundwater flow. It takes time-series of rainfall and potential evapotranspiration as input, and produces a time-series of groundwater level. Hydrographs of flows through the outlets of the groundwater store are also generated, which can potentially be related to river flow measurements.

METRAN is transfer-noise modelling tool for time series modelling, mostly used with piezometric heads as explained variable and precipitation and reference evaporation as explanatory variables.
Tool can also perform factor analysis of residuals of multiple time series models. Simple parametrization of transfer functions, which allows spatial correlation and interpretation of the physical system.

All described tools were used for modelling Vrana lake level based on historic, and predicted future precipitation and temperature data. METRAN was also used to model lake salinity based on precipitations data. It should be emphasized that described modelling tools are primarily developed for modelling groundwater level instead of surface water level in the lake. However, Vrana lake is situated within the karstic environment, and the lake level is strongly influenced by groundwater recharge from the extensive karstic catchment, as well as by discharge through the permeable subsurface to the sea. Groundwater recharge and discharge are largely happening dispersedly along the lake shores and below lake level, so direct measurements of total inflow and outflow are not available nor possible to measure. Usage of lumped groundwater modelling tools enabled to solve the problem of non-measurable total inflow and outflow by modelling level based on lumped values of precipitation and air temperatures over the catchment, as well as lumped values of subsurface permeability and local base level. However, due to specifics related to modelling lake, i.e. surface water instead of groundwater level, several approximations and unrealistic parameter settings in the modelling process were necessary (GARDENIA and AQUIMOD modelling tools).

4.1.2   Climate data

The TACTIC standard scenarios are developed based on the ISIMIP (Inter Sectoral Impact Model Intercomparison Project, see www.isimip.org) datasets. The resolution of the data is 0.5°x0.5°C global grid and at daily time steps. As part of ISIMIP, much effort has been made to standardise the climate data (a.o. bias correction). Data selection and preparation included the following steps:

1. Fifteen combinations of RCPs and GCMs from the ISIMIP data set where selected. RCPs are the Representative Concentration Pathways determining the development in greenhouse gas concentrations, while GCMs are the Global Circulation Models used to simulate the future climate at the global scale. Three RCPs (RCP4.5, RCP6.0, RCP8.5) were combined with five GCMs (noresm1-m, miroc-esm-chem, ipsl-cm5a-lr, hadgem2-es, gfdl-esm2m).
2. A reference period was selected as 1981 – 2010 and an annual mean temperature was calculated for the reference period.
3. For each combination of RCP-GCM, 30-years moving average of the annual mean temperature where calculated and two time slices identified in which the global annual mean temperature had increased by +1 and +3 degree compared to the reference period, respectively. Hence, the selection of the future periods was made to honour a specific temperature increase instead of using a fixed time-slice. This means that the temperature changes are the same for all scenarios, while the period in which this occur varies between the scenarios.
4. To represent conditions of low/high precipitation, the RCP-GCM combinations with the second lowest and second highest precipitation were selected among the 15 combinations for the +1 and +3 degree scenario. This selection was made on a pilot-by-pilot basis to accommodate that the different scenarios have different impact in the various parts of Europe. The scenarios showing the lowest/highest precipitation were avoided, as these end members often reflects outliers.

5. Delta change values were calculated on a monthly basis for the four selected scenarios, based on the climate data from the reference period and the selected future period. The delta change values express the changes between the current and future climates, either as a relative factor (precipitation and evapotranspiration) or by an additive factor (temperature).

6. Delta change factors were applied to local climate data by which the local particularities are reflected also for future conditions.

For the analysis in the present pilot the following RCP-GCm combinations were employed:

Table 1. Combinations of RCPs-GCMs used to assess future climate

		RCP	GCM
1-degree	"Dry"	rcp4p5	hadgem2-es
	"Wet"	rcp6p0	noresm1-m
3-degree	"Dry"	rcp4p5	hadgem2-es
	"Wet"	rcp6p0	hadgem2-es

4.2   Tool(s) / Model set-up

After the preliminary time series analysis, lumped modelling tools were used to model lake level dynamics based on precipitations, potential evapotranspiration (PET) and direct evaporation from the lake surface. GARDENIA (developed by BRGM), METRAN (developed by TNO) and AQUIMOD (developed by BGS) lumped modelling tools were tested for modelling purposes.
Although all used tools were principally developed for modelling groundwater levels in aquifers, they were tested for modelling lake level, which is in strong connection with the surrounding karst groundwater. Water fluxes to the lake are happening mainly dispersedly through the karst subsurface, and consequently impossible to be directly measured and monitored. This prevents modelling the lake level based on direct inflow, outflow and lake geometry. Lumped groundwater modelling tools were used as an option to overcome this problem. GARDENIA and AQUIMOD models enable level modelling based on precipitations and additionally pumping dynamics, which was used as equivalent process to direct evaporation from the lake. METRAN model is pure transfer function-noise model which can use several input time series in order to model output series. Additionally, manually adjusted simple transfer function was also used to model lake salinity response to the low lake levels.

4.3   Tool(s)/ Model calibration/ test

4.3.1   Observation data

58 years (1961-2018.) of monthly average lake level, sea level, air temperature and relative humidity measurements were available for the historical modelling of the Vrana lake level dynamics. Potential evaporation (PET) was calculated based on Turc method (EtpTurc modelling tool, developed by BRGM). Data of direct evaporation from the lake was available only for two

shorter periods (few years in total). High correlation of monthly evaporation with air temperature enabled calculation of direct evaporation from the lake for the whole period based on air temperature measurements solely.
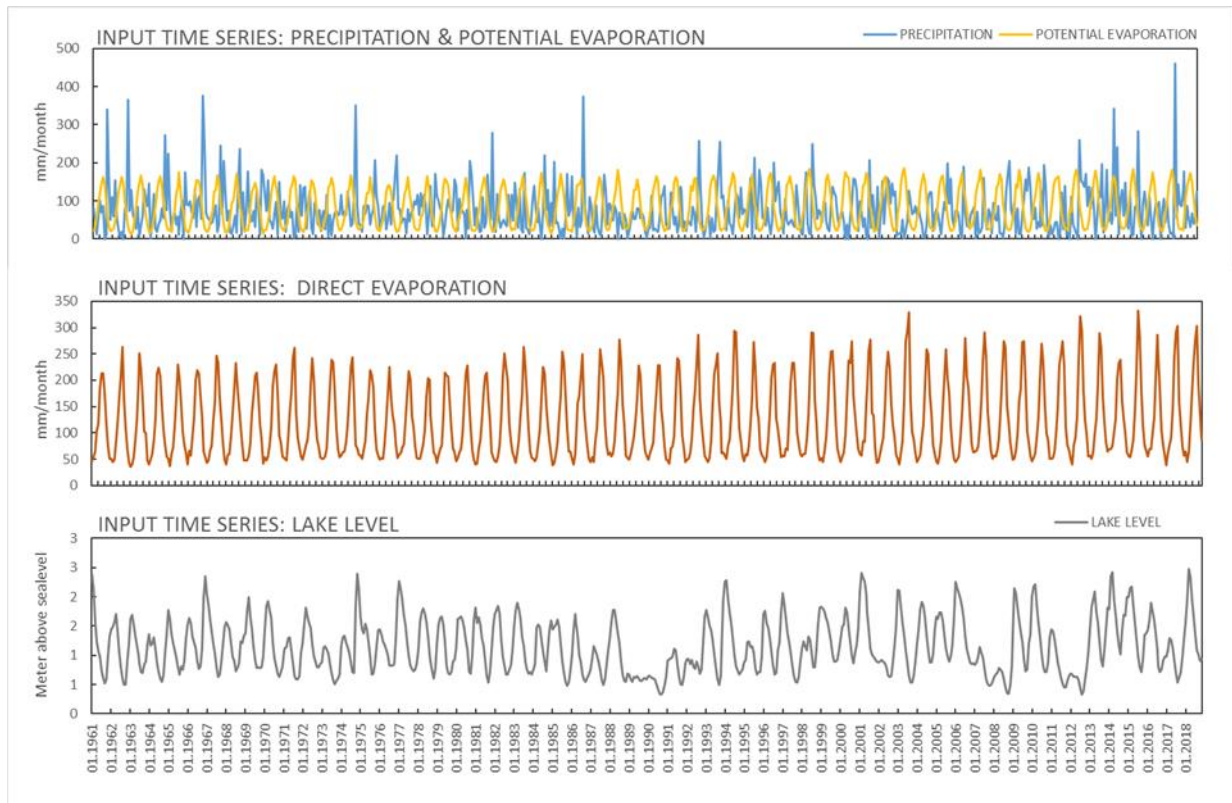
Figure 7. Input time series used for modelling the Vrana lake level dynamics.

4.3.2   Model calibration/adjustment

GARDENIA

GARDENIA modelling tool has a large number of parameters that can be calibrated automatically, or fixed at certain values. Initial calibration attempts, with all parameters non fixed/calibrated ended at unrealistically low effective recharge, accompanied by unrealistically low efficient porosity. Therefore, efficient porosity was fixed at 5%, which is realistic value for the karstified limestone in the area. Base level was also fixed at 0.5 m, as this was average sea level measured close to the Lake, and sea level presents base level for the lake subsurface outflow. Direct lake evaporation was included in the model as pumping. Evaporation was expressed in m^3/s units, converted from monthly evaporation height multiplied by the lake area. GARDENIA model optimize pumping influence on modelled water level by calibration, which enabled efficient inclusion of direct evaporation from the lake surface to the model.

AQUIMOD

Aquimod modelling tool was adjusted in similar way as GARDENIA. The main difference between GARDENIA and AQUIMOD is that AQUIMOD is not able to optimize pumping influence, and therefore inclusion of direct evaporation from the lake in the model resulted with largely exaggerated lowering of the modelled water level. Therefore, direct evaporation could not be included in the model, which resulted in much lower model efficiency comparing to GARDENIA. Therefore, only GARDENIA was used for future climate assessment.

METRAN

Metran transfer-noise modelling tool was used both for modelling lake level based on measured precipitations and air temperatures, and for modelling lake salinity increases based on lake levels. As transfer-noise modelling is purely stochastic model, unlike GARDENIA and AQUIMOD which are physically based lumped models, modelling lake level in METRAN didn't require any approximations and manipulation of input parameters in order to model lake level with groundwater modelling tool. Also, as transfer-noise modelling can be used for modelling any output time serie based on one or more input time series, this model was also used to model lake salinity based on lake level. Prior to modelling lake salinity, critical lake level bellow which lake salinity start to increase was determined. Final model use only lake levels below this threshold value as an input serie.

4.4   Uncertainty

Main source of uncertainty for future CC predictions and scenarios is non-linearity of the processes involved both in lake level response to rainfall and temperature and lake salinity response to low lake levels. All modelling approaches assume linearity of the processes involved in transfer of input to output signal. However, modelled processes are probably not linear, especially lake salinity response in the case of extremely low lake level. Therefore, it can be concluded that presented models are relatively reliable within historically observed conditions, while uncertainty significantly rises in conditions outside them.

5 RESULTS AND CONCLUSIONS

5.1 Performance to historical data

Gardenia model of lake the level (Fig. 8) shows correlation coefficient of 0.83, and NSE of 0.684. However, the greatest importance was atributed to simulation in extremely low lake level conditions, as that are the critical conditions for the lake salinization process. Therefore, model performance is better simulation in drought periods in comparison to the whole modelling period.
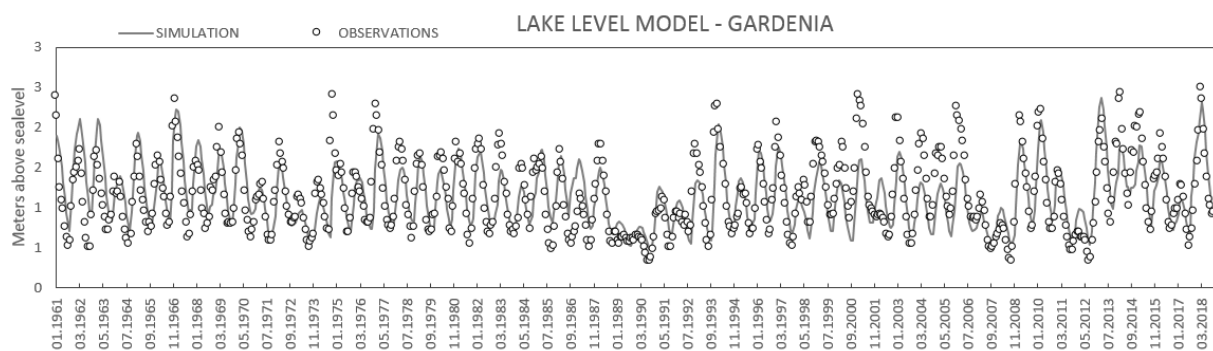
Figure 8. Historical modelling of the Vrana lake level with GARDENIA modelling tool.

As already explained, impossibility to efficiently integrate direct evaporation from the lake surface in the model, AQUIMOD model shows much lower efficiency in comparison to GARDENIA (Fig. 9). NSE of AQUIMOD lake level model is 0.42 wich is not acceptable for reliable lake level predictions. Furthermore, the model was not able to model extremely low lake levels, which are the most important for the lake salinity increases.
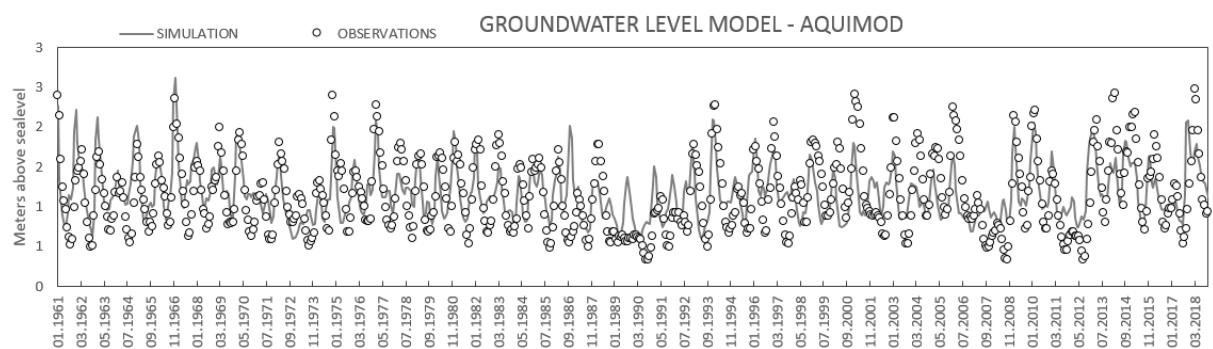
Figure 9. Historical modelling of the Vrana lake level with AQUIMOD modelling tool.

METRAN model shows relatively good efficiency (R^2 = 0.62), and it simulate extremely low levels very well (years 2008 & 2012 in Fig. 10). However, model is designed to work in daily timesteps, and montly timesteps (not exactly same timesteps in days) presented some problems. Adittional problem is related to non-applicability of the modelling with METRAN by non-modelling experts (modelling was done by TNO expert), which slightly reduced posibility to more extensive model

modification and development. However, pure stochastic modelling with METRAN is probably the most correct approach to model Vrana lake level, despite slightly better modelling result obtained with GARDENIA tool.
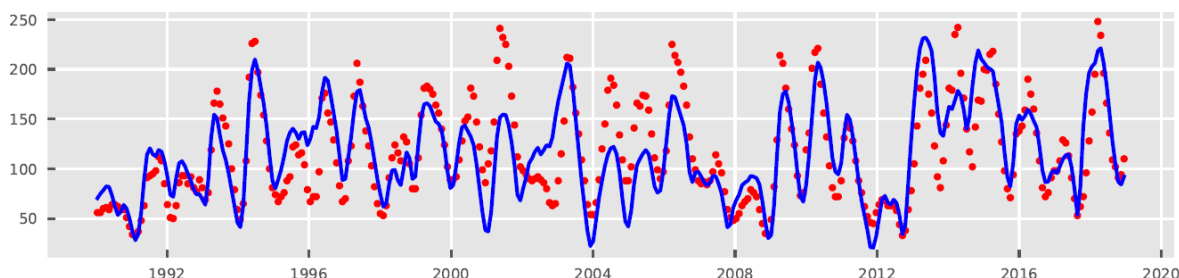
Figure 10. Historical modelling of the Vrana lake level with METRAN modelling tool.

METRAN stochastich transfer-noise model was also posible to used to model the lake salinity with the lake levels as an input. Model performed reasonably well ($R^2 = 0.76$), but it was not able to simulate extremely high salynity values (Fig. 11). If low values bellow natural lake water salinity background in normal conditions had been subsitiued by background values, model would show even higher efficiency.
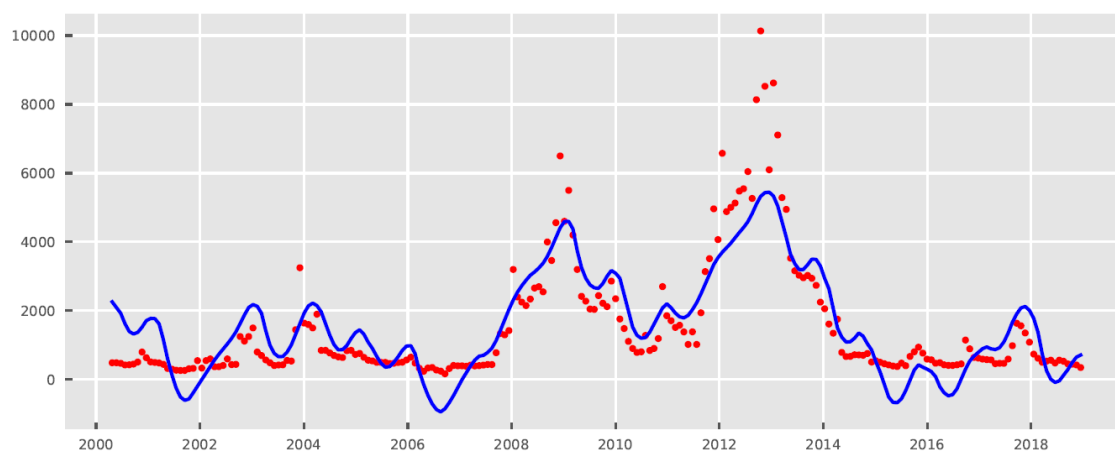
Figure 11. Historical modelling of the Vrana lake salinity with METRAN modelling tool.

Aditional approach to model the lake salinity based on lake level was done by using simple transfer function, manually adjusted in excel software. Simple model uses lake levels below threshold value, determined as a criticall value below which salinity starts to increase, as an input. The model simulate salinity dynamics very well ($R^2 = 0.78$).
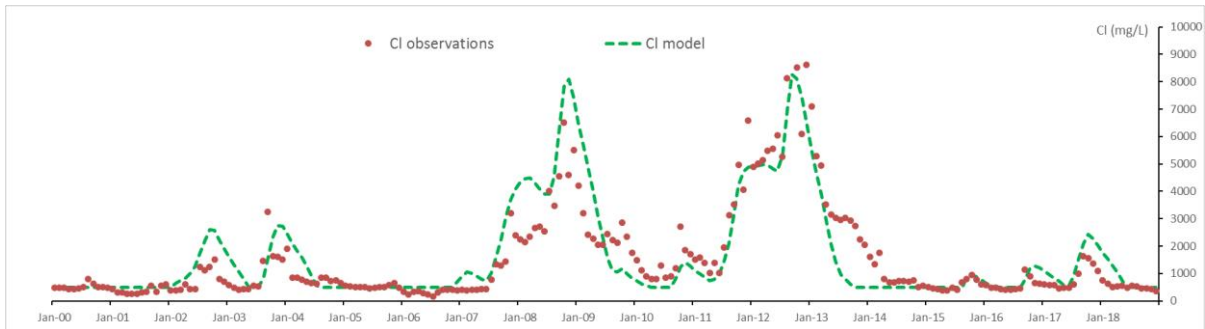
Figure 12. Historical modelling of the Vrana lake salinity with manually calibrated transfer function.

5.2 Results of assessments

Assesment of future CC scenarios, based on four selected scenarios (Table 1) was done with GARDENIA tool, as this tool provided best performance on modelling based on historical observations. Modelled future lake levels based on all four scenarios are considerably lower than historic levels (Figs. 13, 14). The most significant influence on lowering lake levels in GARDENIA model has largely increased direct evaporation from the lake (Fig. 15) due to significantly increased air temperatures in summer months according to all four considered CC scenarios. Moreover, the lake level below determined threshold value of 0.5 m a.s.l., in which case salinity of the lake start to significantly increase, historically appeared only in the cases of severely dry years, while according to the considered future CC scenarios it will appear regularly (Fig. 14). Also, all four CC scenarios ended with relatively close future lake level predictions.
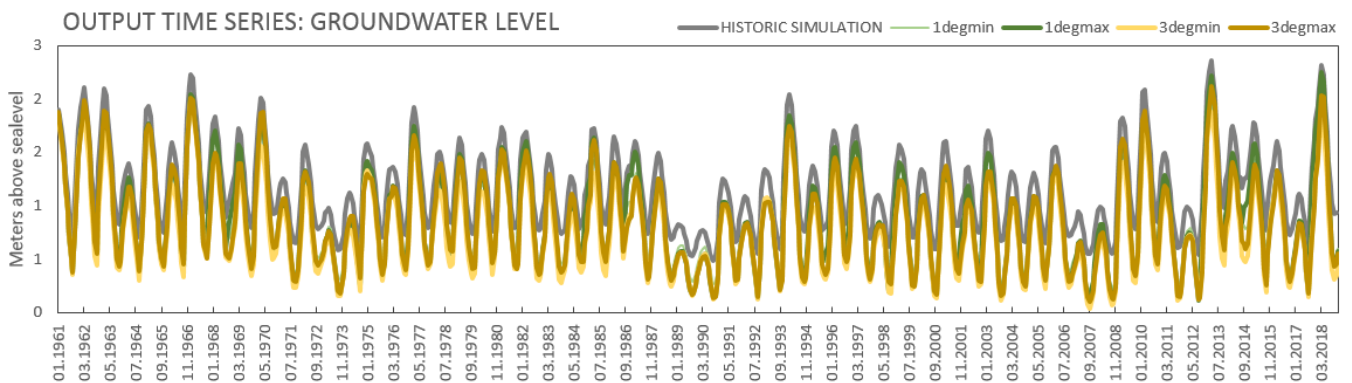
Figure 13. Future projection of the Vrana lake levels for four selected CC scenarios (Table 1), modelled with GARDENIA tool calibrated on historical observations.
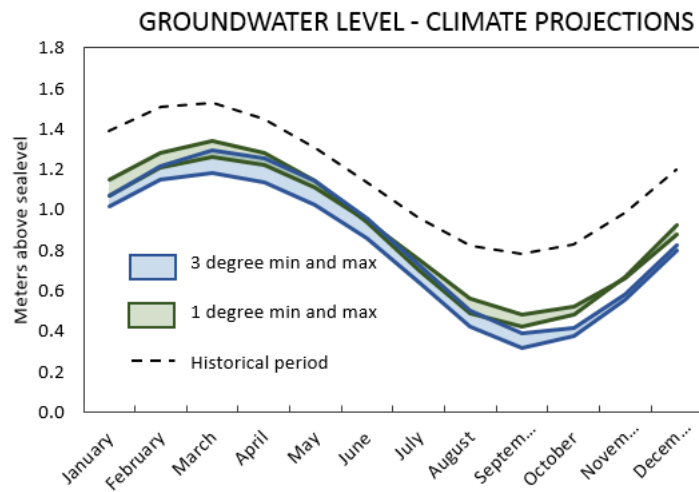
Figure 14. CC projection of the average monthly levels of the Vrana lake, modelled with GARDENIA tool calibrated on historical observations.
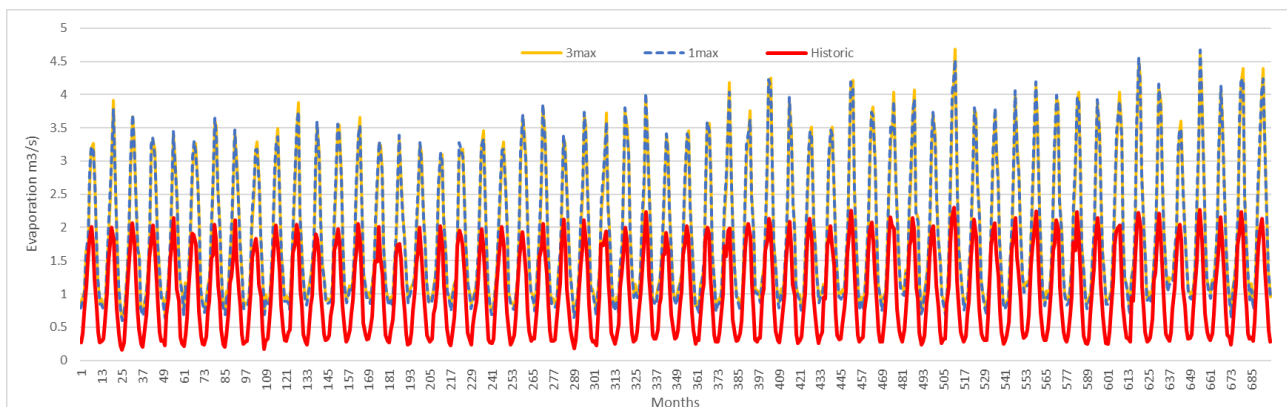
Figure 15. CC projection of direct evaporation from the Vrana lake (m^3/s), based on established relation to air temperatures on historic measurements.

On Figure 16. Future CC projection of the Vrana lake chloride content, based on 3deg max scenario is shown. Future CC projection is modelled by using a simple transfer function. Other future CC scenarios shows similar output, as future levels (input fore chloride model) modelled with GARDENIA (Figs. 13, 14) are relatively close. However, it should be noted that transfer function is linear model, while response of salinity to the low lake levels is probably non-linear. Therefore, modelled future CC salinity results should be regarded as very approximate. Regardless of exact values of expected future salinity increase due to CC, it is certain that generally large increase in the lake salinity is expected, which will result in transition of the system state from mostly fresh water lake with occasional brackish episodes to all the time brackish lagoon with variable salinity (maximum approaching seawater salinity).
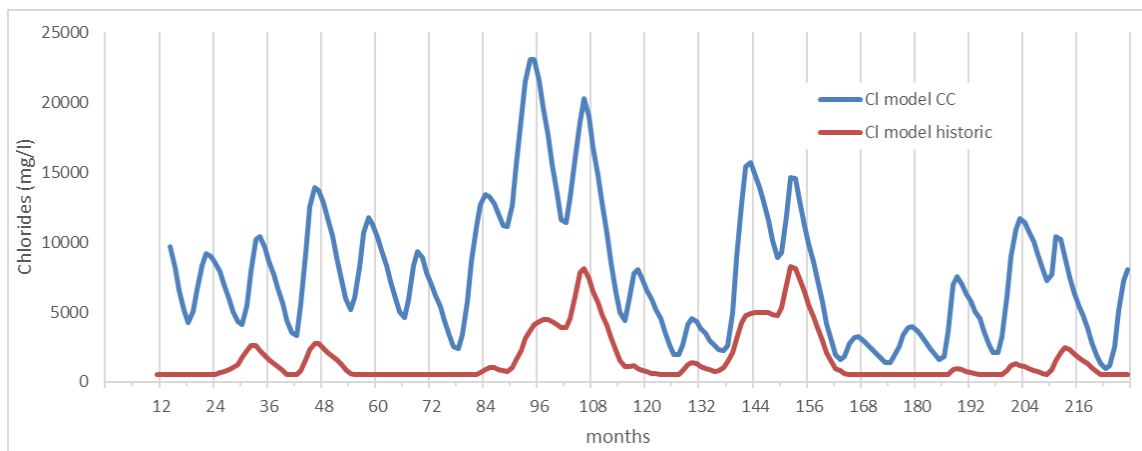
Figure 16. Future projection of the Vrana lake chloride content, modelled by using simple transfer function (Fig. 12).

5.3 Adaptation strategies

Permeable karst terrain separating the lake and the sea enable underground inflow of sea water into the lake during dry periods when lake level drops near (or even below) sea level. Excessive salinization of the lake presents a major threat to the lake ecosystem. The main preventing factor for lake salinization is sufficient lake water level, i.e. sufficient freshwater quantity within the lake. Major sink of the freshwater from the lake during hot and dry summer months is very high evaporation from the lake surface. Due to the large lake volume system has considerable inertia. Therefore, sufficiently high lake level at the beginning of dry period usually prevents subsequent excessive level drop. Also, sufficient inflow of freshwater into the lake during critically low lake levels prevents excessive lake salinization. Consequently, two main factors that can prevent excessive lake salinization are high lake level at the start of dry period, as well as sufficient inflow of fresh water to the lake during dry periods. Adaptation strategies applicable to Vrana lake ecosystem are therefore aimed at achieving these two goals.

Both pumping of groundwater for public water supply and irrigation within the lake catchment lower fresh water inflow to the lake. Therefore, adaptation measures that can be applied and tested include *Water transfer* from neighboring water supply systems and *Integrate water demands in conjunctive systems*. The local water supply system is already connected to the neighboring systems, but due to additional costs, water from other system is used only in the cases of water shortage from local sources. Nevertheless, effects of possible water transfer on reducing lake salinization should be analyzed in more detail. In addition, *improved planning, control and resources allocation* between public water supply, agriculture and freshwater depending ecosystem should be applied. *Improved monitoring and early warning system* should be eatablished in order to anticipate conditions leading to excessive lake salinization, and start applying the *Water transfer* measures.

Additional measures aimed at insuring high water level before start of the dry season include Create/*restore wetlands*, which were historically converted to agricultural lands by digging

artificial evacuation channel for high lake waters. The channel can be partially blocked and actively managed in future, but some of agriculture lands in vicinity of the lake would probably be occasionally drowned (restoration of the wetlands) in order to have sufficiently high lake level in dry season.

Table 2. Adaptation strategies that applicable to Vrana lake system.

DEMAND
REDUCING ENVIROMENTAL IMPACTS
Increase water allocation for ecosystems
Create/restore wetlands
OFFER
COMPLEMENTARY RESOURCES
Water transfer
MIXED (improving resilence & adaptation capacity)
Improve planning, control and resources allocation
Improved monitoring and early warning
Integrate water demands in conjunctive systems

6 REFERENCES

Josip Rubinić & Ana Katalinić (2014) Water regime of Vrana Lake in Dalmatia (Croatia): changes, risks and problems, Hydrological Sciences Journal, 59:10, 1908-1924, DOI: 10.1080/02626667.2014.946417

Croatian water management (1994): Vrana lake – reservoir construction. Preliminary environmental impact study (In Croatian). Unpublished expert report.

Stroj, A. (2012): Vrana lake – hydrogeological study (In Croatian). Croatian Geological survey, unpublished expert report.

Zaninović. K., et al. (2008): Climate atlas of Croatia 1961-1990., 1971-2000 (In Croatian). Croatian Meteorological and Hydrological Service, Zagreb.

Deliverable D5.3

PILOT DESCRIPTION AND ASSESSMENT

Liepaja SWI, Latvia

Authors and affiliation:

Inga Retike, Krišjānis Valters, Dāvis Borozdins

Latvian Environment, Geology and meteorology Centre (LEGMC)

Deliverable Data	
Deliverable number	D5.3
Dissemination level	Public
Deliverable name	Liepaja seawater intrusion pilot description and assessment report for sea/salt water intrusion
Work package	WP5
Lead WP/Deliverable beneficiary	IGME
Deliverable status	
Version	Version 1
Date	24/01/2021

[This page has intentionally been left blank]
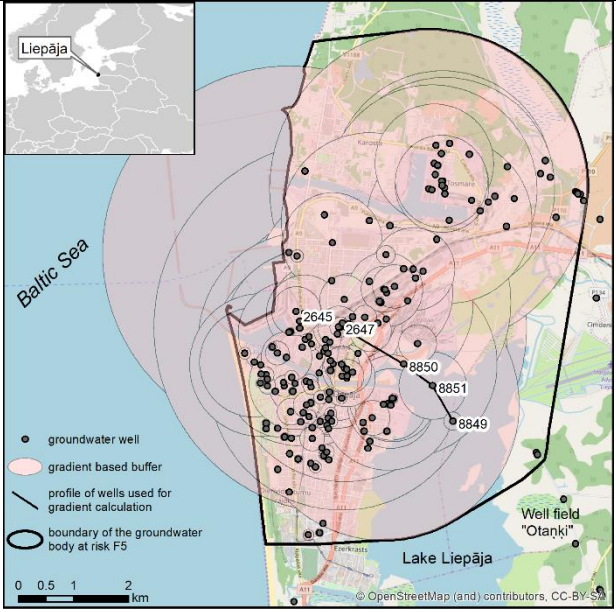
LIST OF ABBREVIATIONS & ACRONYMS

RGWB   Groundwater body at risk according to WFD

LEGMC   Latvian Environment, Geology and meteorology Centre

BL   Background levels

TV   Threshold values

GW   Groundwater

GWB   Groundwater body

SWI   Seawater Intrusion

TABLE OF CONTENTS

1   EXECUTIVE SUMMARY

Pilot name	Liepaja seawater intrusion	
Country	Latvia	
EU-region	Northern Europe	
Area (km^2)	46 km2	
Aquifer geology and type classification	Sandstones and silicatic alternating sequences, other aquifers (dolomites). Porous and fissured	
Primary water usage	Drinking/ industry	The boundary of delineated groundwater body at risk - F5 (**Liepaja seawater intrusion**)
Main climate change issues	In last year's depression cone significantly reduced, thus the area affected by seawater intrusion also decreased. However, these changes are due to high decrease of water consumption from affected aquifers and are related to economic aspects (closing of the largest factory and decrease of working places for inhabitants in that area). Still the area is attractive for business and industry (near the port) as well as for tourism, therefore with the increase of economical growth, the consumption may rise, and the hydrogeological conditions are in favour of seawater intrusion. Climate change together with economic growth may lead to higher water consumption from the aquifers at risk and there are no other, better water sources in the territory or they are too expensive to exploit.	
Models and methods used	Delineation of area affected by seawater intrusion was based on chloride concentration gradient along the well profile and gradient based buffers (Bikše and Retike, 2018). Background (BL) and threshold values (TV) delineated according to BRIDGE methodology with stricter criteria for BL delineation (Retike and Bikše, 2018). Calculation of the size of impact on GW resources was based on calculations of seawater fraction (Appelo and Postma, 2005).	
Key stakeholders	Ministry of Environmental Protection and Regional Development of the Republic of Latvia, LEGMC, water suppliers, companies	
Contact person	Dāvis Borozdins from LEGMC (Latvia) davis.borozdins@lvgmc.lv	

The pilot territoy is located in western part of Latvia, in Liepaja city (affected area by seawater intrusion 46 km^2). In the beginning of the 20th century and intensive groundwater abstraction from Upper Devonian Mūru-Žagares (D3mr-žg) aquifer took place in Liepaja surroundings. First evidence of water level decrease and quality change (high chloride concentrations) in water supply wells were reported in early 1930's. However, regular groundwater monitoring started only in 1961 and already formed depression cone was identified. A decision was made to switch to centralized water supply and install new well field (further from the city, but in the same aquifer). The depression cone continued to expand and it was decided to exploit Middle Devonian Burtnieku and Upper Devonian Gaujas (D$_2$br+D$_3$gj) aquifer to reduce the pressure on Upper Devonian Mūru-Žagares (D$_3$mr-žg) aquifer. New wells in "Otaņķi" in D$_2$br+D$_3$gj aquifer were installed in 1967. Other aquifers in the area contain high sulphate content and mineralization, and therefore are unsuitable for water supply. Depression cone started to decline in the beginning of 1990's when consumption rate dramatically decreased because of the collapse of USSR. In about 15 years groundwater level in D$_3$mr-žg aquifer restored and exceeded the Baltic Sea level. Chloride concentrations decreased in marginal zone of the area affected by seawater intrusion, still in central part of the zone chloride values remain high. Seawater intrusion takes place in freshwater aquifer at city Liepāja - Upper Devonian Mūru-Žagares (D$_3$mr-žg) partly confined aquifer which is formed of weakly cemented sandstones, siltstones and dolomites in total thickness of 44 - 47 m and at depth of 38 - 43 m. D$_3$mr-žg is covered by Upper Devonian clayey formations and Quaternary till and sand around Liepaja city. Dominating land use in the pilot area is artificial surfaces, then fallows water bodies and forests and semi-natural areas.

The seawater intrusion impact and situation assessment was performed using several tools, performing hydrogeological modeling, as well as modeling three climate change scenarios. Statistical analysis was performed quantitatively describe the sea-water intrusion in coastal freshwater aquifers. For the assessment of SWI affected area the Chloride ion concentration interpolated maps were developed. For the geostatistical interpolation of the chloride concentration kriging technique was chosen. With the use of available measurements the experimental variograms characterizing the spatial variability of chloride concentrations were constructed. Three model scenarios were defined: Past (historical), Present and Future. Preliminary model runs showed that at modern conditions no seawater intrusion was likely as modelled groundwater heads were above the sea level. That would be true for Future scenario as well if the groundwater abstraction rate would remain the same, but groundwater recharge would increase significantly as is demonstrated below. Such a model would provide little new useful insight into seawater intrusion problem, therefore it was decided to explore how the SWI would develop if groundwater abstraction would increase threefold in the Future compared to Present. The climate change scenarios were selected from ISIMP climate data ensembles of 15 models (5 GCM's x 3 RCP's). From scenarios with global warming level of +3°C degrees and +1°C relative to a reference period (1980-2010) the 2nd highest and 2nd lowest scenario regarding precipitation change for each region of interest, based on annual mean change were selected. Correction factors for monthly mean temperature, total precipitation and evapotranspiration was provided.

Results of modelling demonstrated that present groundwater abstraction rates in Liepāja city were sustainable, and gradual recovery of freshwater D$_3$*mr-žg* aquifer affected by seawater intrusion was expected to continue confirming previously observed trends in water levels and quality. It was found that in future climatic conditions increased groundwater recharge was to be expected. As a result even three-fold increase of present groundwater abstraction and preserving present configuration of abstraction wells was not likely to trigger renewed seawater intrusion. In a case of climate change scenario with expected 3°C average temperature rise, increased groundwater recharge (by up to 50%) was expected. As a result even threefold increased groundwater abstraction compared to modern situation with current configuration of abstraction wells was not likely to result in renewed seawater intrusion into Upper Devonian Mūri-Žagare aquifer within groundwater body F5 and its surrounding.

2   INTRODUCTION

Climate change (CC) already have widespread and significant impacts in Europe, which is expected to increase in the future. Groundwater plays a vital role for the land phase of the freshwater cycle and has the capability of buffering or enhancing the impact from extreme climate events causing droughts or floods, depending on the subsurface properties and the status of the system (dry/wet) prior to the climate event. Understanding and taking the hydrogeology into account is therefore essential in the assessment of climate change impacts. Providing harmonised results and products across Europe is further vital for supporting stakeholders, decision makers and EU policies makers.

The Geological Survey Organisations (GSOs) in Europe compile the necessary data and knowledge of the groundwater systems across Europe. In order to enhance the utilisation of these data and knowledge of the subsurface system in CC impact assessments the GSOs, in the framework of GeoERA, has established the project "Tools for Assessment of ClimaTe change ImpacT on Groundwater and Adaptation Strategies – TACTIC". By collaboration among the involved partners, TACTIC aims to enhance and harmonise CC impact assessments and identification and analyses of potential adaptation strategies.

TACTIC is centred around 40 pilot studies covering a variety of CC challenges as well as different hydrogeological settings and different management systems found in Europe. Knowledge and experiences from the pilots will be synthesised and provide a basis for the development of an infra structure on CC impact assessments and adaptation strategies. The final projects results will be made available through the common GeoERA Information Platform (http://www.europe-geology.eu).

Liepaja is a coastal city with water supply originating from two Devonian aquifers. One of them – upper Devonian Mūri-Žagare (D_3mr-$\check{z}g$) aquifer – was affected by seawater intrusion that reached its culmination in 80th of the 20th century. After the implementation of certain measures (new well field installation, use of other alternative aqfuifers), the rate of intrusion development started to subside. Due to decreased water abstraction since late 20th century retreat of the seawater intrusion was observed.

The report was compiled under the agreement between the Latvian Environment, Geology and Meteorology Centre (LEGMC) and the University of Latvia.

The aim of this study is to assess the potential impact of climate change on the future development of SWI by modelling different future scenarios and assessing the potential situation. In this coastal urban area, intensive water abstraction resulted in the formation of a depression cone, which led to the development of SWI into the main aquifer that was used for drinking water abstraction. Various measures were performed to reduce the development of intrusion. In the 1990s, water abstraction declined significantly, contributing to the recovery of water levels and the reduction of the intrusion process. Overall, potential future development scenarios and modeling results point to a reduction of SWI impact. In a case of climate change scenario with average temperature rise, increased groundwater recharge was expected.

According to modeling resultsm, even threefold increased groundwater abstraction compared to modern situation with current configuration of abstraction wells was not likely to result in renewed seawater intrusion into Upper Devonian Mūri-Žagare aquifer within groundwater body F5 and its surrounding.

The information obtained in the report would be useful for planning long-term measures to be taken in connection with the development of SWI processes in the area and to identify potential threats to groundwater.

3 PILOT AREA

In the beginning of the 20th century and intensive groundwater abstraction from Upper Devonian Mūru-Žagares (D*3mr-žg*) aquifer took place in Liepāja surroundings. First evidence of water level decrease and quality change (high chloride concentrations) in water supply wells were reported in early 1930's. Depression cone started to decline in the beginning of 1990's when consumption rate dramatically decreased because of the collapse of USSR. In about 15 years groundwater level in D*3mr-žg* aquifer restored and exceeded the Baltic Sea level. Chloride concentrations decreased in marginal zone of the area affected by seawater intrusion, still in central part of the zone chloride values remain high.

Previously the area affected by seawater intrusion in Liepāja was relatively small part of large groundwater body F1 (total area of F1 is 2974 km2) which is in good chemical status. On the one hand it was inappropriate to set whole groundwater body in bad status considering the size of the area really affected by seawater intrusion (les then 20% criterion). On the other hand, GWB must be set in poor status if it is affected by sea or salt water intrusion. Thus, a political decision was made to delineate the area affected by seawater intrusion in Liepāja as a separate groundwater body at risk (RGWB)- F5 in 2018 which is our pilot area.

3.1 Site description and data

3.1.1 *Location of pilot area and historical evolution of seawater intrusion*

The case study is located in western part of Latvia, in Liepaja city (affected area by seawater intrusion 46 km²). See figure 1.
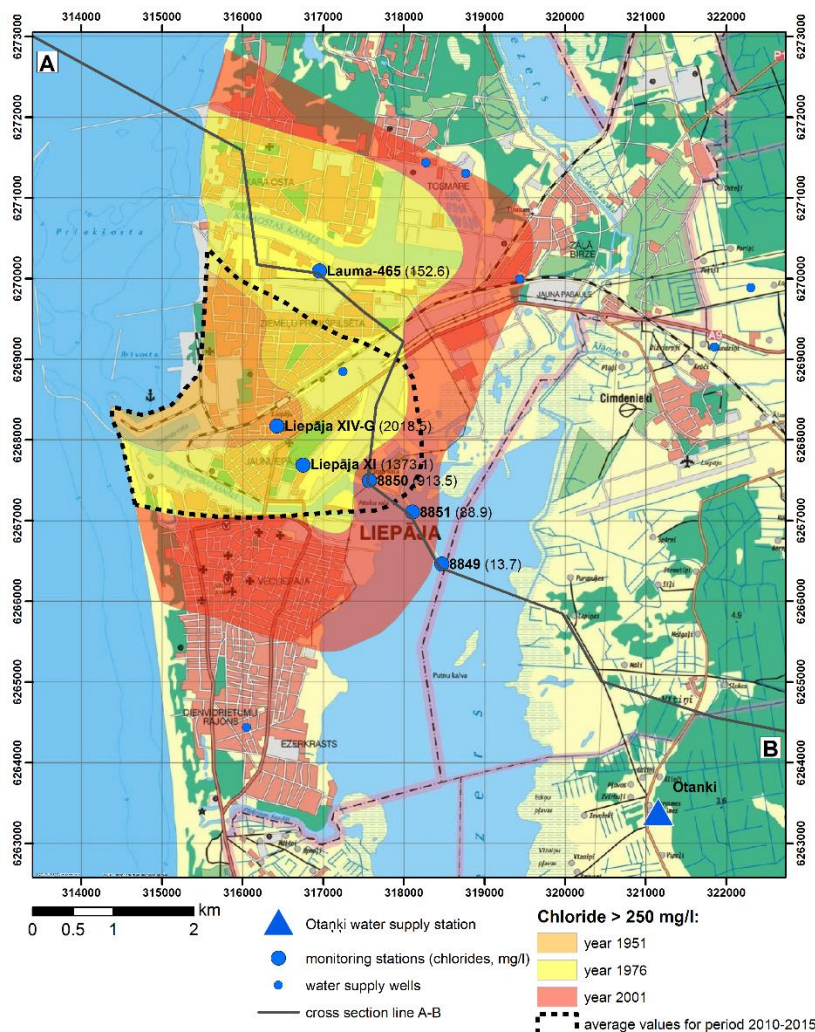
Figure 1. Sea water intrusion evolution in Mūru-Žagares aquifers at city Liepāja from 1951 to 2015

In the beginning of the 20th century and intensive groundwater abstraction from Upper Devonian Mūru-Žagares (D3mr-žg) aquifer took place in Liepaja surroundings. First evidence of water level decrease and quality change (high chloride concentrations) in water supply wells were reported in early 1930's. However, regular groundwater monitoring started only in 1961 and already formed depression cone was identified. A decision was made to switch to centralized water supply and the new well field "Otaņķi" was created in 1961. Still, it abstracted groundwater from the same aquifer - D3mr-žg. As a result, depression cone expanded southeast and in 1976 reached "Otaņķi". In 1986 the center of depression cone was located in "Otaņķi"

area and groundwater levels were reported as 14 m below sea level in D3mr-žg aquifer. In ten years the seawater intrusion has moved 1 km southeast and reached the northern part of the lake "Liepaja". A specific measure was established to prevent further movement of saltwater - an abstraction of the affected water for technical needs (Janikins et al. 1993).
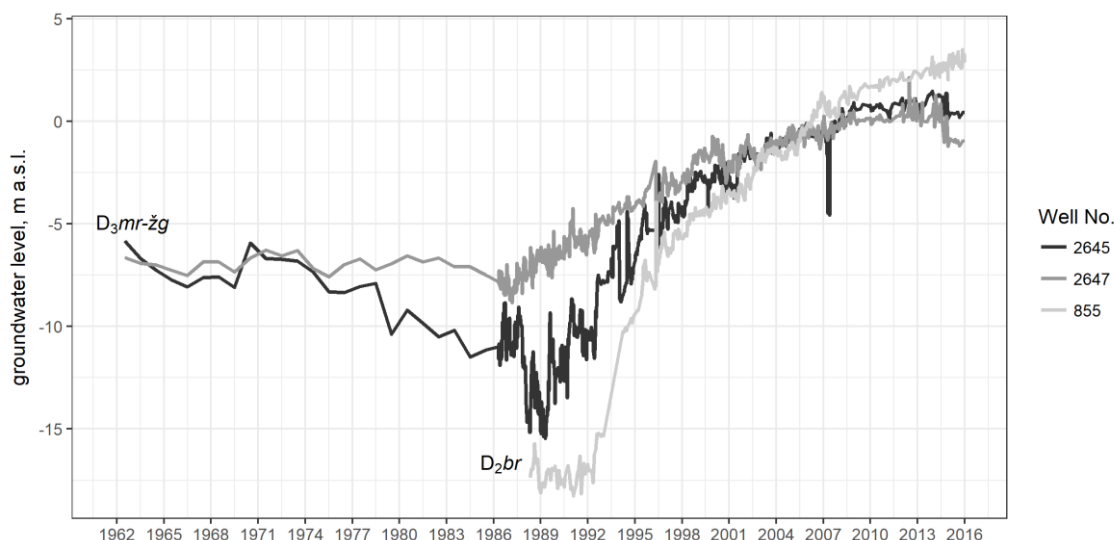
Figure 2. Historical groundwater levels in D$_3$mr-žg and D$_2$br aquifers (Bikše and Retike, 2018)

It was decided to exploit Middle Devonian Burtnieku and Upper Devonian Gaujas (D$_2$br+D$_3$gj) aquifer to reduce the pressure on Upper Devonian Mūru-Žagares (D$_3$mr-žg) aquifer. New wells in "Otaņķi" in D$_2$br+D$_3$gj aquifer were installed in 1967. Other aquifers in the area contain high sulphate content and mineralization, and therefore are unsuitable for water supply.

Depression cone started to decline in the beginning of 1990's when consumption rate dramatically decreased because of the collapse of USSR. In about 15 years groundwater level in D$_3$mr-žg aquifer restored and exceeded the Baltic Sea level (Figure 1). Chloride concentrations decreased in marginal zone of the area affected by seawater intrusion, still in central part of the zone chloride values remain high.

3.1.2 *Hydrogeological setting*

Seawater intrusion takes place in freshwater aquifer at city Liepāja - Upper Devonian Mūru-Žagares (D$_3$mr-žg) partly confined aquifer which is formed of weakly cemented sandstones, siltstones and dolomites in total thickness of 44 - 47 m and at depth of 38 - 43 m. D$_3$mr-žg is covered by Upper Devonian clayey formations and Quaternary till and sand around Liepaja city. Deposits of D$_3$mr-žg aquifer are exposed at the bottom of the Baltic Sea - approximately 5 km from the coast. Cause is the dipping of Devonian deposits towards S-SE (and outcropping at N-NW) and the lack of Quaternary sediments at some areas at the sea.

Underlying formations consist of dolomitic marls, clays, dolomite and sandstones forming several aquitards and minor aquifers. At the depth of 230 - 241 m lies Upper Devonian Gaujas and Middle Devonian Burtnieku formation (D$_2$br+D$_3$gj) - significant hydraulically connected

aquifer with total thickness of more than 100 m consisting of sandstones and clays. The D$_2$br+D$_3$gj aquifer has no direct connection to uppermost aquifers and the Baltic Sea, however, D$_2$br+D$_3$gj aquifer is mainly used for industrial water supply due to elevated mineralization and high sulphate content from gypsum dissolution.

Thus, the most important aquifer for water supply needs in Liepāja surroundings is shallow D$_3$mr-žg freshwater aquifer. It contains good quality drinking water and has been extensively used for decades.
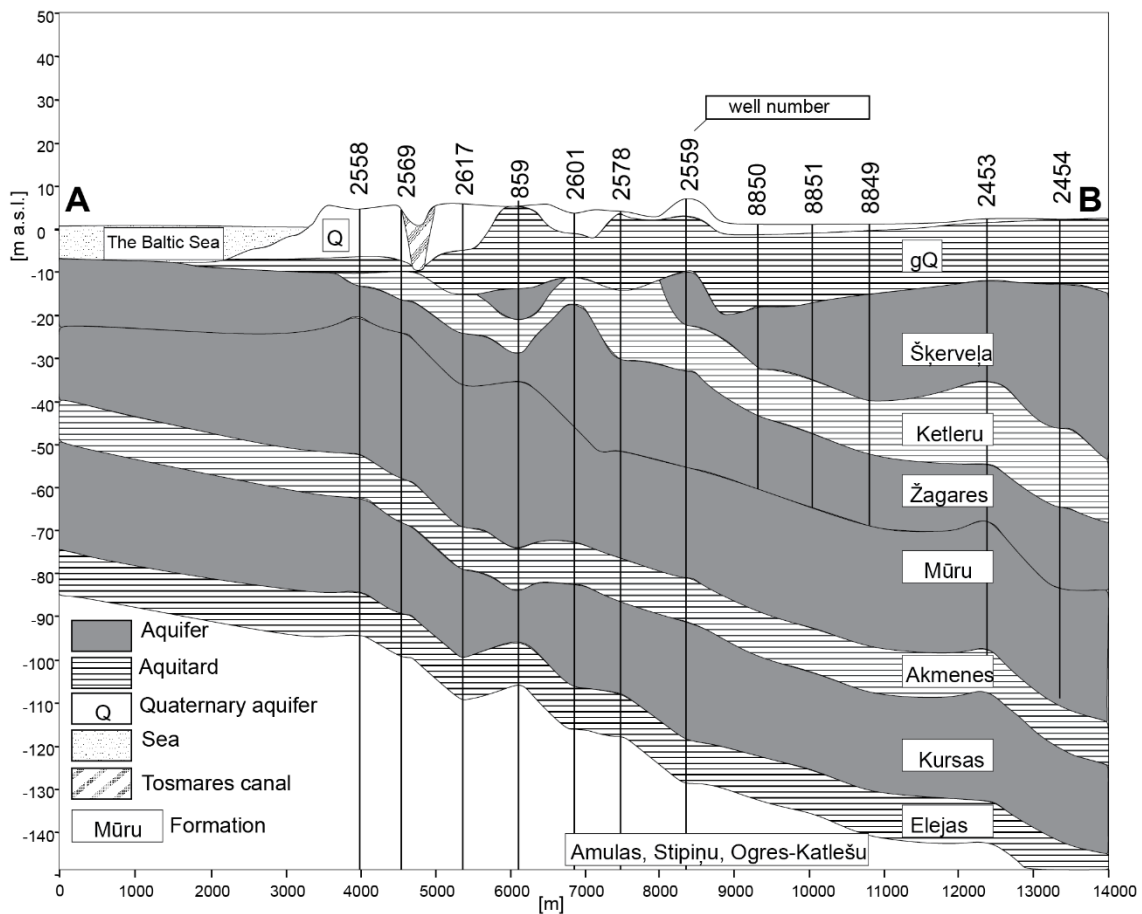
Figure 3. Hydrogeological cross section line A- B (see Fig.1) based on Spalviņš et al. 2004

3.1.3   *Surface water bodies*

Location of case study, surface water bodies (according to WFD) and location of rivers and lakes is presented in Figure 4.
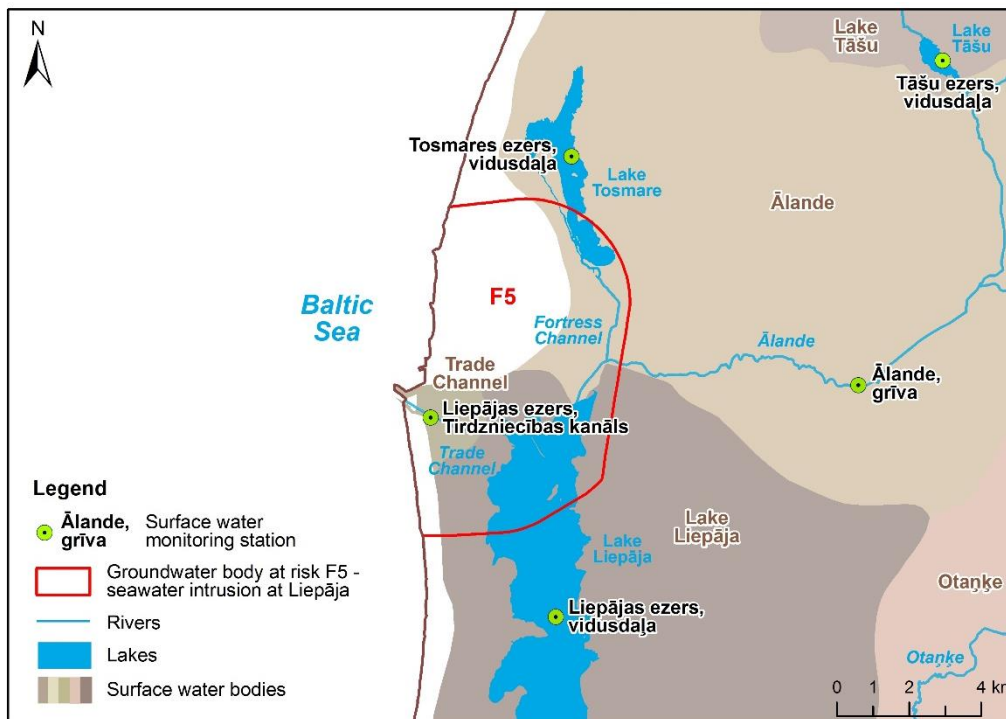
Figure 4. Case study area and surface waters.

3.1.4   *Climate*

The average precipitation in time period from 1966 till 2017 is 700 mm/y, average evaporation is unknown, but it is less than precipitation. Annual mean temperature is 7.3 °C.
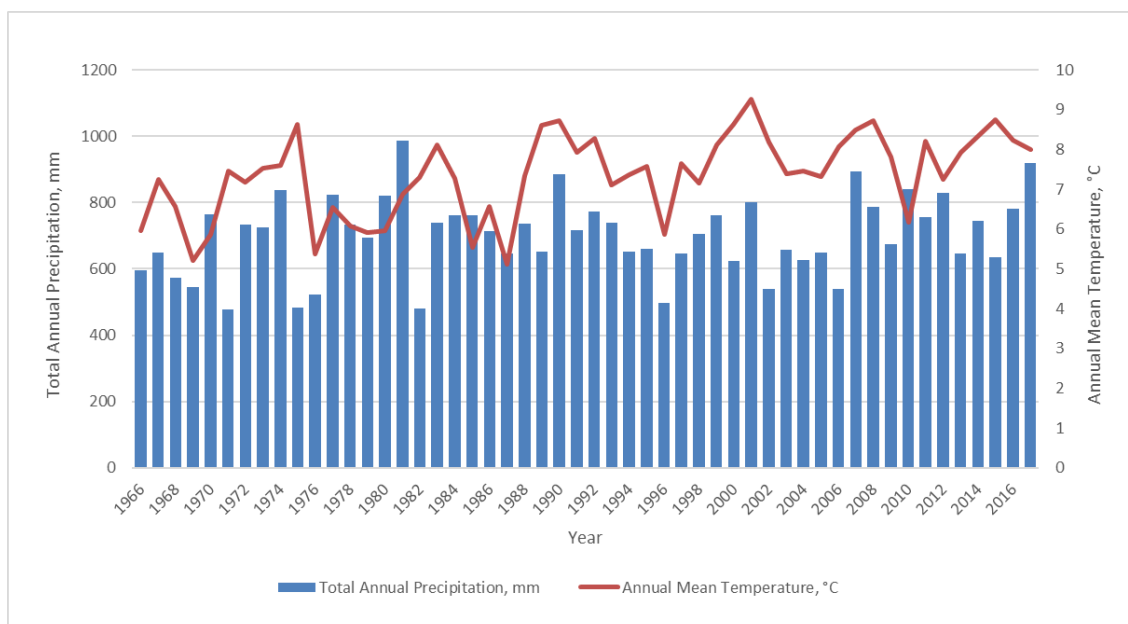
Figure 5. Evolution of annual precipitation and annual mean temperature in nearest meteorological station "Liepaja"

3.1.5 *Land use and soil types, artesian water vulnerability*

Dominating land use in the pilot area is artificial surfaces, then fallows water bodies and forests and semi-natural areas. See figure 6.
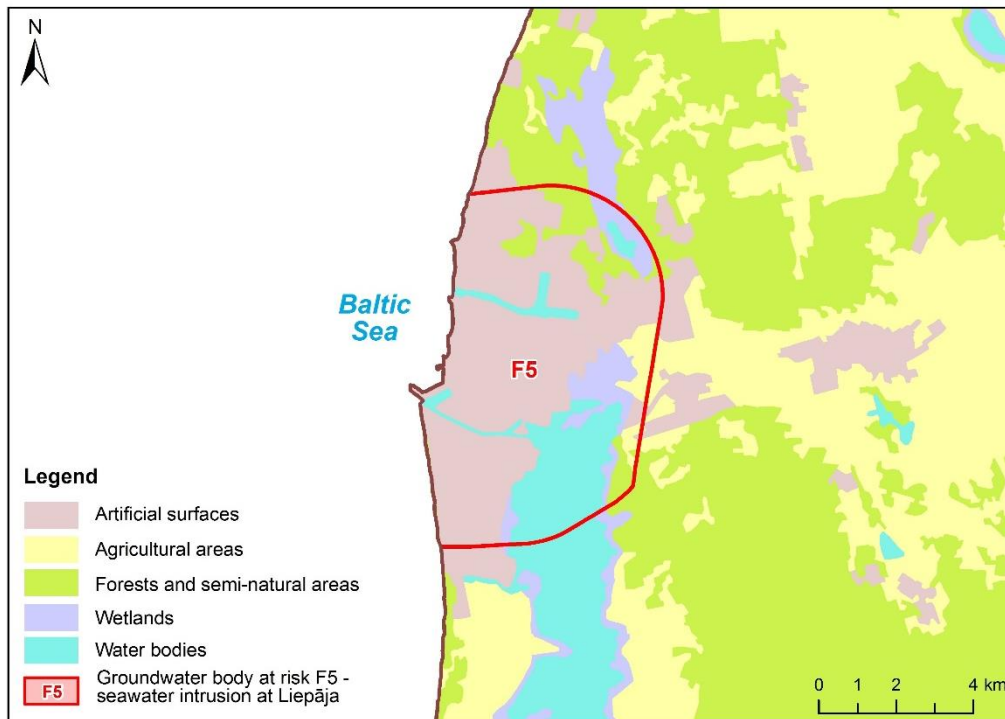
Figure 6. Land use in pilot area from Corine Land Cover

Available data about soil type is only in agricultural lands in small part of pilot's area in Eastern part. Most of the area is dominated by artificial surfaces (city) and water bodies. See figure 7.

Simple vulnerability map shows that pilot area is of low risk of contamination due to upstream areas f artesian waters. See figure 8.
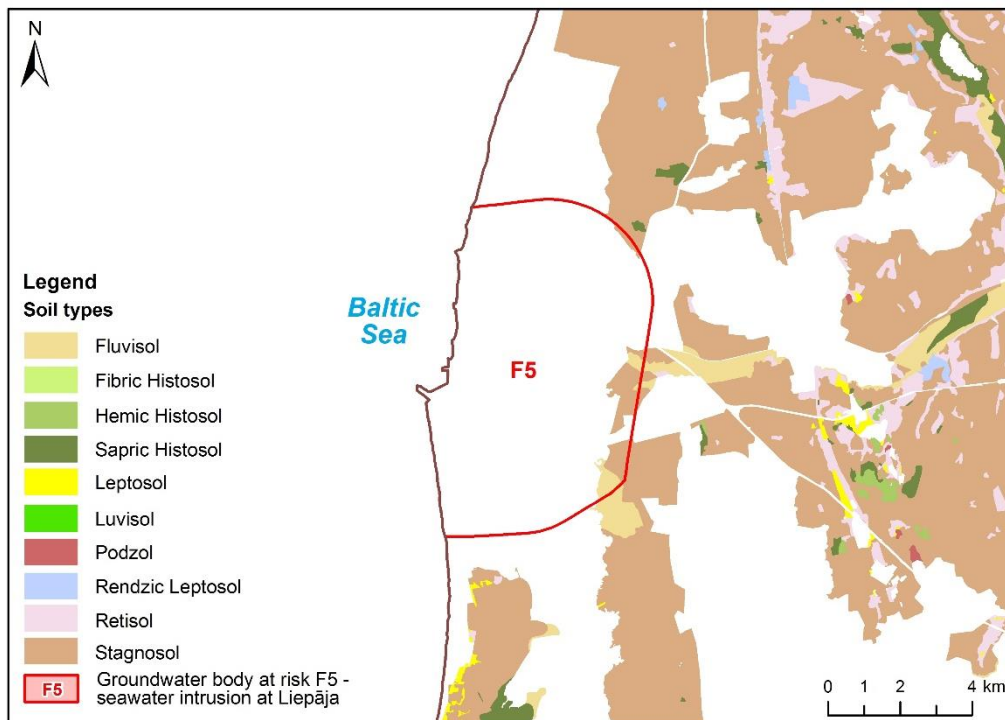
Figure 7. Soil types in agricultural lands in pilot area.
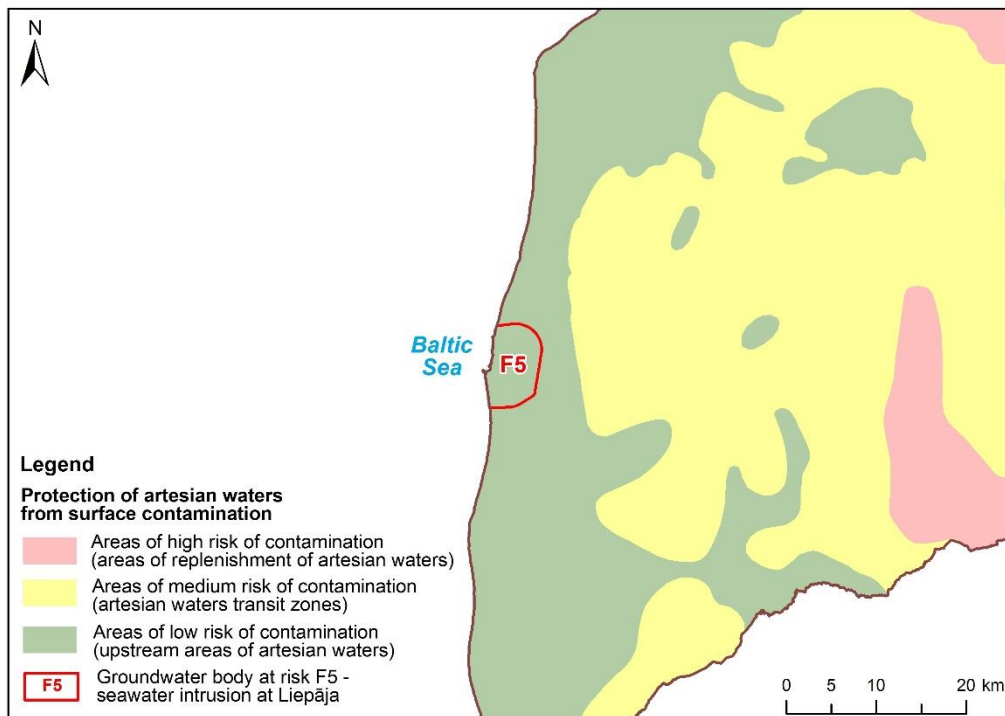
Figure 8. Vulnerability maps for artesian waters

3.1.6 *Abstraction*

There are many water abstraction wells in the pilot area abstracting groundwater directly from the affected aquifer by seawater intrusion and other aquifers. However, we do not have data about small water consumptions (<100 m3/d). See Figure 9.
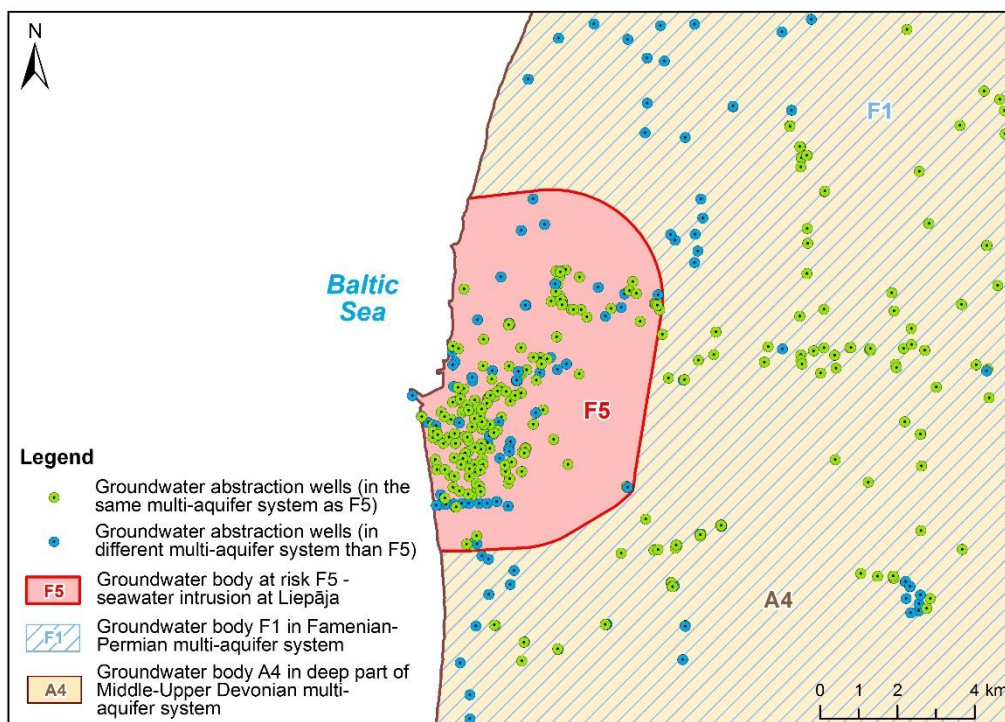
Figure 9. Locations of water abstraction wells in affected aquifer and others

Currently there is a small amount of water abstraction in well fields (areas abstracting groundwater more than 100m3/d) due to bad water quality and low water demand. Liepaja city is mostly supplied with groundwater from Otaņķi water supply station you can see in Figure 10. In Table 1 you can see supply rates in m3 per day in 2017.
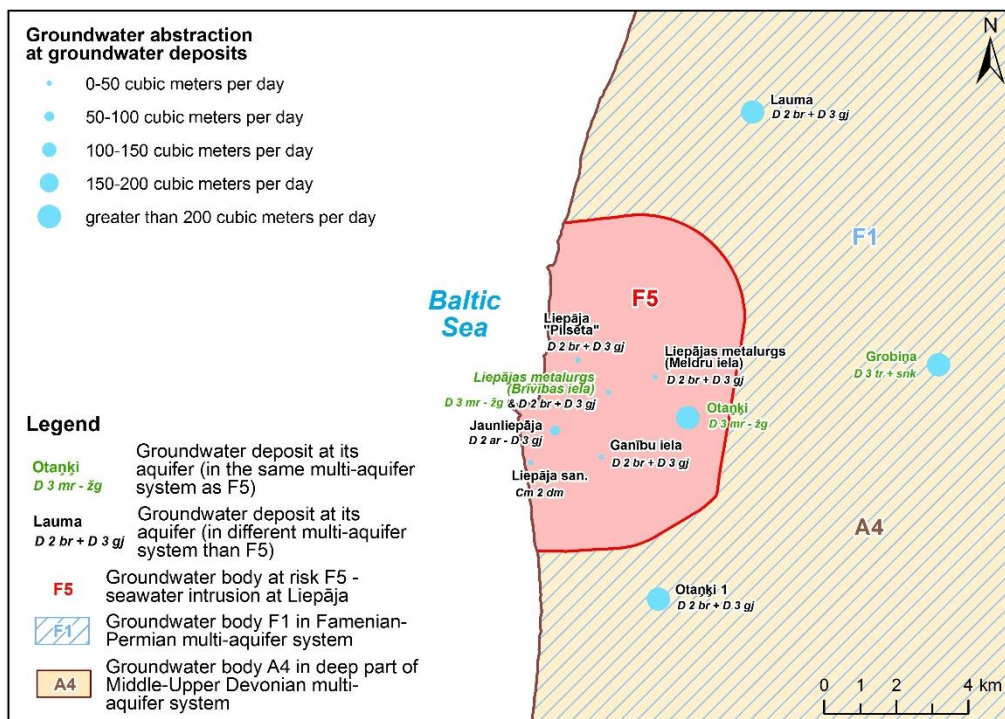
Figure 10. Locations of well fields in affected area

Table 1. Water supply in well fields in 2017 (see locations in figure 10).

Well field	Aquifer	Groundwater type	Purpose of groundwater abstraction	Groundwater abstraction (2017), m³ per day
Ganību iela	$D_2\ br + D_3\ gj$	sulphate freshwater	production, technical and household purposes	23.22
Grobiņa	$D_3\ tr + snk$	freshwater	drinking water production, centralized water supply	415.88
Jaunliepāja	$D_2\ ar$- $D_3\ gj$	sulphate freshwater	drinking water production, decentralized water supply	59.49
Lauma	$D_2\ br + D_3\ gj$	freshwater	drinking water production, centralized water supply	811.71
Liepāja "Pilsēta"	$D_2\ br + D_3\ gj$	sulphate freshwater	drinking water production, decentralized water supply	3.39

Liepāja san.	Cm$_2$ dm	saltwater	medical needs - procedures	0.13
Liepājas metalurgs (Brīvības iela)	D$_3$ mr - $\check{z}g$	freshwater	technical purposes	0.00
	D$_2$ br + D$_3$ gj	sulphate freshwater		0.00
Liepājas metalurgs (Meldru iela)	D$_2$ br + D$_3$ gj	sulphate freshwater	technical purposes	13.99
Otaņķi	D$_3$ mr - $\check{z}g$	freshwater	drinking water production, centralized water supply	3243.68
Otaņķi 1	D$_2$ br + D$_3$ gj	sulphate freshwater	drinking water production, centralized water supply	3556.49

3.2 Climate change challenge

Based on the EEA map, Latvia is expected to be affected by climate change by the issues outlined in Figure 11, which are relevant to Northern europe. The climate changes planned in the territory of Latvia are related to the increase of the average air temperature. This could affect the reduction of snow and ice cover periods. Atmospheric precipitation is also expected to increase, especially in the winter season, and with the increase in average air temperature, the maximum and minimum air temperatures will also increase. Changes in air temperature and precipitation in the future could affect various natural processes - the area will become suitable for heat-loving plants and crops. Warmer winters and less snow and ice cover will reduce the risk of spring floods in the future. An increase in the frequency and intensity of storms in the future could cause great damage to the economy, as well as adversely affect coastal erosion processes and the flooding of large coastal areas as a result of wind surges.

At present, Latvia has sufficient groundwater resources and by ensuring sustainable management of groundwater resources, it is not expected that the quantitative and qualitative status of groundwater could deteriorate. Nevertheless, due to climate change, droughts are increasing during the summer period, causing a seasonal decline in shallow groundwater (according to monitoring data). This problem mainly affects individual households (which use shallow aquifers for drinking water). Droughts also have a direct impact on agriculture, which could lead to an increase in water abstraction for irrigation purposes in the future.

Arctic
Temperature rise much larger than global average
Decrease in Arctic sea ice coverage
Decrease in Greenland ice sheet
Decrease in permafrost areas
Increasing risk of biodiversity loss
Intensified shipping and exploitation of oil and gas resources

Coastal zones and regional seas
Sea-level rise
Increase in sea surface temperatures
Increase in ocean acidity
Northward expansion of fish and plankton species
Changes in phytoplankton communities
Increasing risk for fish stocks

North-western Europe
Increase in winter precipitation
Increase in river flow
Northward movement of species
Decrease in energy demand for heating
Increasing risk of river and coastal flooding

Mediterranean region
Temperature rise larger than European average
Decrease in annual precipitation
Decrease in annual river flow
Increasing risk of biodiversity loss
Increasing risk of desertification
Increasing water demand for agriculture
Decrease in crop yields
Increasing risk of forest fire
Increase in mortality from heat waves
Expansion of habitats for southern
disease vectors
Decrease in hydropower potential
Decrease in summer tourism and
potential increase in other seasons

Northern Europe
Temperature rise much larger than global average
Decrease in snow, lake and river ice cover
Increase in river flows
Northward movement of species
Increase in crop yields
Decrease in energy demand for heating
Increase in hydropower potential
Increasing damage risk from winter storms
Increase in summer tourism

Mountain areas
Temperature rise larger than European average
Decrease in glacier extent and volume
Decrease in mountain permafrost areas
Upward shift of plant and animal species
High risk of species extinction in Alpine regions
Increasing risk of soil erosion
Decrease in ski tourism

Central and eastern Europe
Increase in warm temperature extremes
Decrease in summer precipitation
Increase in water temperature
Increasing risk of forest fire
Decrease in economic value of forests

European Environment Agency

Figure 11. How is climate expected to change in Europe. The European Environment Agency map

4 METHODOLOGY

4.1 Methodology and climate data

4.1.1 *Tools/ model description*

Statistical analysis method, chloride ion cincentration interpolated map development, as well as 3D hydrogeological modeling were used to assess seawater intrusion process.

Statistical analysis

Baena-Ruiz *et al.* (2018) suggested a methodology to quantitatively describe the sea-water intrusion in coastal freshwater aquifers. They suggest summarizing the available data about aquifer affected by saltwater intrusion in a proportionally scaled two-rectangle diagram (**Figure 12**). One rectangle represents the extent and depth of groundwater in its pristine (semi natural) quality and other – groundwater that had been polluted by seawater intrusion as indicated by above-background or above-threshold Cl^- ion concentration. The height and length of the rectangles represent the average depth and extent respectively of pristine and contaminated groundwater. In addition the mass of Cl^- ion intrusion per linear meter of coastline is suggested as measure of severity of contamination.
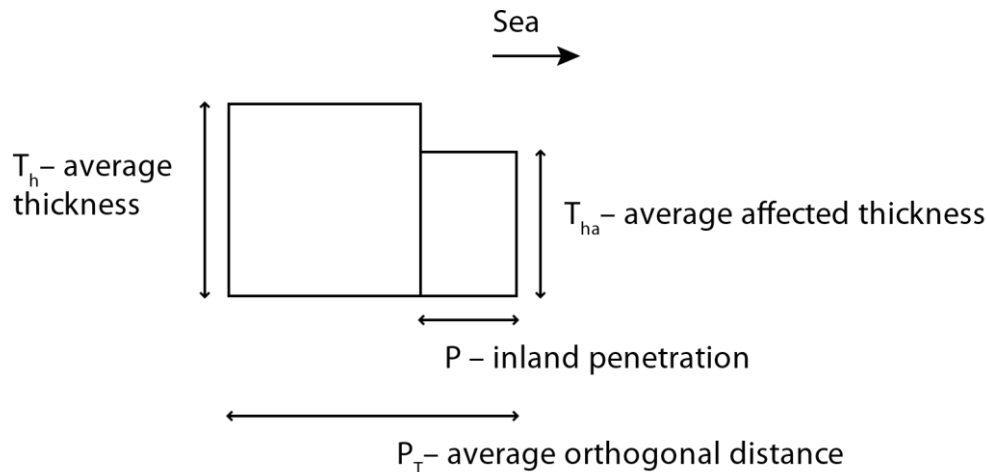
Figure 12 Conceptual visualization of proportion of the groundwater body affected by seawater intrusion as suggested by Baena-Ruiz *et al.* (2018)

Chloride ion concentration interpolated maps

Available observations of the groundwater chemical composition obtained from LEGMC were checked for quality as indicated by charge balance. Only observations where the ion balance error was less than 10% were used. Relatively loose charge balance criteria were selected as we

would be operating with average values thus slight uncertainties in chemical composition data would be smoothed-out.

In many historical observations, the concentrations of the Na^+ and K^+ ions often was expressed as a single aggregated value with unit mg/l. When calculating the charge balance, we used empirically established ratio of 0.276 between K^+ and Na^+ molar concentrations, calculated from the available data at the study region. Using this approach, we significantly increased volume of historical data with enabled charge balance control.

Available observations were selected for to time-intervals from 1975 to 1985 characterising situation in 80-ties of the 20th century and from 2010 to 2020 as modern situation. In total data from 81 and 38 wells respectively was selected in each case. In cases when more than one observation was available the median value of Cl^- concentration was used.

For the geostatistical interpolation of the chloride concentration kriging technique was chosen. With the use of available measurements the experimental variograms characterizing the spatial variability of chloride concentrations were constructed and applied to the ordinary kriging spherical model. Background Cl^- concentration was set as 3.6 mg/l – lowest reported concentration for the D_3mr-žg aquifer in the study area.

3D hydrogeological modelling

Hydrogeological model was developed in MODFLOW environment using GMS software and steady state flow conditions. The transient solute transport was based on steady state flow solution using MT3DMS package.

Model was constructed with 7 geological layers, 4 aquifers and 3 aquitards (**Table 2**) and impermeable basal boundary condition. The infiltration from land surface groundwater recharge was constrained by data from regional hydrogeological model Spalviņš *et al.*, (2018), simplified into 4 recharges zones and adjusted during model calibration.

Table 2 Modelled hydrogeological units

Layer No.	Hydrogeological unit	Aquifer / Aquitard
1	Q_{3-4} sand or till	Aquifer or aquitard
2	Q_{2-3} moraine	Aquitard
3	D_3*fm*	Aquifer
4	D_3*ktl1*	Aquitard
5	D_3*mr-žg*	Aquifer
6	D_3*ak*	Aquitard
7	D_3*jn-ak*	Aquifer

A two-step approach for modelling was devised: initial model calibration for regional model area followed solute transport calculations only for local model (**Figure 13, Table 3**). Regional model was the source of boundary conditions for local model. The two-step approach helped to capture regional flow patterns and reduce computing time for solute transport in local model.
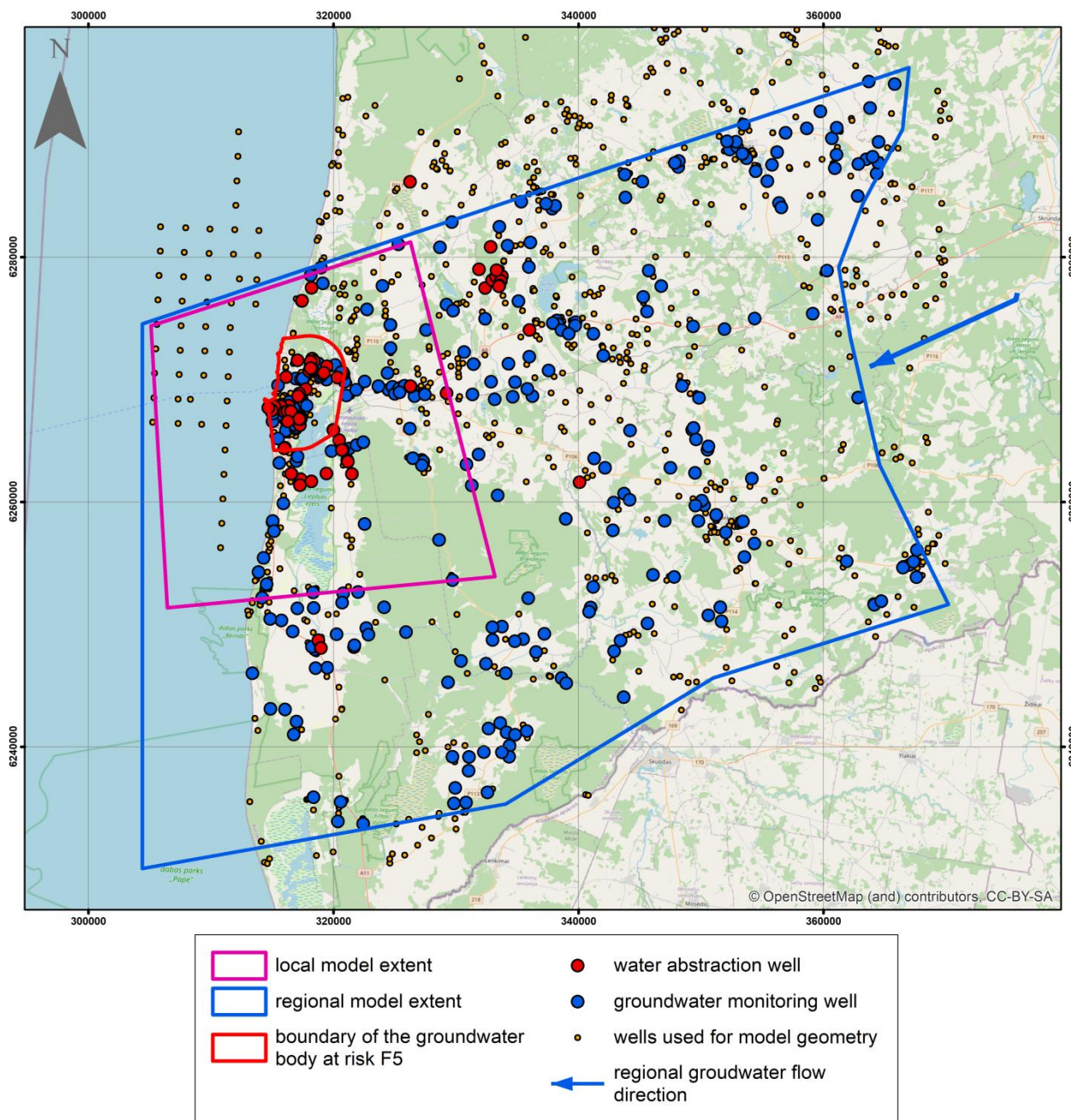
Figure 13 Area of the hydrogeological model for Liepāja seawater intrusion

Regional model area was selected to capture groundwater recharge and discharge areas and to be able to set no flow boundary conditions with no constrains on groundwater head at the model sides. General groundwater flow direction was from East to West. Recharge area was in West Kursa upland that is about 150 m above sea level while the ultimate groundwater discharge area was in the Baltic Sea. Model boundaries were pre-selected according to the regional hydrogeological model of Spalviņš *et al.* (2018). Eastern boundary was set along

groundwater divide in West Kursa upland. The North and South boundary approximately coincide with groundwater flowlines. Finally the western boundary is set under the Baltic Sea.

Table 3 Resolution and size of regional and local models

Parameter	Regional model	Local model
Model dimensions	80 x 54 km	30 x 30 km
Layer	7	7
Cell size	200 x 200 m	200 x 200 m
Rows	240	150
Columns	400	150
Total cells	756 000	157 500
Active cells	459 069	107 477

4.1.2 *Future scenarios. Climate and land use data*

Three model scenarios were defined (**Table 4**): Past (historical), Present and Future. Preliminary model runs showed that at modern conditions no seawater intrusion was likely as modelled groundwater heads were above the sea level. That would be true for Future scenario as well if the groundwater abstraction rate would remain the same, but groundwater recharge would increase significantly as is demonstrated below. Such a model would provide little new useful insight into seawater intrusion problem beside the facts that have been already established – gradual retreat of seawater intrusion (Bikše *et al.*, 2016). Therefore it was decided to explore how the seawater intrusion would develop if groundwater abstraction would increase threefold in the Future compared to Present.

Table 4 Summary of model scenarios

No.	Scenario name	Groundwater abstraction rate (m³/d)	Recharge	Transient solute transport	
				Time frame, years	**Starting conditions Cl⁻ concentration**
1.	Past	57 688	Calibrated	up to 1990	Predefined
2.	Present	11 340	Calibrated	from 1990 to 2040	Output from Past scenario
3.	Future	34 020	Modified according to climate change scenario	from 2040 to 2100	Output from Future scenario

Standard climate change scenarios were provided by the GeoERA (https://geoera.eu/ Establishing the European Geological Surveys Research Area to deliver a Geological Service for Europe) Tactic (Tools for Assessment of ClimaTe change ImpacT on groundwater and adaptation Strategies) project WP3 by by F. S. Weiland, B. van den Hurk and T. Kroon at Deltares, Netherlands. The climate change scenarios were selected from ISIMP climate data ensembles of 15 models (5 GCM's x 3 RCP's). From scenarios with global warming level of +3°C degrees and +1°C relative to a reference period (1980-2010) the 2nd highest and 2nd lowest scenario regarding precipitation change for each region of interest, based on annual mean change were

selected. Correction factors for monthly mean temperature, total precipitation and evapotranspiration was provided. The correction factors for temperature are additive, the correction factors for evaporation and precipitation was multiplicative. Only the scenario for +3°C degrees warming was selected for investigating Liepaja case study and is provided in **Table 5**

Table 5 The correction factors for Liepaja case study (WP5_LEGMC_17_Liepaja_pilot) as prepared by Deltares, Netherlands in scope of GeoERA TACTIC project WP3

scenario	Par	Deg	GCM	RCP	Jan	Feb	Mar	Apr	May	Jun	Jul	Aug	Sep	Oct	Nov	Dec
minchange	PR	_3deg	hadgem2-es	rcp4p5	1.333	1.061	1.083	0.951	0.861	0.827	0.856	0.704	0.930	0.981	1.122	1.126
maxchange	PR	_3deg	miroc-esm-chem	rcp8p5	1.416	1.373	1.187	1.000	0.888	1.099	1.414	1.254	1.309	1.435	1.190	1.255
minchange	TAS	_3deg	hadgem2-es	rcp4p5	1.333	1.061	1.083	0.951	0.861	0.827	0.855	0.704	0.930	0.981	1.122	1.126
maxchange	TAS	_3deg	miroc-esm-chem	rcp8p5	1.417	1.373	1.187	1.000	0.888	1.099	1.415	1.254	1.309	1.435	1.189	1.255
minchange	PET	_3deg	hadgem2-es	rcp4p5	1.168	1.186	1.155	1.139	1.110	1.101	1.084	1.088	1.092	1.120	1.092	1.165
maxchange	PET	_3deg	miroc-esm-chem	rcp8p5	1.222	1.253	1.169	1.122	1.092	1.089	1.083	1.093	1.102	1.090	1.154	1.168
minchange	PR	_1deg	hadgem2-es	rcp6p0	1.190	0.994	0.903	0.951	1.131	0.863	0.995	1.031	0.910	0.868	0.981	1.105
maxchange	PR	_1deg	miroc-esm-chem	rcp4p5	1.245	1.119	1.087	0.950	1.007	1.099	1.134	1.199	1.030	1.316	0.953	0.962
minchange	TAS	_1deg	hadgem2-es	rcp6p0	2.56	2.35	2.14	2.87	3.21	3.42	2.90	3.02	2.76	3.08	2.08	2.71
maxchange	TAS	_1deg	miroc-esm-chem	rcp4p5	2.28	1.91	1.79	2.13	1.13	1.38	1.59	1.78	2.07	1.51	1.75	1.79
minchange	PET	_1deg	hadgem2-es	rcp6p0	1.165	1.148	1.116	1.126	1.112	1.1042	1.082	1.086	1.088	1.120	1.100	1.159
maxchange	PET	_1deg	miroc-esm-chem	rcp4p5	1.154	1.130	1.101	1.093	1.039	1.042	1.045	1.051	1.067	1.058	1.083	1.102

PR – Mean precipitation change per calendar month, multiplier
TAS – Mean temperature change per calendar month, additive
PET – Mean potential evaporation change per calendar month, multiplier
The correction factors for temperature are additive, the correction factors for evaporation and precipitation are multiplicative to avoid negative future precipitation.

The groundwater recharge is a function of local land surface conditions such as land use and soil type and hydrogeological regime of the local groundwater head in topmost aquifer. The later denotes distribution of groundwater recharge and discharge areas. In addition, the groundwater discharge would not be directly affected by climate change: any groundwater leaking to the land surface would be either consumed by evapotranspiration or removed as surface runoff. In contrast, the infiltration of the precipitation water to the groundwater would be affected by climate change: groundwater is recharged only by precipitation water that is not consumed by evapotranspiration or removed as surface runoff. We assumed that changes in balance of the precipitation and evapotranspiration would affect groundwater recharge however there is a site specific unknown partitioning coefficient (k) that controls the proportion of the excess precipitation that is directed towards groundwater and how much of it is removed as surface runoff. Thus, the ratio of groundwater recharge (R) to unknown partitioning coefficient (k) can be estimated by equation (1):

$$\frac{R}{k} = \frac{\sum (PR_i - PET_i, <0 \Rightarrow 0)}{n}, \text{ where} \qquad (1)$$

n – number of months,

PR_i – monthly precipitation,

PET_i – monthly potential evaporation.

Further we assume that value of the partitioning coefficient *k* in future conditions will remain the same while both precipitation *RP* and potential evapotranspiration *PET* will change. To describe present recharge conditions (R_p/k) we used monthly average precipitation and potential evapotranspiration data from ERA-5-land reanalysis (Copernicus Climate Change Service (C3S), 2019) of the model area for the time period from 1990-01-01 to 2019-12-31 calculating the R_p/k as a single average value.

To describe future recharge conditions (R_f/k) we used the scaling factors provided by GeoTACTIC to scale monthly-grid cell values of the PR and PET obtained from era-5-land reanalysis and calculate the future value of the groundwater recharge (R_f/k; eq. 1) as the average across all the monthly values and grid cells.

As the next step we calculated scaling coefficient (k_R) for groundwater recharge due to climate change:

$$k_R = \frac{\frac{R_f}{k}}{\frac{R_p}{k}} = \frac{R_f}{R_p} \ (2)$$

Finally we multiplied the calibrated groundwater recharge rate for the hydrogeological model with k_R to estimate the future groundwater recharge to be used as forcing for hydrogeological model.

We used monthly mean precipitation and potential evaporation from ERA5 land (Copernicus Climate Change Service (C3S), 2019) for model area from 1990 to 2020 as modern meteorological conditions. Future meteorological conditions were characterized by the same data set scaled according to delta-change methodology provide by Deltares for the *maxchange 3deg* scenario (WP5_LEGMC_17_Liepaja_pilot, GCM – miroc-esm-chem, RCP – rcp8p5). According to this scenario in future climate the groundwater recharge is expected to increase by factor of **1.52.** That is we expected around 50% increase in groundwater recharge in future.
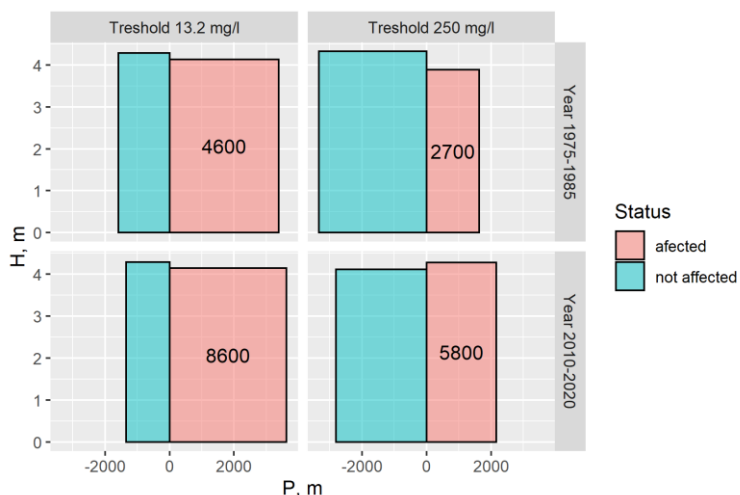
Figure 14 Conceptual representation of the state of the sea-water intrusion into groundwater body F5, Liepāja, Latvia, modified after (Baena-Ruiz *et al.*, 2018): vertical axis (H) is average aquifer thickness in m, horizontal axis (P) is average width of the aquifer affected by seawater intrusion, the number (positive values) and not affected by it (negative values), the number is the extra mas of Cl- ion in the aquifer in kg due to seawater intrusion.

4.2 Tool(s) / Model set-up

Statistical analysis

We used a slightly modified methodology, where the left box represents the proportion of water in aquifer not polluted by seawater intrusion and right box – proportion affected by seawater intrusion (**Figure 15**). We used a subscript *a* to indicated indices considering part of the aquifer affected by seawater intrusion. To indicate parameters considering part of the aquifer not affected by seawater intrusion we used subscript *n*. The concentration of the Cl- above a threshold value (C_R) was used to determine of the groundwater quality at a given location has been affected by seawater intrusion.
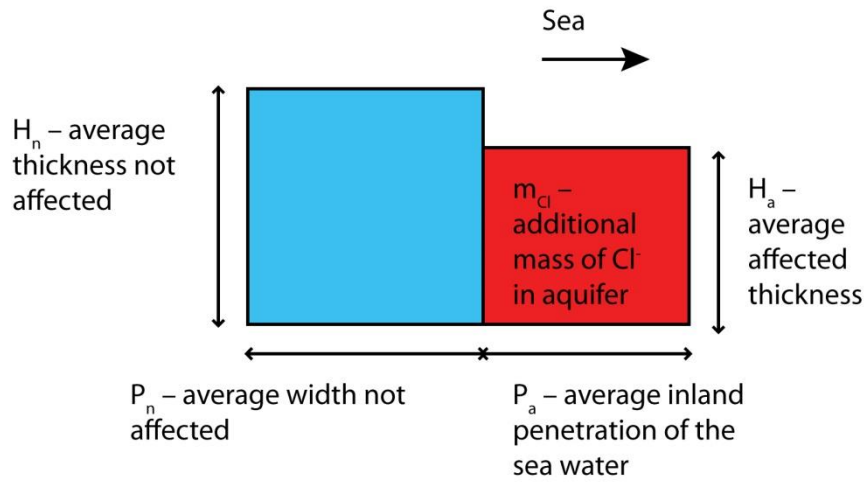
Figure 15 Modified conceptual visualization of proportion of the groundwater body affected by seawater intrusion as suggested by Baena-Ruiz *et al.* (2018)

Storage of water affected by seawater intrusion in grid cell *i* was calculated by equ. (1):

$V_{i,a} = S_{i,a} b_i$ (1), where

$S_{i,a}$ – surface are of the grid cell *i*,

b_i – saturated thickness of the grid cell *i*,

α – active porosity (*storage coefficient* of Baena-Ruiz *et al.*, 2018).

Further the average thickens of the aquifer affected by seawater intrusion H_a and average inland penetration of the sea water P_a was calculated by equ. (2) and (3):

$H_a = \frac{\sum V_{i,a}}{\sum S_{i,a}}$ (2)

$P_a = \frac{\sum S_{i,a}}{L_{coast}}$ (3), where

L_{coast} – coastline length.

The indices describing the average thickness of aquifer not affected by seawater intrusion H_n and its average width P_n were calculated by equations (4), (5) and (6):

$V_{i,n} = S_{i,n} b_i \alpha$ (4), where

$H_n = \frac{\sum V_{i,n}}{\sum S_{i,n}}$ (5)

$P_n = \frac{\sum S_{i,n}}{L_{coast}}$ (6).

Finally, the average concentration of the chloride ion in the affected area *C*, increment of concentration I_C and mass of additional chloride ion $m_{Cl,a}$ was calculated by equ. (7), (8) and (9) as suggested by (Baena-Ruiz *et al.*, 2018):

$C = \frac{\sum(C_{i,a} V_{i,a})}{\sum V_{i,a}}$ (7)

$IC = C - C_R$ (8)

$$m_{Cl,a} = P_a I_C H_a 10^{-3} \qquad (9)$$

3D hydrogeological modelling

Geological information from 1492 wells and boreholes was used to construct the geological structure of the model. Groundwater head was constrained by data from 187 groundwater monitoring wells in historical and 163 in modern situation. Out of these wells 93 and 42 respectively were located in detailed model area. Finally 70 and 21 groundwater abstraction wells in the large model area ad 65 and 12 in the detailed area for historical and modern situation respectively were considered. Wells with insignificant abstraction rates (< 50 m³/day) were excluded from the model.

Cl- ion concentration defined for initial model setup is show in **Table 6.** It was assumed that the first model layer – unsaturated zone and Quaternary sands – in model territory covered by Baltic Sea, was saturated with sea water. Further it was assumed that the groundwater in the rest of model territory had uniform background chemical composition.

Table 6 Cl⁻ ion concentration defined for initial model setup

No.	Cl⁻ (mg/l)	Reference	Description	Model units
1.	4100	monitoring data	Sea water	Baltic sea and first model layer Quaternary sands
2.	176	monitoring data	Lake Liepāja	Lake Liepāja
3.	13.2	Background groundwater composition in D₃mr-žg aquifer (Retike and Bikše, 2018)	Groundwater	All geological units except where seawater was present
4.	3.6	Least observed Cl⁻ concentration in groundwater in model area, LEGMC data	Precipitation	Groundwater recharge

4.3 Tool(s)/ Model calibration/ test

After several preliminary and exploratory model runs best results were obtained calibrating the regional model against the historical situation and using this regional calibrated model as a basis for all further calculations (**Figure 16**). For present day and Future scenarios groundwater level distribution was re-calculated using respective values of groundwater abstraction and recharge imposed to the regional calibrated model. A local model area engulfing groundwater body at risk 5F, Otaņķi wellfield and Baltic Sea region where likely intrusion of seawater into aquifers was taking place was selected for solute transport – seawater intrusion – modelling. For each modelling scenario respective regional model was used to select the boundary conditions for the local model. Further, the transport modelling was performed sequentially running the three model scenarios and using the result – distribution of Cl⁻ concentration in groundwater – of one scenario as an input to the next scenario model.
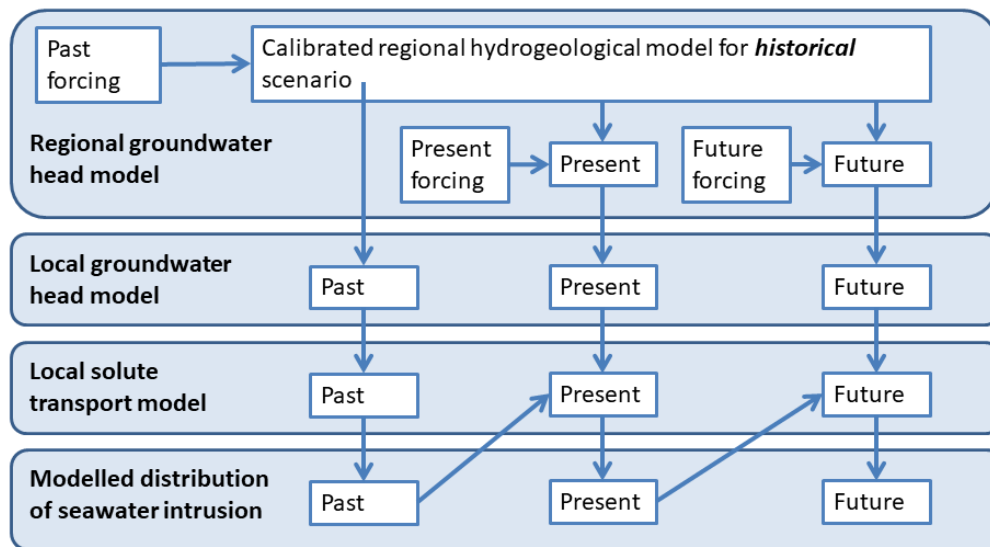
Figure 16 Modelling workflow

Calibrated hydrogeological model parameters are given in **Table** 7 while the calibrated recharge values across recharges zones are in **Table 8**, future recharge was calculated by multiplying calibrated recharge with coefficient 1.52.

Table 7 Calibrated hydrogeological model parameters

Model layer No.	Material, formation	Horizontal hydraulic conductivity m/day	Anisotropy (Horizontal /vertical conductivity)	Poro sity	Long. disper sivity
1.	Quaternary, aquitard upper glacial till	0.12	5	0.05	1
	Quaternary, aquifer sand	7.90	1	0.25	20
2.	Quaternary, aquitard lower glacial till	0.01	3	0.05	1
3.	Carboniferous, Permian and Devonian Famenian, aquifer dolomites and sandstones	1.05	2	0.15	20
4.	Devonian Ketleri Formation, aquitard dolomite marl and clay	7.73E-05	5	0.01	1
5.	Devonian Muri – Zagare, aquifer dolomites and sandstones	7.34	2	0.15	20
6.	Devonian Akmene Formation, aquitard marl and clay	3.00E-04	3	0.01	1
7.	Devonian Joniski - Akmene aquifer dolomites and sandstones	2.71	2	0.15	20

Table 8 Groundwater recharge values across recharge zones

Recharge zones	Recharge value, m/day	
	Past and Present	**Future**
Recharge zone 0 (sea)	0	0
Recharge zone 1	2.13E-08	3.23E-08
Recharge zone 3	1.11E-04	1.69E-04
Recharge zone 2	6.62E-06	1.01E-05

4.4 Uncertainty

Model uncertainties (errors) are summarized in **Table 9** and **Figures** 17 and 18. Positive mean error (ME) indicate that modelled groundwater head was higher than observed as the model errors are calculated as modelled head minus observed head. Mean absolute error (MAE) is a measure of average absolute deviation of modelled head from observed head. Relatively large errors were likely due to close proximity of observations wells and groundwater abstraction wells. Time-variable groundwater abstraction rates from individual wells and relatively coarse spatial resolution of our reginal model preclude fine simulation of groundwater head near wells used for water extraction.

In addition it is likely that the groundwater flow in the 80-ties of the 20t century in Liepaja city were not at stationary state. That would explain the negative mean error of the local model for the Past scenario as well as positive mean error for the present scenario.

Table 9 Regional model uncertainties (errors) or residuals expressed as difference between observations and model: ME – mean error, MAE – mean absolute error; RMSE – root mean squared error.

Scenario	ME (m)	MAE (m)
Past, regional model	0.4	4.2
Past, local model	-2.2	3.4
Present, regional model	2.6	5.4
Present, local model	4.7	5.2

Computed vs. Observed Values
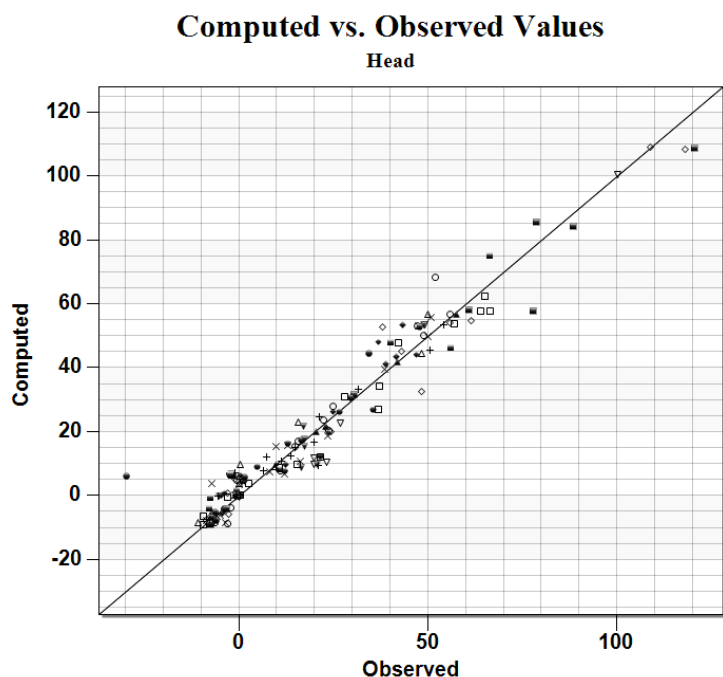
Head

Figure 17 Comparison of the observed and modelled groundwater heads (m a.s.l.) Past scenario, full (regional) model, symbols non-uniquely indicate different groundwater observation wells.

Computed vs. Observed Values
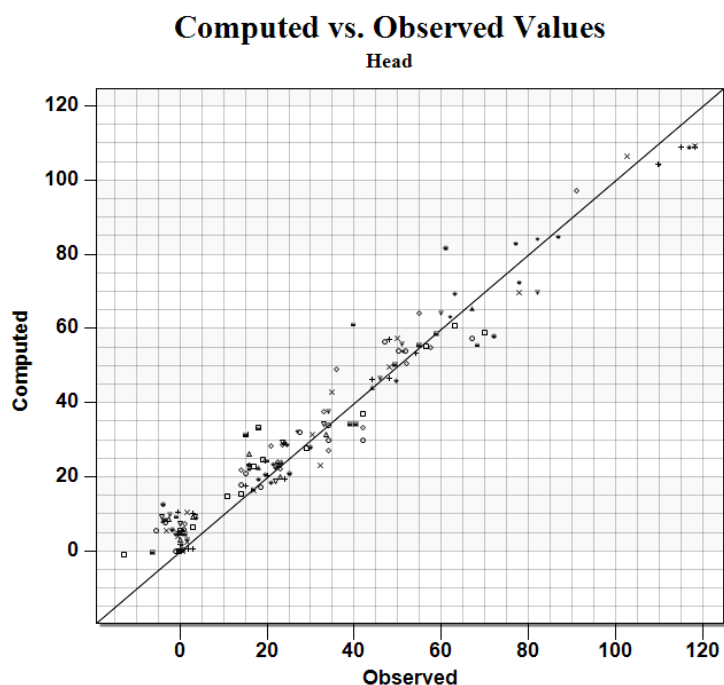
Head

Figure 18 Comparison of the observed and modelled groundwater heads (m a.s.l.) present scenario, full (regional) model, symbols non-uniquely indicate different groundwater observation wells.

5 RESULTS AND CONCLUSIONS

5.1 Statistical analysis

The extrapolated Cl$^-$ ion concentration in D$_3$*mr-žg* aquifer in the 80-ties of the 20th century and modern situation is shown in **Figures 19**. Interestingly we found that the apparent seawater intrusion extent and volume was greater in modern situation rather than in the past when groundwater abstraction was at its peak (**Figure 14**). In part that might be due to methodological reasons: for the past conditions data about groundwater salinity was available for more wells (81 wells) than in modern situation (38 wells). In addition the wells used for interpolation in past and modern situation overlap only partly. Thus the current representation cannot be used to directly asses the evolution of the seawater intrusion, however it is useful for examining the proposed methodology (Baena-Ruiz *et al.*, 2018).

The Baltic coastline in the study region is trending in N-S direction and forms the Western boundary of the F5 groundwater body. Therefore we have taken the N-S extent of the F5 groundwater body as a good approximation for the coastline length (L_{coast}), that was needed to calculate the indices describing seawater intrusion along the methodology adopted from (Baena-Ruiz *et al.*, 2018). Thus the value of L_{coast} was found to be 9343 m.
Guidance document elaborated by LEGMC (LVĢMC, 2018) suggests that the active porosity (α) for the Upper Devonian Mūri-Žagare aquifer ranges from 0.08 to 0.12, for our calculations we used value 0.1.

As noted by Retike and Bikše (2018) in two adjacent wells data base No 2645 and 2647, contrasting Cl$^-$ concentrations were observed: median Cl$^-$ concentration from 2010 to 2020 was 8.6 and 2000 mg/l respectively. They explained that two wells tap different depths intervals of the Mūri-Žagare aquifer. Similar contrast in these wells was observed for Cl$^-$ concentration measured from 1975 to 1985. Therefore, to avoid obtaining geologically unreasonable concentration gradients we exclude the well No 2645 from interpolation of the Cl$^-$ load.
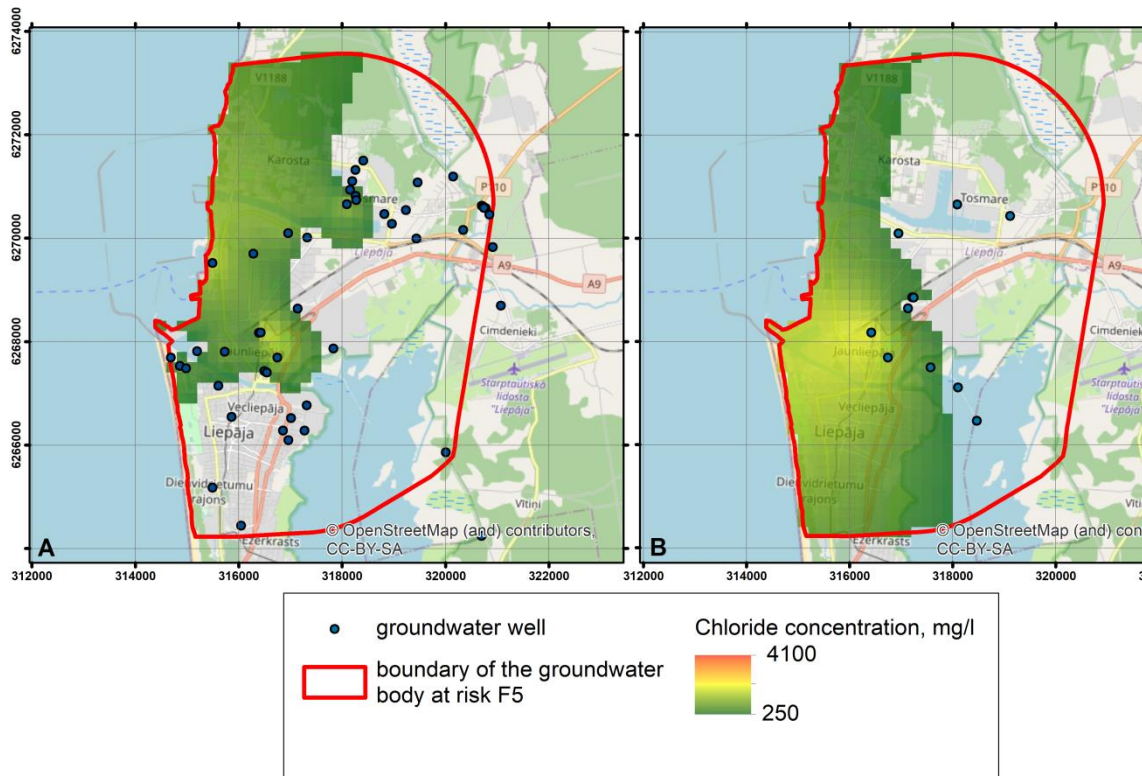
Figure 19 Interpolated Cl⁻ concentration in the groundwater of the Mūri-Žagare Upper Devonian aquifer, median values for observations from 1975 to 1985 (left) and from 2010 to 2020 (right).

5.2 Modelling results

Modelled groundwater head distribution and extent of the seawater intrusion asilustrated by Cl⁻ concentration in D_3mr-$žg$ aquifer for the Past, Present and Futures scenarios are presented in **Figures** from **20** to **27**.

Results for Past scenario demonstrated that groundwater depression cone clearly extended below the Baltic Sea (**Figure 20 and 21**) indicating significant potential for sea water intrusion. That was confirmed by solute transport model. Albeit, with provided model setup, it was found that about 250 years of water abstraction was necessary for development of the seawater intrusion similar to one that was historically observed. This apparent discrepancy most likely was due to necessary model initiation time to achieve realistic starting conditions. Further it was considered that the model still provides valuable insights into development of seawater intrusion and is further elaborated in discussion chapter. Further transient solute transport simulation results were considered to be consistent with observations. We have elaborated the question in discussion section.

For the Present scenario only insignificant depression of groundwater head due to groundwater abstraction for stead state situation was modelled (**Figure 22 and 23**). Groundwater depression cone had not developed around groundwater abstraction sites within detailed model area. Thus

it can be concluded that any remaining seawater intrusion was inherited form the peak of groundwater abstraction during 20th century, indicating that the seawater intrusion was no longer. This is in line with this previous finding, that the groundwater heads in last decades had rebounded and the Cl- concentration in the aquifer was declining (Bikše and Retike, 2018). Furthermore we examined the modelled state of the seawater intrusion for year 2027 when next planning cycle for water management was due to start. A slight reduction of the modelled extent of the seawater intrusion was expected (**Figure 24 and 25**) however generally it was expected to change negligibly.

Steady state groundwater head simulation for Future scenario – 3-fold increase of present groundwater abstraction rate and 1.52-fold increase in groundwater recharge – indicate that depression cone had developed around Otaņķi wellfield (**Figure 26 and 27**). However the groundwater head in $D_3mr\text{-}\check{z}g$ aquifer remains above the sea level and no significant sea-ward extension of groundwater depression cone within F5 groundwater body and Otaņķi wellfield next to it was detected. These model results indicate that renewed seawater intrusion in Liepāja city even for increased groundwater consumption was unlikely.
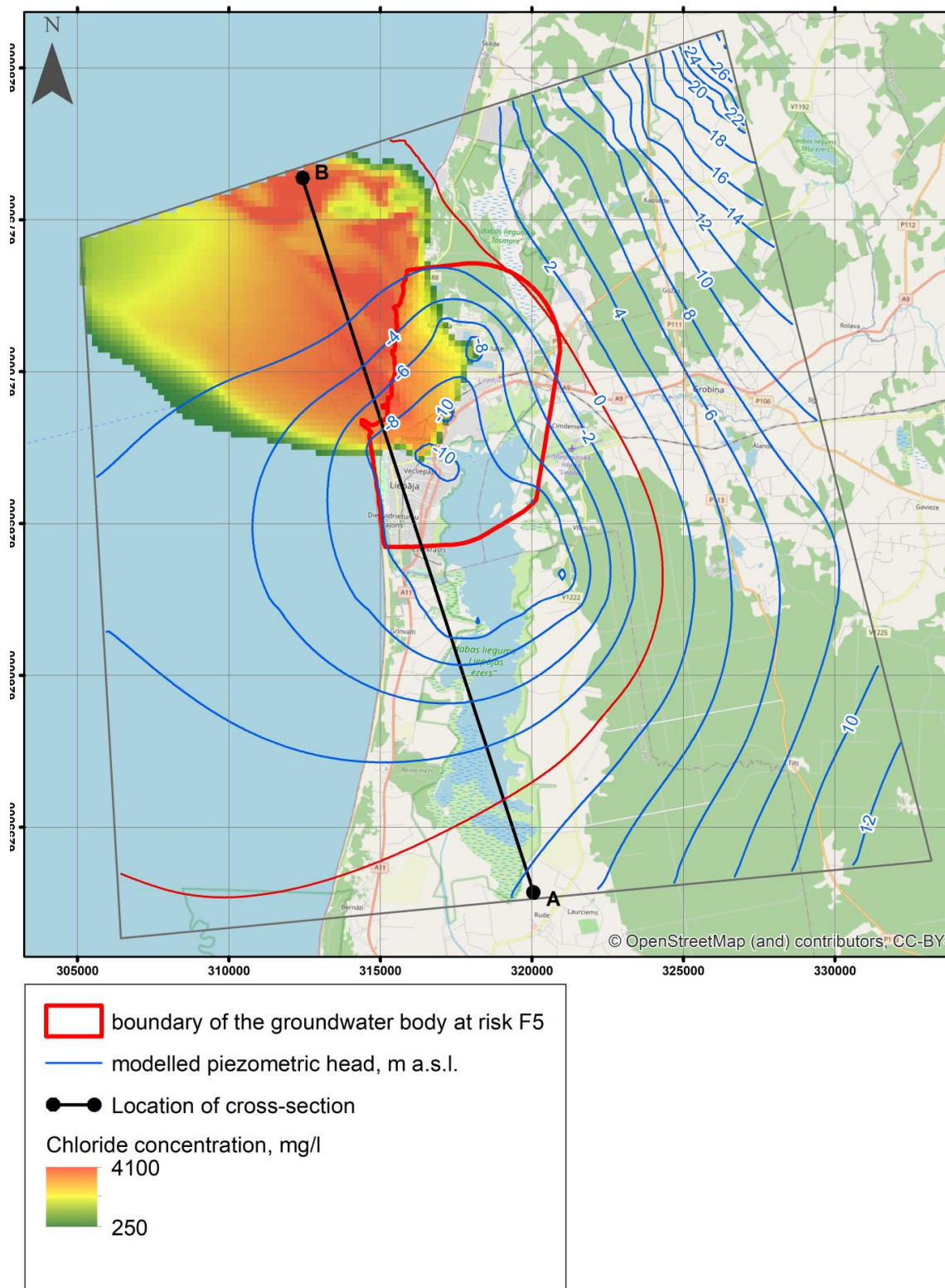
Figure 20 Modelled groundwater head (m a.s.l.) and Cl⁻ concentration (mg/l) distribution in D$_3$*mr-žg* aquifer around 1980, Past scenario
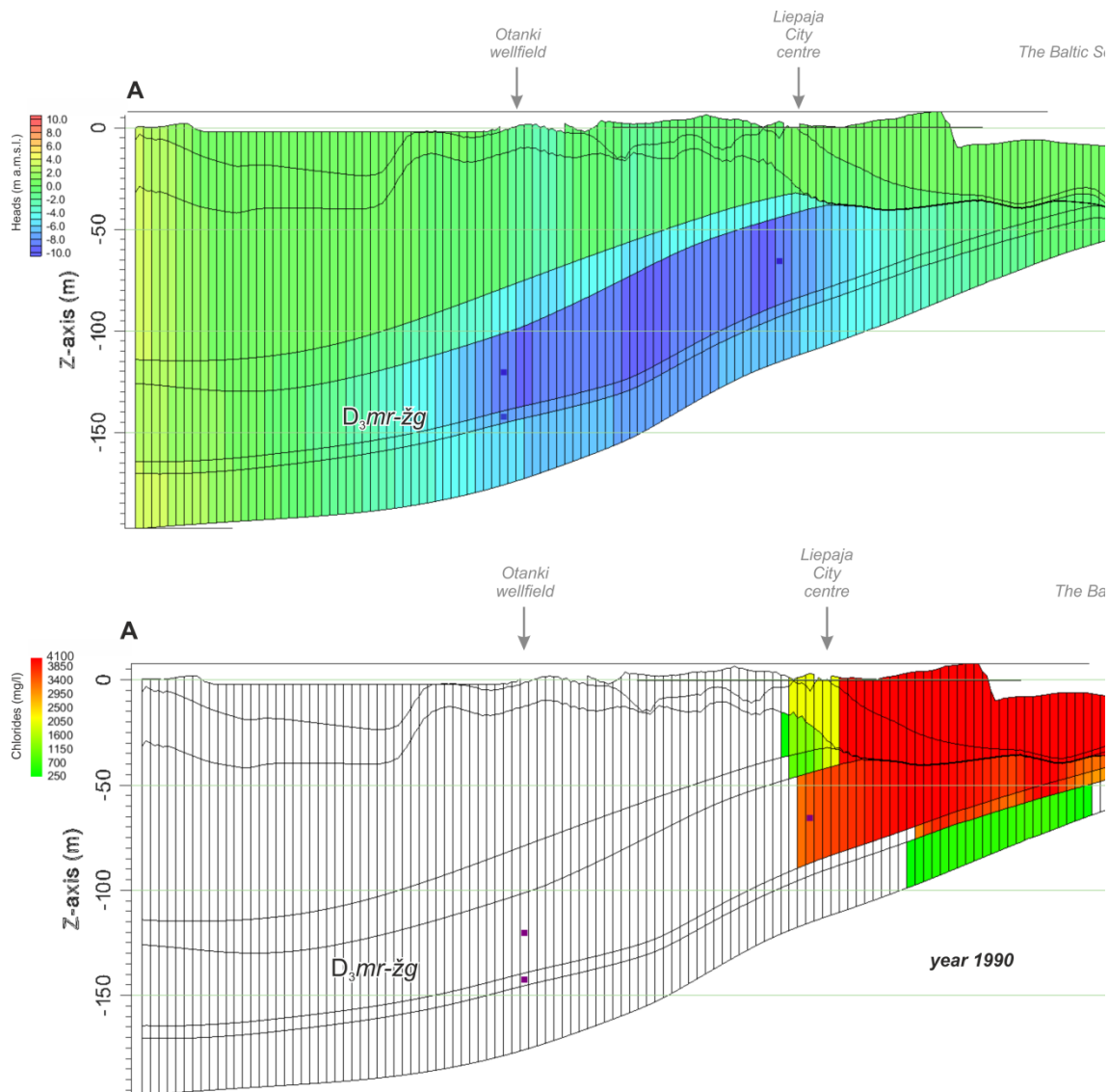
Figure 21 Vertical cross-section along A-B line (**Figure**): top – groundwater head (m a.s.l.); bottom - Cl⁻ concentration (mg/l) around 1980, Past scenario
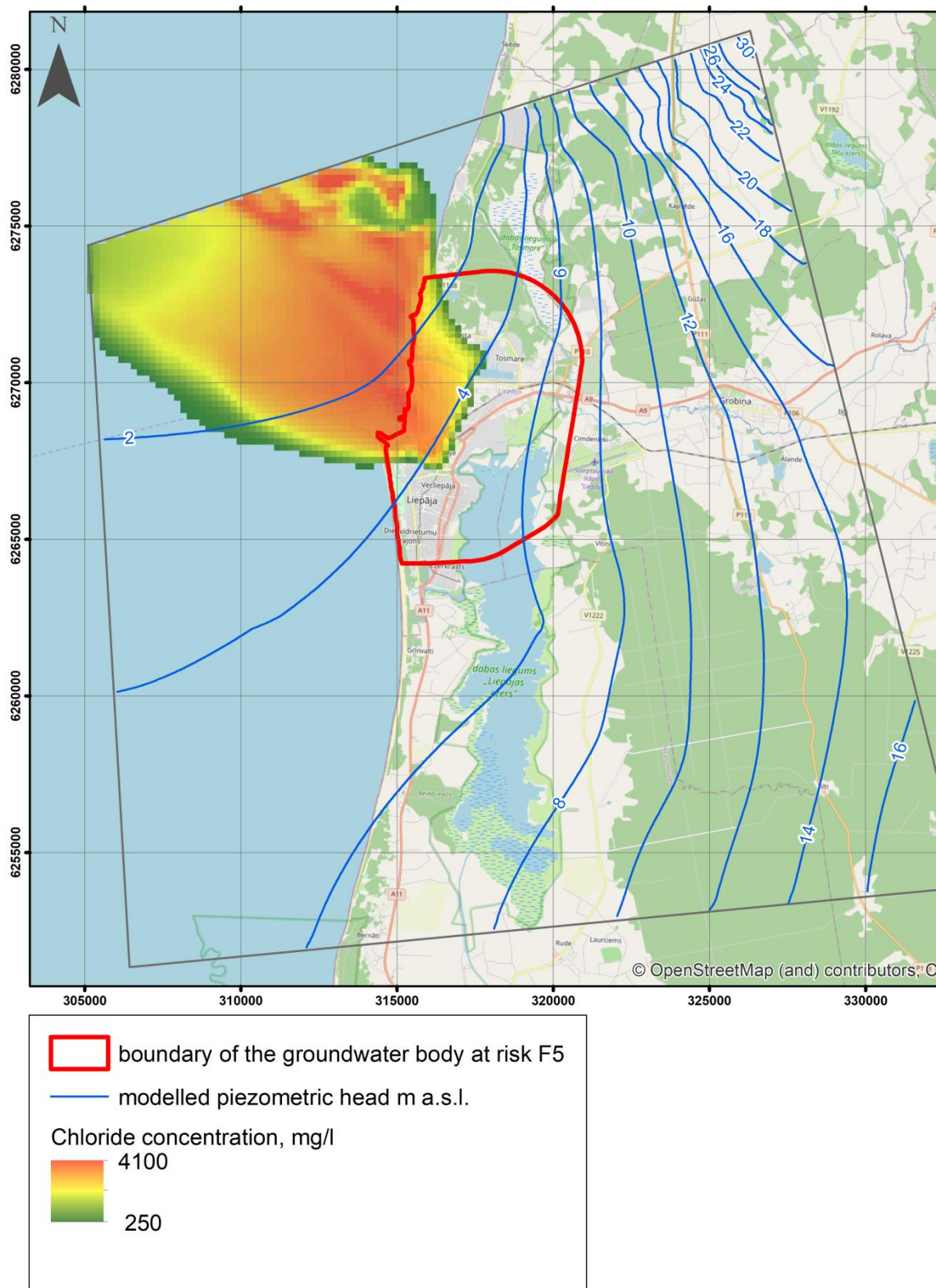
Figure 22 Modelled groundwater head (m a.s.l.) and Cl⁻ concentration (mg/l) distribution in D₃*mr-žg* aquifer around 2015, Present scenario
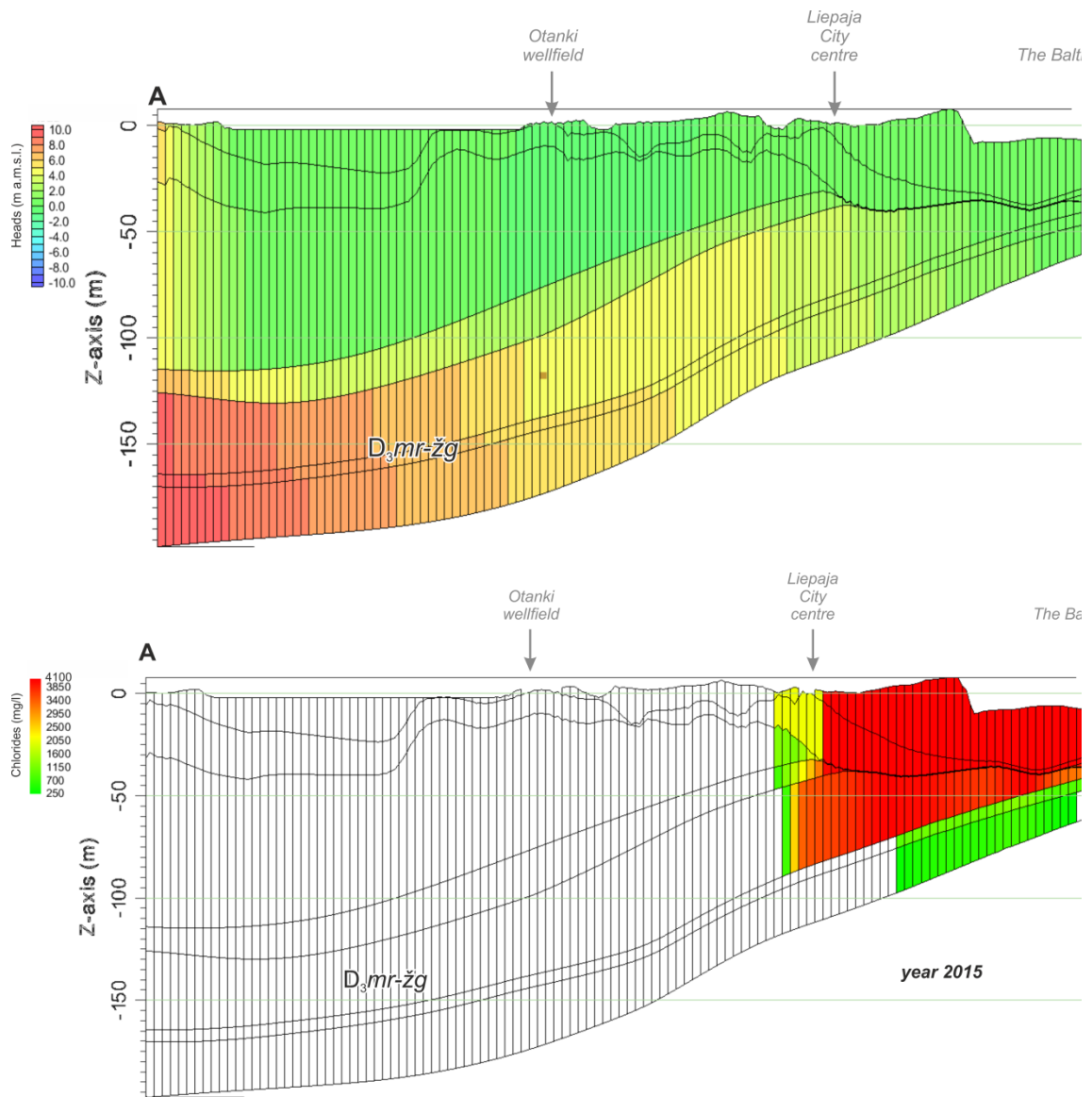
Figure 23 Vertical cross-section along A-B line (**Figure 20**): top – groundwater head (m a.s.l.); bottom - Cl⁻ concentration (mg/l) aquifer around 2015, Present scenario
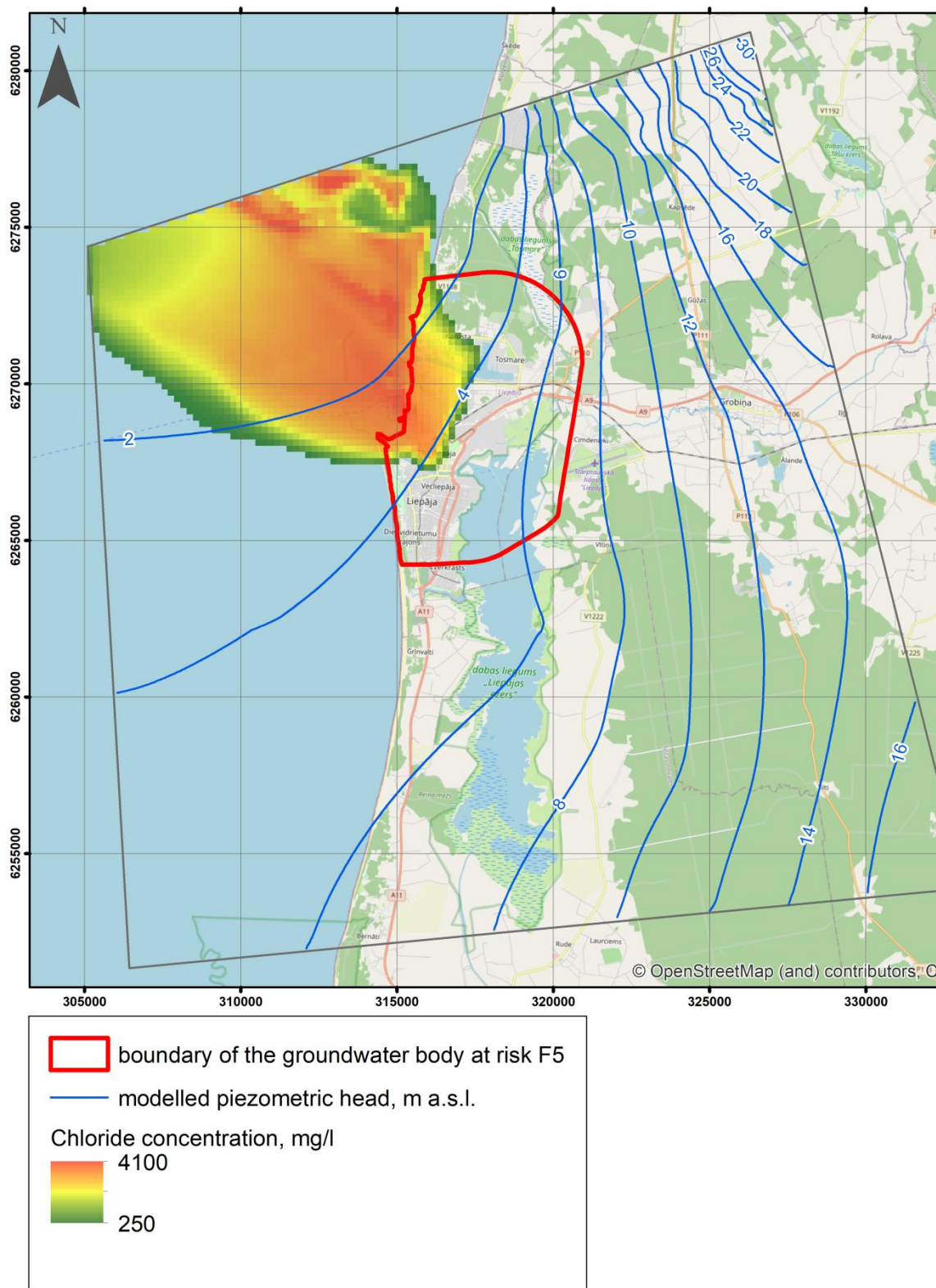
Figure 24 Modelled groundwater head (m a.s.l.) and Cl⁻ concentration (mg/l) distribution in D₃mr-žg aquifer around 2027
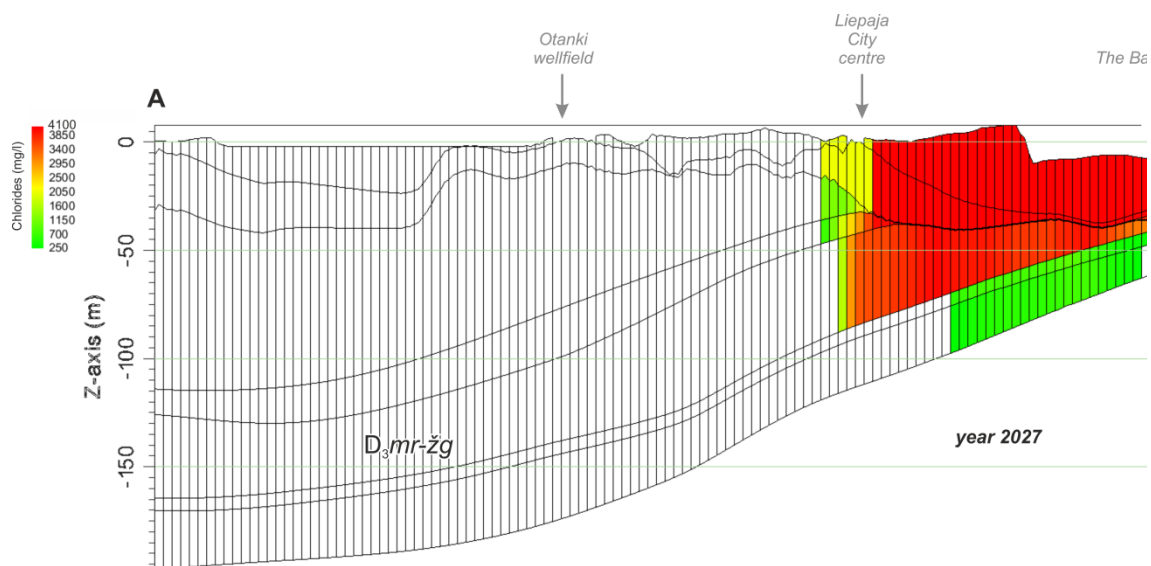
Figure 25 Vertical cross-section along A-B line (**Figure 20**): Cl$^-$ concentration (mg/l) around 2027
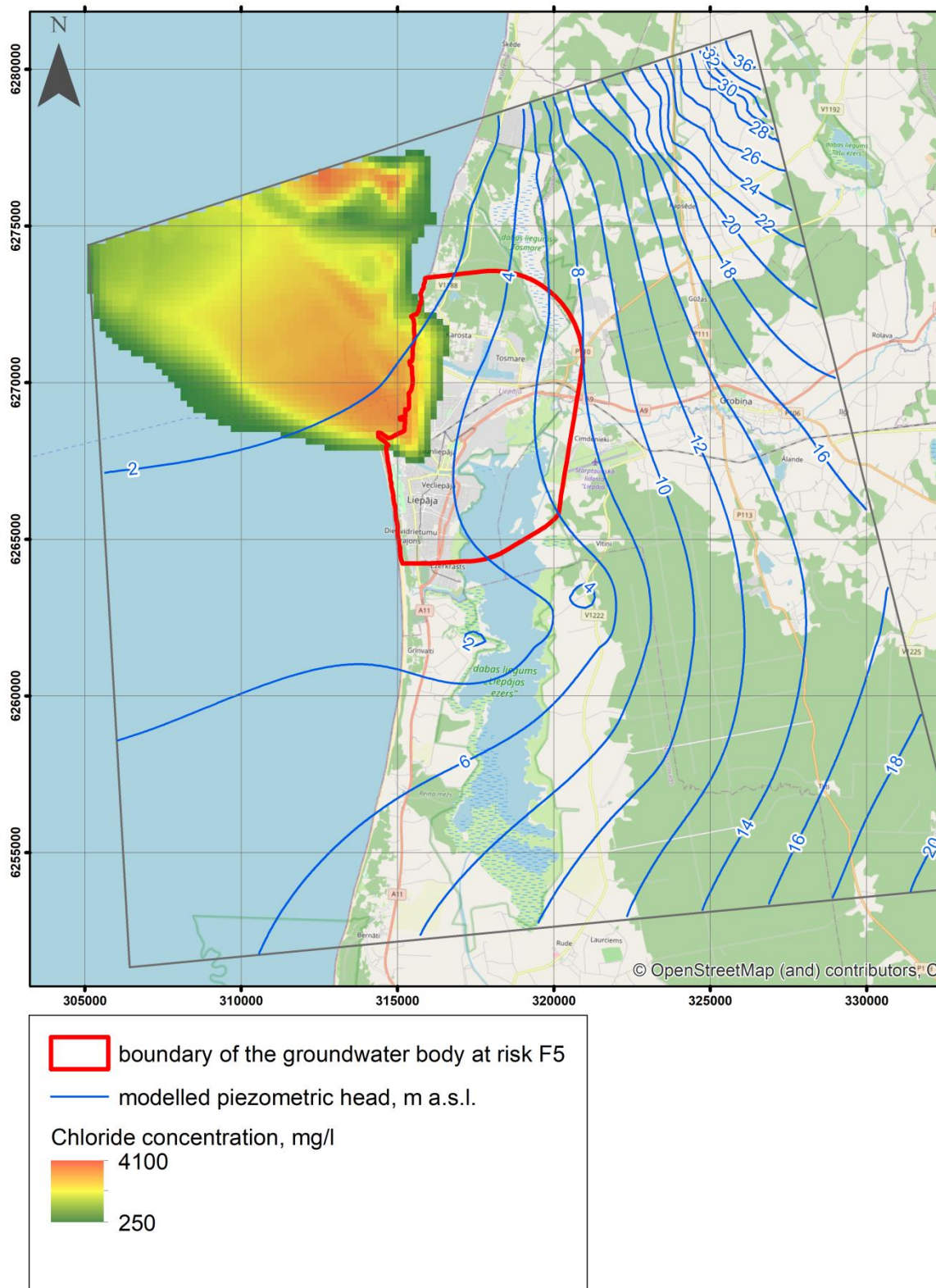
Figure 26 Modelled groundwater head (m a.s.l.) and Cl⁻ concentration (mg/l) distribution in D$_3$mr-žg aquifer around 2100, Future scenario
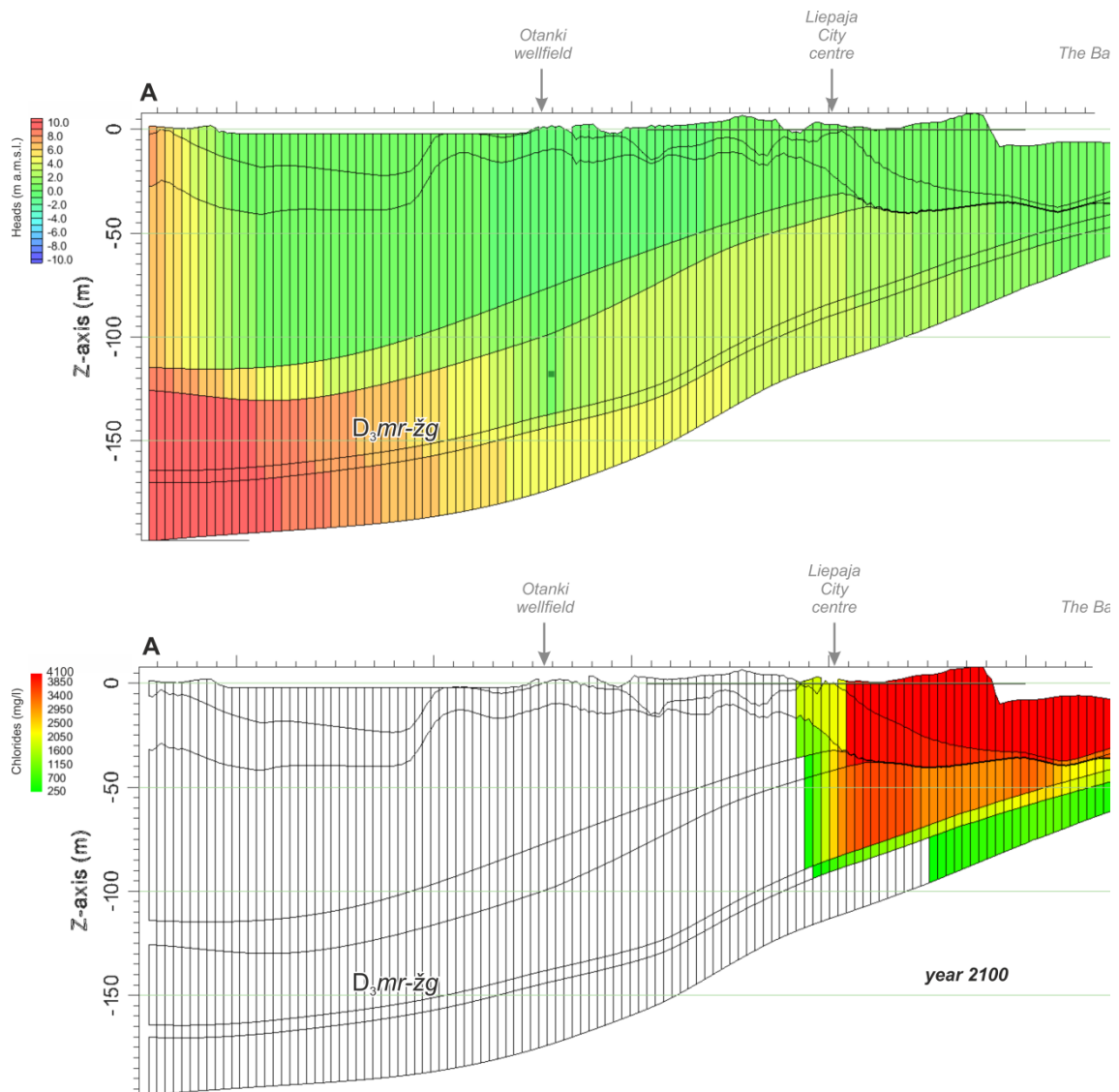
Figure 27 Vertical cross-section along A-B line (**Figure 20**): top – groundwater head (m a.s.l.); bottom - Cl⁻ concentration (mg/l) around 2100, Future scenario

5.3. Conceptual representation of the state of seawater intrusion

Results of the conceptual representation of the state of seawater intrusion according to modified methodology by Baena-Ruiz *et al.*, (2018; **Figure 28**) show gradual retreat from its peak in late 20th century. However, despite significantly increased groundwater recharge, even by the end of 21st century the tracer of historical seawater intrusion was expected to be found in groundwater body F5.
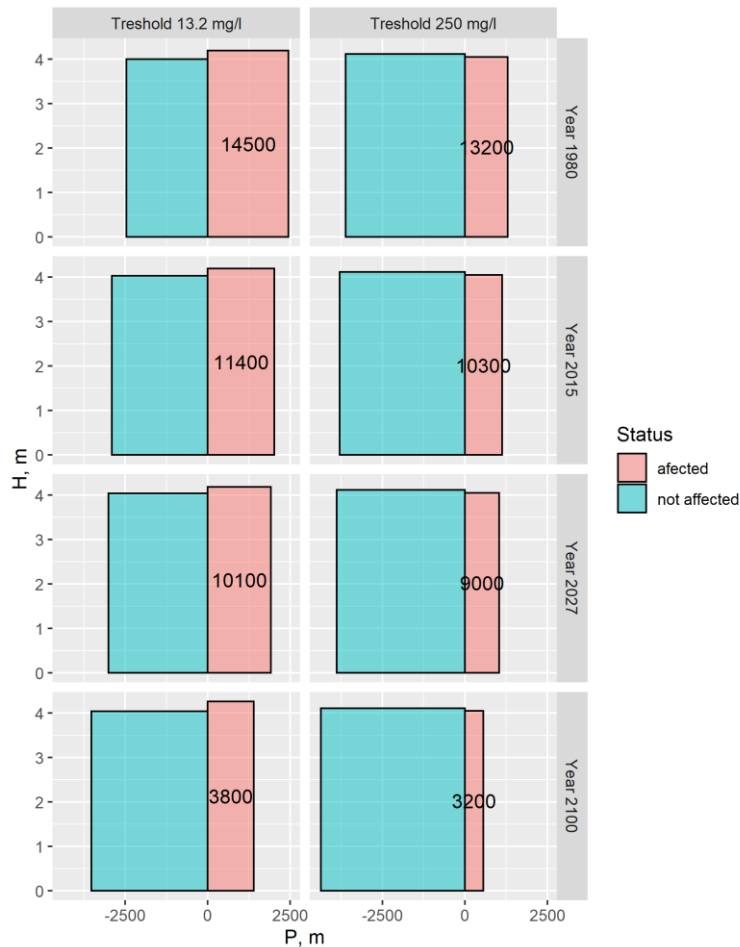
Figure 28 Conceptual representation of the state of the sea-water intrusion into groundwater body F5, Liepāja, Latvia, modified after (Baena-Ruiz *et al.*, 2018), see symbol explanation in **Figure 15**

5.4. Performance to historical data

3D hydrogeological modelling

Simulation of the seawater intrusion into D_3 Mūri-Žagare aquifer yielded controversial results: at least 250 years of historically high groundwater abstraction was needed to have the state of seawater intrusion as historically observed. However the modelled retreat of the seawater intrusion after decrease of abstraction rate largely followed the observations. This indicate that either assumptions of initial chloride distribution in aquifer was inaccurate or model setup does not satisfactory reflect actual geological situation.

In literature (Semjonovs *et al.*, 1997) there were indications about groundwater salinization already in 30-ties of the 20th century. If this is the case, then it is likely that at natural state significant portion of aquifers bellow the Baltic Sea were saturated with saltwater rather than

freshwater. In our model setup we have assumed that the brackish (salinity of about 10‰) water of Baltic Sea has the same density as fresh water, therefore little or no natural penetration of seawater into aquifers would take place. In model initiation only the topmost layer was marked as saturated with seawater. Much earlier inland penetration of seawater in D$_3$*mr-žg* aquifer would be modeled if on model initiation saltwater would be present in the aquifer under the Baltic Sea.

D$_3$*mr-žg* aquifer is made of both sandstones, dolomites and impervious interlayers of fined grained sediments (Lukševičs *et al.*, 2012), however in model setup it was represented as uniform aquifer. Thus actual configuration of locally significant aquitards could significantly influence the propagation rate of seawater intrusion into aquifer. In addition carbonate aquifers are known to have a dual porosity: water movement in fissures and cracks are much faster than in fine pores in blocks separated by the fissures. Thus actual penetration of intrusion in fissured rocks would be faster compared clastic sediments.

Furthermore both more heterogeneous geological structures of the study site as well as speculated antecedent sea water in sedimentary formations below Baltic Sea would result in development of more dispersed sea water intrusion. Configuration of observed seawater intrusion actually was more complex and dispersed compared to our model output. Both hypotheses deserve further attention, but are outside the scope of current work.

Conceptual representation of the state of intrusion

Interpolated results of the Cl$^-$ concertation in D$_3$*mr-žg* aquifer clearly did not adequately illustrated the state of the seawater intrusion. That was evident by overall smoothing and patchiness of the maps. Consequently conceptual representations are equally uncertain. However the rather wide distribution of low-level Cl$^-$ contamination (**Figure 19**) might be rather realistic, particularly if compared to the modeled sharp gradients of Cl$^-$ concentration.

Conceptual representation of the statistically interpolated state of intrusion have greater extent but leaser total mass of above-threshold Cl$^-$ intruded into aquifer (**Figure 14**) if compared to the modeled one (**Figure 28**). Arguably the area of the aquifer affected by intrusion was better represented by the 3D hydrogeological model, despite some of regions (near lake Liepāja, **Figure 19 and 20**) know to have elevated Cl$^-$ concentration does not show up in modeled maps. That might be due to simplification of geological complexity in geological model or inaccurate representation of the actual groundwater abstraction.

In contrary it is likely that the total mas of extra Cl$^-$ ion in D$_3$*mr-žg* aquifer were more closely represented by the interpolated observations as generally higher concentrations were calculated by modeling compared to actual observations. This discrepancy between modeling results and observation very likely was due to simplified representation of complex geological stricter in the model.

Interpolation of the observed Cl$^-$ concentration in D$_3$*mr-žg* aquifer gives an impression that the intrusion has spread since the 80-ties of the 20th century. Most likely that was not the case as groundwater abstraction rates had decreased and observed levels of Cl$^-$ concentration are decreasing (Bikše *et al.*, 2016). Non-overlapping observation wells were the source of this misleading result, demonstrating the need for continuous and consequent monitoring. It is unlikely that the geology will experience similar explosion of high resolution, near-continues

availability of remote sensing data, like some other earth sciences had in recent decades year. Lack of knowledge about detailed structure of the geological environment will remain a major challenged in hydrogeological modeling. Thus continuation of ongoing monitoring work is important as ever ensuring that the same parameters are being observed at the same locations.

5.5 Results of assessments

1. Using 3D stationary groundwater flow model we did not found any evidence of ongoing seawater intrusion into $D_3mr\text{-}\check{z}g$ aquifer, thus we conclude that elevated Cl^- concertation in this aquifer was the historical pollution that is gradually removed by natural groundwater flow.

2. Results of hydrogeological modelling demonstrated that present groundwater abstraction rates in Liepāja city were sustainable, and gradual recovery of freshwater $D_3mr\text{-}\check{z}g$ aquifer affected by seawater intrusion was expected to continue confirming previously observed trends in water levels and quality.

3. It was found that in future climatic conditions increased groundwater recharge was to be expected. As a result even three-fold increase of present groundwater abstraction and preserving present configuration of abstraction wells was not likely to trigger renewed seawater intrusion.

4. Unrealistically long initiation period of historically high groundwater abstraction rates was necessary to model state of seawater intrusion similar to observations, however modelled retreat of intrusion after reduction of groundwater abstraction reflected observations satisfactory. It is likely that already at natural state seawater was a penetrating sedimentary rock below Baltic Sea near Liepāja, resulting in fast development of inland intrusion when intensive groundwater abstraction was initiated in early 20th century. In addition geological heterogeneous and possibly fissured, dual-porosity layers within $D_3mr\text{-}\check{z}g$ aquifer would have contributed in faster than expected inland penetration of seawater. Both these aspect deserve further investigation.

5. In a case of climate change scenario with expected 3°C average temperature rise, increased groundwater recharge (by up to 50%) was expected. As a result even threefold increased groundwater abstraction compared to modern situation with current configuration of abstraction wells was not likely to result in renewed seawater intrusion into Upper Devonian Mūri-Žagare aquifer within groundwater body F5 and its surrounding.

6. The inherent difficulties in using simple statistical interpolation to represent the state of seaware intrusion in to complex geological environment underlain the need for continues monitoring of the same groundwater parameters at the same locations.

6   REFERENCES

Baena-Ruiz L, Pulido-Velazquez D, Collados-Lara AJ, Renau-Pruñonosa A, Morell I. 2018. Global Assessment of Seawater Intrusion Problems (Status and Vulnerability). *Water Resources Management* 32 (8): 2681–2700 DOI: 10.1007/s11269-018-1952-2

Bikše J, Retike I. 2018. An Approach to Delineate Groundwater Bodies at Risk: Seawater Intrusion in Liepāja (Latvia). *E3S Web of Conferences* 54: 00003 DOI: 10.1051/e3sconf/20185400003

Bikše J, Retiķe I, Kalvāns A. 2016. Historical evolution of seawater intrusion into groundwater at city Liepāja, Latvia. *XXIX Nordic Hydrological Conference 8-10 August 2016, Kaunas, Lithuania* **21**: 171

Copernicus Climate Change Service (C3S). 2019. C3S ERA5-Land reanalysis. *Copernicus Climate Change Service*

Levins I, Levina N. 2001. Assesment of centralized water supply sources for Liepaja; Fund # 12430 (in Latvian). Riga.

Lukševičs E, Stinkulis Ģ, Mūrnieks A, Popovs K. 2012. Geological evolution of the Baltic Artesian Basin. In *Highlights of Groundwater Research in the Baltic Artesian Basin*, Dēliņa A, , Kalvāns A, , Tomas S, , Bethers U, , Vircavs V (eds).University of Latvia; 7–52.

LVĢMC. 2018. Metodiskie norādījumi par hidroģeoloģiskās izpētes pārskatu sagatavošanu un noformēšanu: aizsargjoslu ap pazemes ūdens ņemšanas vietām noteikšanas metodika. Pārskatos par hidroģeoloģisko izpēti biežāk sastopamo kļūdu apskats.: 29 Available at: https://www.meteo.lv/fs/CKFinderJava/userfiles/files/Geologija/Geologiska_izpete/Metodis kie_noradijumi.doc

Marandi A, Karro E. 2008. Natural background levels and threshold values of monitored parameters in the Cambrian-Vendian groundwater body, Estonia. *Environmental Geology* 54: 1217–1225 DOI: 10.1007/s00254-007-0904-6

Müller D, Blum A, Hart A, Hookey J, Kunkel R, Scheidleder A, Tomlin C, Wendland F. 2006. Final proposal for a methodology to set up groundwater treshold values in Europe. Report to the EU project '"BRIDGE"' 2006, Deliverable D18 Available at: http://hydrologie.org/BIB/Publ_UNESCO/SOG_BRIDGE/Deliverables/WP3/D18.pdf

Retike I, Bikše J. 2018. New Data on Seawater Intrusion in Liepāja (Latvia) and Methodology for Establishing Background Levels and Threshold Values in Groundwater Body at Risk F5. *E3S Web of Conferences* 54: 00027 DOI: 10.1051/e3sconf/20185400027

Semjonovs I, Bebris RA, Kokoreviča A, Konošonoka R, Skolmeistare R, Lustiks I, Gavena I, Doniņa I, Levina N, Aleksāns O, et al. 1997. *Pazemes ūdeņu aizsardzība Latvijā (in Latvian)*.

Izdevniecība Gandrs: Rīga.

Spalvins A, Slangens J, Janbickis R, Lace I, Eglite I, Skibelis V. 2004. Hydrogeological model for well field Otanki of Liepaja, Latvia. *Scientific Proceedings of Riga Technical University in series 'Computer Science'* 21 (46): 162–171

Spalviņš A, Krauklis K, Aleksāns O, Lāce I. 2018. Latvijas hidroģeoloģiskā modeļa LAMO izveidošana, izmantošana un pilnveidošana (Development, Application and Upgrading of the Hydrogeological Model of Latvia LAMO; in Latvian). *Boundary Field Problems and Computer Simulation* 57: 5–14 DOI: 10.7250/bfpcs.2018.001

Tolstovs J. 1994. Preparation of materials for modelling of water suply for Liepaja, Fund # 11261. Rīga.

Deliverable 5.3

PILOT DESCRIPTION AND ASSESSMENT

Campina de Faro Aquifer System (Portugal)

Authors and affiliation:

Judite Fernandes, Carla Midões, Adelaide Ferreira, Ana Castanheira e Fernando Monteiro, Ana Pereira, José Sampaio (Geological Survey of Portugal - LNEG)

Edite Reis (Portugal Environment Agency - APA/ARH Algarve)

Rui Hugman, Luís Costa, Kathleen Standen e José Paulo Monteiro (Algarve University - UALG)

Deliverable Data	
Deliverable number	D5.3
Dissemination level	Public
Deliverable name	Pilot description and assessment
Work package	WP5, Assessment of salt-/sea water intrusion status and vulnerability
Lead WP/Deliverable beneficiary	Institution IGME
Deliverable status	
Version	Version 1
Date	2020/4/19

[This page has intentionally been left blank]

LIST OF ABBREVIATIONS & ACRONYMS

CC	Climate Change
CF	Campina de Faro Aquifer System
FW	Freshwater
SW	Seawater
SWI	Seawater intrusion

TABLE OF CONTENTS

TABLE OF FIGURES

1   EXECUTIVE SUMMARY

Pilot name	CAMPINA DE FARO AQUIFER SYSTEM (Code M12)	
Country	Portugal	
EU-region	Mediterranean region	
Area (km^2)	86.4 km^2	
Aquifer geology and type classification	Sands and gravels of Quaternary deposits cover biocalcarenites from Miocene. Porous and karstified Aquifer System.	
Primary water usage	Irrigation, industry, drinking water (few people).	
Main climate change issues	Abstraction for the tourism sector has been intensified over the last years with the irrigation of golf courses located in Vale de Lobo and Quinta do Lago (sector W of the aquifer system). Long-term piezometric time series show that water levels have been persistently negatives since 2010, accompanied by a constant increase of chlorides, which may indicate an ongoing saline intrusion process. The decrease of annual precipitation, river flow and recharge will lead to the need to implement mitigation measures such as the intensification of natural recharge and reuse of treated wastewater for irrigation of golf courses.	
Models and methods used	Chemical indicators, time series analysis, statistical analysis, lumped indices, integrated hydrological model (although the lack of reliable recharge).	

Key stakeholders	Portugal Environment Agency (APA), Portuguese Environmental Ministry, Algarve University.
Contact person	Judite Fernandes, LNEG Portuguese Geological Survey, judite.fernandes@lneg.pt

Campina de Faro Aquifer System (M12) is a coastal aquifer along Algarve coast (southern of Portugal), with an area of 86.4 km^2 and it was the pilot selected for Tactic project. The aquifer system is an exploitation target for agricultural supply. However, over the last years, the extraction for the tourism sector has been intensified with the irrigation of golf courses located in Vale de Lobo and Quinta do Lago (sector W of the aquifer system), causing a depletion on groundwater levels. Sands and gravels of the Plio-Quaternary deposits (30 - 60 m thick) gives support to a shallow phreatic aquifer, which covers a confined multi-layered aquifer installed in the Miocene sandy limestones (300 m thick). Evaporites are injected into faults at 90 to 120 m depth. In the past, there was evidence of artesianism in some areas, showing the hydraulic independence of the two aquifers. Nowadays, bad drilling practices caused hydraulic connection between them, increasing the vulnerability to contamination of the deepest aquifer. Natural flow goes from north to south towards the sea, locally changing due to the extractions. The shallow aquifer receives direct recharge from precipitation, while the Miocene aquifer receives indirect recharge from the Jurassic-Cretaceous limestones located up to north and also from influent streams/rivers along faults. Downstream, the rivers and streams have an effluent behaviour and maintain sensitive ecosystems dependent on groundwater discharge. In the W sector of the aquifer system, time series show that water levels have been persistently negative since 1995. Since 2010, this trend has been followed by a constant increase of chlorides, which may indicate an ongoing seawater intrusion process.

Climate models projection results predict a virtually systematic decline in water table recharge and river flow, due to temperature rise and effective rainfall decrease. Significant SW encroachment would be expected under climate change and groundwater water use conditions, making abstraction for agriculture and golf course irrigation unfeasible and completely reducing the freshwater discharge in streams and into the Ria Formosa lagoon.

Chemical indicators were helpful to get an update overview of seawater intrusion status allowing the definition of an area of 4.6 Km^2 currently impacted by SWI. Ratios rCl /rHCO3 and rSO4 / rHCO3 discretized groundwaters affected by seawater intrusion from those affected by evaporites dissolution + fertilizers input. The vulnerability to SWI of the aquifer system was assessed applying Galdit method. There is a good agreement between highly vulnerable areas and SWI impacted area. A density-dependent flow and transport model was able to simulate future SWI impacts considering 3 different scenarios of recharge reduction (5%, 10% and 20%) according to climate change predictions in this region. Simulations show that Miocene deep aquifer is more affected by SWI than the Plio-Quaternary phreatic aquifer, an expected result since the deep aquifer is affected by a higher rate of abstraction. This becomes more evident in

the western sector of the aquifer (Vale do Lobo sector), which is subject to a higher and more concentrated water abstraction, hence being more vulnerable to seawater intrusion processes.

Adequate management measures and changes in water use practices are needed to counteract SWI like intensification of natural recharge and reuse of treated wastewater for irrigation of golf courses, among others. Although further work is still needed to improve the understanding of the system and provide reliable predictions of the impact of changes to water use and climate, results provided here already show that groundwater management needs to be adapted to avoid serious problems in the future.

2 INTRODUCTION

Climate change already have widespread and significant impacts in Europe, which is expected to increase in the future. Groundwater plays a vital role for the land phase of the freshwater cycle and has the capability of buffering or enhancing the impact from extreme climate events causing droughts or floods, depending on the subsurface properties and the status of the system (dry/wet) prior to the climate event. Understanding and taking the hydrogeology into account is therefore essential in the assessment of climate change impacts. Providing harmonised results and products across Europe is further vital for supporting stakeholders, decision makers and EU policies makers.

The Geological Survey Organisations (GSOs) in Europe compile the necessary data and knowledge of the groundwater systems across Europe. In order to enhance the utilisation of these data and knowledge of the subsurface system in CC impact assessments the GSOs, in the framework of GeoERA, has established the project "Tools for Assessment of ClimaTe change ImpacT on Groundwater and Adaptation Strategies – TACTIC". By collaboration among the involved partners, TACTIC aims to enhance and harmonise CC impact assessments and identification and analyses of potential adaptation strategies.

TACTIC is centred around 40 pilot studies covering a variety of CC challenges as well as different hydrogeological settings and different management systems found in Europe. Knowledge and experiences from the pilots will be synthesised and provide a basis for the development of an infra structure on CC impact assessments and adaptation strategies. The final projects results will be made available through the common GeoERA Information Platform (http://www.europe-geology.eu).

Campina de Faro Aquifer System (M12) is a coastal aquifer along Algarve coast (southern of Portugal) and it was selected due it´s unbalanced water budget. Groundwater removed from the aquifer system for human use is almost equal to total estimated recharge, placing the system at risk of seawater intrusion. The evidence of SWI in the western sector where few boreholes are already salinized confirms that CF is currently overexploited in an un-sustainable way. Groundwater dependent ecosystems are seriously threatened, especially those dependent of effluent streams.

Assessment of seawater intrusion status, aquifer vulnerability to seawater intrusion and scenarios of seawater intrusion impacts due recharge reduction are the main goals of the work here presented.

3   PILOT AREA

3.1   Site description and data

3.1.1   *Location and extension of the pilot area*

The pilot area corresponds to the Campina de Faro Aquifer System, a coastal aquifer along Algarve coast (southern of Portugal), with an area of 86.4 km^2.
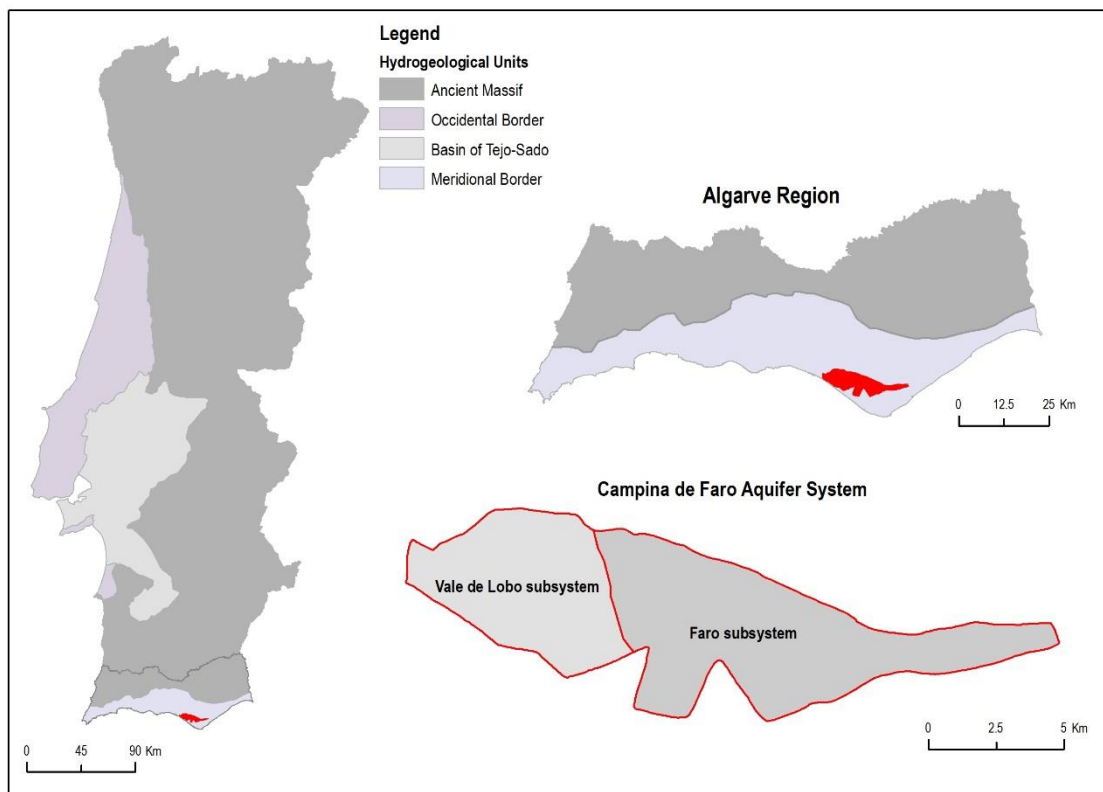

Figure 1. Location and extension of the Campina de Faro Aquifer System

The aquifer system of Campina de Faro is divided into two subsystems: Faro and Vale do Lobo. Both of them have several spatial discontinuities from the potentiometric and hydrogeochemical point of view, and a certain independence between them can be seen.

Our focus will be mainly on Vale do Lobo subsystem, which occupies an area of about 32 km^2, west located.

3.1.2 Geology /aquifer system main characteristics

The aquifer system of Campina de Faro consists of two overlapping aquifers:

At the surface, the detrital sediments (clayey sandstones with intercalations of pebbles and gravels, sands and alluvial deposits of the Quaternary) gives support to a phreatic aquifer, porous type with variable thickness, reaching in some places 65 m depth (Quinta do Lago), representing the preferential recharge area of this groundwater body.

In depth, there is another aquifer associated with fossiliferous limestones, biocalcarenites, and carbonate sandstones from Miocene. This porous/karstic aquifer type has a confined/semi-confined behaviour and its thickness can reach 300 m (Almeida et al., 2000).

Cretaceous formations are the substrate on which the above-mentioned aquifer formations are based (Silva, 1988). A sequence of marbles, limestones and dolostones constitute the C 1-2 formation followed by clay, sandstones, limestones and dolostones of the C 1 formation.

The shallow aquifer and the deep aquifer are separated by a clayed confining layer, that makes the lower part of the aquifer system independent from the upper part. However, in some places, there may be a hydraulic connection between both, due to the absence of the confining layer (Almeida et al., 2000).

The vertical and lateral variability of lithologic facies of this groundwater body is thus reflected in the formation of a multi-aquifer system, subdivided into a phreatic shallow aquifer at the top, and an underlying multi-layered semi-confined/confined aquifer.
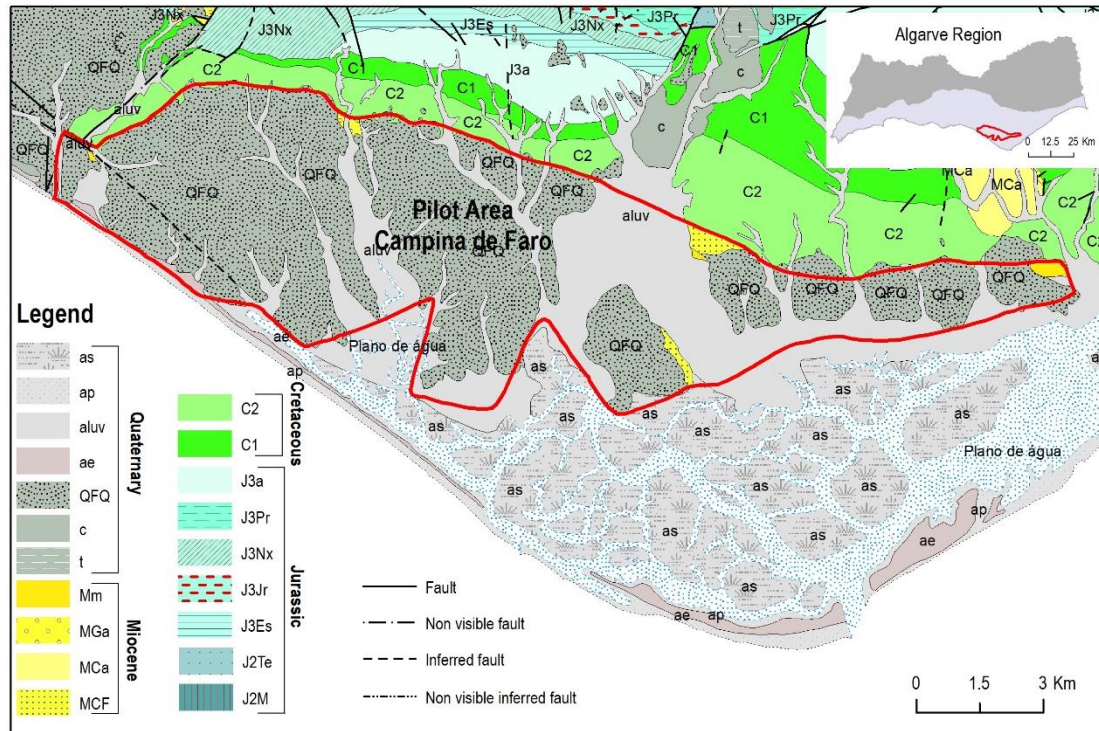
Figure 2. Geological formations of the Campina de Faro Aquifer System.

The geological structure corresponds to a monocline with a smooth slope (20°) towards south. The Miocene formations were deposited in a basin, graben type, controlled by faults, whose directions reflect the alignments of the main watercourses. Another aspect to be taken into account is the presence of diapiric structures which outcrops in Faro city, also recognized in geophysical studies (gravimetry) and confirmed by drill cores between depths of 91 (Quinta da Penha) and 120 m (Pontes de Marchil) at N of Faro (Silva, 1988).
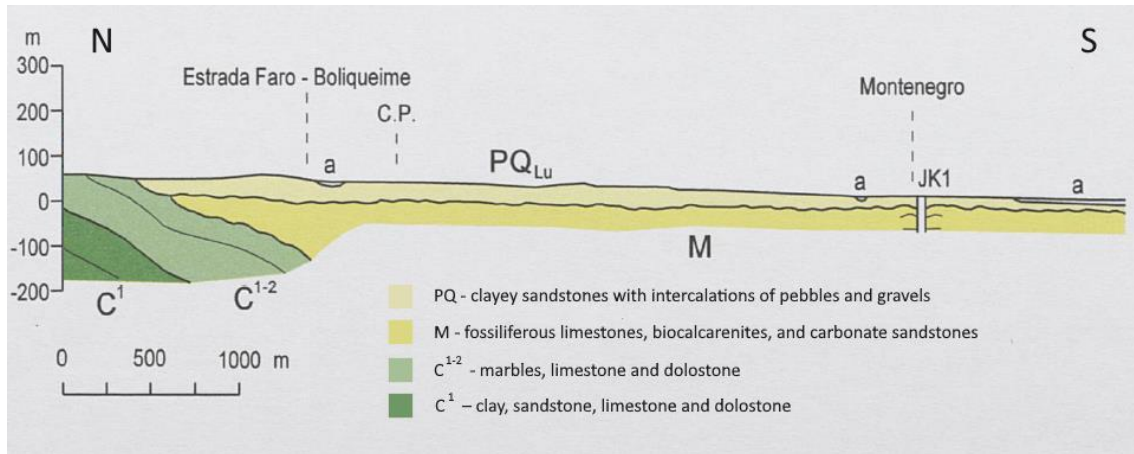
Figure 3. Geologic North-South Cross-section of the Campina de Faro Aquifer System, extracted from Manuppella, 2017.

The shallow aquifer receives direct recharge from the precipitation, while the Miocene aquifer receives indirect recharge from the Cretaceous and Jurassic limestones located at North, and this is the most important recharge source. However, in the absence of the confining layer there is also recharge from upper aquifer and from the streams located along faults that cross the aquifer system, namely the streams of Rio Seco and Ribeira da Biogal (Faro subsystem) and of S. Lourenço and Corgo da Gondra (Vale do Lobo subsystem).

From the geological point of view, there are still structural differences, with the existence of NW-SE and N-S faults, which cause formations compartmentalization in several blocks. These faults play an important role in the groundwater flow, with N-S faults functioning as preferential groundwater flow directions, whereas NW-SE faults act as a barrier (Stigter et al., 1998).

According to piezometric data, the regional groundwater flow pattern in natural conditions shows fluxes from north to south-SW, towards the sea.

Discharge occurs along the end part of streams into the Ria Formosa coastal lagoon and into the Atlantic Ocean.
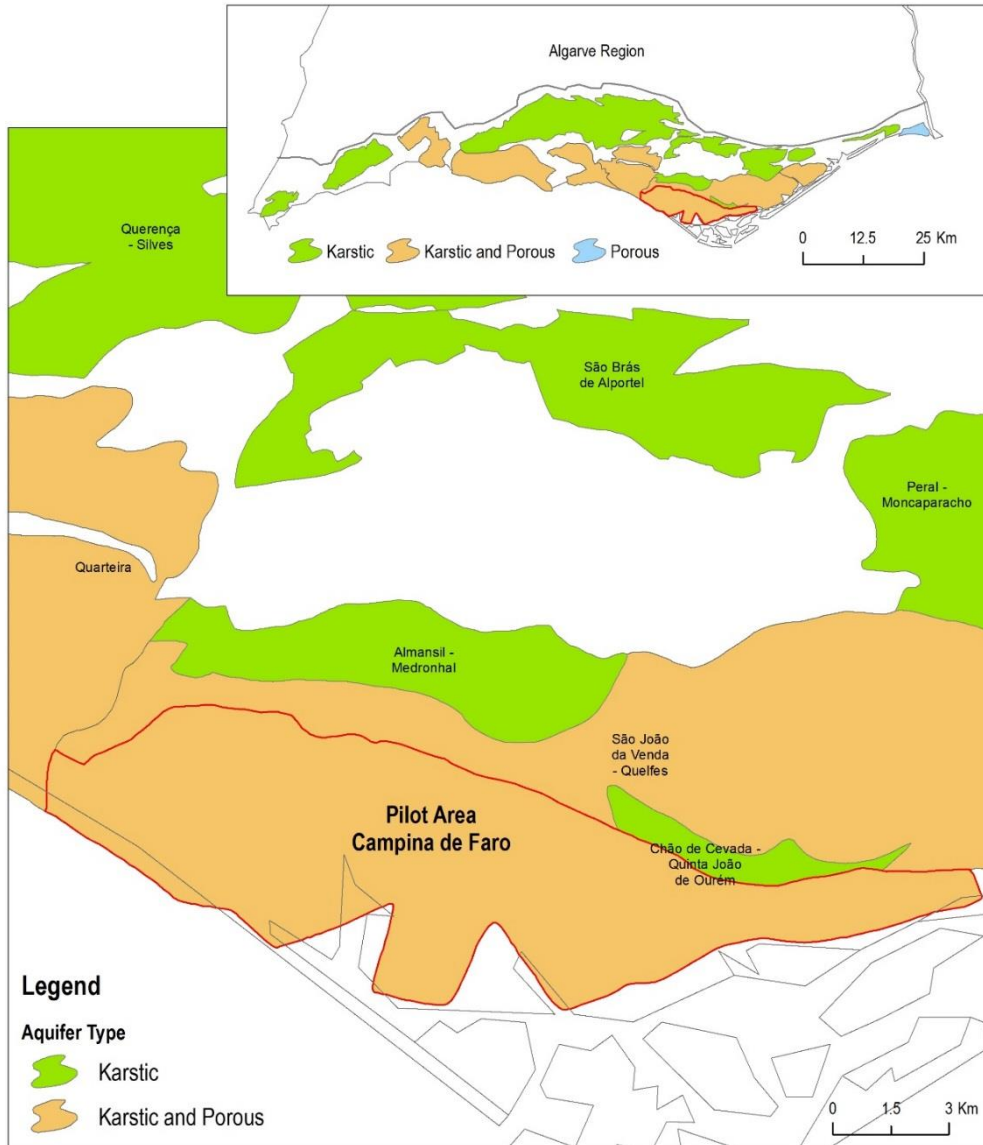
Figure 4. Aquifer Type of the Campina de Faro Aquifer System.

3.1.3 Topography and soil types

The area occupied by the aquifer system corresponds to an extensive flattening coastal plain, with heights ranging between 30 and 40 m. It is practically occupied by the sands and gravels of

Faro-Quarteira and alluviums. This area is crossed by several streams, on its terminal section, slightly embedded, which flow into the Ria Formosa coastal lagoon.
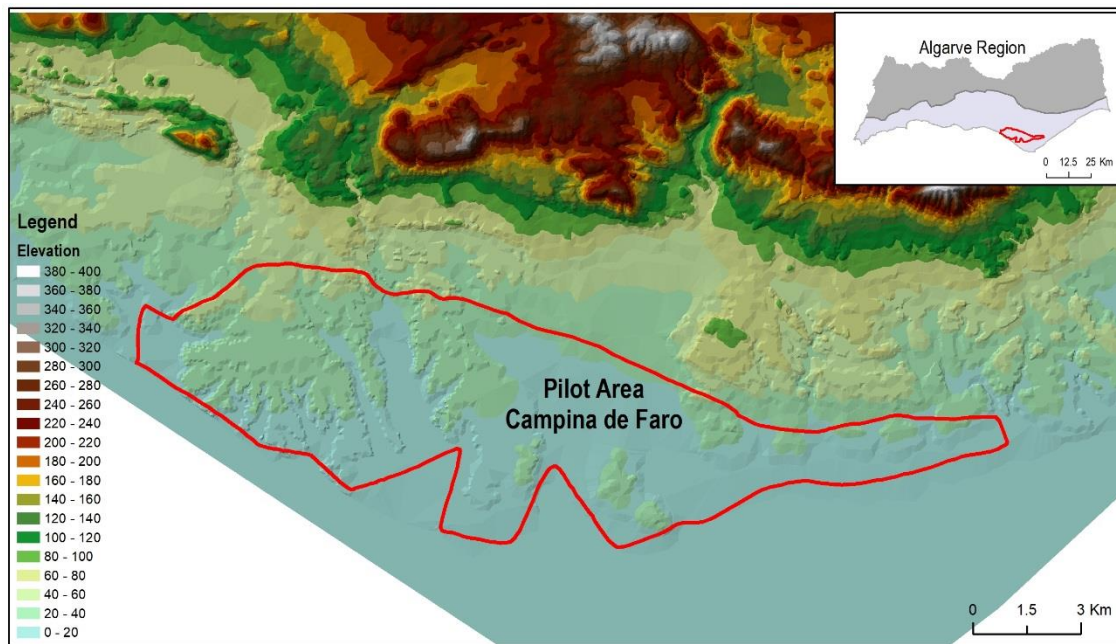
Figure 5. Digital Terrain Model of the Campina de Faro Aquifer System.

The soils lie on a sandy substrate with smooth slopes, predominantly lower than 3% (Management Plan for the Hydrographic Region of the Ribeiras do Algarve, 2016). The most abundant soils are the Mediterranean Soils, red or yellow, from compact limestone or dolomite (Vcd). Other soils, also important in the area under analysis, are: i) Calcareous soils from Climatic Xeric Regime, developed on non-compacted limestone (Pc); ii) Lithosoils, no humus, slightly insaturated, developed on coarse sandstones (Vt); and iii) Red calcareous soils, from Climatic Xeric Regime, of limestones (Vc). It can be said that only Lithosoils are originated from Areias e Cascalheiras of Faro-Quarteira Formation (Management Plan for the Hydrographic Region of the Ribeiras do Algarve, 2016).
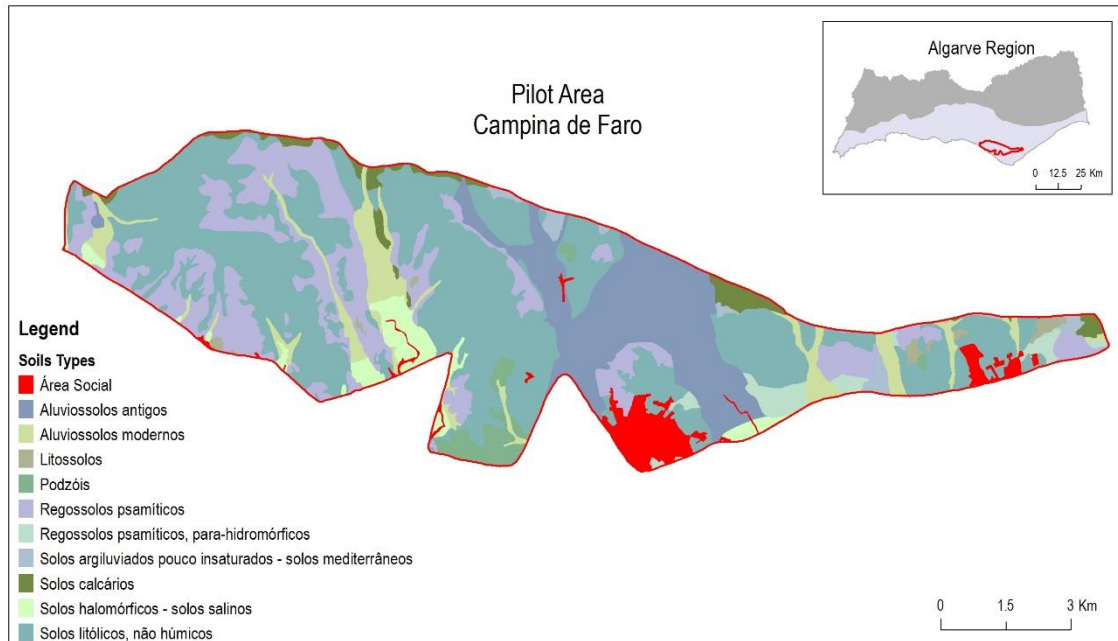
Figure 6. Soils Types of the Campina de Faro Aquifer System (Portuguese Classification).

3.1.4 Surface water bodies

The surface water bodies within the area covered by the aquifer system of Campina de Faro are: the Carcavai and S. Lourenço streams in the Vale do Lobo subsystem area and the Biogal, Rio Seco and Bela Mandil streams in the subsystem of Faro.

With an approximate direction N – S all these waterlines are tributaries of the Ria Formosa coastal lagoon, belonging to the drainage basin of Ria Formosa barrier islands and coastal lagoon system. The streams have a temporary regime, being dry during much of the dry semester and their flow regime presents a high interannual and seasonal variability. They also present an important interaction with groundwater, being influent upstream and effluent downstream already within the Ria Formosa lagoon system.
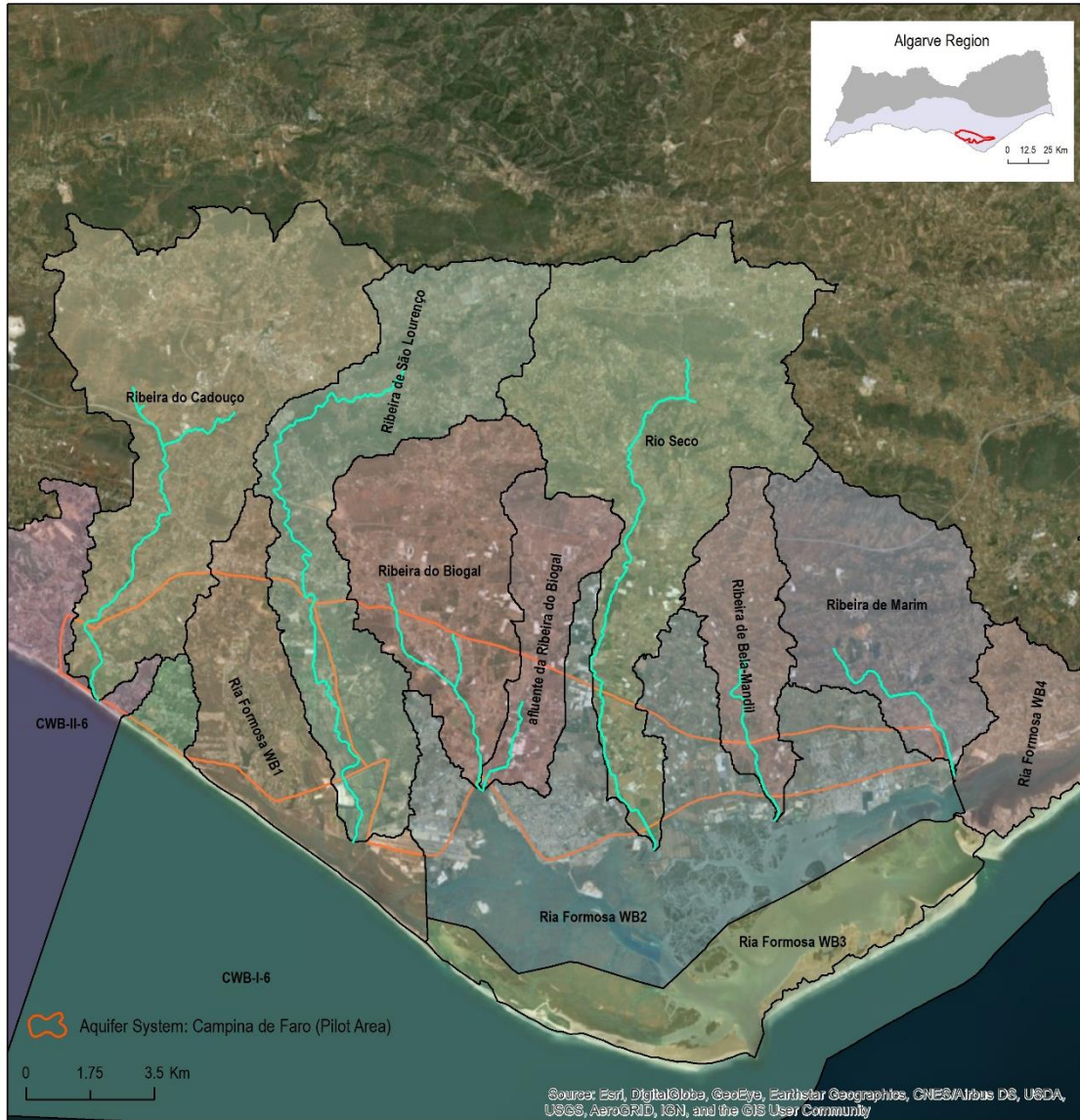
Figure 7. Surficial water bodies, Hydrographic basins and main streams (Management Plan for the Hydrographic Region of the Ribeiras do Algarve, 2016).

3.1.5   Hydraulic Head evolution and Hydrochemical aspects

Monitoring of piezometric levels in the study area began in the early 1980s. Piezometric network has 20 piezometers which have been monitored on a monthly basis for 30 years. It was carried out continuously in some points and during certain periods of time in other points, the reason

why the observation series have about 30 years. Groundwater quality monitoring network has 23 points, where electrical conductivity, pH and temperature have been measured twice a year since 1995. Laboratory physical-chemical analysis have been also carried out twice a year.
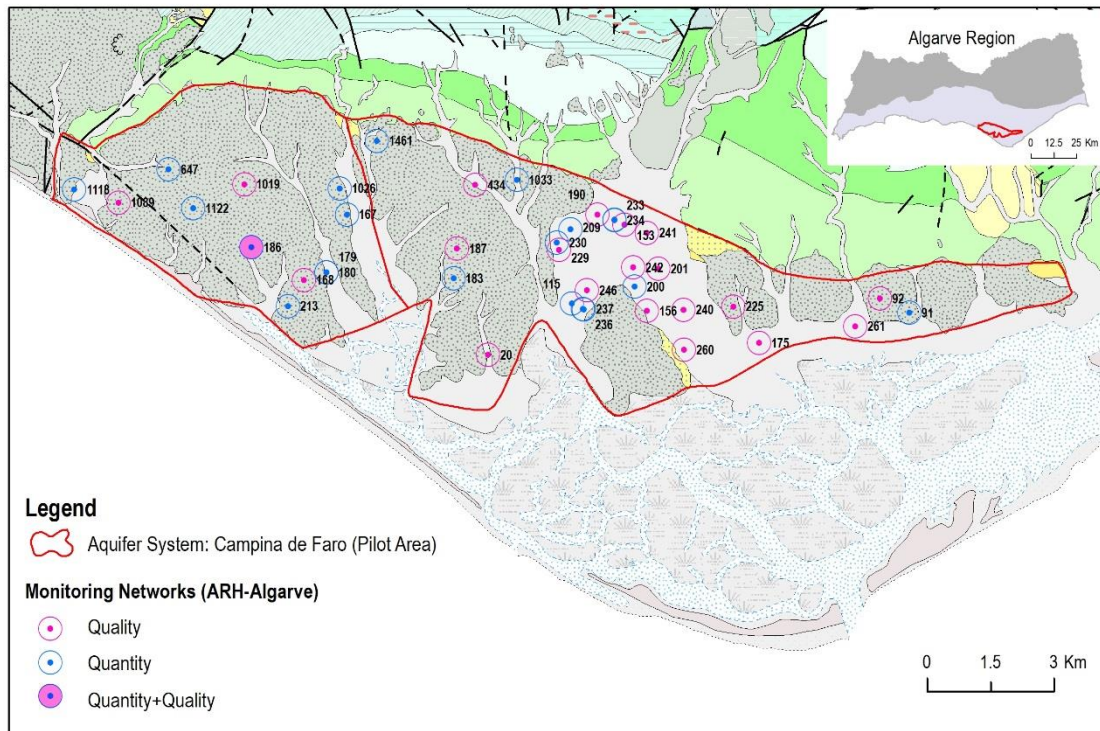
Figure 8. Monitoring quality and quantity networks (APA - ARH Algarve).

Both subsystems of the aquifer system present a relative differentiation in the hydrogeochemical and piezometric characteristics.

Figure 9 shows the piezometric surface from April 1984 and Figures 10 and 11 present recent piezometric surfaces for May 2018 (end of the rainy season) and October 2017 (end of the dry season), respectively.

A comparison of piezometric surfaces shows that sector E of the Campina de Faro has recovered to positive water levels whilst levels depletion within sector W of Vale do Lobo has worsened, presenting negative values.
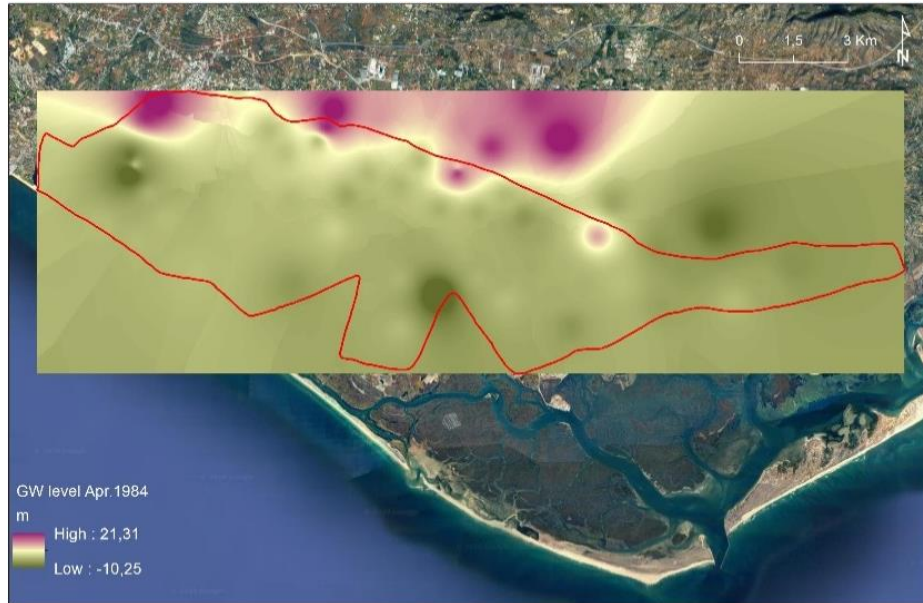
Figure 9. Piezometric surface for April 1984 (end of the rainy season).
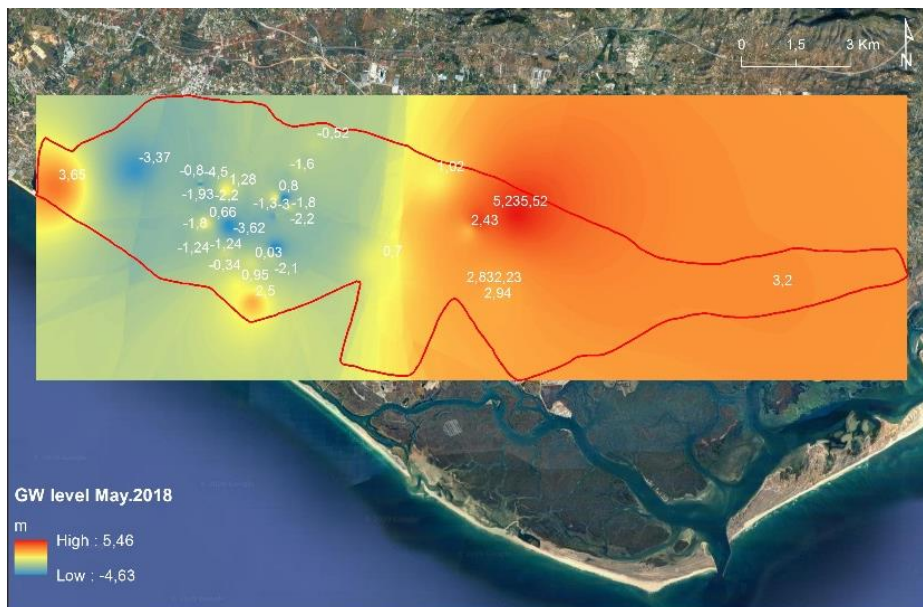
Figure 10. Piezometric surface for May 2018 (end of the rainy season).
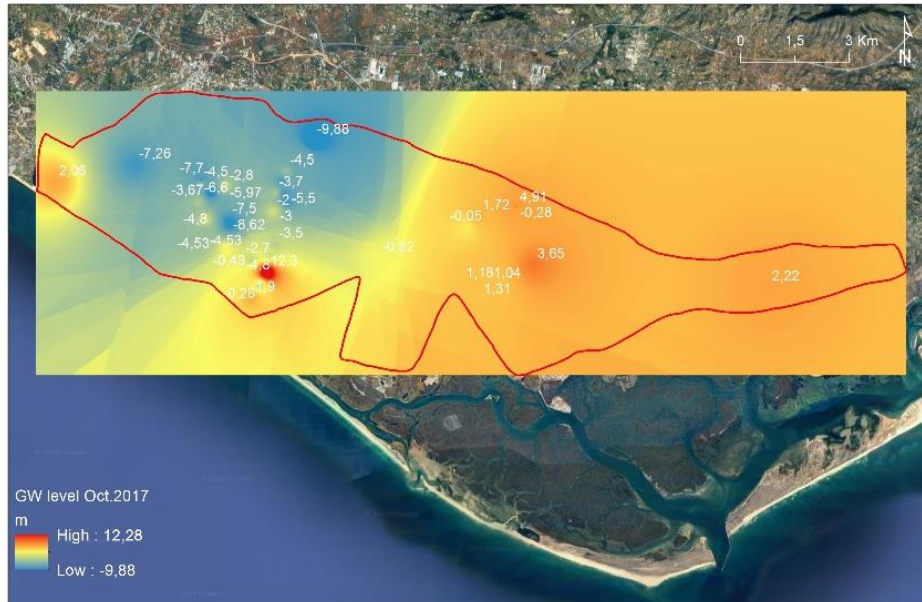
Figure 11. Piezometric surface for October 2017 (end of the dry season).

In the Vale do Lobo subsystem, the observation of about 30 years of piezometric levels indicates a downward trend especially from 2010 onwards, which is more pronounced in the East, due the combined effect of the decrease of the precipitation and, consequently, of the recharge and the increase of water withdrawals.

From the mid-1990s onwards, in points that have been exploiting the upper aquifer, piezometric levels have been negative almost of the time (APA-ARH Algarve).

The maximum amplitude of oscillation of the water levels is about 15 m and the inter-annual oscillations vary between 5 to 6 m (APA-ARH Algarve).

In the Faro Subsystem, this situation does not occur, showing always positive water levels without a downward trend.

These differences have been attributed mainly to the geological context which condition the recharge in depth (Management Plan of the Hydrographic Region of the Ribeiras do Algarve, 2016), but strong water abstraction for irrigation purposes leading to depressions on the piezometric surface, especially during summers and intensified by drought years, must be also considered.

Seawater intrusion is ongoing at SE of Vale do Lobo subsystem causing complete groundwater deterioration (Figure 12). On Faro Subsystem, groundwater quality problems are related with nitrates concentrations resulting mainly from bad agricultural practices for several years. Throughout the aquifer system, there are problems of evaporites leaching that are injected along the faults leading to high concentrations of sulphate and chloride.
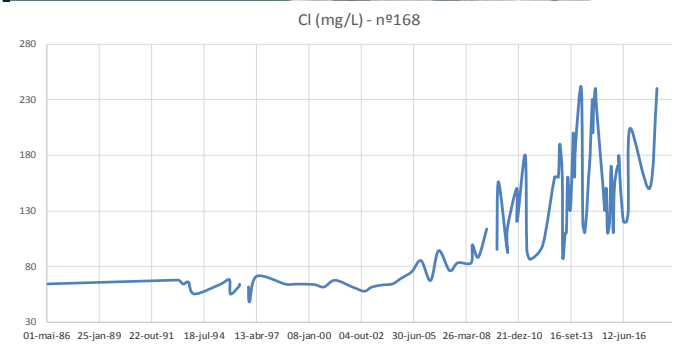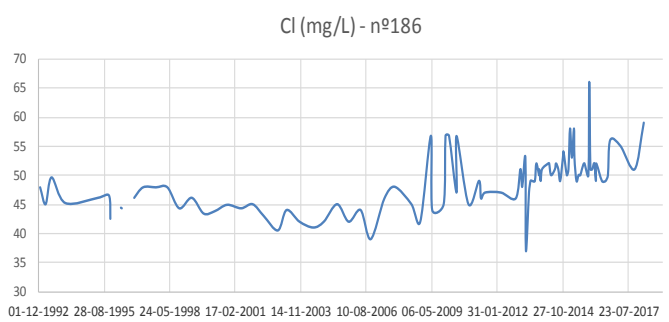
Cl (mg/L) - nº1089

Cl (mg/L) - nº1019
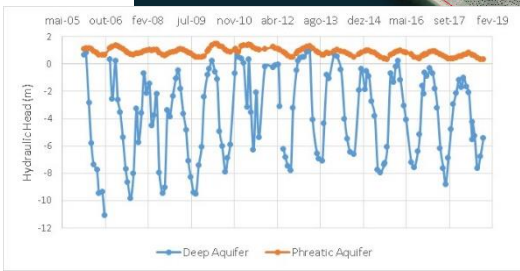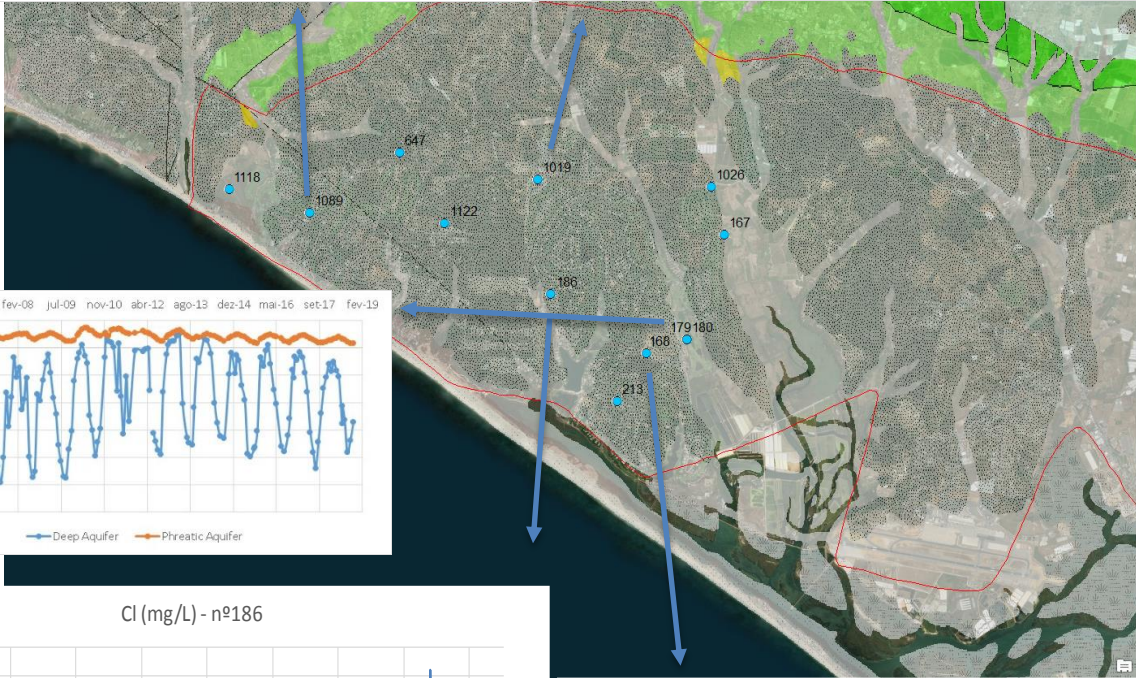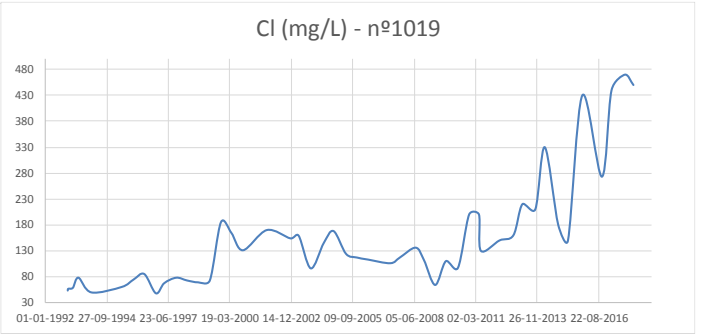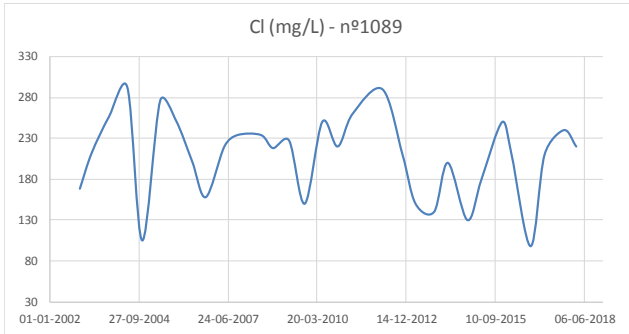
Cl (mg/L) - nº186

Cl (mg/L) - nº168

Figure 12. Cl time series in Vale de Lobo subsystem (W sector) and hydraulic head of both aquifers (APA - ARH Algarve), where can be seen positive hydraulic head for shallow aquifer and negative height for deep confined aquifer followed by a rising trend of chlorides concentration (mg/L).

From the hydrogeochemical point of view, groundwater presents sodium chloride (Na-Cl) and calcium bicarbonate (Ca-HCO$_3$) *facies*. Although two sources for Cl rising must be considered, one from seawater and other from evaporites, the recent increase in Cl should be preferentially related with the advance of seawater intrusion.

3.1.6   Hydraulic parameters

Pumping tests give some values for hydraulic parameters. Silva (1988) obtained a transmissivity value of 300 m^2/day from a recovery test in a borehole located in Quinta do Lago that pumps the lower aquifer.

A pumping test on deep aquifer conducted by DRAH in Gambelas gave the following results:

Transmissivity T =397 m^2/dia and Storage coefficient S= 1,3 X 10^{-4}

In the Campina sector, another pumping test provided transmissivity values ranging from 140 to 284 m2/day for the deep aquifer (Silva, 1988).

For the upper aquifer no data are available on hydraulic properties, except for some values of hydraulic conductivity determined by Silva (1988). These indicated a very low permeable medium. However, given the evident heterogeneity of the upper detrital unit, probably there are some areas characterized by significantly higher values of that parameter.

Based on 470 flow rate data Almeida et al., 2000, calculates Q1-Q3 ranging from 4.2 to 8 L/s and the maximum flow rate is about 44 L/s.

3.1.7   Climate

The Algarve coast, where the study area is located, has a Mediterranean climate, with two evident seasons, a warm and dry season and a wet season. Temperatures in the summer months are attenuated by the effect of the ocean. The mountains located at north have a protective effect in the winter months, preventing the advance of the continental polar air masses over the region, also called "nortadas" (Nemus, 2002).

According with data recorded at the Patacão station (Direção Regional de Agricultura e Pescas do Algarve (DRAPALG)), located inside the area covered by the Campina de Faro subsystem, the average annual rainfall is about 600 mm. The months of heaviest rainfall go from October to March and those of smaller rainfall go from June to August. The average annual temperature is

17.3°C. The warmest months are July and August with average monthly temperatures of around 24°C and the coldest months are January and February, with around 11°C. Potential evapotranspiration has an average value of about 876 mm/year (Faria et al., 1981, in Stigter, 2005), which largely exceeds precipitation. The actual evapotranspiration was estimated between 75 and 88% of the precipitation, depending on the method of determination (Silva, 1984; Silva, 1988; Stigter et al., 1998; De Bruin, 1999 in Stigter, 2005).
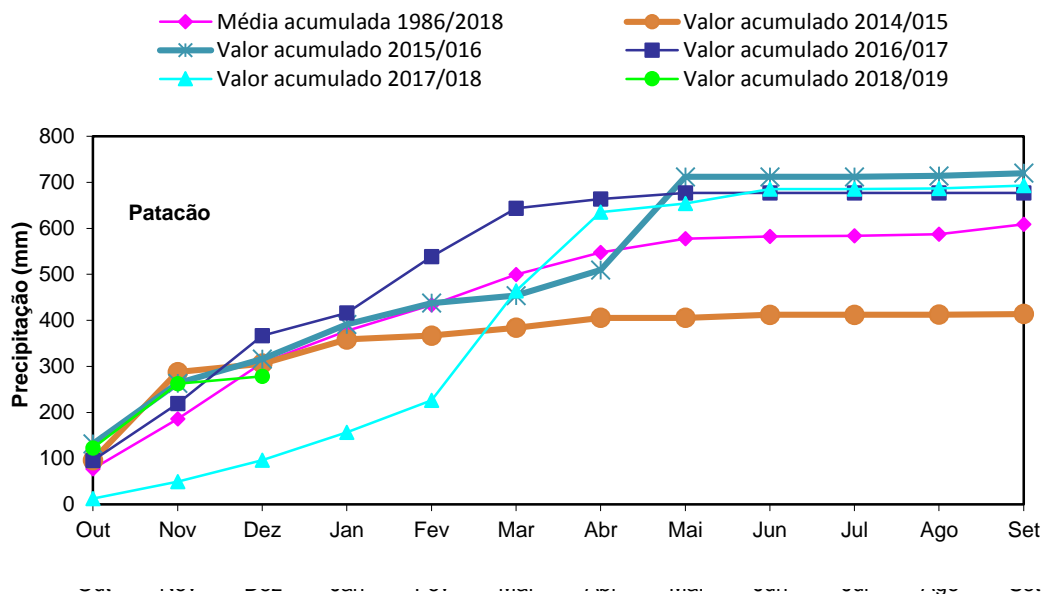
Figure 13. Cumulative annual rainfall (mm, 1986 – 2018). Source: DRAPALG.
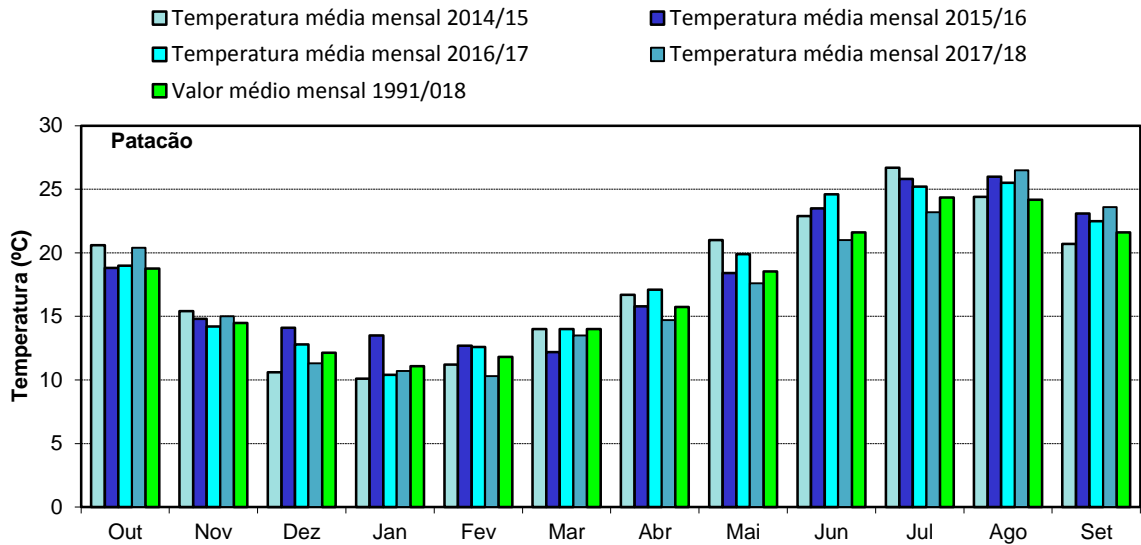
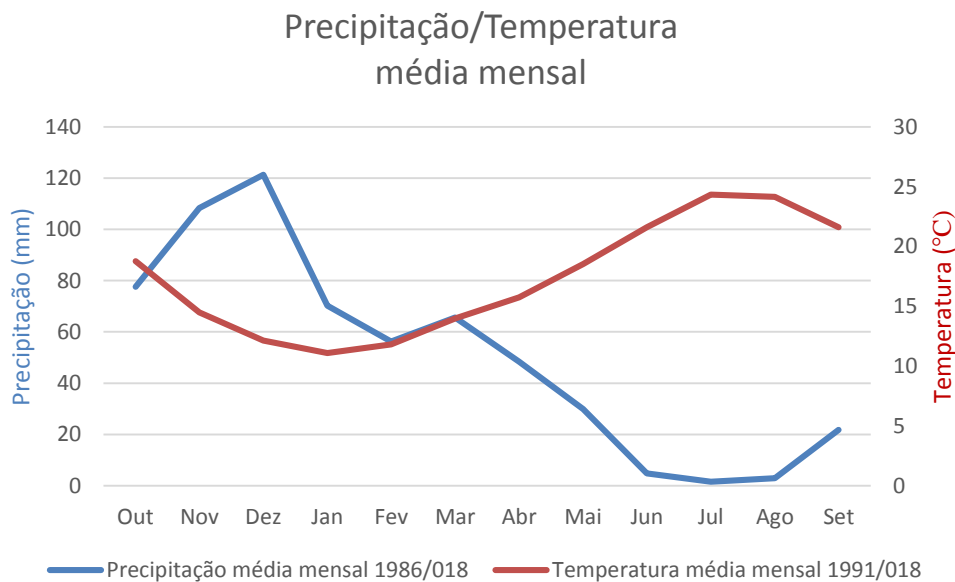*Figure 14. Average seasonal temperature (°C, 1991 – 2018). Source: DRAPALG.*

Figure 15. Average monthly rainfall and temperature (mm 1986/°C 1991 – 2018). Source: DRAPALG.

3.1.8   Land Use

In the current occupation of the soil, agricultural use predominates (mainly citrus groves and watercress production), tourist (golf courses and urbanizations with large garden areas) and pinewoods.
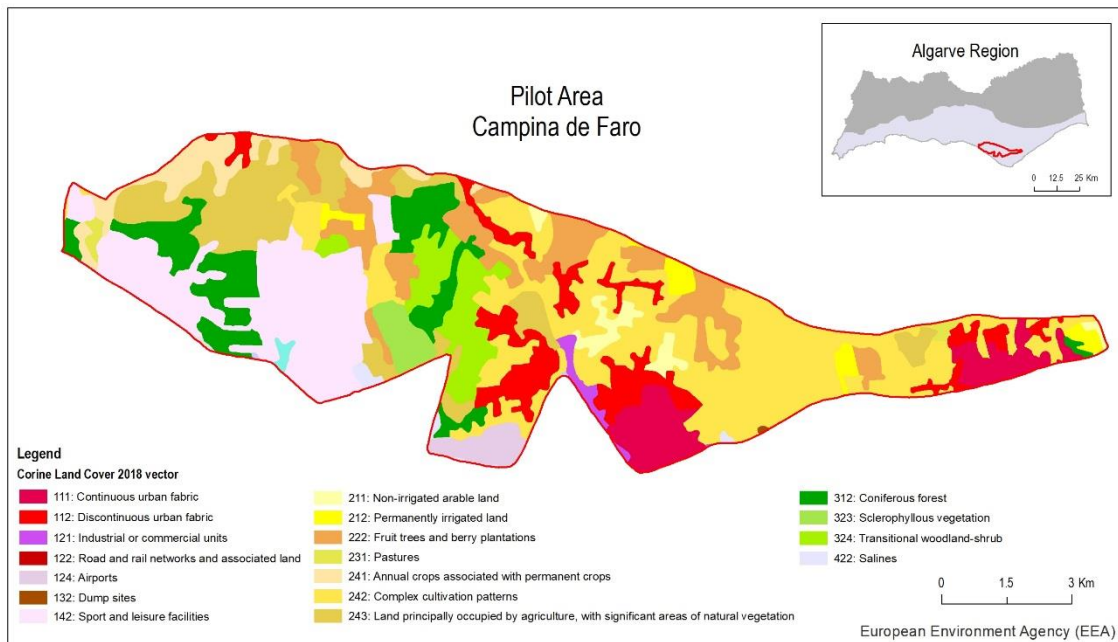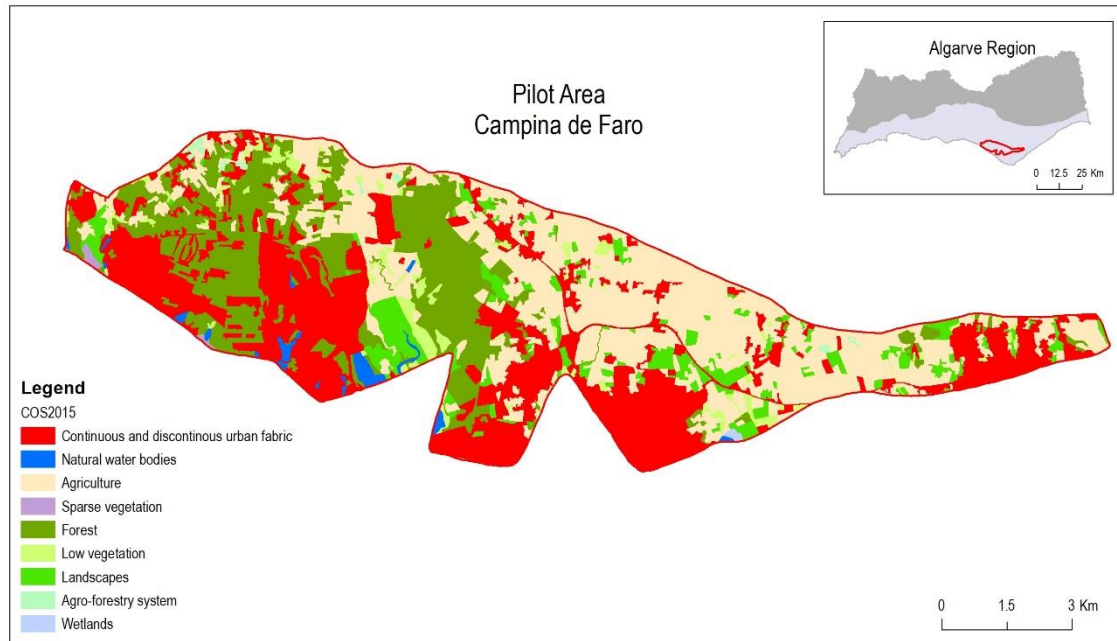

Figure 16. Corine Land Cover 2018. https://land.copernicus.eu/pan-european/corine-land-cover/clc2018?tab=mapview

Figure 17. Land Use Mapping 2015.

https://snig.dgterritorio.gov.pt/rndg/srv/por/catalog.search#/search?anysnig=COS2015&fast=index

3.1.9   Abstractions/irrigation

3.1.9.1   Vale do Lobo subsystem

According to Reis (2018), in the Vale do Lobo subsystem 625 abstractions of groundwater (boreholes and wells) are currently inventoried.

The withdrawal is mainly for irrigation of golf courses and agriculture, namely citrus fruits. The irrigation of private gardens also demand significant groundwater volumes. Private human consumption and swimming pools are uses that consume smaller volumes. Table 1 shows the volumes of private abstractions for uses referred above, according to the volumes authorized in use permits of groundwater resources. Total volume of abstractions from the Vale do Lobo subsystem, giving the above data, is 4.3 hm^3/year.

Table 1 - Volumes of groundwater withdrawals according to the volumes authorized in the use permits of water resources, Reis (2018).

Use	Consumption (hm³/year)
Garden watering	0.48
Agricultural irrigation	1.32
Golf	2.26
Human consumption	0.18
Swimming pools	0.005
Total	**4.25**

As the volumes authorized in the use permits may not often coincide with the volumes actually abstracted, another method was applied to calculate the consumption for agriculture and garden irrigation, based on land use of the orthophoto maps of 2007. After determining the irrigated area, an irrigation volume was attributed, according to the existing crop, for a critical year. Data on human consumption and golfing were obtained from data submitted by the owners. Total volume of water abstractions of the Ludo - Vale do Lobo water body by the referred method is 5.4 hm³/year.

Table 2 - Volumes of groundwater abstraction according to land use and owner's data, Reis (2018)

Use	Consumption (hm³/year)
Garden watering	0.25
Agricultural irrigation	1.87
Golf	3.25
Human consumption	0.024
Total	**5.39**

3.1.9.2   Faro subsystem

According to Reis (2018), in the Faro subsystem 563 abstractions of groundwater are presently inventoried. Currently, there is no exploitation for public supply.

The private consumption is mainly used for agriculture irrigation, namely horticulture and citrus. Giving the authorized volumes in use permits of groundwater resources, abstractions for irrigation are around 1.7 hm³/year.

Another method applied to calculate irrigation consumption was based on land use, using the orthophoto maps of 2007. After the determination of the irrigated area, an irrigation volume was attributed, according to the existing crop, for a critical year. The abstractions obtained for irrigation purposes of Faro sub-system are 5.4 hm³ / year.

The difference among the two calculation methods is significant, being probably the value achieved by the second method closer to reality. The withdrawal obtained by the second method represents about 87% of the average annual recharge in the long term. However, the recharge of this groundwater body is underestimated due the lack of knowledge of depth groundwater transfers from the water bodies at the north. It should be noted that the present-day piezometric levels are high when compared to the time series and show no downward trend.

3.1.10   Water Balance

Evaluation of water inputs for the Vale do Lobo subsystem is carried out through the contribution of the various sources of recharge. The shallow aquifer receives direct recharge from the precipitation, while the Miocene aquifer has the most important source of recharge as indirect recharge from the Jurassic-Cretaceous limestones located at North.

Average annual rainfall in this groundwater body is around 600 mm. Using the recharge rate of 16% (Stigter et al., 2009), a natural recharge value of 3.1 hm³/year is reached (96 mm/year) for the entire area of the Vale do Lobo subsystem (32 km²).

This subsystem is crossed by streams that contribute to its recharge. The most important is the S. Lourenço stream, where a hydrometric station is located upstream of this groundwater body. The existing data series have a very short sampling period and adequate data treatment has not been carried out yet. However, it is estimated that the average recharge of the aquifer from this stream will be about 1.5 hm³/year, so it was considered that the annual average long-term recharge is about 4.6 hm³/year.

In addition to the aforementioned sources of recharge, there is also the deep recharge from the water infiltration in the northern limestones, for which there is no data that allow estimation. Therefore, the average annual recharge value will be higher than the above-referred value.

Campina de Faro subsystem presents the same behaviour of the Vale do Lobo subsystem. In addition to recharge from rainfall (5.2 hm^3/year), the Rio Seco stream is an important source of recharge. Of the Jurassic-Cretaceous limestones in the North, a deep recharge reaches the sandy limestone aquifer mainly through faults and fractures.

Regarding the water outputs from the whole system, in addition to the abstractions mentioned in the previous subchapter, there are also natural discharges, which sustain groundwater dependent ecosystems, such as the Ria Formosa lagoon and the end sectors of the S. Lourenço, Biogal, Rio Seco and Bela-Mandil streams. There is no data to estimate the volumes of these discharges.

Considering the inputs and outputs of the groundwater body, the water balance is then presented in tables 3 and 4.

Table 3 - Water balance for the Vale do Lobo subsystem (hm^3/year), Reis(2018)

Vale do Lobo (subsystem)		
Input		
Natural recharge(hm^3/year)		3.1
Influent recharge from surficial water (hm^3/year)		1,5
Annual average long-term recharge (hm^3/year)		>4.6
Output		
Discharge to aquatic and terrestrial ecosystems (hm^3/year)		?
Abstractions (hm^3/year)	Known (permits)	4.3
	Estimated (land use)	5.4
Water Balance (hm^3/year)	Known (permits)	0.3
	Estimated (land use)	-0,8

Table 4 - Water balance for the Faro subsystem (hm^3/year), Reis(2018)

Campina de Faro (subsystem)		
Input		
Natural recharge(hm^3/year)		5.2
Influent recharge from surficial water (hm^3/year)		1
Annual average long-term recharge (hm^3/year)		>6.2
Output		
Discharge to aquatic and terrestrial ecosystems (hm^3/year)		?
Abstractions (hm^3/year)	Known (permits)	1.7
	Estimated (land use)	5.4
Water Balance (hm^3/year)	Known (permits)	4.5
	Estimated (land use)	1,7

3.2 Climate change challenge

Climate change will not affect the water resources in the whole Europe the same way, depending on various factors, which are mostly related to climate, geology, pedology and land use (Figure 18).
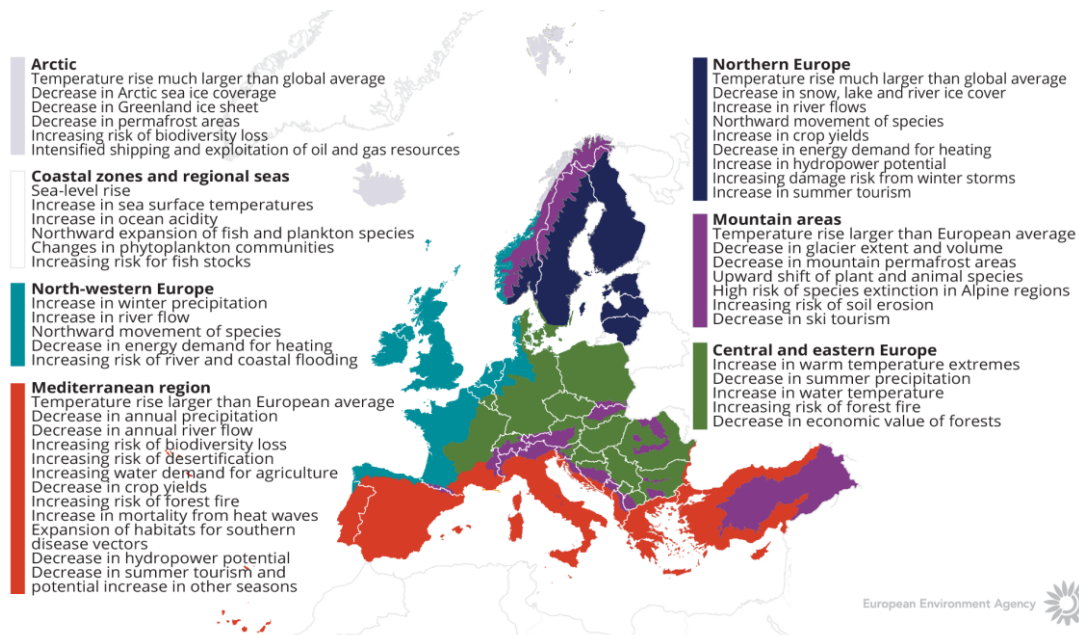

Arctic
Temperature rise much larger than global average
Decrease in Arctic sea ice coverage
Decrease in Greenland ice sheet
Decrease in permafrost areas
Increasing risk of biodiversity loss
Intensified shipping and exploitation of oil and gas resources

Coastal zones and regional seas
Sea-level rise
Increase in sea surface temperatures
Increase in ocean acidity
Northward expansion of fish and plankton species
Changes in phytoplankton communities
Increasing risk for fish stocks

North-western Europe
Increase in winter precipitation
Increase in river flow
Northward movement of species
Decrease in energy demand for heating
Increasing risk of river and coastal flooding

Mediterranean region
Temperature rise larger than European average
Decrease in annual precipitation
Decrease in annual river flow
Increasing risk of biodiversity loss
Increasing risk of desertification
Increasing water demand for agriculture
Decrease in crop yields
Increasing risk of forest fire
Increase in mortality from heat waves
Expansion of habitats for southern disease vectors
Decrease in hydropower potential
Decrease in summer tourism and potential increase in other seasons

Northern Europe
Temperature rise much larger than global average
Decrease in snow, lake and river ice cover
Increase in river flows
Northward movement of species
Increase in crop yields
Decrease in energy demand for heating
Increase in hydropower potential
Increasing damage risk from winter storms
Increase in summer tourism

Mountain areas
Temperature rise larger than European average
Decrease in glacier extent and volume
Decrease in mountain permafrost areas
Upward shift of plant and animal species
High risk of species extinction in Alpine regions
Increasing risk of soil erosion
Decrease in ski tourism

Central and eastern Europe
Increase in warm temperature extremes
Decrease in summer precipitation
Increase in water temperature
Increasing risk of forest fire
Decrease in economic value of forests

European Environment Agency

Figure 18. Observed and projected climate change and impacts for the main biogeographical regions in Europe (European Environmental Agency).

3.2.1 How is the climate expected to change in the area?

In the SIAM, SIAM_II and CLIMAAT_II projects, climate change scenarios for Portugal were analysed using simulations of different climate models. The simulation control of the model with the higher spatial resolution was compared with the observed values, indicating a high level of adherence in the variables mean temperature and precipitation. Together with the results of other models analysed in the referred projects, the following climatic scenario is suggested for the period 2080-2100:

All models in all scenarios predict a significant increase in mean temperature in all regions of Portugal by the end of the 21st century;

An increase in summer maximum temperature on the continent, between 3°C in the coastal zone and 7°C in the inland, together with an increase in the frequency and intensity of heat waves;

All weather indexes related to temperature also show changes in the climate scenario. The increases are large in the number of warm days (maximum over 35°C) and tropical nights

(minimums over 20°C), while reductions in cold weather indexes are expected (eg, frost days or days with minimum temperatures lower than 0°C);

Regarding rainfall, the uncertainty of the future climate is substantially greater. However, almost all the models analysed foresee a reduction of precipitation in Continental Portugal during Spring, Summer and Autumn. One of the climate models foresees reductions in the amount of precipitation in the Continent, that can reach values corresponding to 20% to 40% of the annual precipitation (due to a reduction in the duration of the rainy season), with the largest losses occurring in the southern regions. The regional model, with greater regional disaggregation, points to an increase in precipitation during the winter, due to increases in the number of days of strong precipitation (above 10 mm/day).

In the scope of the climate portal project (http://portaldoclima.pt/) meteorological/climatological data from the IPMA stations (Instituto Português do Mar e da Atmosfera), installed in the District capitals, with records for the study period from 1970 to 2016, were processed to forecast scenarios until the end of the XXIst century.

The model data were obtained using the same methodology adopted in all the processes, and for this validation process, the average value of the 4 points of the matrix around the meteorological/climatological station location was used. The statistics corresponding to the models (modeling history and projections) are calculated from average values of each of the models according to the indicated period (annual, monthly or seasonal).

Data is available for 4 series:

• hist-obs: historical observed (1971-2016)

• hist-mod: historical modeling (1971-2005)

• proj-mod: future projections (2006-2100, divided into two scenarios (RCP 4.5 and RCP 8.5))

Ongoing climate change in Portugal based on IPMA time series data (30 years) and SIAM, SIAM_II and CLIMAAT_II Project Reports, can be summarized as follows:

1) A significant increase in an average of the maximum and minimum temperatures with reduction of thermal amplitude;
2) Increase in the number of "summer days" and "tropical nights", as well as in the annual rate of heat waves;
3) Decrease of cold days and nights and in the number of cold waves;
4) Great irregularity in precipitation but no significant trends (increase or decrease) in the annual average value;
5) An important reduction in the precipitation on the month of March in the whole territory;

6) Smaller but significant reduction in precipitation in February.

The results for the Faro station located in the study area are presented below.

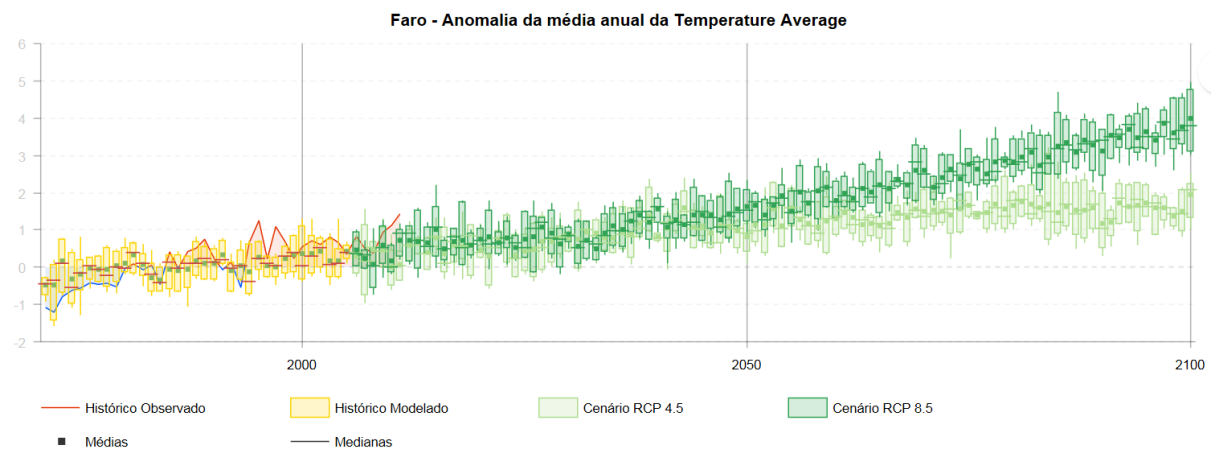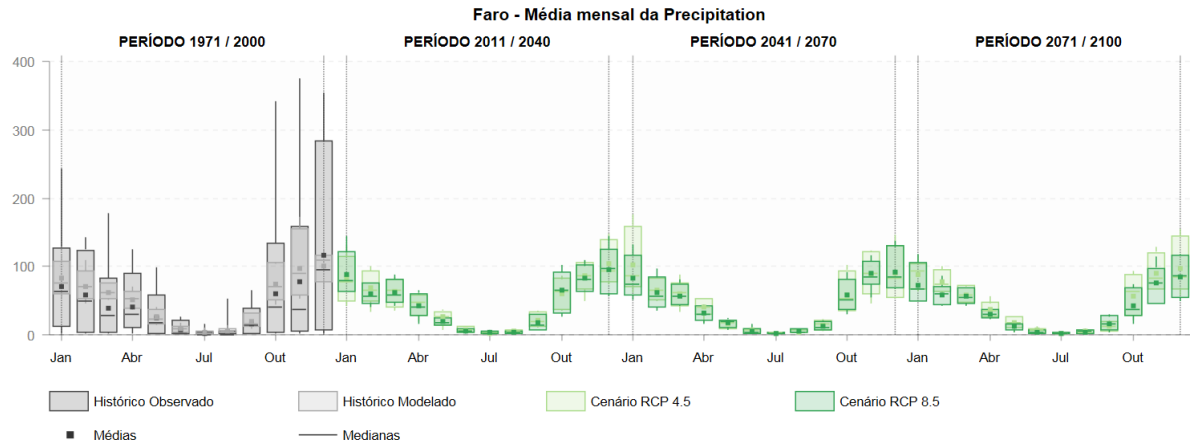## Monthly analysis
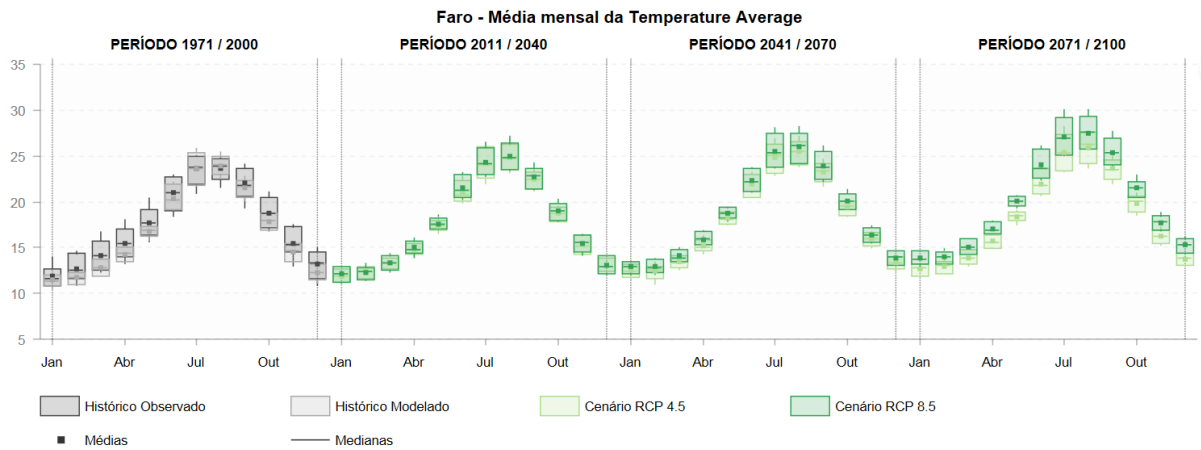
Annual analysis

Figure 19. Temperature Predictions up to 2100 for Faro Station. http://portaldoclima.pt/
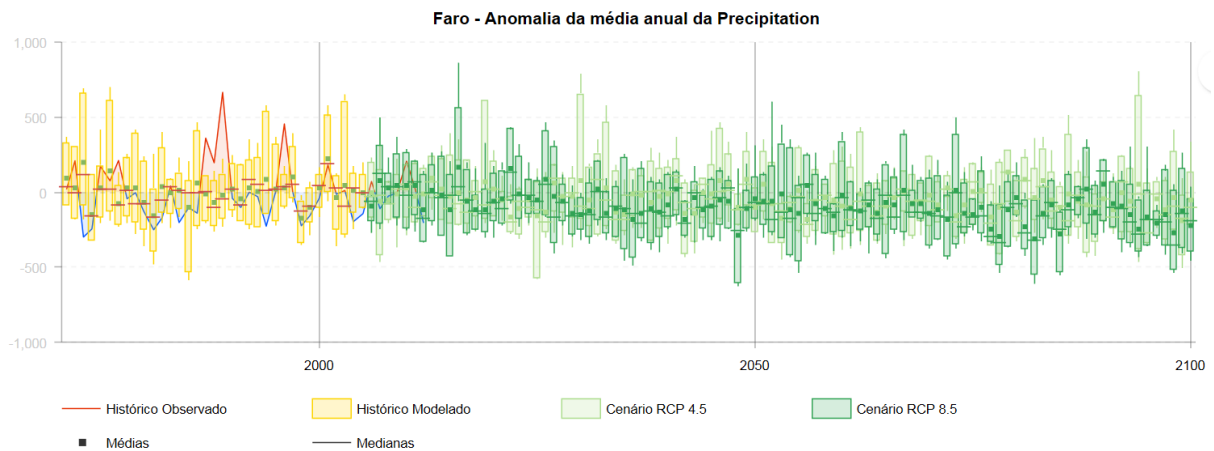
Monthly analysis

Faro - Média mensal da Precipitation

Annual analysis

Faro - Anomalia da média anual da Precipitation

Figure 20. Precipitation Predictions up to 2100 for Faro Station. http://portaldoclima.pt/

3.2.2   What are the challenges related to the expected climate change?

As shown above, the rise of temperature and, consequently, the rise of the potential evapotranspiration (ETp) together with the decrease in annual precipitation will lead to dry soils, decline in average river flow and in water table recharge, as well as potential loss of groundwater resources.

Under these circumstances, the risk of events with potential significant impact will rise, like the increase of the frequency and intensity of droughts and heat waves, rainstorms, especially in winter and floods.

Due to the incidence of these events, other impacts are expected, namely:

1) Forest fires, biodiversity loss and desertification, changes in land use and soil capacities, decrease in crop yields;
2) High risk of groundwater dependent ecosystems, increase in water demand for public supply, industry, and agriculture, decrease in hydropower production;
3) Related with sea-level rise, the rise of waves overtopping on coastal areas, coastal erosion, saline intrusion due to the loss of groundwater resources;
4) Expansion of Habitats for southern disease vectors, dehydration and breathing problems for the elderly and children.

These will lead to the need for implementation of control and mitigation measures, for instance:

1) Reforestation with native species adapted to dry climates, change of practices in agriculture without destruction of the organic matter layer to retain more water in the soil, development of new underground irrigation technologies that avoid evapotranspiration;
2) Increase the water monitoring surveillance, promote rainfall collect, intensification of natural recharge, reuse other sources of water like treated wastewater for irrigation of golf courses, promote hydric use efficiency, installation of hydraulic barriers against seawater intrusion progression with the injection of treated wastewater close to the coast;
3) Creation of infrastructures to sustain floods and promotion of infiltration, removal of human settlements in the flood beds and areas subject to flooding;
4) Rethink the planning of land use in the coastal area, shifting the population and agriculture with greater demand for water from the coast;
5) Energy production from other renewable sources;
6) Health education for climate change.

4 METHODOLOGY

Chemical indicators were applied to get an update overview of seawater intrusion status and the area/volume impacted by SWI was defined. Aquifer system vulnerability was assessed applying Galdit method. A density-dependent flow and transport model was able to simulate future impacts of SWI on the aquifer system considering 3 different recharge reduction scenarios according to climate change predictions in this region.

4.1 Assessment of seawater intrusion status through chemical indicators

Some chemical parameters and relationships between them quickly provide an insight on seawater intrusion status within the aquifer. The concentration and spatial distribution of Cl, Br and Sr, strongly related to seawater, allow us to make a first assessment.

Secondly, ratios like rCl/rBr ~655 for seawater, rCl/rHCO3 = 1-5 for inland waters and 20-50 for seawater, rMg/rCa = 5 for seawater (Custodio and Llamas,1983), have been proved to be useful grouping groundwater samples affected by seawater intrusion. At Campina de Faro, high concentrations of Cl may have evaporites dissolution in addition to seawater intrusion as sources. To distinguish waters affected by each process, the ratios rCl /rHCO3 and rSO4 / rHCO3 were applied.

Thirdly, in the piper diagram the relative proportions of the major ions indicates which process is going on for each groundwater sample. Their spatial distribution allows us defining the affected area and calculate the affected aquifer volume.

In order to get an updated overview of seawater intrusion status, field work was carried out, collecting groundwater samples for physicochemical analysis.

4.2 GALDIT (PT) - Assessment of aquifer vulnerability to seawater intrusion in coastal aquifers

The Galdit index (CHACHADI and LOBOFERREIRA, 2001, 2005) was developed on the assumption that the vulnerability of groundwater to seawater intrusion can be defined as "the sensitivity of groundwater quality to an imposed groundwater pumpage or sea level rise or both in the coastal belt, which is determined by the intrinsic characteristics of the aquifer". To apply the method the bottom of the aquifer(s) must lies below the mean sea level.

The most important mappable factors that control the seawater intrusion were found to be:

• **G**roundwater Occurrence (aquifer type; unconfined, confined and leaky confined).

• **A**quifer Hydraulic Conductivity.

• Height of Groundwater **L**evel above Sea Level.

• **D**istance from the Shore (distance inland perpendicular from shoreline).

• **I**mpact of existing status of seawater intrusion in the area.

• **T**hickness of the aquifer, which is being mapped.

GALDIT Index = (1*G + 3*A + 4*L + 4*D + 1*I + 2*T)/15

The vulnerability of the area to seawater intrusion is assessed based on the magnitude of the GALDIT Index. In a general way, lower the index less vulnerable to seawater intrusion.

Sr. no.	GALDIT-Index Range	VULNERABILITY CLASSES
1	≥ 7.5	Highly vulnerability
2	5 to 7.5	Moderately vulnerability
3	< 5	Low Vulnerability

Height of Groundwater Level above Sea Level and Impact of existing status of seawater intrusion in the area are 2 out of a total of 6 parameters that might vary over time. Thus Galdit's vulnerability mapping remains more or less constant if no significant changes in land use and water abstractions occur.

4.3 Flow and transport model

4.3.1 Model description

A three-dimensional density-coupled flow and transport model for the aquifer system was developed by Hugman, 2016, to provide an insight into local SWI processes. Long-term changes in land use within Vale do Lobo subsystem are unlikely to occur once tourism is well established with several golf courses, resorts and villas. The greatest pressure on the system will be the maintenance of the current abstractions alongside with the reduction of the recharge due to climate change. Based on the forecast of climate change in this area (section 3.2.1), three scenarios of 5%, 10% and 20% of recharge reduction have been simulated to predict the progress of the SWI.

4.3.2 Model set-up

A detailed description of the model set-up can be seen in Hugman, 2016. A summary of the main aspects is presented as follows.

A three-dimensional (3D) geological representation of the three layers (sandy phreatic aquifer, clay aquitard and sandy limestone aquifer) of the CF was created, based on a digital elevation model (DEM), data collected from borehole logs and results from previous geophysical studies. On-shore, the outer limits were extended to include the coastal lagoon and a 500 m offshore extent where the CF connects directly with the Atlantic Ocean. Elevation of the sea-floor was based on detailed bathymetry data.

Mesh generation took into account the location of the geological units, fault-lines, main streams and channels of the lagoon.

Recharge from rainfall was assigned to the top layer, with a uniform value of 17.5% of average annual rainfall. Monthly rainfall data was used to determine recharge for transient simulations. Estimated abstraction rates for the several golf courses active within the aquifer limits were assigned to boreholes inventoried within their respective areas of operation. Abstraction for agriculture was arbitrarily distributed with 25% in the phreatic and the remaining 75% in the semi-confined aquifer. Transient simulations considered constant abstraction for irrigation concentrated from mid-May to mid- September.

Porosity affects the rate of contaminant movement. Therefore, minimum values were assumed, as they represent the worst-case scenario where SWI occurs faster.

Hydrogeological parameter ranges in Hugman, 2016

Layer	Porosity	Specific Yield (S_y)	Hydraulic Conductivity (K) (m.d^{-1})
Phreatic (sand)	0.22-0.38 *	0.20-0.35 *	0.0167-46.32 *
Aquitard (clay)	0.35-0.60 **	0.00-0.05 *	0.005 *
Semi-Confined	0.05-0.40 **	0.001 ***	0.19-3.97 ***

*(Roseiro, 2009); **(Fitts, 2002); ***(Silva (1988)

To determine the potential amount of lateral recharge to the CF, the average annual groundwater budget of the area to the north was estimated (Hugman, 2016). The average water budget from 1983 to 1999, assuming constant irrigation and public water supply demands, results in a excess water budget of 1.0×10^6 m^3.yr^{-1}. With the decrease in abstraction for public water supply from 1999 to 2008, average groundwater available for lateral recharge was estimated at 4.2×10^6 m^3.yr^{-1}.

4.3.3   Model calibration

A detailed description of the model calibration can be seen in Hugman, 2016. A brief summary of the main aspects is presented as follows.

K and b were calibrated by trial-and-error for the period between 2000-2007. This period was chosen for the large amount of continuous time-series. Subsequently storage parameters (Sy Specific Yield and Ss Specific Storage) were calibrated by trial-and-error using transient data for the period between 1990 to 1999. Simulated variation in hydraulic head was compared to measured values from the official monitoring network. Results were validated by extending the simulation to 2007.

4.3.3.1 Observation/Simulated data

Simulated temporal variation in hydraulic head for the 1990-2007 period was compared with observed values for selected piezometers in Figures 21 and 22.

Best fit for simulated hydraulic head was obtained with K values of 5.62 m.d^{-1} (phreatic), 0.0045 m.d^{-1} (aquitard) and 0.95 m.d^{-1} (semi- confined) and with an S_y of 0.05 (phreatic), 0.01 (aquitard) and 0.2 (semi- confined) (Hugman, 2016).

Both phreatic and aquitard layers were not sensitive to Ss, and the default 0.0001 m^{-1} was maintained, whilst the best fit for the semi-confined layer was obtained with a value of 0.0003 m^{-1} (Hugman, 2016).
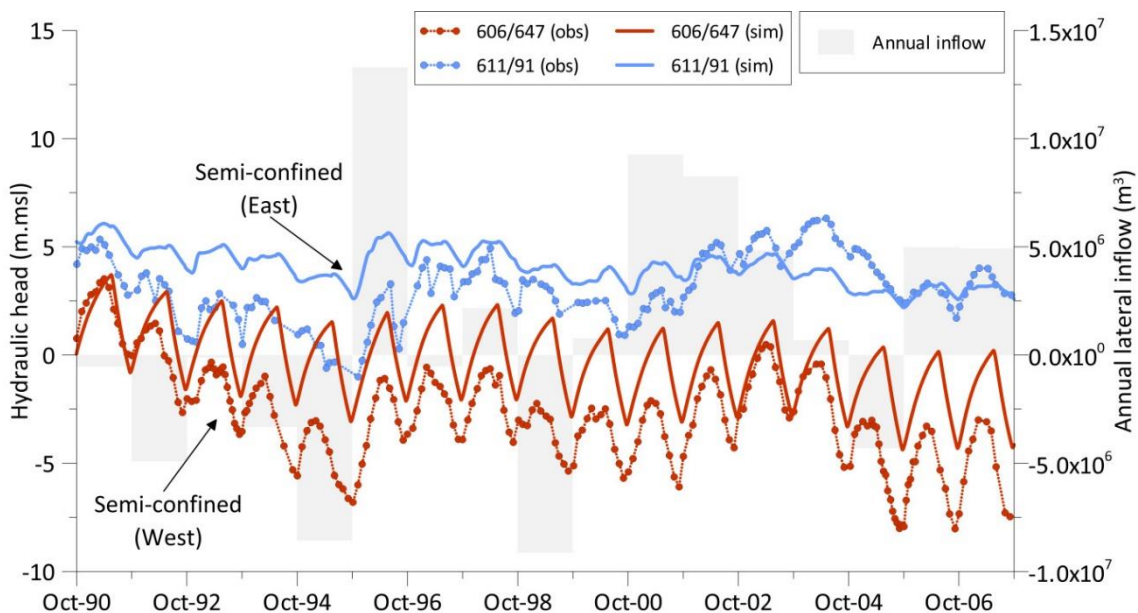
Figure 21. Time-series of simulated and observed hydraulic head between 1990 and 2007 in the east and west sectors of the CF, extracted from Hugman, 2016.
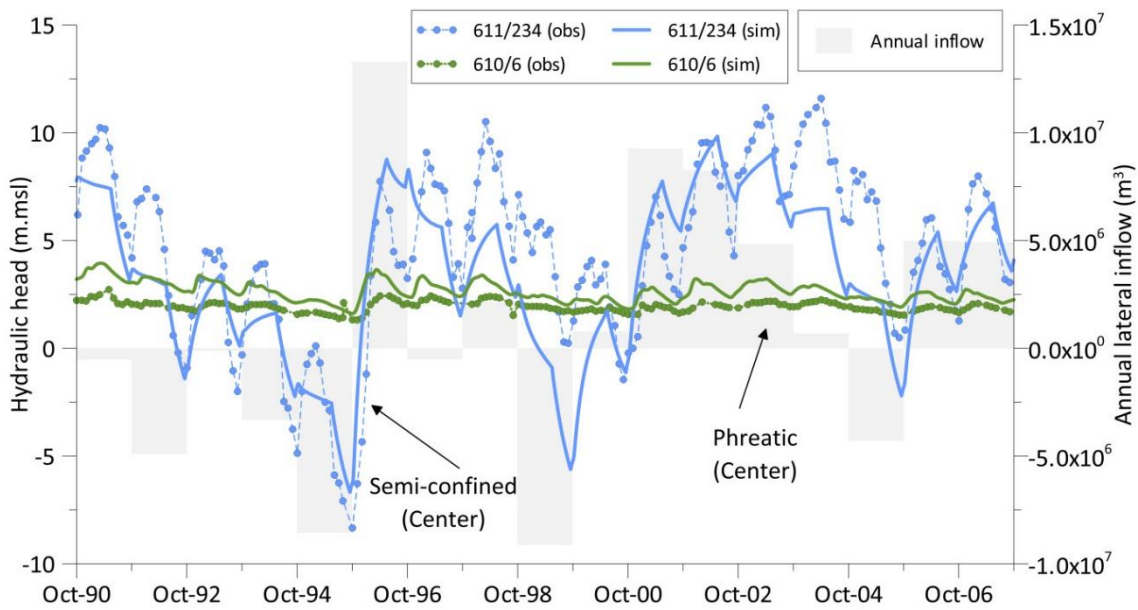
Figure 22. Time-series of simulated and observed hydraulic head between 1990 and 2007 in the central sector of the CF, extracted from Hugman, 2016.

4.3.4   Uncertainty

The good fit between observed and simulated hydraulic heads, for an acceptable range of hydraulic parameters, corroborates the conceptual model of lateral inflow through fractures/faults contributing to groundwater budget of the system (Hugman, 2016). Lateral recharge to the CF is subject to a large amount of uncertainty and calls   for further work in constraining the estimate of lateral inflow, as this is an important part of the CF water budget.

Discharge into aquatic and terrestrial ecosystems is also a source of uncertainty and does not allow greater accuracy in the water balance.

5 RESULTS AND CONCLUSIONS

5.1 Assessment of seawater intrusion status

High Cl, Na, Br, Sr concentrations clearly show the affected area, as can be seen in Figures 23, 24 and 25. Seawater intrusion is ongoing on SW area, in the South of Vale do Lobo subsystem.

High concentrations of Cl and Br are also observed within the aquifer system, in aligned points, coinciding with trending faults W-E and NW-SE. In fact, there are evaporites injected into these faults at a depth of about one hundred meters which are responsible to these high concentrations accompanied by high concentrations of sulphate.

Figure 23. Spatial distribution of Cl concentration(mg/L) on October2019.

Figure 24. Spatial distribution of Sr concentration(mg/L) on October2019.
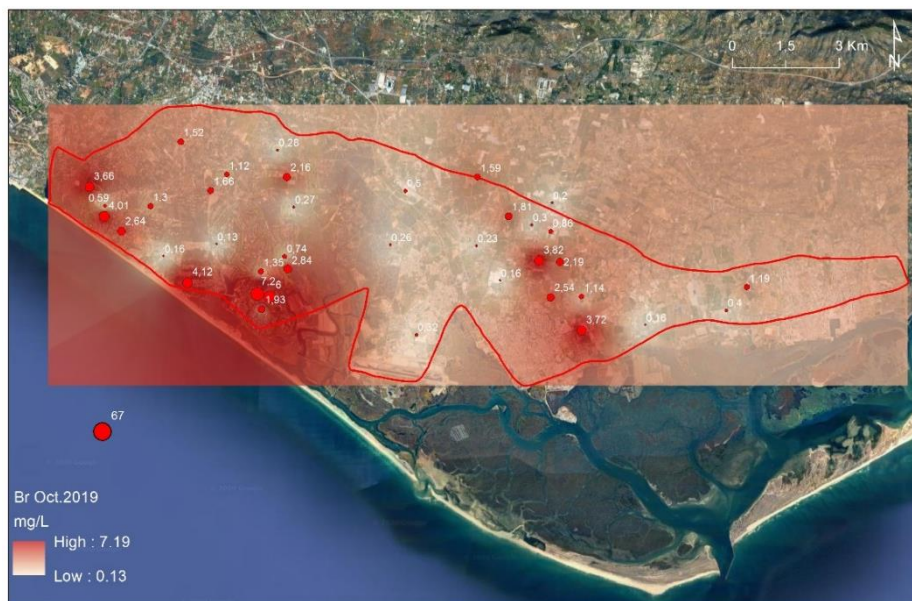
Figure 25. Spatial distribution of Br concentration(mg/L) on October2019.

Ratios such as rCl/rBr, rCl/rHCO3 (Figure 26) and rMg/rCa allowed us to clarify which are the sampling points whose chemical composition results from mixing with seawater.

Additionally, the ratios rCl /rHCO3 and rSO4 / rHCO3 were calculated and projected one against other on a scatter plot in order to discretized groundwaters affected by seawater intrusion from those affected by evaporites dissolution + fertilizers input (Figure 27). Two distinct groups of groundwaters are observed. There is a group of 4 samples showing a strong mixture with seawater, namely San Lorenzo - Green 10 (610/228), San Lorenzo - Hole 2 (610/195), Infraquinta (610/211) and JJW - Formosa Park Hotel (610/256) corresponding to the highest values of rCl / rHCO3 (Figure 26). In the other group, the discretization of groundwater can be seen according to the concentration of sulphates from the dissolution of evaporites, sometimes masked with the input of fertilizers (Figure 27).

rCl / rBr ratio was not very conclusive, highlighting only the sampling point 610/195 of the group of 4 and pointing out also 606/1098 and 606/1019, both located inland, 1600m and 3000 m far from the coast.
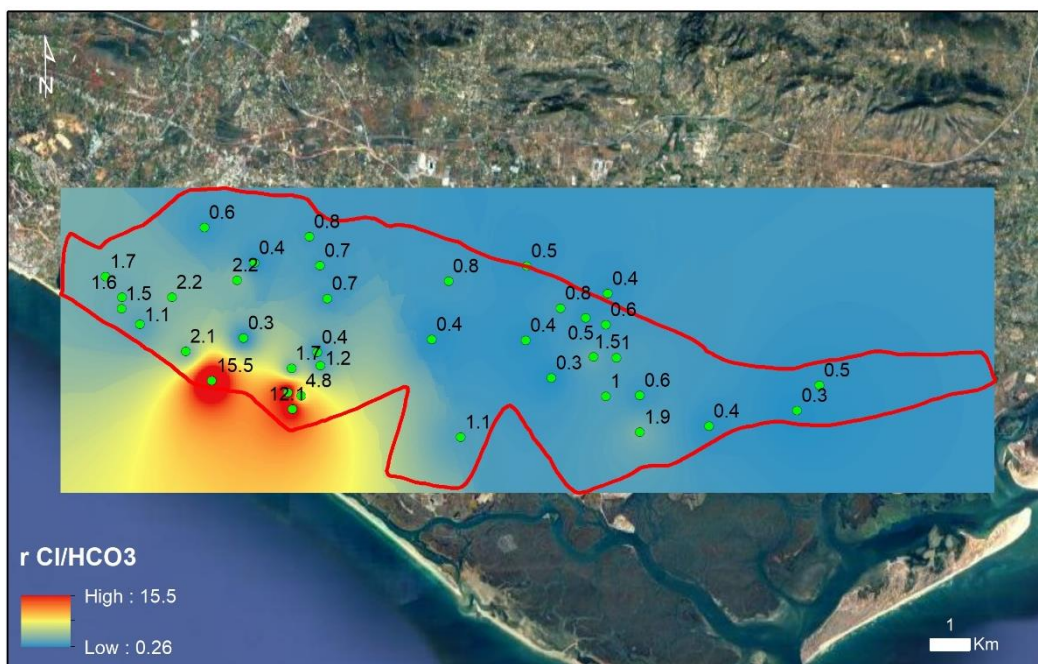
Figure 26. rCl/rHCO3 mapping on October2019. Values >5 indicate seawater intrusion.
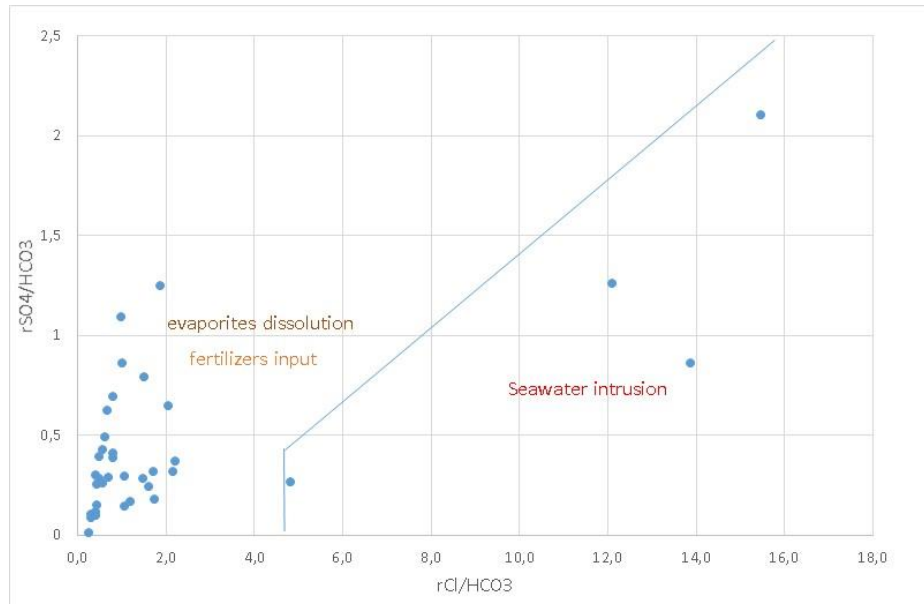
Figure 27.Scatter plot between rCl/rHCO3 and rSO4/rHCO3 on October2019. 2 distinct groups affected by seawater intrusion and evaporites dissolution can be observed.

On the piper diagram, the relative proportions of the major ions indicates which process is going on in each groundwater sample (Appelo and Postma, 1996, Figure 28).
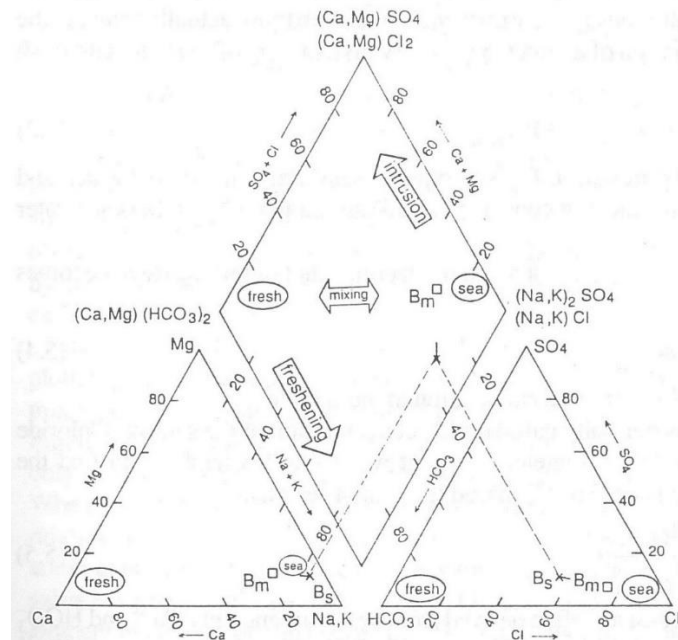
Figure 28. Processes that are taking place in groundwater can be identified with the Piper diagram (Appelo and Postma, 1996)

Plotting groundwater samples from Vale do Lobo subsector (Figure 29, right), it can be seen that the group of 4, mentioned above, are over the intrusion domain.

On Campina de Faro subsector, samples 611/201, 611/242 and 611/260 are aligned with a NW-SE fault and also present high concentrations of Cl, Br, SO4 related with evaporites dissolution (Figure 29, left, orange highlighted).

On the E of the aquifer system, sample 611/261 is very different from the other samples (Figure 29, left, blue highlighted). In fact, this sample is from a borehole that has been without extraction and the groundwater was not renewed prior to sampling, having been collected with a sampler. This sample is not representative and should not be considered in the assessment.

Figure 30 shows how relative proportions of the major ions are spatial distributed on the aquifer system showing an agreement with previous results.
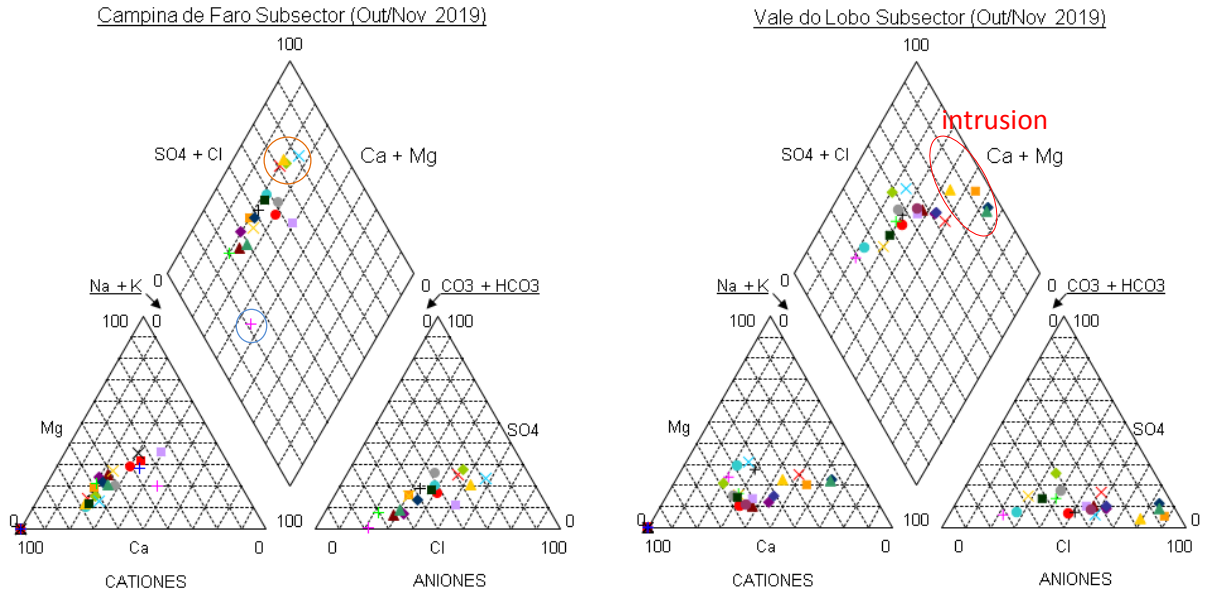
Figure 29. Processes that are taking place in groundwater from Campina de Faro and Vale do Lobo subsectors.

Figure 30. Relative proportions of major ions in the aquifer system.

The overlapping of various indicators allows the delimitation of an area of 4.6 Km² impacted by seawater intrusion, which corresponds to 14.4% of Vale do Lobo subsystem. If we take into account 250 m of aquifer thickness, we can estimate that a volume of $1150 \times 10^6 m^3$ of the aquifer matrix is currently impacted.

5.2   Assessment of aquifer vulnerability to seawater intrusion

The application of the Galdit method to Campina de Faro is shown below in figures 31 to 37.

G (**G**roundwater Occurrence (aquifer type; unconfined, confined and leaky confined)

Indicator	Weight	Indicator Variables	Importance Rating
Groundwater occurrence/Aquifer type	1	Confined Aquifer	10
		Unconfined Aquifer	7.5
		Leaky confined Aquifer	5
		Bounded Aquifer (recharge and/or impervious boundary aligned parallel to the coast)	2.5
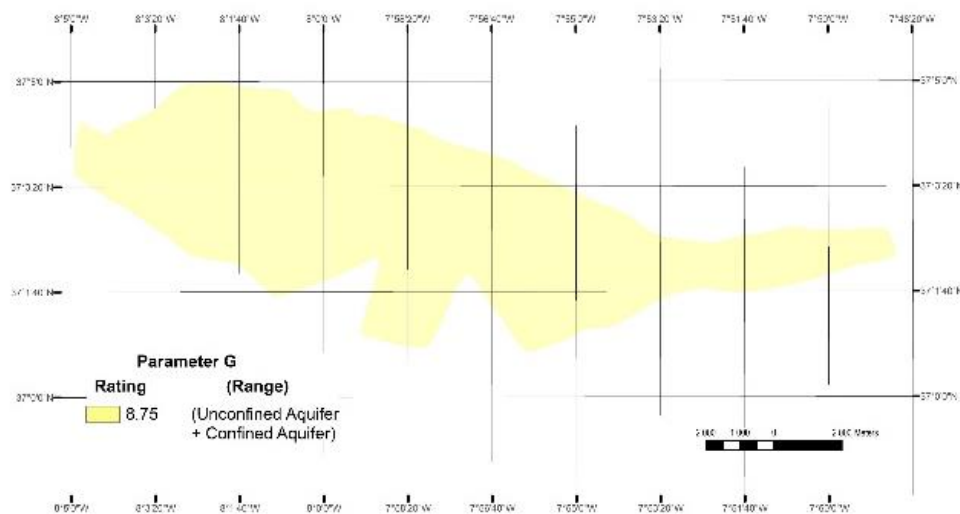
Figure 31. Parameter G - Groundwater occurrence/aquifer type.

A (**A**quifer Hydraulic Conductivity)

Indicator	Weight	Indicator Variables		Importance Rating
		Class	Range	
Aquifer Hydraulic Conductivity (m/day)	3	High	>40	10
		Medium	10-40	7.5
		Low	5-10	5
		Very low	<5	2.5
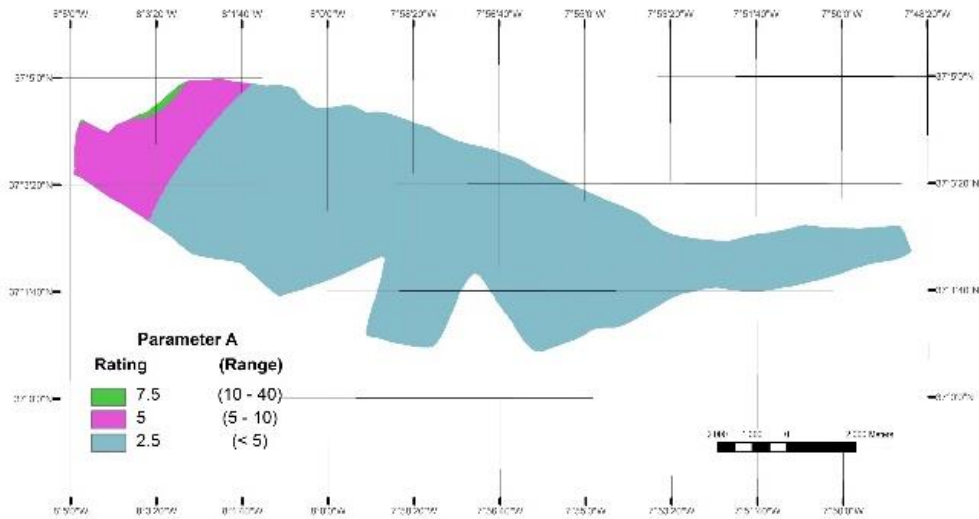
Figure 32. Parameter A - Aquifer Hydraulic Conductivity.

L (Height of Groundwater Level above Sea **L**evel)

Indicator	Weight	Indicator Variables		Importance Rating
		Class	Range	
Height of ground water Level above msl (m)	**4**	High	<1.0	10
		Medium	1.0-1.5	7.5
		Low	1.5-2.0	5
		Very low	>2.0	2.5
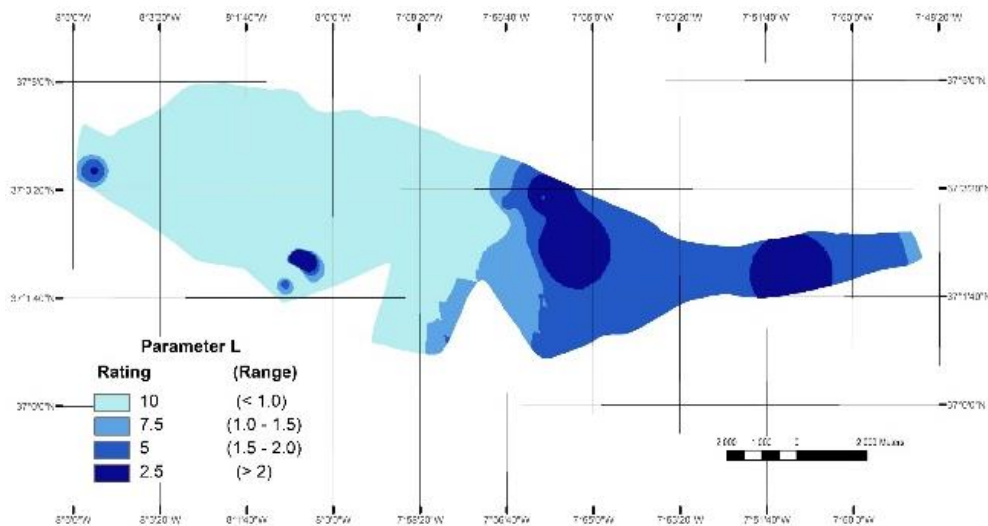
Figure 33. Parameter L - Height of Groundwater Level above Sea Level.

D (**D**istance from the Shore)

Indicator	Weight	Indicator Variables		Importance Rating
		Class	Range	
Distance from shore / High Tide (m)	4	Very small	<500	10
		Small	500-750	7.5
		Medium	750-1000	5
		Far	>1000	2.5
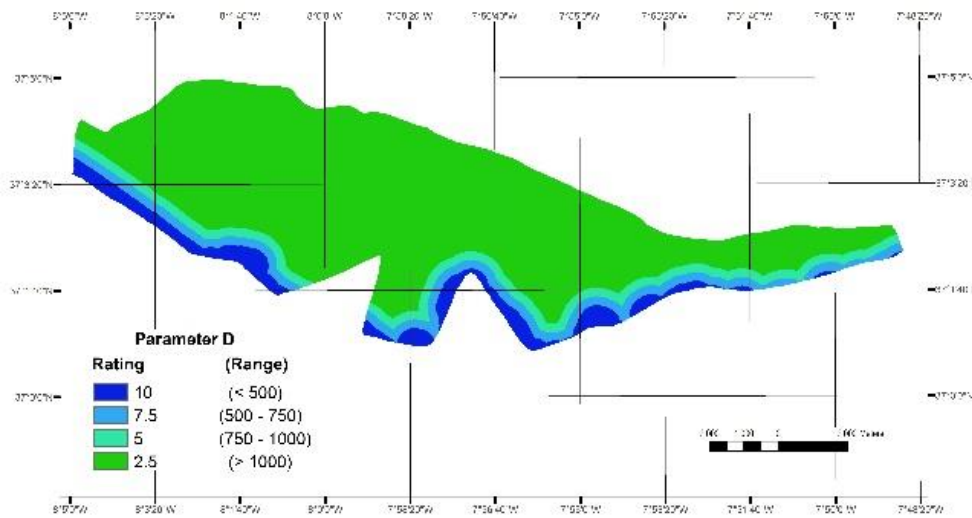
Figure 34. Parameter D - Distance from the Shore.

I (**I**mpact of existing status of seawater intrusion in the area)

Indicator	Weight	Indicator Variables		Importance Rating based on Cl⁻ / [HCO₃⁻¹ + CO₃²⁻], ratio of ground water
		Class	Range of Cl^- / [HCO_3^{-1} + CO_3^{2-}], ratio in epm in ground water	
Impact status of existing seawater intrusion	1	High	>2	10
		Medium	1.5-2.0	7.5
		Low	1-1.5	5
		Very low	<1	2.5
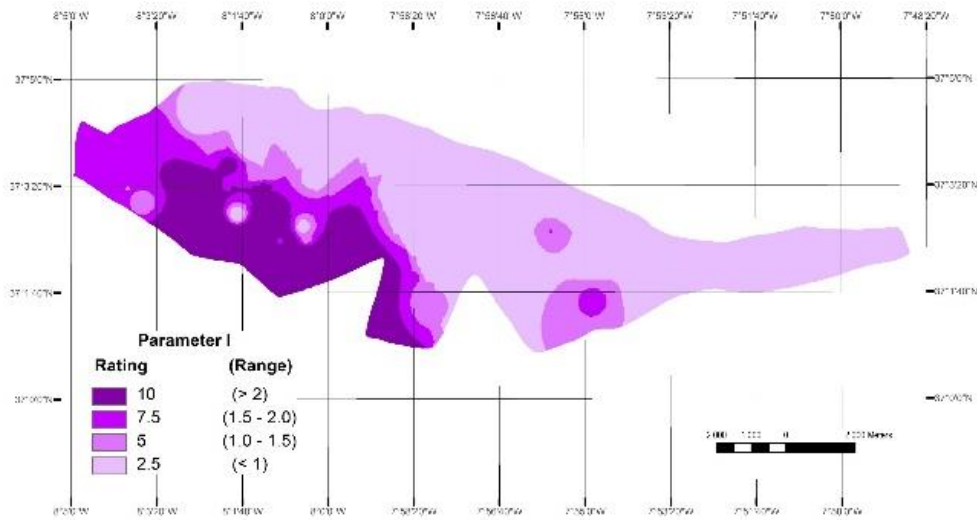
Figure 35. Parameter I - Impact of existing status of seawater intrusion in the area.

T (**T**hickness of the aquifer)

Indicator	Weight	Indicator Variables		Importance Rating based on the saturated aquifer thickness
		Class	Range	
Aquifer thickness (saturated) in metres	2	Large	>10	10
		Medium	7.5-10	7.5
		Small	5-7.5	5
		Very small	<5	2.5
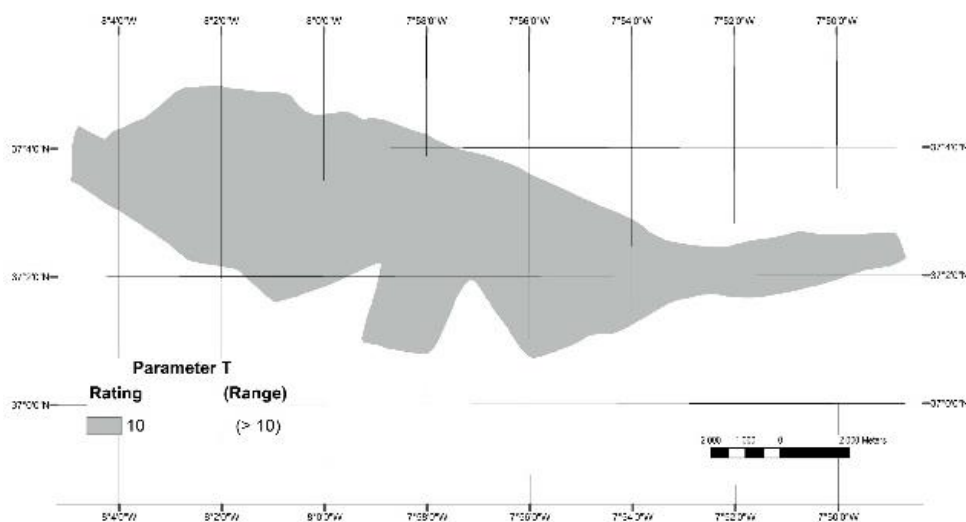
Figure 36. Parameter T - Thickness of the aquifer.

Figure 37. Galdit index.

In figure 37 it can be seen that the results of Galdit Index are very consistent with what is seen in the aquifer system.

The eastern sector of the Campina de Faro is less vulnerable than the western sector of Vale do Lobo. Within the highly vulnerability area of Vale do Lobo we can find the boreholes affected presently by seawater intrusion.

5.3 Scenarios of seawater intrusion impacts due recharge reduction

Due to predicted climate change for the region, reduced rainfall will hit the aquifer in two ways. On the one hand, direct recharge is automatically reduced and, on the other hand, surplus recharge from aquifers systems at the north will also be reduced decreasing the lateral recharge in CF. It is unexpected long-term changes in land use once tourism and agriculture are well established. So, the greatest challenge of the system will be maintaining currently demand alongside with recharge reduction.

Based on the forecast of climate change in this area (section 3.2.1), three scenarios of 5%, 10% and 20% of recharge reduction have been simulated to foresee SWI impact.

Results for the simulation of the density driven flow model are shown on Figure 38 to Figure 45.

4 scenarios have been simulated according to: Scenario A – Business as Usual; Scenario B – reduction of 5% recharge; Scenario C – reduction of 10% recharge; Scenario D – reduction of 20% recharge

The spatial distribution of the seawater-freshwater (SW-FW) fraction for the different scenarios is shown in figures 38 to 41 respectively, for the following slices:

Slice 1 – Top of Plio-Quaternary aquifer;

Slice 4 – Bottom of Plio-Quaternary aquifer;

Slice 6 – Top of Miocene aquifer;

Slice 8 – Upper mid slice of Miocene aquifer;

Slice 12 – Lower mid slice of Miocene aquifer;

Slice 18 – Bottom of Miocene aquifer;

Most of the abstractions in the area occur within slices 8 and 12.

According to the spatial distribution of the SW-FW, it can be seen that scenario A (BAU) results in the scenario with lower extent of area affected by SWI, when compared with the remaining scenarios of recharge decrease. As expected, the area affected by SWI increases when the recharge decreases, which can be seen when comparing the same slice of different scenarios. It can also be observed that for all the scenarios, the mixing zone becomes wider with depth. A particular increase of the width of the mixing zone towards the interior of the aquifer appears to occur at slice 8, which could be due to the effect of the abstractions wells, since most abstractions wells fall within slices 8 and 12. Results obtained suggest that the western sector of this aquifer (Vale do Lobo sector) appears to be more vulnerable to seawater intrusion processes, as can be seen by the larger mixing zone in this sector, when compared to the easternmost sector.

Figure 38. Scenario A – Business as Usual; Fraction SW – FW (1 = fully seawater, 0 = fully freshwater)
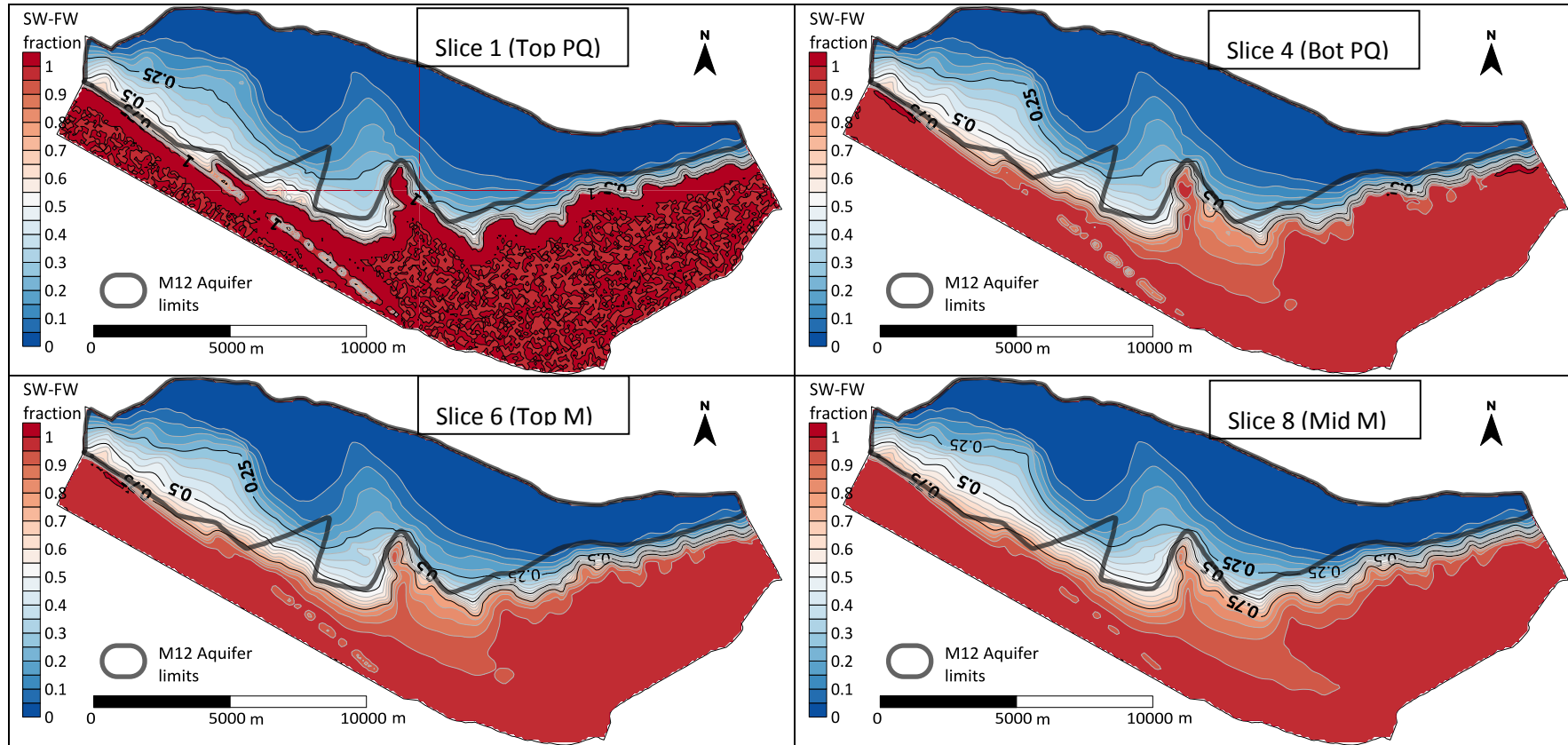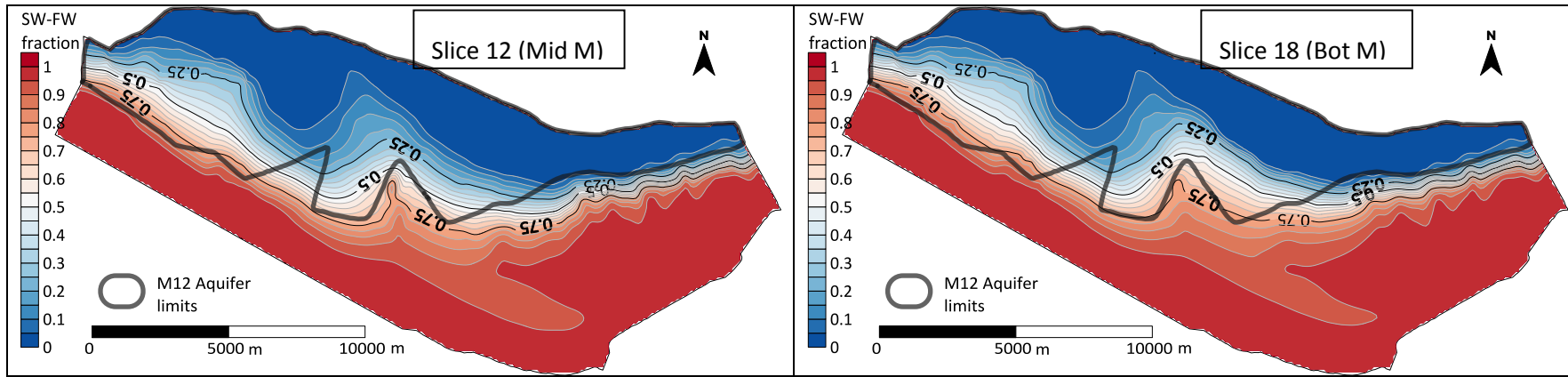
Figure 39.Scenario B – Recharge reduction – 5%; Fraction SW – FW (1 = fully seawater, 0 = fully freshwater)
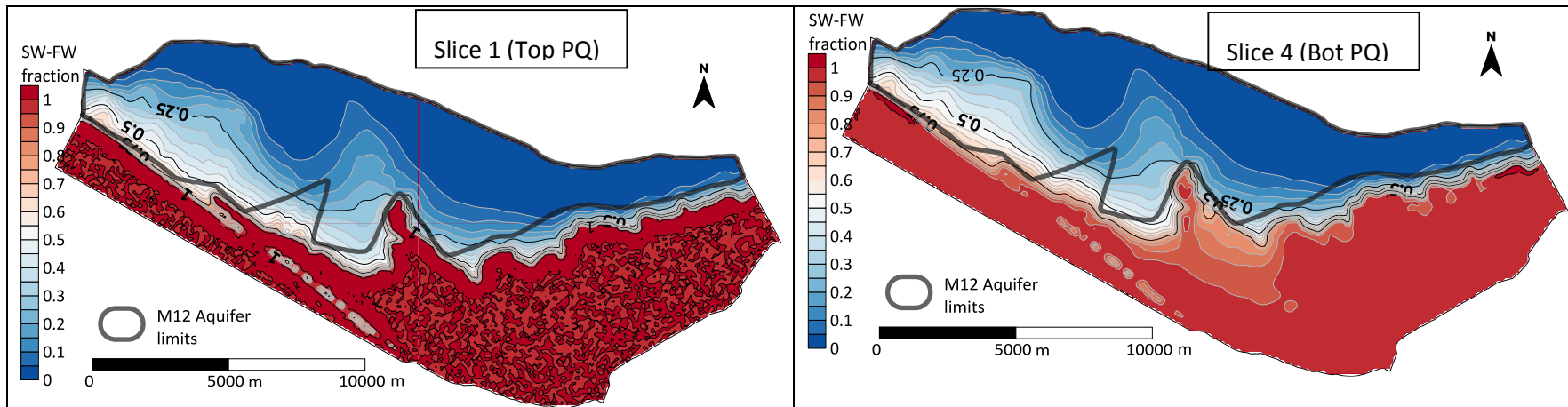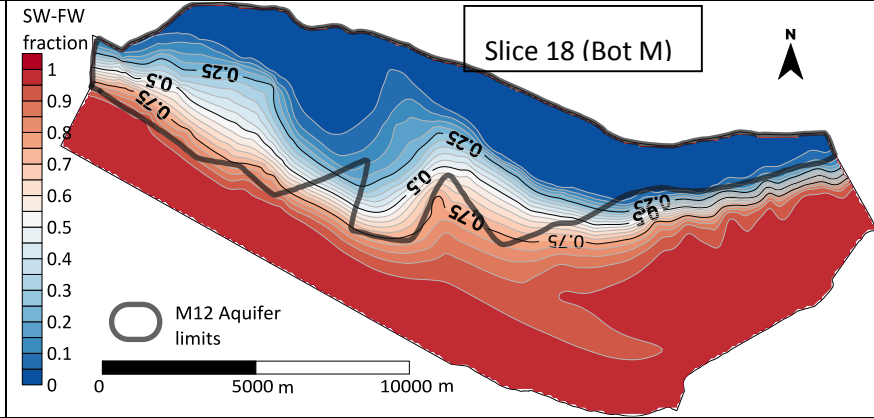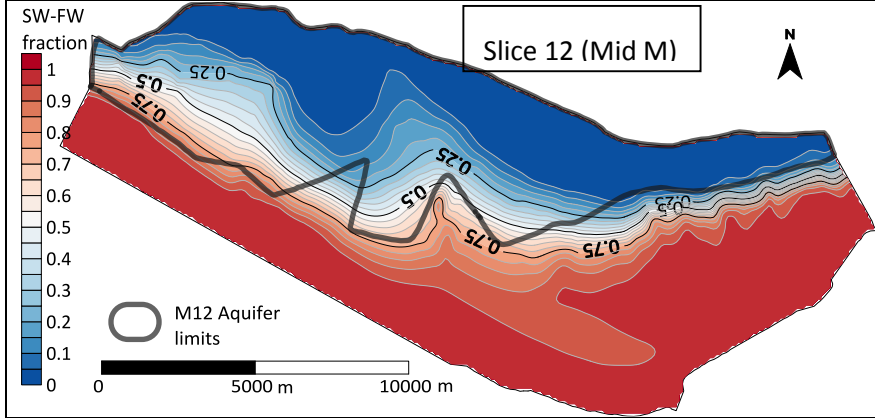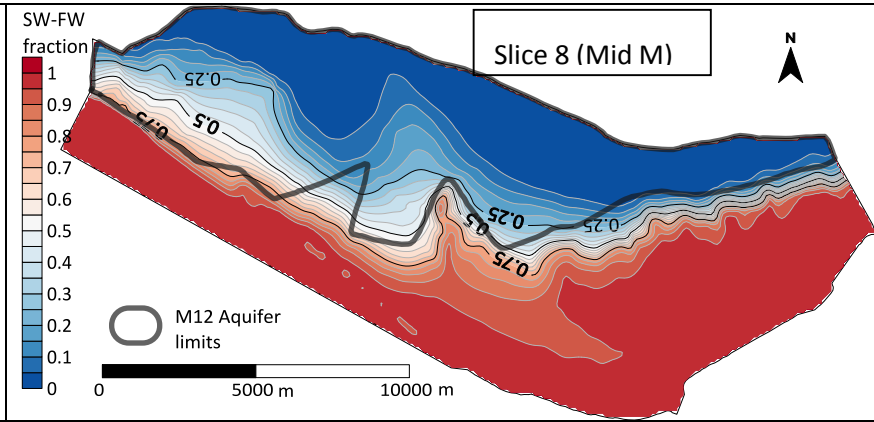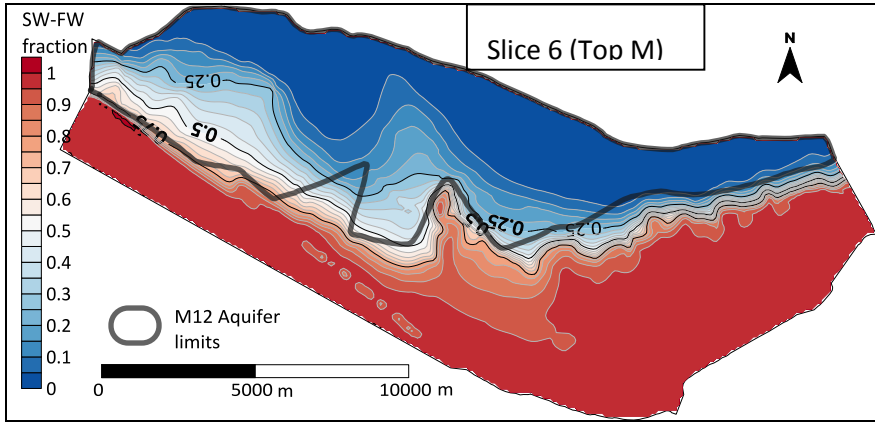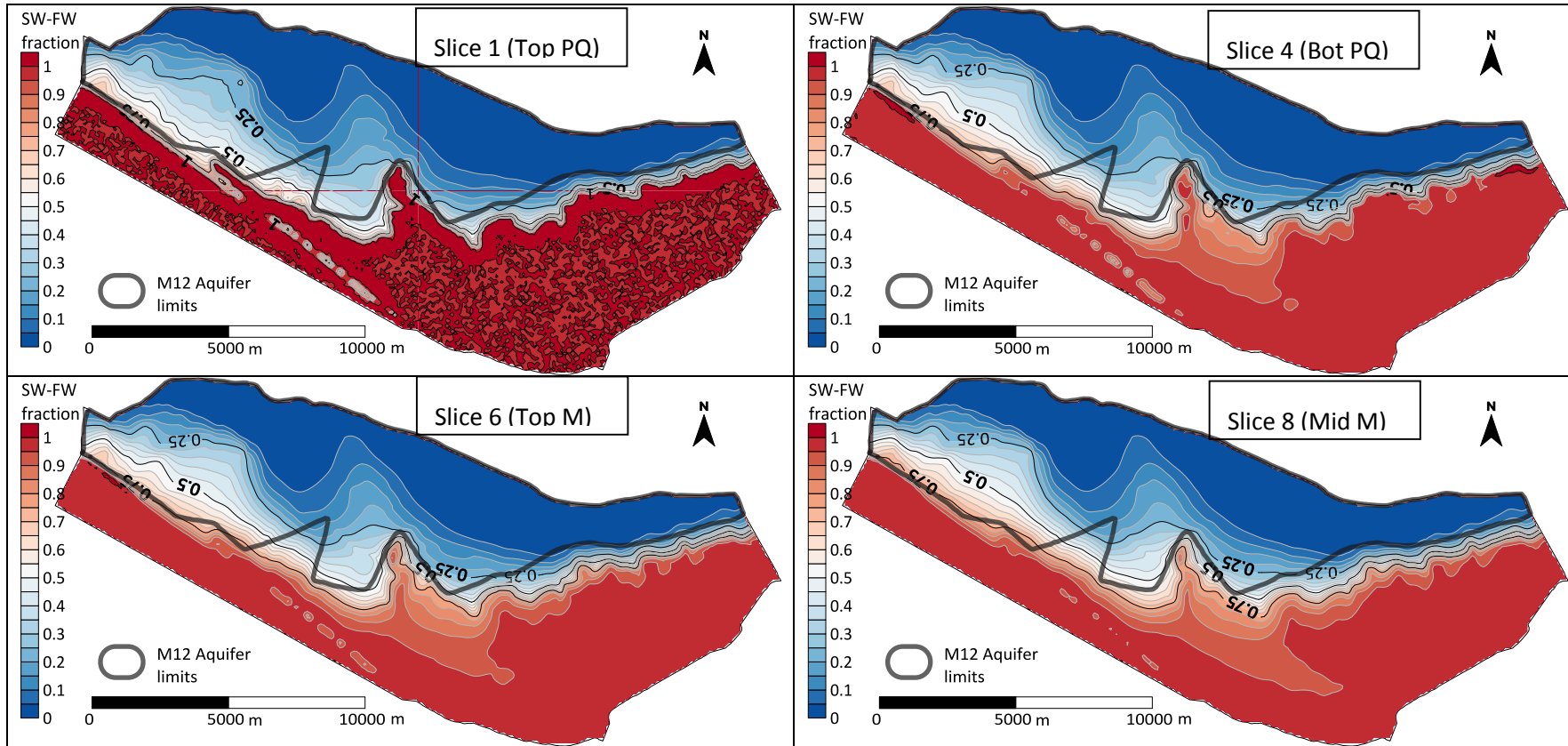
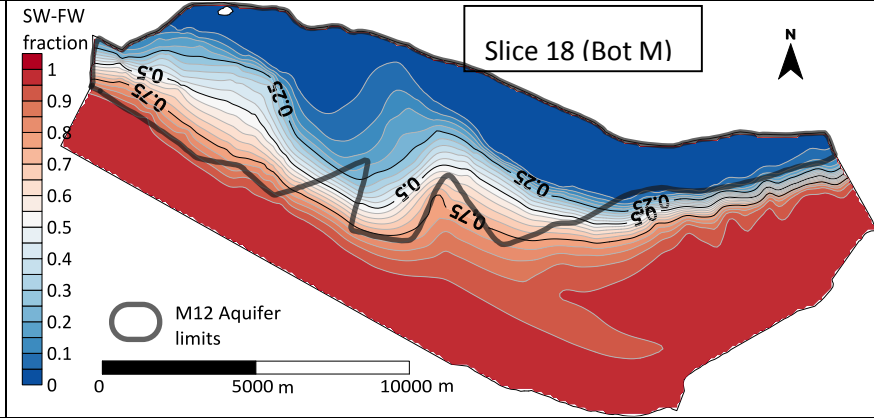*Figure 40. Scenario C – Recharge reduction – 10%; Fraction SW – FW (1 = fully seawater, 0 = fully freshwater)*
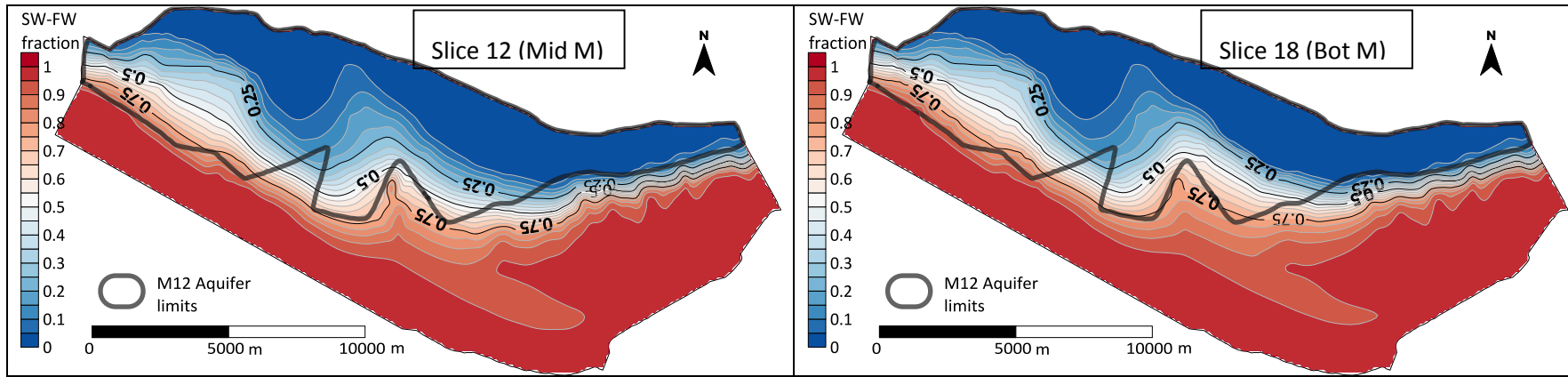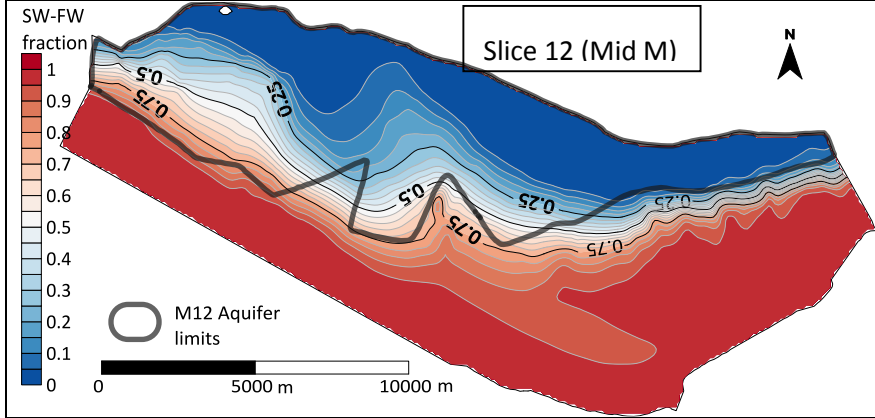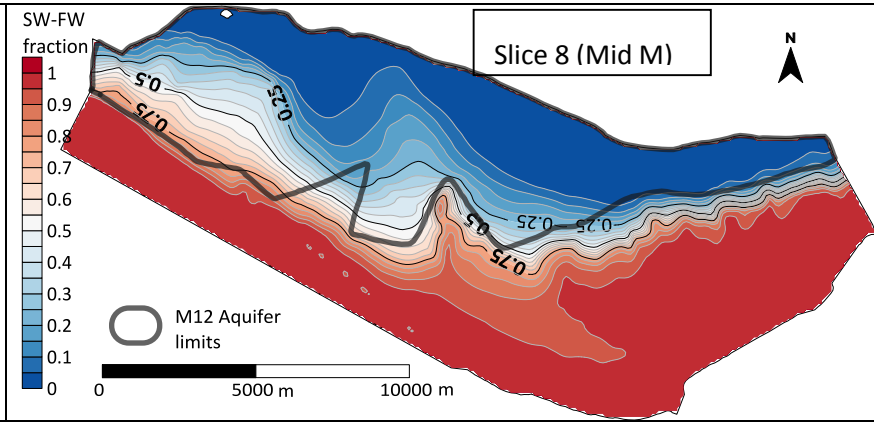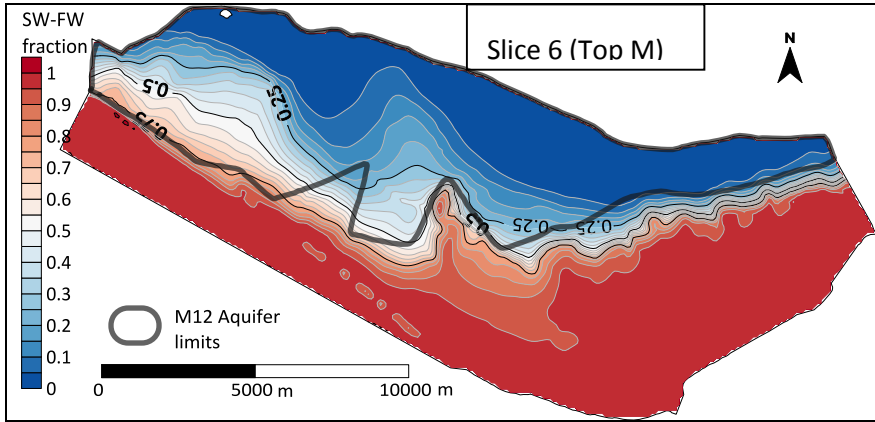
Figure 41. Scenario D – Recharge reduction – 20%; Fraction SW – FW (1 = fully seawater, 0 = fully freshwater)
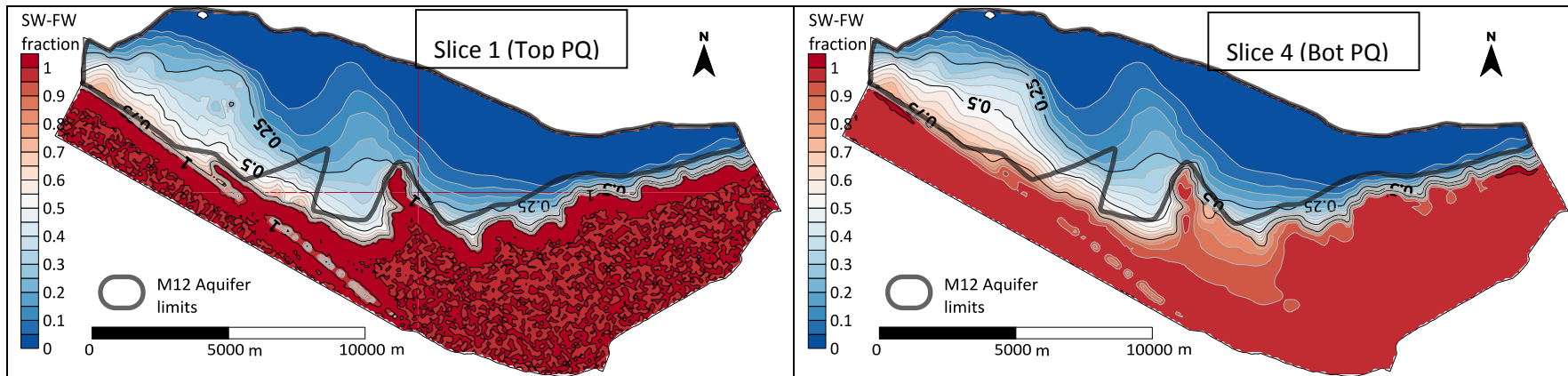
Figures 43 to 44 show two N-S cross sections with the calculated SW-FW fraction in the aquifer system. Two cross sections have been analysed, namely, Vale do Lobo (VL), in the Western sector and Rio Seco (RS) in the Eastern sector of the aquifer system and the location of such cross sections is shown in figure 42. With the analysis of both cross-sections, it becomes clear that the semi-confined Miocene aquifer appears to be more affected by seawater intrusion than the upper Plio-Quaternary aquifer, since a higher extension of this system shows higher SW fraction. As previously mentioned upon the analysis of the SW-FW fraction spatial distribution, the cross sections also show that the Vale do Lobo sector have a higher extent of seawater fraction towards the inside of the aquifer system, in the Miocene aquifer.
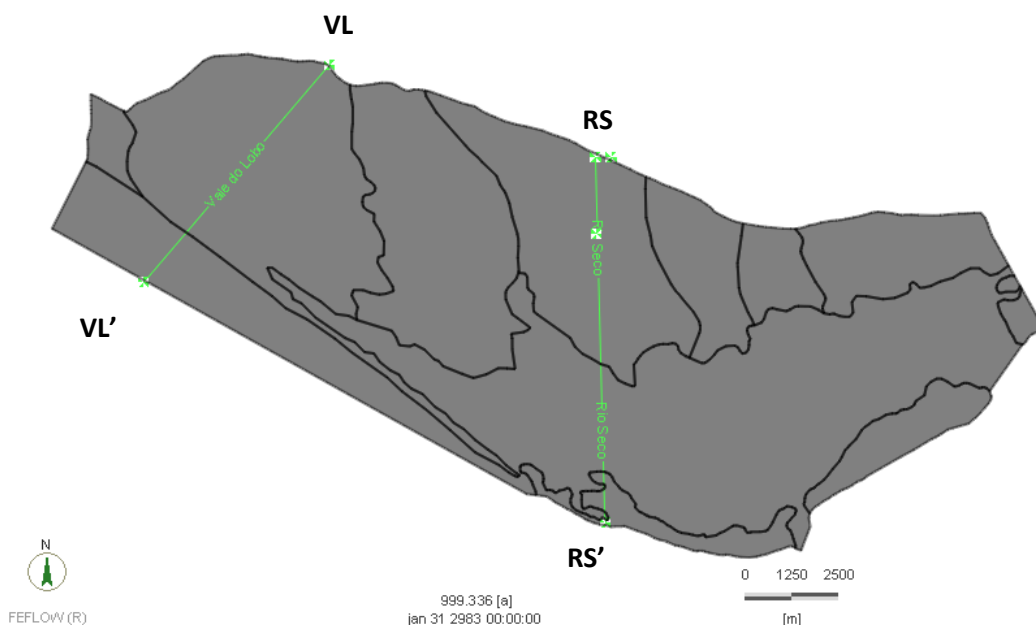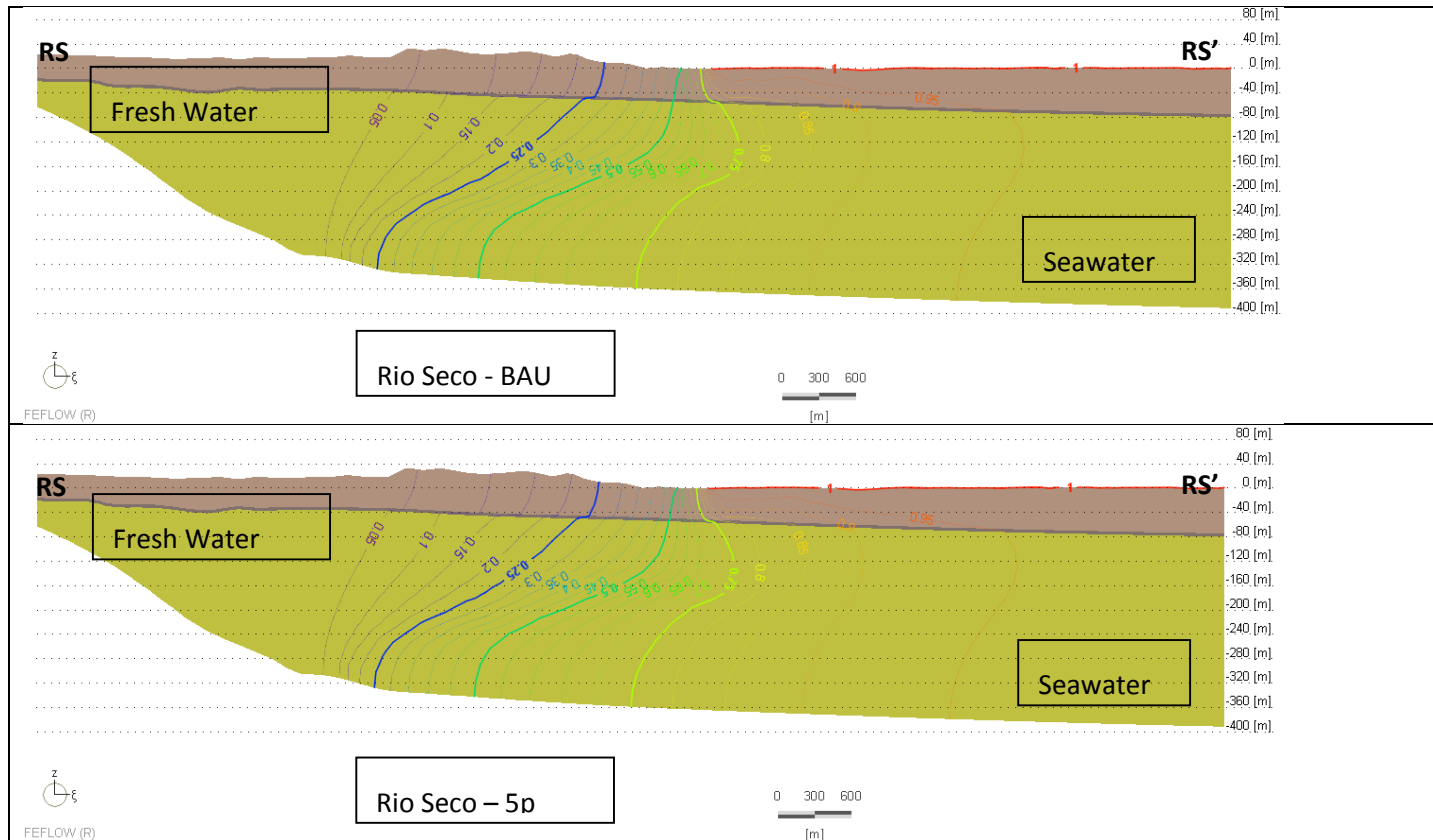

Figure 42. Cross Sections location; VL = Vale do Lobo cross section; RS = Rio Seco cross section

In order to present a better representation of the differences of SW-FW fraction amongst the simulated scenarios, a residual map is presented in figure 45, showing the residual between scenario A (Business As Usual) and the worst case scenario D (decrease of 20% recharge). Within this figure, negative values, represented in red shades, indicates increase of SW fraction, when comparing scenario D to A, i.e., it indicates areas where scenario D shows higher fraction of seawater than scenario A. On the opposite, green shades indicate areas where scenario A shows higher fraction of SW comparing with scenario D.

Figure 43. Rio Seco Cross Section with SW-FW fraction
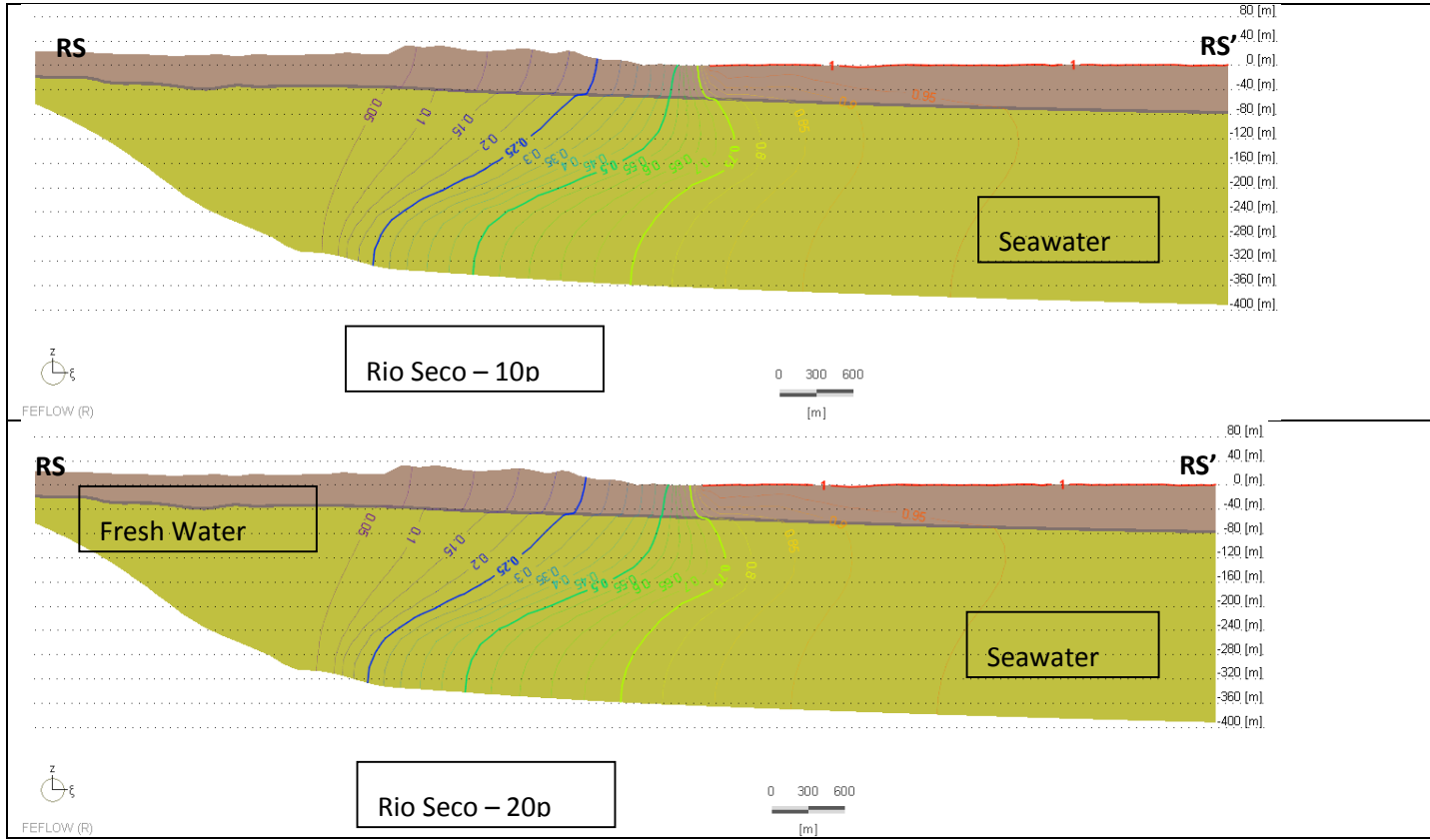
RS   RS'

Seawater

Rio Seco – 10p

0   300   600
[m]

FEFLOW (R)

RS   RS'
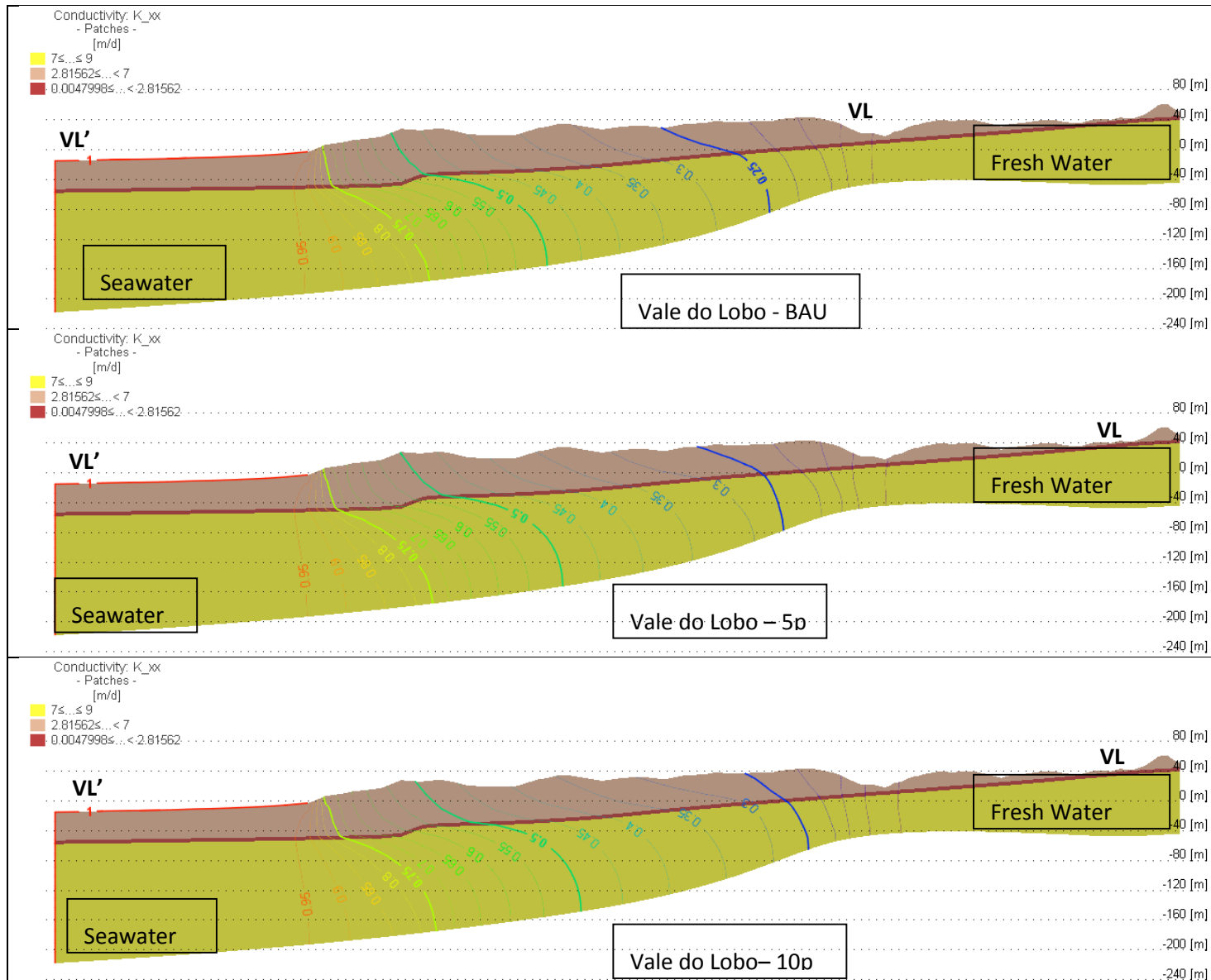
Fresh Water

Seawater

Rio Seco – 20p

0   300   600
[m]

FEFLOW (R)

Figure 44. Vale do Lobo Cross Section with SW-FW fraction
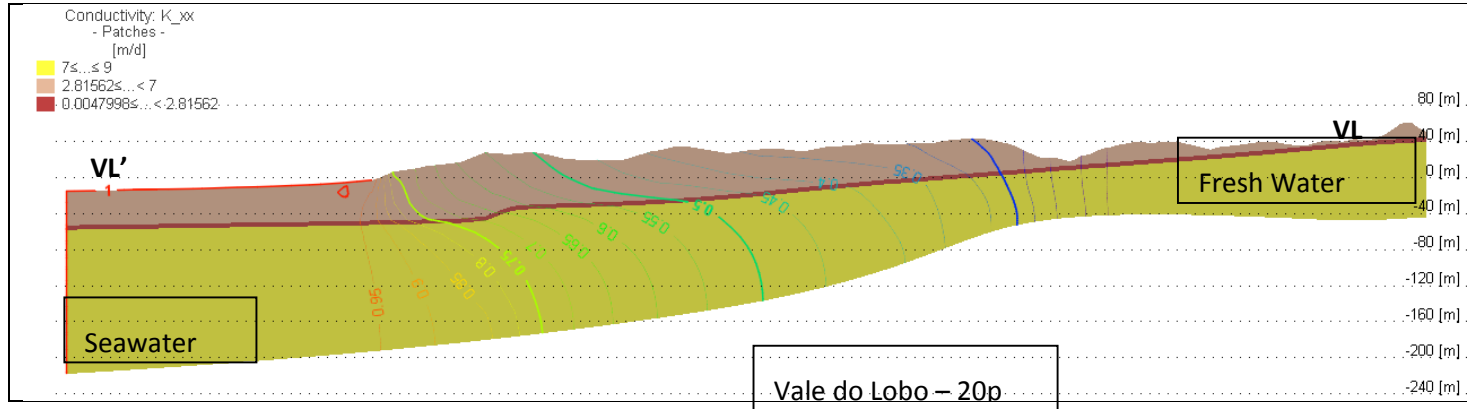
Figure 45. Residuals between Scenario BAU and Scenario D – Decrease of 20% recharge

Residual [BAU] – [D]

Modelled results are as expected, showing that for the entire aquifer limits, SW fraction affected areas are higher for scenario D. There are some areas in which the opposing is happening, i.e., scenario A shows higher 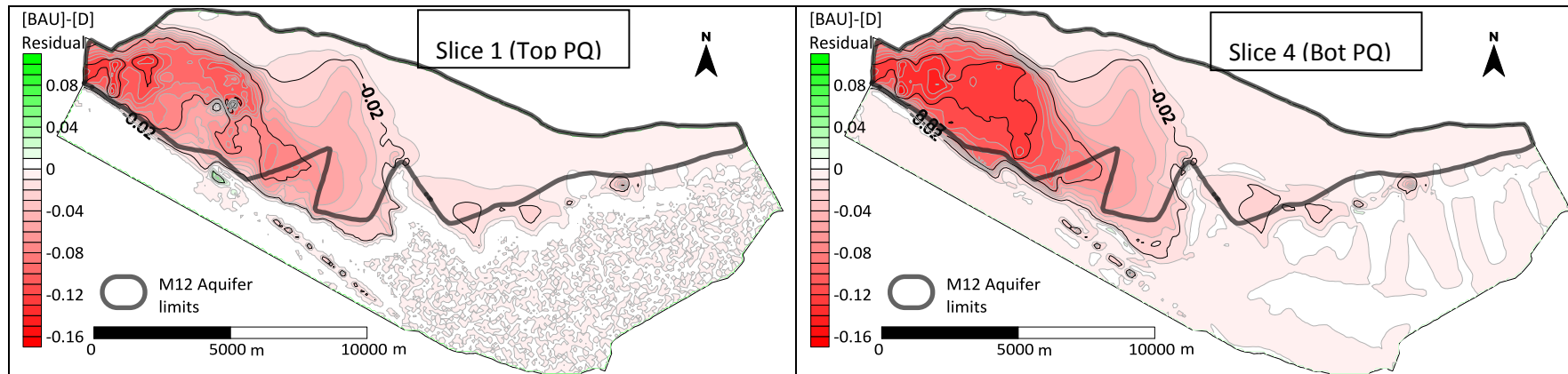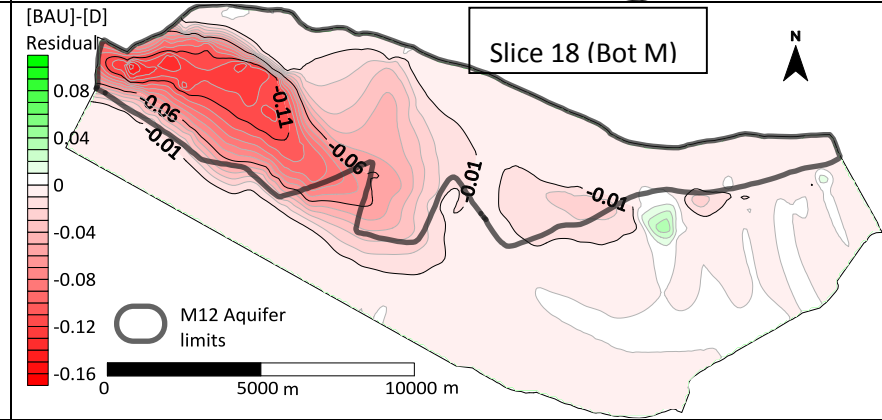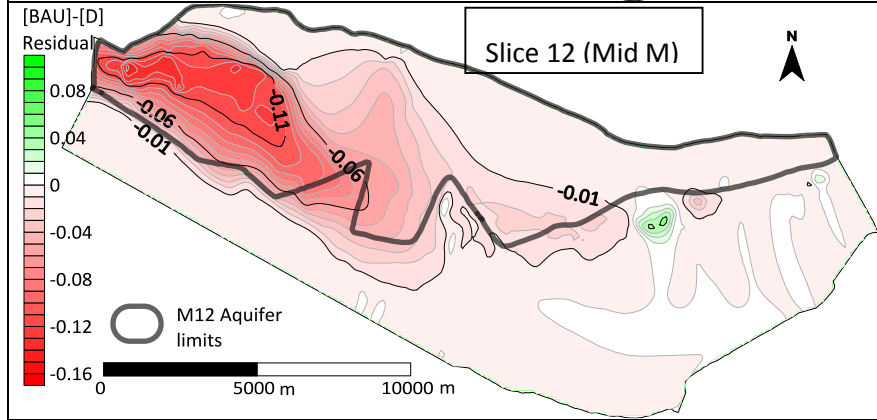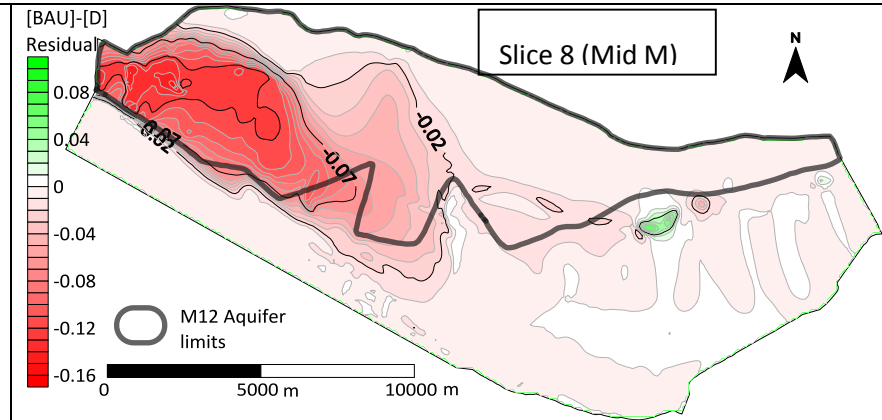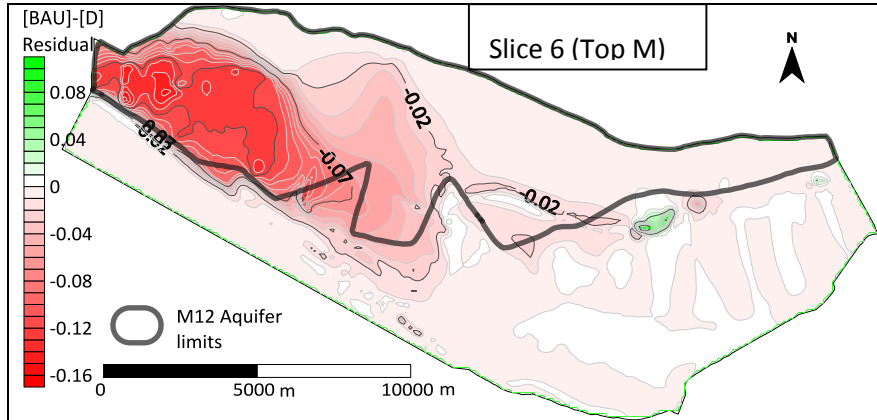fraction of SW, but those happen outside of the aquifer system limits, and could be due to numerical instability of the model. The residual map clearly shows the most affected areas by the decrease in recharge, which, as already suggested before, is in the western sector of Vale do Lobo, while the remaining sector of the aquifer is only mildly affected.

This pedagogical analysis shows in general that the Miocene aquifer of this aquifer system is more affected than the Plio-Quaternary aquifer. This is an expected result since the Miocene aquifer is affected by a higher rate of abstraction. This becomes more evident in the western sector of the aquifer, the Vale do Lobo sector, which is subject to a higher and more concentrated water abstraction, hence being more vulnerable to seawater intrusion processes.

5.4   Conclusions

A good results agreement can be seen among major ions (Cl, Na, Br, Sr) spatial distribution, whose high concentrations has seawater as source, the rising trend in Cl time series, ratio rCl/rBr ~655 and the ongoing processes as showed by piper diagram. As high concentrations of Cl may have evaporites dissolution in addition to seawater intrusion as sources, ratios rCl /rHCO3 and rSO4 / rHCO3 were applied to distinguish waters affected by each process.

Time series of piezometric levels and chemical parameters showed that average piezometric surface of the western sector for deep aquifer has been below sea level since 1980s and Cl concentration increasing has started in 2005.

The joint of several data allows the delimitation of an area of 4.6 Km^2 currently impacted by seawater intrusion, which corresponds of about 14.4% of Vale do Lobo subsystem (Figure 46).

The highest vulnerability areas accessed by Galdit method also contain the above impacted area.

Figure 46. Area currently affected by seawater intrusion in Vale do Lobo subsystem.

Although the uncertainty of the Water balance, it can be seen that groundwater removed from the CF for human use is almost equal to total estimated recharge, placing all the system at risk of SWI. The evidence of SWI in the western sector confirms that is currently overexploited in an un-sustainable way. Groundwater dependent ecosystems, especially those located at streams end section, are seriously threatened.

Due reduction of recharge foreseen by Climate Change, simulations show that Miocene deep aquifer is more affected by SWI than the Plio-Quaternary phreatic aquifer, an expected result since the deep aquifer is affected by a higher rate of abstraction. This becomes more evident in the western sector of the aquifer (Vale do Lobo sector), which is subject to a higher and more concentrated water abstraction, hence being more vulnerable to seawater intrusion processes.

Adequate management measures and changes in water use practices are   needed to counteract SWI. Among other measures to be evaluated, the following are suggested:

1) Reuse other sources of water like treated wastewater for irrigation of golf courses and installation of hydraulic barriers against seawater intrusion with the injection of treated wastewater close to the coast;

2) Intensification of natural recharge through private systems of rain water collection from the roofs and injection into boreholes or wells; replacement of waterproofed areas by

wooden decks to promote water infiltration; Increase the water monitoring surveillance;

3) Reforestation with native species adapted to dry climates, change of practices in agriculture without destruction of the organic matter layer to retain more water in the soil, development of new underground irrigation technologies that avoid evapotranspiration;

4) Rethink the planning of land use in the coastal area shifting agriculture with greater water demand from the coast;

5) Education for climate change promoting hydric use efficiency.

6 REFERENCES

Almeida, C., Mendonça, J. J. L., Jesus, M. R., Gomes, A. J., 2000. Sistemas Aquíferos de Portugal Continental. Vol. III. CGUL e Instituto da Água. DOI: 10.13140/RG.2.1.2036.6163.

Almeida, C., Silva, M. L. (1987) - Incidence of Agriculture on Water Quality at Campina de Faro (South Portugal), IV Simposio de Hidrogeología. Palma de Maiorca. Hidrogeología y Recursos Hídricos (XII). Ed. Ass. Esp. Hidrología Subterránea, pp. 249-257.

Appelo, C.A.J. and Postma, D. (1996). Geochemistry, Groundwater & Pollution. Balkema, Rotterdam.

Costa, F. E., Brites, J. A., Pedrosa, M. Y., Silva, A. V. (1985) - Carta Hidrogeológica da Orla Algarvia, esc. 1:100 000. Notícia Explicativa. Serviços Geológicos de Portugal, Lisboa.

Chachadi A.G. & Lobo-Ferreira, J.P. (2001), Sea water intrusion vulnerability mapping of aquifers isung GALDIT method. Proc. Workshop on modeling in hydrogeology, Anna University, Chennai, pp.143-156, and in COASTIN A Coastal Policy Research Newsletter, Number 4, March 2001. New Delhi, TERI, pp. 7-9, (cf. http://www.teriin.org/teri-wr/coastin/newslett/coastin4.pdf).

Chachadi A.G & Lobo-Ferreira, J.P (2005), Assessing aquifer vulnerability to sea-water intrusion using GALDIT method: Part 2 – GALDIT Indicator Descriptions. IAHS and LNEC, Proceedings of the 4th The Fourth Inter Celtic Colloquium on Hydrology and Management of Water Resources, held at Universidade do Minho, Guimarães, Portugal, July 11- 13, 2005.

Dias, R. P., 2001. Neotectónica da Região do Algarve. Dissertação de doutoramento, Fac. Ciências, Univ. Lisboa, 369 p.

Geirnaert, W., van Beers, P. H., de Vries, J. J., Hoogeven, H. (1982) - A geo-electric survey of the Miocene aquifer between Quarteira and Olhão, Algarve (Portugal). Comun. Da III Semana de Hidrogeologia, Dep. de Geologia da FCUL, pp. 143-153.

Hugman, 2016. Numerical Approaches to Simulate Groundwater Flow and Transport in Coastal Aquifers – From Regional Scale Management to Submarine Groundwater Discharge. PhD thesis. Universidade do Algarve.

Lobo-Ferreira, J.P, Chachadi, A.G., Diamantino, C., & Henriques, M.J. (2005), Assessing aquifer vulnerability to sea-water intrusion using GALDIT method: Part 1 – Application to the Portuguese Aquifer of Monte Gordo. IAHS and LNEC, Proceedings of the 4th The Fourth Inter Celtic Colloquium on Hydrology and Management of Water Resources, held at Universidade do Minho, Guimarães, Portugal, July 11- 13, 2005.

Management Plan for the Hydrographic Region of the Ribeiras do Algarve, 2016/ Plano de Gestão da Região Hidrográfica das Ribeiras do Algarve, aprovado pela Resolução do Conselho de Ministros n.º 52/2016, de 20 de setembro (Republicado em anexo à Declaração de Retificação n.º 22-B/2016, de 18 de novembro).

Manuppella, G., Oliveira, J. T., Pais, J., Dias, R. P. (1992) - Carta Geológica da Região do Algarve, escala 1:100 000. Notícia Explicativa. Serviços Geológicos de Portugal, Lisboa. 15 pág.

Manupella, G., Ramalho, M., Antunes, A. T., Pais, J. (2007) - Carta Geológica de Portugal na escala 1:50 000, Notícia Explicativa da Folha 53-A, FARO. Serviços Geológicos de Portugal. 40 pág.

Moura, D. e Boski, T. (1994) - Ludo Formation - a New Lithostratigraphic Unit in Quaternary of Central Algarve. Gaia, Lisboa, 9: pp. 95-98.

Nemus, 2002- Estudo de Impacte Ambiental do campo de golfe dos Pinheiros Altos.

Pais, J. (1992) - Cenozóico, in Manuppella, G. (coord.), 1992. Nota Explicativa da Carta Geológica da Região do Algarve, escala 1/100 000. pp. 8-9.

Reis, E. (2018) - Cálculo do Balanço Hídrico do Sistema Aquífero da Campina de Faro do Algarve. Technical Report.

Roseiro, C. (2009) - Recarga artificial de aquíferos: aplicação ao sistema aquífero da   Campina de Faro. Dissertação para a Obtenção do Grau de Doutor em Hidrogeologia. Universidade de Lisboa. 272 pág.

Silva, A. V., Portugal, A., Freitas, L. (1986) - Modelo de Fluxo Subterrâneo e Salinização dos Aquíferos Costeiros entre Faro e Fuzeta. Com. Serv. Geol. Portugal, 72(1/2), pp. 71-87.

Silva, M. L (1988) - Hidrogeologia do Miocénico do Algarve. Dissertação para a Obtenção do Grau de Doutor em Geologia. Departamento de Geologia da FCUL. 377 pág.

Silva, M. L., C. Almeida, 1989. Aspectos Hidrogeológicos das Formações Miocénicas do Algarve. Geolis, revista da Secção de Geologia Ec. e Aplicada, II(2): 115-132.

Silva, M. O. e Silva, M. L. (1992) - Impactos da Agricultura na Qualidade Química das Águas Subterrâneas. Os exemplos da Campina da Luz (Tavira) e da Campina de Faro. Geolis, vol. 6 (1 e 2), pp. 136-145.

Stigter, Van Ooijen, Post, Appelo, 1998. A hydrogeological and hydrochemical explanation of the groundwater composition under irrigated land in a Mediterranean environment, Algarve, Portugal. Journal of Hydrology, vol. 208, pp 262-279.

Stigter, 2005. Integrated analysis of hydrogeochemistry and assessment of groundwater contamination induced by agricultural practices. PhD thesis. Universidade Técnica de Lisboa.

Terrinha, P. A. G., 1998. Structural Geology and Tectonic Evolution of the Algarve Basin, South Portugal. Unpublished PhD Thesis, Imperial College, London, 430.

Victor, L. A. M. e Martins, I. J. (1978) - Estudo de Anomalias Gravimétricas nas Regiões de Moncarapacho e Campina de Faro, Publicação n.º 15 do Inst. Geof. Infante D. Luis, F.C.U.L.

Deliverable 5.3

PILOT DESCRIPTION AND ASSESSMENT

Falster, Denmark

Authors and affiliation:

Per Rasmussen, Klaus Hinsby, Denitza Voutchkova, Birgitte Hansen

[GEUS]

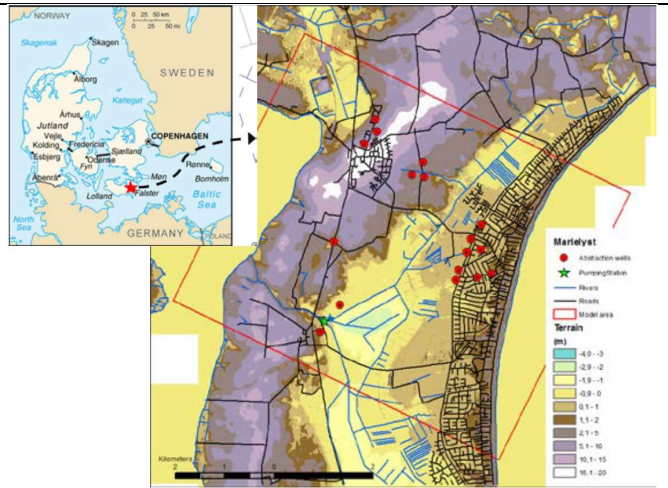| Deliverable Data	
Deliverable number	D5.3
Dissemination level	Public
Deliverable name	*Pilot description and assessment*
Work package	WP5 & 6: *Assessment of salt-/sea water intrusion status, vulnerability and adaptation strategies*
Lead WP/Deliverable beneficiary	*IGME*
Deliverable status	
Version	*1*
Date	28/04/2021

[This page has intentionally been left blank]

LIST OF ABBREVIATIONS & ACRONYMS

TABLE OF CONTENTS

1 EXECUTIVE SUMMARY

Pilot name	Falster
Country	Denmark
EU-region	Central and eastern Europe
Area (km²)	32
Aquifer geology and type classification	Chalk, fractured
Primary water usage	Drinking water supply

Main climate change issues	Increasing sea levels is expected to increase the risk of saltwater intrusion to the coastal confined chalk aquifer. Groundwater modeling studies have shown that a potential decrease in precipitation for extended periods may also increase the risk of saltwater intrusion to the local groundwater aquifer. Other effects of projected climate change impacts include an increase in the number and size of extreme rain events resulting in floodings along drainage canals if measures are not taken to avoid this.
Models and methods used	Geophysical measurements (e.g. electromagnetic, both airborne and groundbased, as well as geophysical borehole logging) have been conducted to find the existing fresh-saltwater boundary and support the development of a geological and an integrated groundwater-surface water model for climate change impact assessment and adaptation. Field tracer experiments were completed in order to estimated dual-domain flow parameteres for density dependent groundwater modelling using MODFLOW, MT3DMS and SEAWAT. Analyses of groundwater and surface water including age dating and emerging contaminants were performed for characterization of water qualities. Salinity sources were assessed by the use of self-organizing maps (SOM) for the analysis of the distribution of selected trace elements. Natural backgroundwater values were furthermore estimated by different methods and used to assess groundwater threshold values and chemical status according to the Water Framework Directive.
Key stakeholders	Marielyst Waterworks, Land Reclamation Society Bøtø Nor, Farmers, Dike Guild of Falster, Homeowners Association, tourist- and business associations, Gedser bird watching station.
Contact person	Klaus Hinsby (khi@geus.dk), Per Rasmussen (pr@geus.dk)

Saltwater intrusion to the coastal chalk aquifer on the southern part of the Falster island is a significant challenge and threat to water supply in the area in the near and far future (Rasmussen et al., 2013, 2015) as in many other coastal areas in Europe (Hinsby et al., 2011) and globally (Post and Abarca, 2010). The main climate change impact and adaptation issues with the Falster pilot area include potential saltwater intrusion from the Baltic Sea, deeper saline parts of the aquifer and other parts of the confined chalk aquifer and aquifer system (Hinsby et al., 2012), which locally seems not to have been completely freshened during the Pleistocene and Holocene (Knudsen et al., 2021). In addition flooding of low-lying areas and droughts during extreme events have occurred during recent years and is expected to increase in the area according to climate change projections for Northwestern Europe.

The upper part of the chalk aquifer at a depth between typically 15 – 25 meter below surface locally has elevated chloride contents to concentrations above the drinking water standard of 250 mg/l. Depending on location the observed elevated concentrations may originate from the aquifer itself as an old marine sediment, the Baltic Sea and Holocene marine sands above the aquifer (Hinsby et al., 2012, Rasmussen et al., 2013, Knudsen et al., 2021).

The understanding of the salinity sources and the migration of dissolved chloride in the chalk aquifer is important for developing efficient measures to control saltwater intrusion and protect water supply wells from increasing chloride e.g. by temporary groundwater storage / water banking and other subsurface water solutions (Hinsby et al., 2018), while potentially protecting the built environment in the area at the same time (Hinsby et al., 2015, 2016, 2019).

2   INTRODUCTION

Climate change (CC) already have widespread and significant impacts in Europe, which is expected to increase in the future. Groundwater plays a vital role for the land phase of the freshwater cycle and has the capability of buffering or enhancing the impact from extreme climate events causing droughts or floods, depending on the subsurface properties and the status of the system (dry/wet) prior to the climate event. Understanding and taking the hydrogeology into account is therefore essential in the assessment of climate change impacts. Providing harmonised results and products across Europe is further vital for supporting stakeholders, decision makers and EU policies makers.

The Geological Survey Organisations (GSOs) in Europe compile the necessary data and knowledge of the groundwater systems across Europe. In order to enhance the utilisation of these data and knowledge of the subsurface system in CC impact assessments the GSOs, in the framework of GeoERA, has established the project "Tools for Assessment of ClimaTe change ImpacT on Groundwater and Adaptation Strategies – TACTIC". By collaboration among the involved partners, TACTIC aims to enhance and harmonise CC impact assessments and identification and analyses of potential adaptation strategies.

TACTIC is centered around 40 pilot studies covering a variety of CC challenges as well as different hydrogeological settings and different management systems found in Europe. Knowledge and experiences from the pilots will be synthesised and provide a basis for the development of an infrastructure on CC impact assessments and adaptation strategies. The final projects results will be made available through the common GeoERA Information Platform (http://www.europe-geology.eu).

The Falster pilot area in Southeastern Denmark has been investigated for about a decade to improve the understanding of salinity sources (Hinsby et al., 2012, Knudsen et al., 2021), climate impacts on salt water intrusion to a coastal aquifer that secure water supply for a summer housing areas in the southeastern part of the Falster Island (Marielyst), which experiences increasing salinity and risk of flooding.

3   PILOT AREA

The local waterworks, Marielyst Waterworks, located in the Falster pilot area has experienced problems with increasing salt (chloride) concentrations in water supply wells during the last two to three decades (Fig. 1). The waterworks have had to close several existing water supply wells due to chloride concentrations above the drinking water standard in the coastal aquifer. The main aquifer in the area is a shallow chalk aquifer highly fractured in the upper 10-20 meter. The land use in the study area is dominated by agriculture and settlements of summer cottages, although a few small permanent villages have developed on top of the push moraine hills in the western part of the area. Today there are more than 5000 summer cottages. Although most of these are built on the original barrier islands in the eastern part of the investigated area, the most recent housing areas have spread into the reclaimed areas and some of these are therefore located at or below mean sea level. The freshwater supply for the villages and the summer cottages is based solely on groundwater.
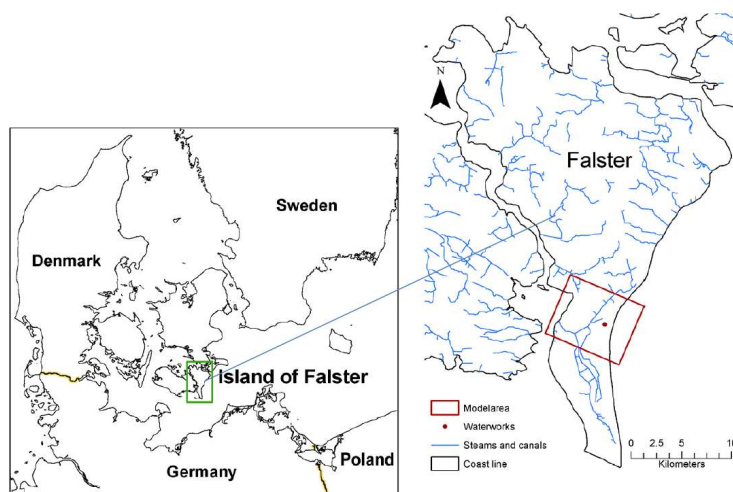

Fig. 1. Location of Falster pilot area

The Falster test site area was studied in the three previous EU and National research projects: "BaltCICA" (www.baltcica.org) was part-funded by the BONUS programme on the Baltic Sea (www.bonusportal.org), "Water4Coasts" was part-funded by the Ecoinnovation program of the Danish Ministry of Environment and Food (http://eng.ecoinnovation.dk/), and "SUBSOL" (www.subsol.org) received funding from the European Union's Horizon 2020 research and innovation programme (https://ec.europa.eu/programmes/horizon2020/en). Main results from the three projects can be found in Rasmussen et al. (2013), Hinsby et al. (2016), and Hinsby et al. (2018).

The main objective of the studies conducted in BaltCICA was to assess climate change impacts on the freshwater-saltwater boundary in the Chalk aquifer in the investigated area. Geophysical measurements (e.g. electromagnetic, both airborne (SkyTEM) and ground based, as well as geophysical borehole logging) were conducted to find the existing freshwater-saltwater boundary and to support the development of a geological and an integrated groundwater-surface water model for climate change impact assessment and adaptation (Fig 2 and 3).
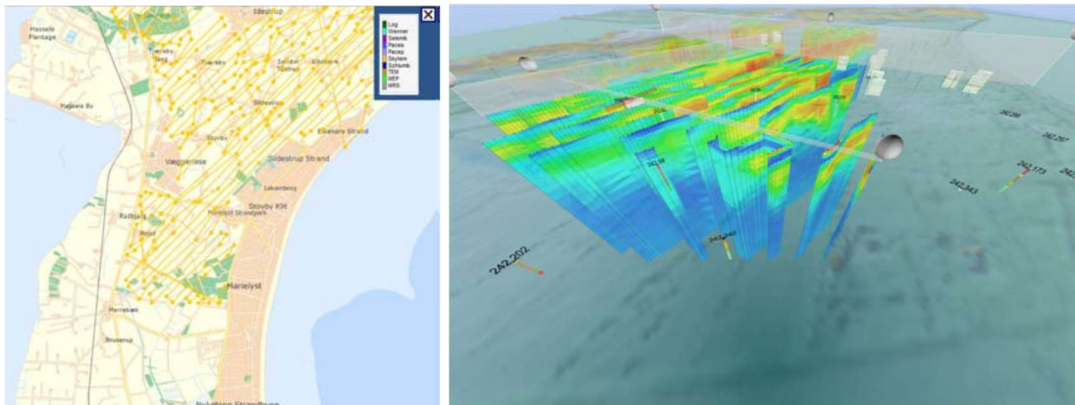
Fig. 2. SkyTEM flight lines (left). SkyTEM resistivities displayed in 3D (right)
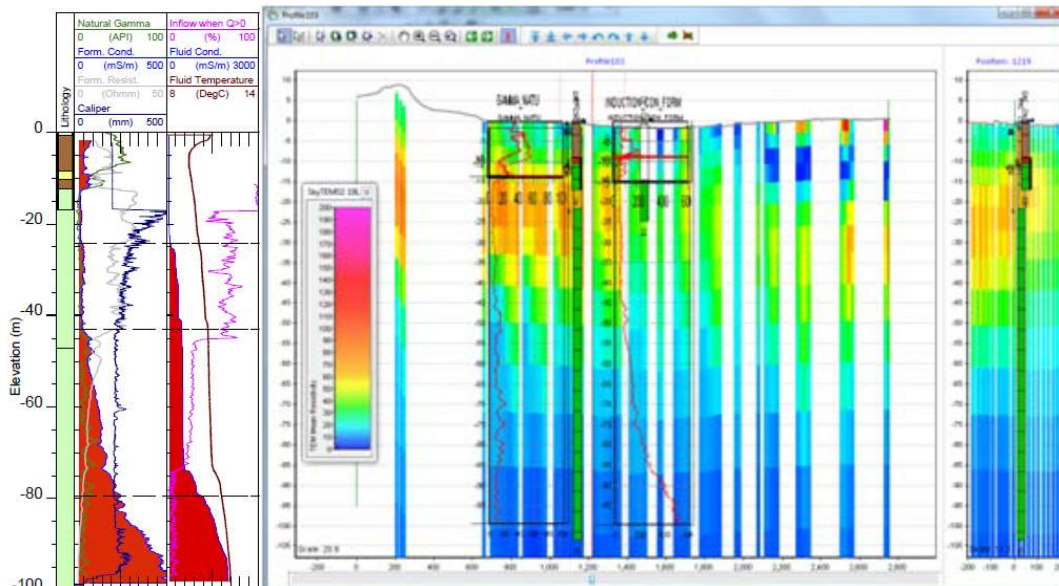

Fig. 3. Geophysical borehole logs (left). Combined plot of formation conductivity from wireline logging and SkyTEM resistivities (right)

The main objective of the Water4Coasts study was to initiate the assessment of the potential application of new innovative techniques to control saltwater intrusion and protect freshwater resources in the fractured Chalk aquifer of the Falster Island and similar settings, globally (Hinsby et al, 2016). The studies demonstrated that several issues needed to be investigated further before concrete solutions could be recommended. The recommendations included more detailed analyses of the hydraulic properties of the fractured chalk aquifer. Other suggestions dealt with further analysis of water quality of groundwater and surface waters. Surface water could potentially be used after treatment for injection and water banking e.g. between wet winter periods with low demands and abstraction and dry summer periods with high demands and abstraction.

In the SUBSOL project, the Falster area was selected as one of the areas to assess whether the subsurface water solutions (SWS) developed for single porosity granular aquifers in the Netherlands may be applied with similar success and designs in dual-porosity fractured

carbonate aquifers. The conducted investigations indicate that dual porosity systems are very well suited for the application of SWS techniques, globally, but that fracture distributions and e.g. glaciotectonical impacts affects the hydraulic behaviour in complicated ways that require additional investigations and assessments (Fig. 4).
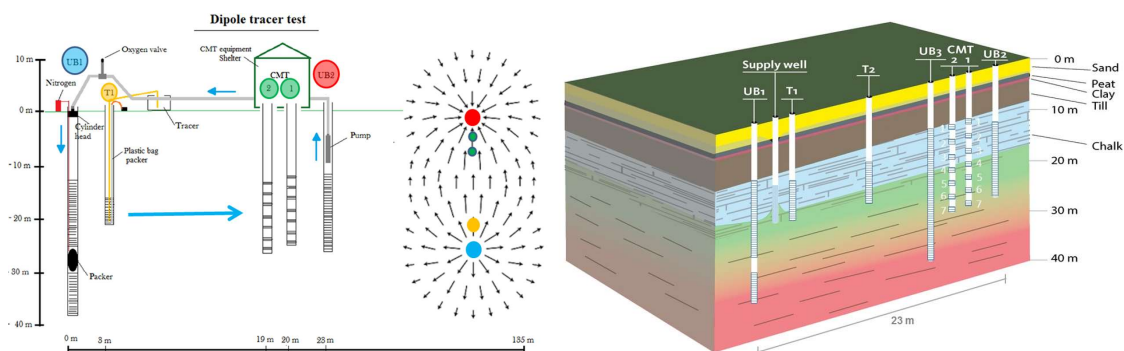

Fig. 4. The developed dipole tracer test setup in the SUBSOL project, blue arrows in the left diagram show the water movement. Tracer was injected in T1 or T2 (right diagram) and tracer breakthroughs were observed in the multi-level screens of CMT1 and 2

The aim of this case study was to further assess the salt-/seawater intrusion status and vulnerability in the shallow fractured chalk aquifer in Falster. The vulnerability assessments of the aquifer includeed effects of future climate predictions concerning risks of a drier climate with less precipitation resulting in reduced groundwater recharge, increased frequency and intensity of intense rainfall resulting in flooding. The aim was also to look at the possibility for using MAR (Managed Aquifer Recharge) as a tool for the long-term protection, sustainable management and improvement of local groundwater resources.

3.1   Site description and data

Location of pilot area
The pilot area is located in the south-eastern part of Denmark on the island of Falster. Towards the east the area is bounded by the Baltic Sea and towards the west of the strait of Guldborgsund (Fig. 5). The local waterworks are abstracting groundwater from the shallow Chalk aquifer overlain by quaternary and post glacial sediments of mainly clayey tills and sands. The well fields located closest to the Baltic Sea coast have seen an increasing chloride concentration in the abstracted groundwater during the last decades.
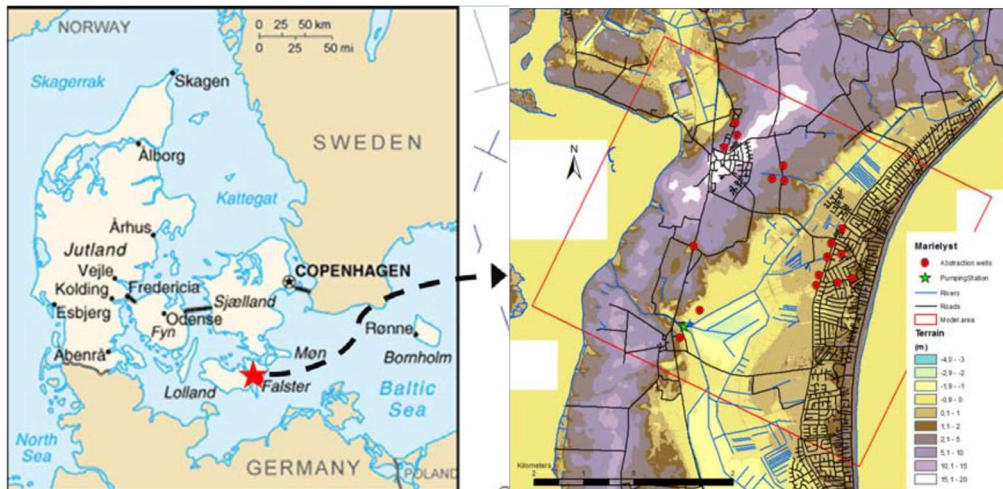
Fig. 5. Location of pilot area, abstraction wells, drainage canals and pumping station

Climate

The climate in Denmark is characterized by the country's close location to the Atlantic Ocean and the Gulf Stream. The predominant occurrence of western winds means that the coastal climate is dominant. The coastal climate and the location in the west wind belt mean that Denmark usually has relatively cool summers and mild winters. However, when the wind comes from the continent, periods of continental climate (hot summers and cold winters) can occur.

The sea is surrounding Denmark, which also means that the temperature difference between night and day is relatively small.

The average daily temperature in Denmark is around 15-16 degrees in summer and around or just above the freezing point in winter. Winters with a prolonged supply of cold air from the continent occasionally give rise to hard winters, where the inland waters freeze.

The average annual precipitation in the area is approximately 700 mm and the actual evapotranspiration is approximately 450 mm.

Topography

The elevation varies from 19 m a.s.l. (above sea level) in the west to -3 m a.s.l. in the central eastern part of the area. The landscape is mainly developed from north-south trending push moraine hills of clayey tills along the coast in the western part of the island, which were formed during the last glaciation by an east to west moving glacier. During the Holocene, small barrier islands with eolian sand dunes, which constitute the eastern part of the island and a lagoon developed in front of the glacial moraine hills. As the barrier islands grew it became possible to reclaim the low-lying wetland area between the push moraine and the barrier islands in the central part of the study area.

Land use

The land use in the study area is dominated by agriculture and settlements of summer cottages, although a few small permanent villages have developed on top of the push moraine hills in the western part of the area.

Soil types

The dominant soil types in the Falster pilot area are clayey till, marine sand, and eolian sand dunes (Fig. 6).
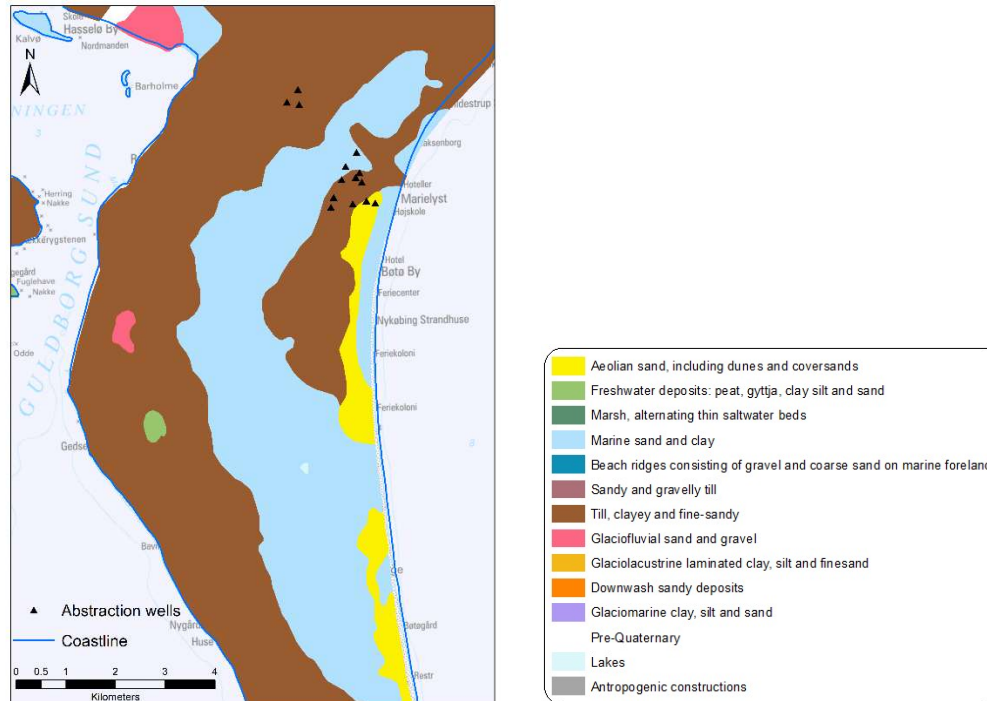
Fig. 6. Soil types (location map, see Fig. 7 A)

Geology/Aquifer type

In the pilot area, the top surface of the Upper Cretaceous chalk aquifer is situated at about 10 m below the surface. It is overlain by a 5 m thick unit of glacial sediments and 5 m marine sand. However, at a depth of 15 to 18 m there is a layer of chalk with gravel and pebbles of basement rocks.

Based on an evaluation of data from other wells in the area, it has become evident that another zone with basement gravel and pebbles existed even deeper at a level from 30 to 40 m below the surface. These findings have implications for the understanding of groundwater flow around the wells as the complexity of the hydraulic characteristics markedly changes the aquifer's behaviour. A model of the glaciotectonite occurrence was established based on a glaciodynamic concept of the area (Pedersen et al., 2018) (Fig. 7).

Fig. 7. Hydrogeological investigation site on Falster: A: geological map of the area demonstrating the glacial geological setting. C: block diagram illustrating the features and glacitectonites in the Upper Cretaceous beds (Pedersen et al., 2018)

The main aquifer for water supply in the area is the upper chalk. The Quaternary glaciations have caused fracturing of the upper 20–30m o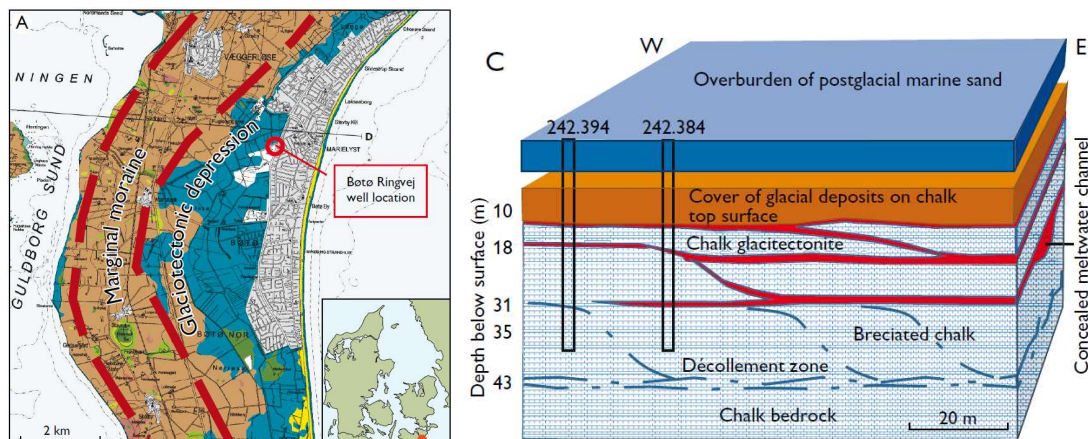f the chalk. In this part, the chalk is fully or partly refreshed due to fast advective groundwater flow through the fractures. Previous studies of chalk aquifers in Denmark have shown that the residual saltwater typically is completely flushed out in the upper 50–80m of the chalk by infiltrating freshwater. Below this zone a mixing zone with elevated chloride concentrations is seen, where the number of fractures and the effective hydraulic conductivity is gradually decreasing compared to the fully refreshed zone above. Below this depth, matrix diffusion is the dominating transport process for saltwater. At depth below 150–200m the saltwater is of oceanic concentration with total dissolved solids (TDS) concentrations above 35 000 mg/l and chloride concentrations above 19 000 mg/l.

Surface water bodies
The surface water system is dominated by the artificial drainage canal system. A few minor creeks flow towards the drainage system or towards Guldborgsund. The drainage system is lowering the water table in the area where the ground surface has elevations between +1 and −3 m a.s.l. The pumping station is aiming at keeping a constant water level in the drainage canals.

Groundwater abstractions/irrigation
The Marielyst Waterworks supplies water to 5200 households. Due to the high percentage of summer cottages in the area, the groundwater supply varies considerably during the year with a maximum of 2000 m³/day in July to a minimum of 300 m³/day in January. The waterworks has 12 active abstraction wells, which are located in three separate well fields. The oldest well field is located about 0.5 km from the coast, a second group of wells are approximately 1 km from the coast (established 1975–1990) and both well fields are located on one of the former barrier islands. The newest well field is located in the central part of the island 2.5 km from the coastline. It was established in 2005 in or very close to the main groundwater recharge area in the push moraine hills.

All 12 groundwater abstraction wells of Marielyst Waterworks are drilled to a depth of 10–15m into the upper fractured chalk aquifer. Significant groundwater abstraction has taken place since

the 1960s. The annual groundwater production reached its maximum around 470 000 m^3/year in the beginning of the 1980s and has since then decreased to the present level of around 250.000 m^3/year, mainly due to repair of leaky water pipes. Additionally, groundwater abstraction takes place from two other minor waterworks and a few irrigation wells, which add up to approximately 150.000 m^3/year.

3.2   Climate change challenge

The Falster pilot area is located in the Central and Eastern Europe climate zone (EEA map Fig. 8) where a decrease in summer precipitation is expected along with an increase in warm temperature extremes. In the Falster pilot area higher summer temperatures and lower precipitation will most probably result in a higher demand for groundwater, both for domestic use and for irrigation of e.g. golf courses. Lower summer precipitation will also affect the surface water bodies being subject to more water stress. A decrease in summer precipitation is not expected to affect the groundwater recharge that is mainly taken place from October to April.

The most likely climate scenario for the pilot area also predicts an increase in sea level, and an increase in winter precipitation, which will most probably result in an increase in groundwater recharge. Rising sea level will most probably result in further seawater intrusion into the coastal Chalk aquifer, causing a reduction in the available groundwater resource for the local freshwater supply. In addition, an increase in the frequency and the intensity rainfall is predicted, which might result in more severe flooding events.
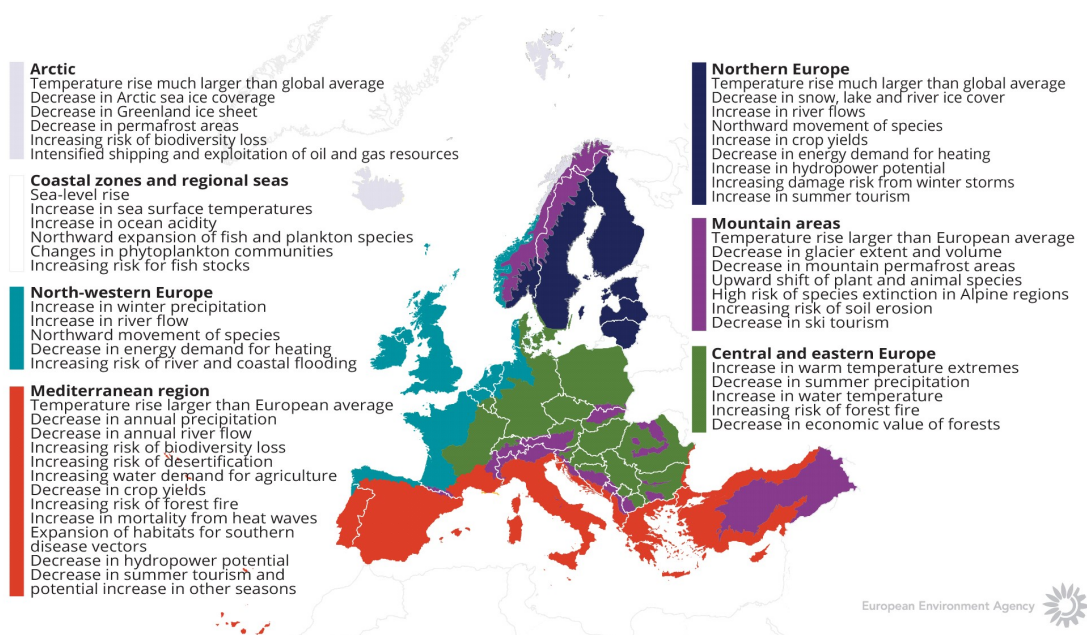

Fig. 8. Observed and projected climate change and impacts for the main biogeographical regions in Europe (European Environmental Agency)

4 METHODOLOGY

4.1 Methodology and climate data

4.1.1 Tools/ model description

For the pilot area on the island of Falster a 3D variable density groundwater model has been setup with the aim of analysing actual and future risk of saltwater intrusion to the local coastal aquifer. The modelling packages MODFLOW, MT3D, and SEAWAT were used. The setup of the MODFLOW/MT3D/SEAWAT model, its functionalities, applications and basic assumptions are described by Rasmussen et al. 2013, which can be found in a special issue of Hydrology and Earth System Sciences (Hinsby et al. 2011). Focus of the modelling were on 1) getting the initial saltwater concentrations right by modelling the transition of part of the pilot area, which over the last two to three centuries has changed from a saltwater lagoon to reclaimed land, 2) the increase in groundwater abstraction from the costal aquifer due to a significant development of summer cottages and the possible effect of seawater intrusion, 3) and impacts of climate change, change in precipitation and sea level rise, on seawater intrusion.

A minor local and simplified 3D variable density model based on the above described model has been setup with the purpose of analysing the applicability and effectiveness of subsurface water solutions (SWS) in a fractured chalk aquifer. The SWS "Freshkeeper" was tested, where freshwater is injected in to the aquifer with the aim of storing freshwater from winter to summer were, and at the same time prevent saltwater from entering the aquifer by creating a freshwater lens in the aquifer around the groundwater abstraction wells (Hinsby et al. 2018).

4.1.2 Climate data

The model scenarios on future risk of saltwater intrusion to coastal aquifer were based on predictions of sea level rise and on change in groundwater recharge due to projected changes in precipitation for the Danish area. The expected change in groundwater recharge for the Pilot Falster was based on the predicted change in groundwater recharge for a comparable area in Denmark (van Roosmalen et al. (2007). These studies used output from regional climate models representing IPCC (2000) scenarios A2 and B2.

The tested climate change effects of sea level rise and changes in groundwater recharge were gradually implemented in the groundwater model over a simulation period of 90 years. For an additional 200-year simulation period both recharge and sea level were kept constant in order to assess the long-term effects of the imposed climate changes (Rasmussen et al. 2013).

The groundwater model could be improved in a couple of ways, e.g. by including 1) an ensemble of the latest climate models for different emission scenarios including downscaling (see www.aquaclew.eu), 2) the latest predictions for expected sea level rise, and 3) the expected change in the demand for groundwater with predicted longer and warmer summer periods with less precipitation than today.

4.2 Tool(s) / Model set-up

The groundwater model was based on the large scale Danish national hydrological model, the DK-Model (Henriksen et al. 2003) with later updates. The geological information in the model was refined using data from geological soil maps, and from various types of borehole tests and borehole wireline logs. The canal and drainage system were refined using local maps and field surveys.

4.3 Tool(s)/ Model calibration/ test

The groundwater model was calibrated using groundwater head observations and discharge data from the main drainage canal. The variable density model simulations of saltwater intrusion were validated against groundwater chemical data and geophysical data (borehole logging data and data from both ground and airborne transient electromagnetic surveys).

4.3.1 Observation data

Time series of groundwater head, groundwater chemistry and river discharge were available for model calibration and validation. Some of the historical data series up to or more than 30 years long. During the resent project periods more intensive monitoring programmes were organised.

4.4 Uncertainty

The geological uncertainty was the major source of uncertainty for the groundwater density model. The knowledge in general and also site-specific knowledge about flow and transport characterises for the fractured and double porosity chalk aquifer was limited. The geological interpretation and the implemented geological model for the coastal zone was uncertain, there were only limit geological available in the coastal zone, few boreholes exist as groundwater interests are limited and geological information collected for exploration for off-shore raw material exist only further out in the sea. The degree and the extent of the refreshening of saline water in the chalk aquifer by fresh groundwater recharge was also a source of uncertainty.

These uncertainties were to some extent addressed by field campaigns including borehole wire logging, electromagnetic surveys, both airborne (SkyTEM) and ground based, and onsite field tracer tests. More investigations are needed to really improve the flow and transport processes in the double fractured chalk aquifer.

4.5 Saltwater intrusion and groundwater chemical status

The national Threshold Value (TV) for Cl is set to 250 mg/l, which is the same as the drinking water quality standard. The natural background levels (NBL) for Cl were estimated at the national scale for different types of aquifers and locations. However, because these NBLs were lower than the national TV, they were not used in the chemical status assessment of the Danish groundwater bodies.

The NBL for Cl relevant to Falster is for the carbonated aquifers on Sjælland, which was estimated to be 157.2 mg/l, based on the representative Cl values for 1283 sampling points. The

representative value was determined as the mean of the annual mean concentrations for the period 2000-2018 (incl.).

5 MODELLING AND MONITORING RESULTS

5.1 Modelling results and climate change impact assessments

5.1.1 Performance to historical data

The calibration results for the groundwater heads for the steady-state models were are regarded as satisfactory with a RMS value of 1.53 m. The used groundwater heads for model calibration were all measured in boreholes with low salinity and density effects on hydraulic heads are insignificant. For the transient calibration a R^2-value (the Nash–Suthcliffe coefficient) of 0.88 was found for the drainage canal main gauging station based on monthly data, which in general is an acceptable calibration result (Rasmussen et al. 2013).

A comparison between the modelled saltwater distribution and SkyTEM surveys showed both good agreement in some areas and areas with some discrepancy (Fig. 9). See Rasmussen et al. 2013 for further discussions of the model validation and the electromagnetic surveys.
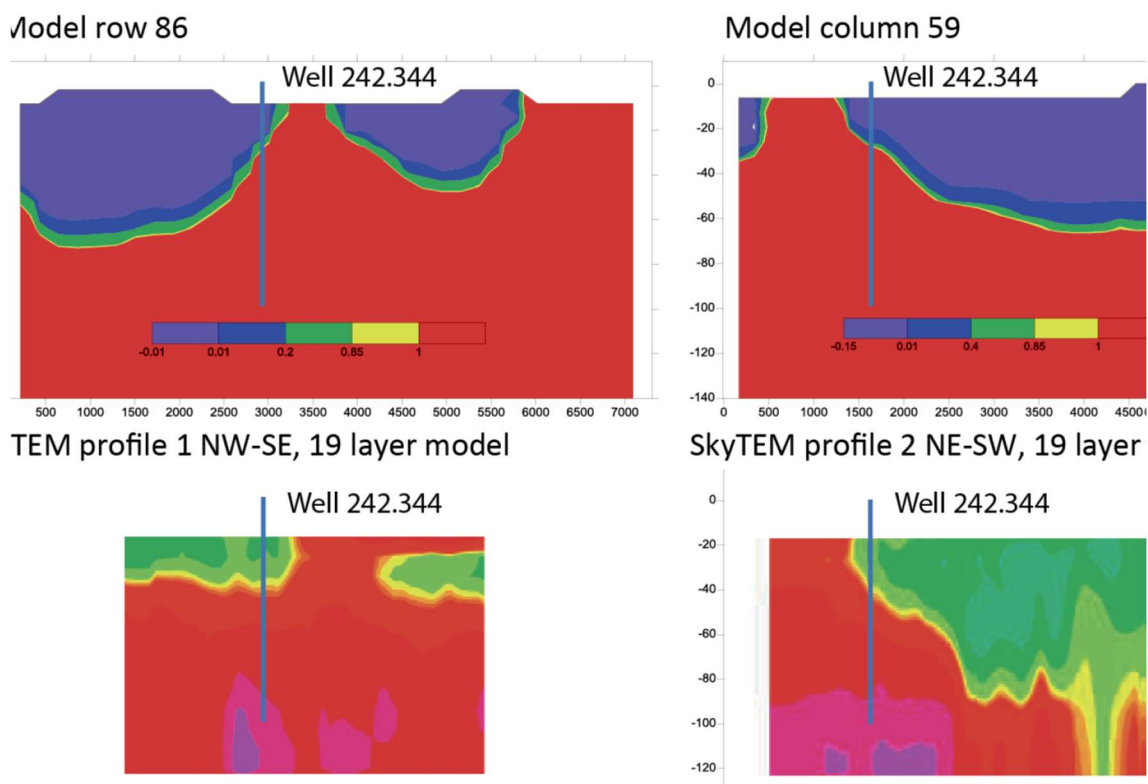

Fig 9. Comparison between the results of model simulations (upper cross sections) and SkyTEM surveys (lower cross sections). The colour scales are defined such that blue/green colours indicate freshwater of drinking water quality ([Cl−]<250 mg L−1). Yellow is breaching a threshold value of 150 mg L−1, and red breaches the drinking water guideline (Rasmussen et al. 2013)

5.1.2   Results of assessments

The study shows that saltwater intrusion in the Falster Pilot is sensitive to changes in sea level, groundwater recharge and stage of the drainage canals. The changes in recharge were found to be the most important factor, whereas minor sea level rises do not seem to affect the sea water intrusion as much. For the abstraction wells at risk the model studies show that the chloride concentrations are most sensitive to the stage of the drainage canals and to the groundwater recharge. However, the combination of significant changes in groundwater recharge, sea level rise, groundwater abstraction, and canal maintenance are crucial for the development of the groundwater quality (Rasmussen et al. 2013).

5.2 Monitoring data and chemical status assessments

5.2.1 Time series of chloride concentrations

The dataset covers the period 1985 to 2020 and includes groundwater Cl samples taken at 14 abstraction wells used by Marienlyst Vandværk for drinking water production (Table 1 and Figure 10 and 11). In addition, the Cl samples of the treated drinking water taken at the exit of Marienlyst Vandværk (after all treatment) are also presented for comparison purposes.

Table 1. Summary statistics for the Cl dataset with information on the number of samples, the sampling period, the minimum, 10th and 50th percentiles (p10 and p50 respectively), maximum, mean and standard deviation (SD)

Sampling point		Samples	Period		Cl concentrations (mg/l)					
DGU number	VV Boring	n	y_1	y_n	min	p10	p50	max	mean	SD
242. 172	3	115	1985	2020	60	120	160	260	156.8	39.3
242. 178	2	115	1985	2020	190	208	280	300	262.8	33.2
242. 189	5	115	1985	2020	40	70.8	176	250	162.2	55.4
242. 190	4	57	1985	2005	156	238	270	316	267.2	29.2
242. 212	9	112	1985	2020	76	110	140	236	148.4	34.5
242. 213	10	57	1985	2005	195	204	220	260	221.5	15.1
242. 230	6	115	1985	2020	39	54	80	144	86.3	30.2
242. 231	7	115	1985	2020	60	70	104	180	102.1	28
242. 239	11	107	1993	2020	11	39.2	78	160	74.7	33.1
242. 317	new 4	58	2005	2020	32	35	40	50	40.7	5.1
242. 319	12	58	2005	2020	34	38	40	60	42.1	5.3
242. 320	new 10	58	2005	2020	26	30	40	52	39.7	7.7
242. 332	8	115	1985	2020	76	116	148	180	144.7	21.7
242. 44B_1	1	59	1985	2006	130	239	280	320	271.3	37.9
242. 44B_2	1	44	2009	2020	20	32	40	80	41.9	13.9
Marielyst Vandværk		115	1985	2020	40	105	124	186	126.5	26

Seven of the wells have been used in the entire period (1985 – 2020). Two (242. 190 and 242. 213) were used until 2005 and after that they were replaced by other two new wells (242. 317 and 242. 320) (Figure 10)
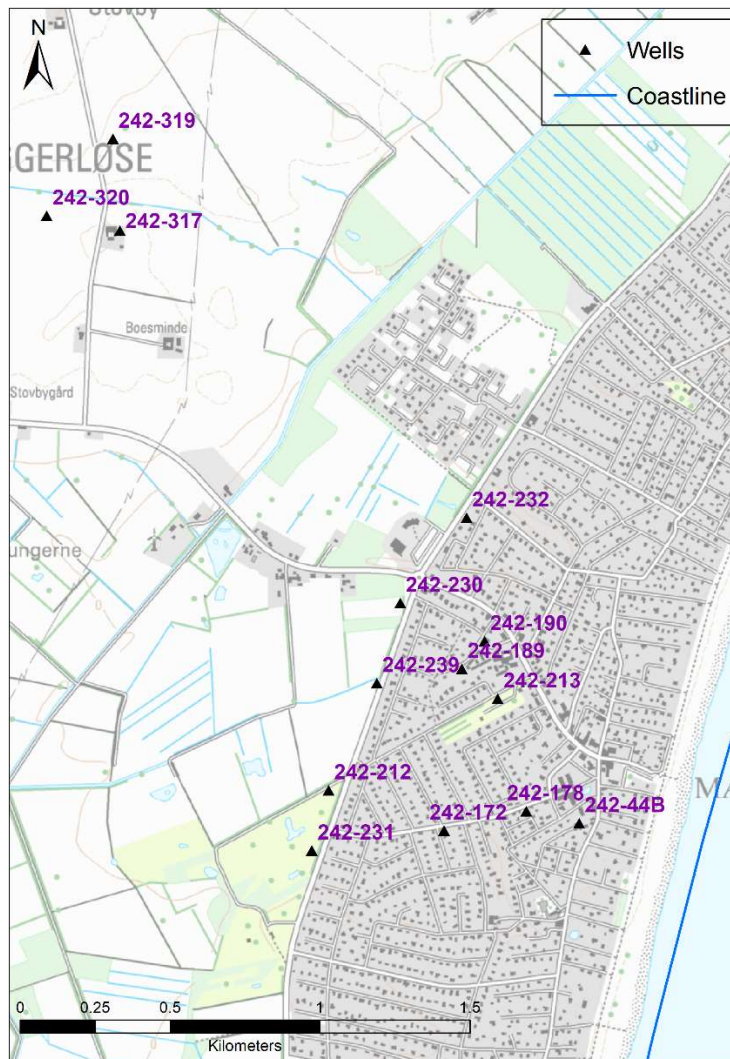
Fig. 10. Location of sampling wells

Well 242. 44B was re-established (deepened) in 26 Jan 2007, so the time-series have a gap from 2006 to 2009. The concentration before and after this intervention differ significantly, so in both Table 1 and Figure 11 those are shown separately and are treated as different sampling points. In the first period, the Cl concentrations were showing an increasing trend with concentrations exceeding the national TV of 250 mg/l, while after the intervention the median Cl concentration was 40 mg/l (max concentration 80 mg/l).
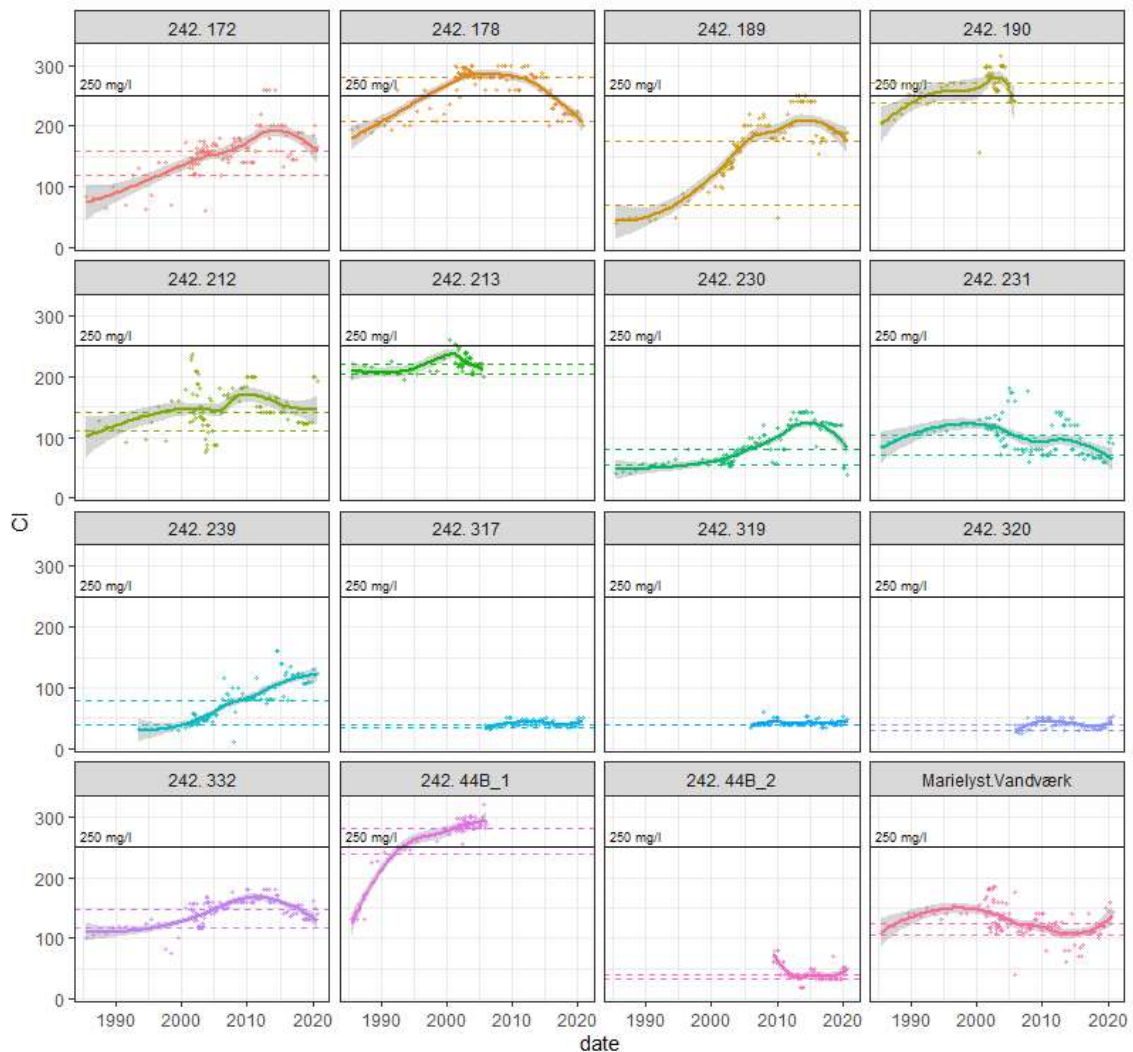
Fig. 11. Time-series of Cl concentrations (mg/l) (y-axis) in groundwater samples for the period1985-2020 at the abstraction wells of Marielyst Vandværk; Each measurement is visualized with a point, the trend is shown with a loess (local polynomial regression) and its 95% confidence interval. The DGU numbers of the abstraction wells are provided above each panel. The Marielyst Vandværk panel shows the Cl concentrations in the treated drinking water at exit waterworks. The national Threshold Value (250 mg/l) is drawn with a black horizontal line, while the representative value for each sampling point based on the 10th and 50th percentiles are shown with dashed lines; DGU n. 242.44B was re-established (deepened) in 26 Jan 2007, so the time-series are split for the two periods (before and after)

5.2.2 Natural background levels (NBLs) for Chloride based on time series data

In order to calculate NBLs (based on the 90th percentile), first a representative concentration level should be chosen for each sampling point. The representative concentration level for a specific period can be calculated based on different summary statistics. For example, in the River Basin Management Plan, the mean of the annual mean concentrations is used to account for the irregularity of the time-series, so each year is weighed equally. The mean is however very

sensitive to outliers, so the median has been suggested by the BRIDGE method. In the recent work done in TACTIC, both the median (50th percentile, p50) and the 10th percentile were tested. Table 1 presents both p10 and p50 for each of the sampling points, both of which are considered here as "representative" levels. These sampling-point specific levels are also shown in Figure 11 together with the time-series and the national TV level.

The p10 representative level for all abstraction wells is below the national TV (250 mg/l). Two sampling points have high p10 (238-239 mg/l), but both of these are no longer in use (242. 190 was replaced, and 242. 44B was deepened).

The p50 representative level, however, is higher than the TV (250 mg/l) for:
- DGU n. 242. 178 (1985-2020), p50 is 280 mg/l and the max Cl concentration is 300 mg/l
- DGU n. 242. 190 (1985-2005), p50 is 270 mg/l and the max Cl concentration is 316 mg/l
- DGU n. 242. 44B (before intervention, 1985-2006), p50 is 280 mg/l and the max Cl is 320 mg/l

The NBL (90th percentile) calculated based on the abstraction wells of Marienlyst Vandværk (15 sampling points with data in the study period) are:
- 226 mg/l with p10 as a representative value
- 276 mg/l with p50 as a representative value (> national TV of 250 mg/l)

Both of these NBLs are higher than the NBL calculated for the carbonated aquifers on Sjælland as part of the River Basin Management Plan (157.2 mg/l). This could indicate that the Cl concentrations observed in these sampling points are influenced by saltwater intrusion due to groundwater abstraction. However, the time-series also show that for most of these sampling points there is a trend-reversal in the last 5-10 years. The new wells established after 2005 have generally low median Cl concentrations (40 mg/l), which could be considered as the natural background at this part of the aquifer.

It could be argued that in general p10 represents better the "natural" background at each of the sampling locations, because the medians at some of the sampling points are influenced by the increasing trends or the trend-reversals. Future work should include detrending of the time-series before estimating NBLs.

Even though the Cl concentrations at some of the abstraction wells of Marienlyst Vandværk are elevated, the drinking water produced at the waterworks has relatively low levels of Cl (median 124 mg/l) which has never exceeded the drinking water standard (250 mg/l) in the study period.

6   CLIMATE CHANGE ADAPTATION STRATEGIES

Saltwater intrusion in coastal aquifers is an increasing problem, and increasing sea levels increase the concern and need for protecting groundwater resources in coastal regions, globally. Hence, efficient adaptation strategies are of increasing importance for projection of the water supply of small cities as well as metropolis in coastal areas around the world. Managed aquifer recharge and other subsurface water solutions provides many options for protecting coastal freshwater resources and temporarily store water e.g. from wet winters to dry summers (Hinsby et al. 2015, 2016, 2018; Zuurbier et al., 2014, 2015, 2017). Sources of fresh water to be stored in groundwater reservoirs / aquifers include desalinized deep brackish groundwater (less energy demanding than seawater desalinization) and purified rain and drainage waters.

The Falster pilot area with its test site facilities for tracer test studies provide excellent opportunities for studying and analysing the efficiency and impact of temporarily storing different types of freshwaters in fractured carbonate aquifer to control salt water intrusion and protect groundwater resources in coastal regions. Studies of climate change impacts in the area (Rasmussen et al., 2013; Hinsby et al., 2018) indicate that such subsurface water solutions may be the only efficient way to protect groundwater resources in similar areas. Hence, such solutions should be more widely tested and optimized in coastal areas around the world.

7 REFERENCES

Henriksen, HJ, Troldborg, L., Nyegaard, P., Sonnenborg, T.O., Refsgaard, J., and Madsen, B. (2003). Methodology for construction, calibration and validation of a national hydrological model for Denmark, J. Hydrol., 280, 52–71.

Hinsby, K., Jakobsen, R., Rasmussen, P., Sonnenborg, T.O., Sø, H.U., Aamand, J., Pedersen, S.A.S., Knudsen, C., Krüger, U.S., Gram, S., Andersen, H., Rasmussen, N.S. (2018). Road map for full scale implementation of SWS for fractured chalk aquifer. SUBSOL deliverable D2.2, 71 pp, http://www.subsol.org/.

Hinsby, K., Johnsen, A.R., Rasmussen, P., Sonnenborg, T.O., Sørensen, S.R., Postma, D., Thorn, P., Scharling, P.B.and Gudbjerg, J. (2016). Water4Coasts - New methods for integrated management and protection of coastal aquifers. Danish Ministry of Environment and Food, 2016, In Danish, but with English Summary and three Technical GEUS reports in English as appendix, 160 pp.

Hinsby, K., Johnsen, A., Sørensen, S. and Postma, D. (2015). Water4Coasts - Evaluation of water quality issues before application of managed aquifer recharge in a coastal chalk aquifer. Danmarks og Grønlands Geologiske Undersøgelse Rapport 2 0 1 5 / 9 3.

Hinsby, K., Jessen, S., Larsen, F. and Postma, D. (2012). A groundwater chemistry and multi-tracer study of sources of saltwater intrusion – the Island of Falster, Denmark. Proceedings of the 22nd Salt Water Intrusion Meeting, Rio de Janeiro, Brasil, http://www.swim-site.nl/pdf/swim22.html.

Hinsby K, Auken E, Essink GHPO, de Louw P, Siemon B, Sonnenborg TO, Wiederholdt A, Guadagnini A, Carrera J, (eds.) (2011). Assessing the impact of climate change for adaptive water management in coastal regions. Hydrol. Earth Syst. Sci., special issue 149, https://hess.copernicus.org/articles/special_issue149.html

Hinsby K., Condesso de Melo MT and Dahl M (2008). European case studies supporting the derivation of natural background Levels and groundwater threshold values for the protection of dependent ecosystems and human health. Science of the Total Environment, 401, 1-20.

Knudsen, C., Hinsby, K., Jakobsen, R., Kjaergaard, L.J. and Rasmussen, P. 2021. Fingerprinting sources of salinity in a coastal chalk aquifer using trace elements. GEUS Bulletin, accepted.

Kolind-Hansen, I. (2017). Investigation of a coastal fractured chalk aquifer, Marielyst, Denmark. Master Thesis, University of Copenhagen, February 2017, 138 pp.

Pedersen, S.A.S., Graversen, P. and Hinsby, K. (2018). Chalk-glacitectonite, an important lithology in former glaciated terrains covering chalk and limestone bedrock. Geological Survey of Denmark and Greenland Bulletin, 41, 21-24, Open access: www.geus.dk/bulletin.

Post, V. and Abarca, E. 2010. Preface: Saltwater and freshwater interactions in coastal aquifers. Hydrogeology Journal, 18, 1-4, preface to special issue, https://link.springer.com/journal/10040/volumes-and-issues/18-1

Rasmussen, P., Sonnenborg, T.O. and Hinsby, K. (2015). Water4Coasts - Modelling the effects of hydraulic barriers to control saltwater intrusion in a coastal chalk aquifer. Danmarks og Grønlands Geologiske Undersøgelse Rapport 2015/92.

Rasmussen P, Sonnenborg TO, Goncear G and Hinsby K (2013). Assessing impacts of climate change, sea level rise, and drainage canals on saltwater intrusion to coastal aquifer, Hydrol. Earth Syst. Sci., 17, 221-243.

van Roosmalen L, Christensen BSB and Sonnenborg TO (2007). Regional differences in climate change impacts on groundwater and stream discharge in Denmark, Vadose Zone J., 6, 554-571.

Zuurbier, Koen G., Klaasjan J. Raat, Marcel Paalman, Ate T. Oosterhof, and Pieter J. Stuyfzand. 2017. "How Subsurface Water Technologies (SWT) Can Provide Robust, Effective, and Cost-Efficient Solutions for Freshwater Management in Coastal Zones." Water Resources Management 31 (2): 671–87. https://doi.org/10.1007/s11269-016-1294-x.

Zuurbier, Koen G., Jan Willem Kooiman, Michel M.A. Groen, Bas Maas, and Pieter J. Stuyfzand. 2015. "Enabling Successful Aquifer Storage and Recovery of Freshwater Using Horizontal Directional Drilled Wells in Coastal Aquifers." Journal of Hydrologic Engineering 20 (3): 1–7. https://doi.org/10.1061/(ASCE)HE.1943-5584.0000990.

Zuurbier, Koen G., Willem Jan Zaadnoordijk, and Pieter J. Stuyfzand. 2014. "How Multiple Partially Penetrating Wells Improve the Freshwater Recovery of Coastal Aquifer Storage and Recovery (ASR) Systems: A Field and Modeling Study." Journal of Hydrology 509: 430–41. https://doi.org/10.1016/j.jhydrol.2013.11.057.